The Dissertation Committee for Yang Peng Certifies that this is the approved version of the following Dissertation:

Importance of Mixed Energy in the Pliocene Development Orinoco Delta Lobes, and the Impact of Large Volumes of Amazon Fluid Mud

Committee:

Ronald J. Steel, Supervisor

Cornel Olariu

Wonsuck Kim

David Mohrig

Craig S. Fulthorpe

Importance of Mixed Energy in the Pliocene development Orinoco Delta Lobes, and the Impact of Large Volumes of Amazon Fluid Mud

by

Yang Peng

Dissertation

Presented to the Faculty of the Graduate School of

The University of Texas at Austin

in Partial Fulfillment

of the Requirements

for the Degree of

Doctor of Philosophy

The University of Texas at Austin

August 2018

Acknowledgements

Firstly and foremost I would like to express my sincere gratitude to my advisor, Ronald Steel, who has been very supportive and provided me with guidance throughout this difficult but meaningful period. No matter how busy he was and wherever he was, he was always there providing timely guidance whenever I needed. I have been extremely lucky to have a supervisor who always encouraged and motivated me. I'd also like to thank Cornel Olariu who is greatly appreciated for insightful discussions and helpful advice that have improved the quality of my work tremendously. Committee members Wonsuck Kim, David Mohrig, and Craig S. Fulthorpe are sincerely thanked for their input during the PhD study. I would like to thank the RioMAR consortium of companies (Statoil, Shell, ExxonMobil, Devon, Chevron, ENI and Woodside) for financial support, as well as Ronald K. DeFord Field Scholarship Fund, and fellowships from the Graduate School. Shunli Li, Clarke A. Clayton, and Cory Hughes are greatly appreciated for their excellent assistance in the field. Georgia Huggins and Ariana Osman are thanked for repeated local support on Trinidad. Juergen Schieber and his students at Indiana University are thanked for their help with the SEM work on the mudstones although it's not included in this dissertation.

I also would like to thank all my colleagues in the Dynamic Stratigraphy workgroup as well as other friends from Jackson School of Geosciences who made this journey in my life a very pleasant experience. Finally, I would like to thank my family and Meng Yu. Without their love, support and encouragement, I wouldn't have walked this far.

Abstract

Importance of Mixed Energy in the Pliocene development Orinoco Delta Lobes, and the Impact of Large Volumes of Amazon Fluid Mud

Yang Peng, PhD

The University of Texas at Austin, 2018

Supervisor: Ronald J. Steel

This research focuses on how river-, wave- and tidal current energy is interpreted to have mixed and been preserved in well-exposed Pliocene strata of both wave-dominated and tide-dominated Orinoco delta lobes. A new method of process facies analysis has been adopted, allowing a more quantitative interpretation. In addition, the very large volumes of Amazon-derived mud that impact the front of the Orinoco Delta today are followed back through the Pliocene Orinoco record, and documented here for the first time. The detection of mixed energies and the additional impact of large mud volumes on the delta front are important because most previous studies on ancient systems have commonly attempted to focus on the dominant process and tended to overlook the complexity of process mixing. The research was carried out in the Pliocene Orinoco Delta on Trinidad using four datasets: an outcrop dataset of 1190 m of measured sections from the topset segments of shelf margin clinoforms of the Moruga Formation; a 260 m outcrop segment from the outer shelf to upper slope environments of the Moruga Formation; a 125 m thick outcrop segment from a tide-dominated delta lobe of the

Manzanilla Formation; and three selected outcrop examples (15-80 m thick) from the Morne L'Enfer, Manazanilla and Mayaro formations.

The results demonstrate how fluvial and wave signals have mixed as the shelf margin clinoform developed in a strong storm wave-dominated setting. The data suggest that the fluvial signals (including parts of distributary channel-fills and delta fronts) were preserved because of unusually high subsidence rates (averaging >1 km/My on the topsets) and rapid sediment burial probably with a sheltered coastal morphology on this early Atlantic shelf margin, preventing some of the fluvial deposits from being completely reworked by storm waves. Some of the tide-dominated segments of the Pliocene Orinoco Delta are shown to have had a compound deltaic clinoform that reveals detailed interaction of river, wave, and tide processes with the impinging fluid mud. This part of the research suggests that the abundant fluid mud caused wave damping and the preferred preservation of river and tidal signals on the subaqueous delta platform due to the reduced wave action. The Amazon-derived mud tended to accumulate on the subaqueous platform in tide-dominated delta lobes, whereas it was more likely to be eroded and re-deposited into a deeper setting on storm wave-dominated delta lobes.

Table of Contents

List of Tables

List of Figures

Figure 3.1: (A) Simplified Map illustrating that Trinidad is located in the foreland basin between the Caribbean plate and South American plate. The Paleo-Orinoco River delivered sediment and filled Eastern Venezuela Basin, onshore southern Trinidad, and offshore Columbus Basin. Previous changing courses of the paleo-Orinoco River from Paleocene to recent are illustrated by successive black dashed lines (numbered by 1 to 3) to the solid line from the west to the east (modified from Escalona and Mann, 2011). (B) Interpreted seismic data across the entire Orinoco shelf-margin prism exhibit progradation and aggradation of shelf deltas into the offshore Columbus Basin (from Dixon, 2005). Note that all deltaic units (TP95 down to TP30, in offshore stratigraphic terminology of Sydow et al., 2003) become shelf-edge deltas and rollover into deepwater slope deposits at the shelf break. The studied Moruga delta can also be seen to occupy a shelf edge position and occurs just below stratigraphic level TP35. (C) Composite well log in the offshore Columbus Basin [location in (B)] (Sydow et al., 2003) shows some 16 coarsening-upward units (each *ca* 200 m thick) indicating repeated stacking of regressive-transgressive Orinoco-Delta units, each becoming shelf-edge deltas on approach to the shelf-slope break. (D) Late Miocene–Pliocene shelf and shelf margin stratigraphy in the onshore Southern Basin of Trinidad in transition to offshore, illustrating four major deltaic growth stages separated by mud-prone flooding surfaces (modified from Steel et al., 2007). This same succession is much more growth faulted and thickened in the offshore Columbus Basin (Sydow et

Chapter 1: Introduction

PROBLEM AND SIGNIFICANCE

Most modern shoreline systems are under the mixed influence of river, wave and tidal processes, and they exhibit dynamically spatial and temporal changes in process regime and morphology (Bhattacharya and Giosan, 2003; Yang et al., 2005; Dalrymple and Choi, 2007; Hampson et al., 2008; Ainsworth et al., 2011; Olariu, 2014), although previous depositional models attempted to focus on the dominant processes using the ternary delta classification (Coleman and Wright, 1975; Galloway, 1975; Boyd et al., 1992). The mixed-process systems result from a variable combination of river, wave and tidal processes which can change through time on different scales, and this will cause complex variation in facies distributions. Examples of such mixed-energy systems have been increasingly documented (Gani and Bhattacharya, 2007; Vakarelov et al., 2012; Ainsworth et al., 2016; Rossi and Steel, 2016; Wei et al., 2016), but the complexity of this mixing is still understudied.

The Pliocene Orinoco delta lobes provide an excellent opportunity to apply the mixed-energy approach in that two separate but broadly coeval reaches (Moruga and Manzanilla formations) of the Pliocene Orinoco, as the modern Orinoco Delta, show both wave-dominated and tide-dominated delta lobes, thus allowing us to examine how river-, wave- and tidal current energy mixed in cases. In addition, the Moruga Formation, the main focus of this study, not only has a shallow-marine stratigraphic record, but also shows the coeval deep-water slope of the continental margin in the early-mid Pliocene parts of the system. This continuous sedimentary record provides insight into the facies

and stratigraphic architecture of the Orinoco shelf-margin growth, given that the extraordinary subsidence rates (2km/My for Pliocene-Pleistocene) would have preserved a more continuous and reliable record than most other margins.

Another research theme taken up herein is that the modern Orinoco Delta receives very large amounts of mud (approximately at least half of the sediment deposited along the Orinoco Delta) from the Amazon River via the northwest-directed Guyana littoral current. However, the influence of these huge volumes of Amazon fluid mud (some 10^8 tons/year of Amazon mud is transported to the Modern Orinoco coast) on the paleo-Orinoco Delta succession is completely unknown. The well-exposed outcrops of the paleo-Orinoco Delta from the late Miocene to Pliocene allow this mud to be examined in delta lobes dominated by different processes (waves, tides, and river currents).

OBJECTIVES

The objectives of the research in this dissertation are:

1. To investigate how the preserved, fluvial and wave signals were mixed in the wave-dominated, Pliocene Orinoco delta lobes by documenting the main facies and stratigraphic architecture during the development of the Moruga Formation within a setting of rapid, long-term syn-depositional subsidence.
2. To examine the growth of an unstable shelf margin that exhibits a transition from a storm wave-dominated delta front on the outermost shelf to gullied upper slope during the early-mid Pliocene development of the Moruga Formation.

3. To document the mixing of river-, wave-, and tidal processes in the tide-dominated delta lobes of the Manzanilla Formation using a new quantitative methodology for highlighting process mixing. In addition, we evaluate how the voluminous mud, coming partly from the impinging Guyana littoral current, impacted wave, tide, and river processes during construction of the muddy delta lobes.
4. To characterize the Amazon fluid mud layers and document how this mud tended to have a differing impact on tide- and wave-dominated settings. A hypothesis that the Guyana mud current is likely to have been effective mainly during rising and highstand of sea level and less so during falling stage and lowstand of sea level is also introduced.

OVERVIEW OF CHAPTERS

Chapter 2: Early-mid Pliocene shelf-margin growth (Moruga Fm.) on southeastern Trinidad: rapid subsidence and preservation of fluvial signals in an otherwise wave-reworked delta front succession

Chapter 2 presents the main facies and stratigraphic architecture of the Moruga Formation (southeastern Trinidad) which initially exhibits, a highly progradational low-angle rising shelf-edge trajectory, but subsequently changed to a moderate aggradational growth. The high progradation rate during the early development of the Moruga wedge was caused by the extremely high sediment supply outpacing the relatively sea-level rise. During the late-stage development of the Moruga Formation, the shelf margin probably subsided more rapidly and shows a greatly increased storage of sediment on the shelf. The studied outcrops exhibit thick, coarsening-upward successions that are mainly storm

wave-dominated delta fronts. An unusual aspect of this succession is the preservation of segments of subaqueous channels and mixed-energy delta fronts, despite the very high degree of storm-wave reworking in the succession. It is suggested that coastal morphology, lack of strong storms, very high rates of subsidence and burial may have protected some the original fluvial signals from being entirely reworked.

Chapter 3: Transition from storm wave-dominated outer shelf to gullied upper slope: The mid-Pliocene Orinoco shelf margin, South Trinidad

Chapter 3 is a manuscript already published in *Sedimentology* (Peng et al., 2017). This paper focuses on a 260 m thick succession (St. Hilaire Silstone and Trinity Hill Sandstone, Morgua Formation) which demonstrates a continuous transition from gullied uppermost slope (with sediment gravity flow and mass-transport deposits) upward to storm wave-dominated delta front on the outermost shelf. This study demonstrates that storm wave-dominated shelf margins do allow sediment bypass down into deepwater areas, even though other literature studies have suggested that exactly this type of margin often tends to be highly inefficient at bypassing sand to deepwater areas.

Chapter 4: Mixed-energy process interactions read from a compound-clinoform delta (paleo-Orinoco Delta, Trinidad): preservation of river and tide signals by mud-induced wave damping

Chapter 4 presents a tide-dominated segment from the Pliocene Orinoco Delta (Manzanilla Formation, coeval to Moruga Formation) that preserved a compound deltaic clinoform. The clinoform reveals details of the interaction of river, wave, and tide

processes with fluid mud at a scale of tens of meters to centimeters in the deposits. This chapter has been published in *Journal of Sedimentary Research* (Peng et al., 2018). This research is one of few studies that demonstrates process mixing in an ancient delta example with a compound clinoform. The mixing of interacting river, wave, and tide processes in this succession is documented using a new quantitative methodology for highlighting process mixing.

Chapter 5: Amazon fluid mud impact on tide- and wave-dominated Pliocene lobes of the Orinoco Delta

Chapter 5, submitted for publication to *Marine Geology*, characterizes Amazon-derived fluid-mud layers in the deltaic succession and shows how littoral fluid mud banks tended to accumulate on the subaqueous platform of strongly tide-influenced delta lobes, whereas on wave-dominated lobes the mud was commonly eroded and reworked farther out into deeper settings.

Chapter 2: Early-mid Pliocene shelf-margin growth (Moruga Fm.) on southeastern Trinidad: rapid subsidence and preservation of fluvial signals in an otherwise wave-reworked delta front succession

ABSTRACT

The early-mid Pliocene Orinoco Delta succession demonstrates the facies and stratigraphic architecture of a shelf margin developed in a setting of rapid, long-term syn-depositional subsidence (averaging about 1 km/My; Wood, 2000; Chen et al., 2018). The studied Moruga clastic wedge of the Orinoco Margin consists of a series of shelf to deepwater clinoforms with six identified facies associations namely channelized sandstones, river and mixed-process delta front, wave-dominated delta front, shoreface, prodelta-offshore transition-shelf, and upper-slope channels and mass-transport deposits. The succession is very sandy and generally consists of coarsening- and thickening-upward units of delta front with HCS/SCS sandstones and wave-ripple lamination indicating dominant storm wave regime particularly when the delta lobes were sited on the outer shelf. Several distributary channels are unusually well preserved and characterized by cross-bedded to parallel-laminated sandstones with mud clast lags in their lower parts and overlain by HCS/SCS sandstones in their upper parts. River-dominated and mixed-process delta front deposits occur in places within stacked, coarsening-upward trends. The river-dominated delta front is characterized by parallel-laminated to current ripple-laminated intervals, and normally graded thin beds changing upward to parallel lamination and low-angle cross bedding. The mixed-process delta front also exhibits wave and bidirectional current ripples as well as discrete intervals of HCS/SCS. The preservation of the channel-base and mouth-bar deposits in the otherwise storm wave-dominated setting suggest a sheltered coastal morphology, low-frequency of

large storms during that time, together with unusually rapid subsidence and burial that may have prevented the fluvial signals from being completely reworked by the storm waves in places.

INTRODUCTION

Shelf-margin clinoforms are large-scale (hundreds of meters) accretionary units that build out from continental and shallow-marine areas to deepwater areas of the continental margin. The shallow and deep sediment facies are separated by the shelf-slope break or shelf edge. The clinoform topsets are built by repeated, regressive and transgressive transits of deltas and other shoreline systems (Steel et al., 2008). As the sediment delivery systems repeatedly reach the pre-existing shelf edge, the shelf margin accretes basinwards. Shelf-margin growth is controlled mainly by sediment flux from the continent and sometimes indirectly by sediment drift along depositional strike, rate of relative sea-level change, and basinal dispersal processes (Carvajal et al., 2009; Dixon et al., 2012b; Gong et al., 2016).

Among prograding shelf margins that grow for longer time intervals (millions to 10s of millions of years), three main types of shelf-margin architecture can be recognized based on their relative progradation and aggradation tendencies (Fig. 2.1). Any margin can also change or gradually evolve from one of these types to another, as seen on the long term development of the currently studied Orinoco shelf margin (Fig. 2.2). Type I clinoform margins have a highly aggradational to slightly progradational architecture with an overall steeply rising shelf-edge trajectory, on the time scale stated above (Fig. 2.1A). Type II margins show highly progradational with only moderate aggradational stacking patterns and a flat to very, low-angle rising shelf-edge trajectory (Fig. 2.1B).

Type III margins are extremely progradational and can have an erosional toplap relationship (incisional channels or valleys) between the topset and underlying deepwater slope component of the clinoforms. They can also be unusually aggradational on basin floor (bottomset) component of the clinoforms, and their shelf edges can exhibit a flat to slightly falling trajectory (Fig. 2.1C).

The Lower Pliocene, Orinoco shelf margin during development of the studied Moruga Formation, is an example of a Type II shelf margin, that initially exhibits a fairly, low-angle rising shelf-edge trajectory with a relatively high progradation rate (TP20-TP32; from Lower Forest Clay flooding surface up to top Gros Morne Sand in Figure 2.2). However, its then takes on an overall moderate aggradational component of growth (TP32-TP38; Top Gros Morne Sand to Top Casa Cruz Sand, Fig. 2.2). Such long-term changes of growth pattern on the accreting Orinoco Late Miocene to Pleistocene shelf margin (Fig. 2.2A) were mainly due to the imbalance between an extremely high sediment supply from the Orinoco River and high rates of subsidence on the margin itself. This resulted in up to 12000 m of Late Miocene through Pleistocene sediment deposited in the Columbus Basin (Wood, 2000), and a significant eastward migration of the paleoshelf-edge from onshore mid-southern Venezuela to its present location 150 km off the modern Orinoco (progradation rate of 16-38 km/My) (Di Croce et al., 1999; Sydow et al., 2003; Carvajal et al., 2009), despite very high subsidence rates (up to 1000 m/My; Wood, 2000) on this margin.

The objectives here are 1) to document the main facies and stratigraphic architecture of the early phase of this rapid to moderately prograding portion of the Orinoco margin during the development of the Moruga Formation, and 2) to examine

how the preserved depositional facies reflect a setting of rapid, long-term syn-depositional subsidence.

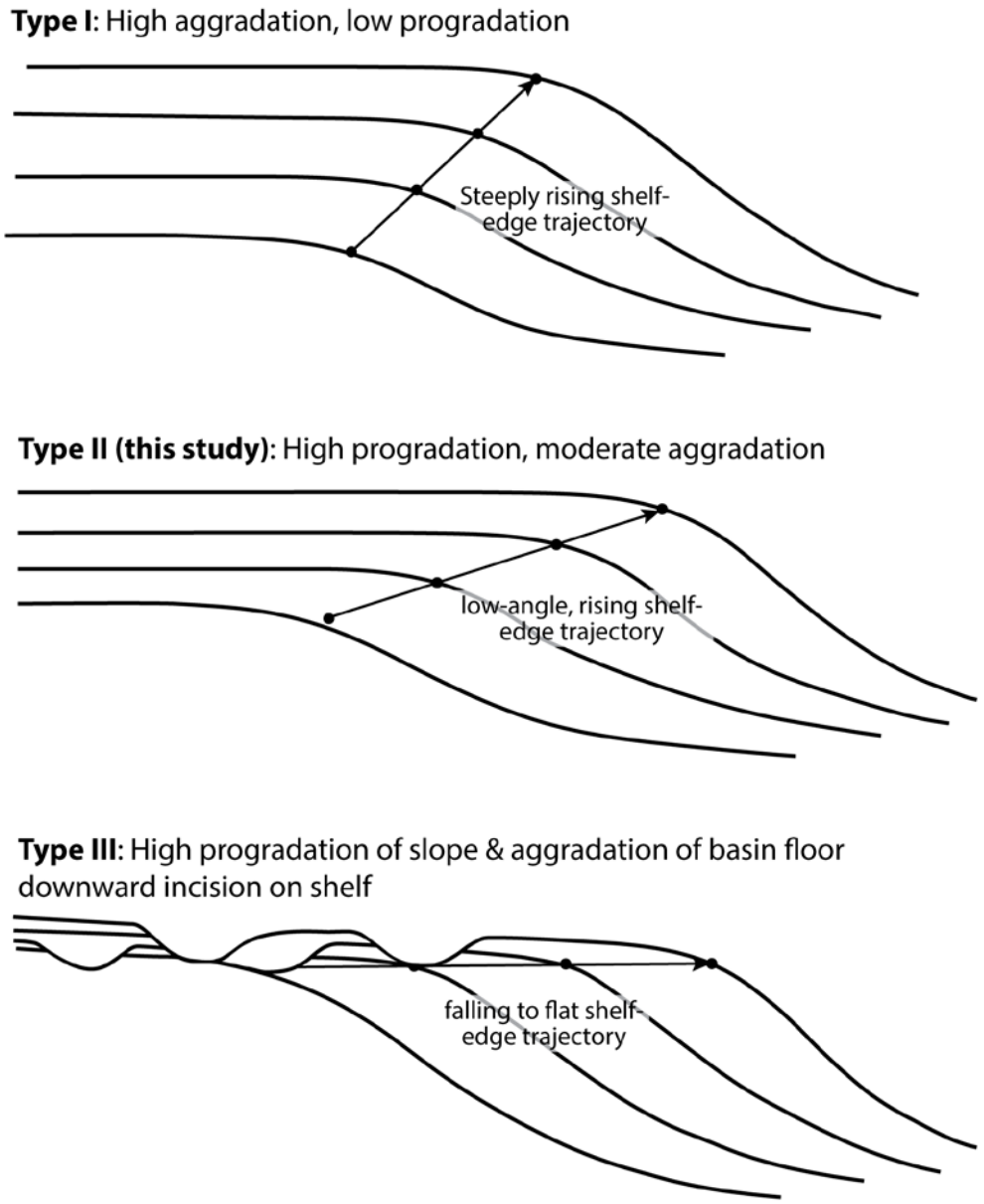

Figure 2.1: Three types of progradational shelf margin with their associated shelf-edge trajectory trends.

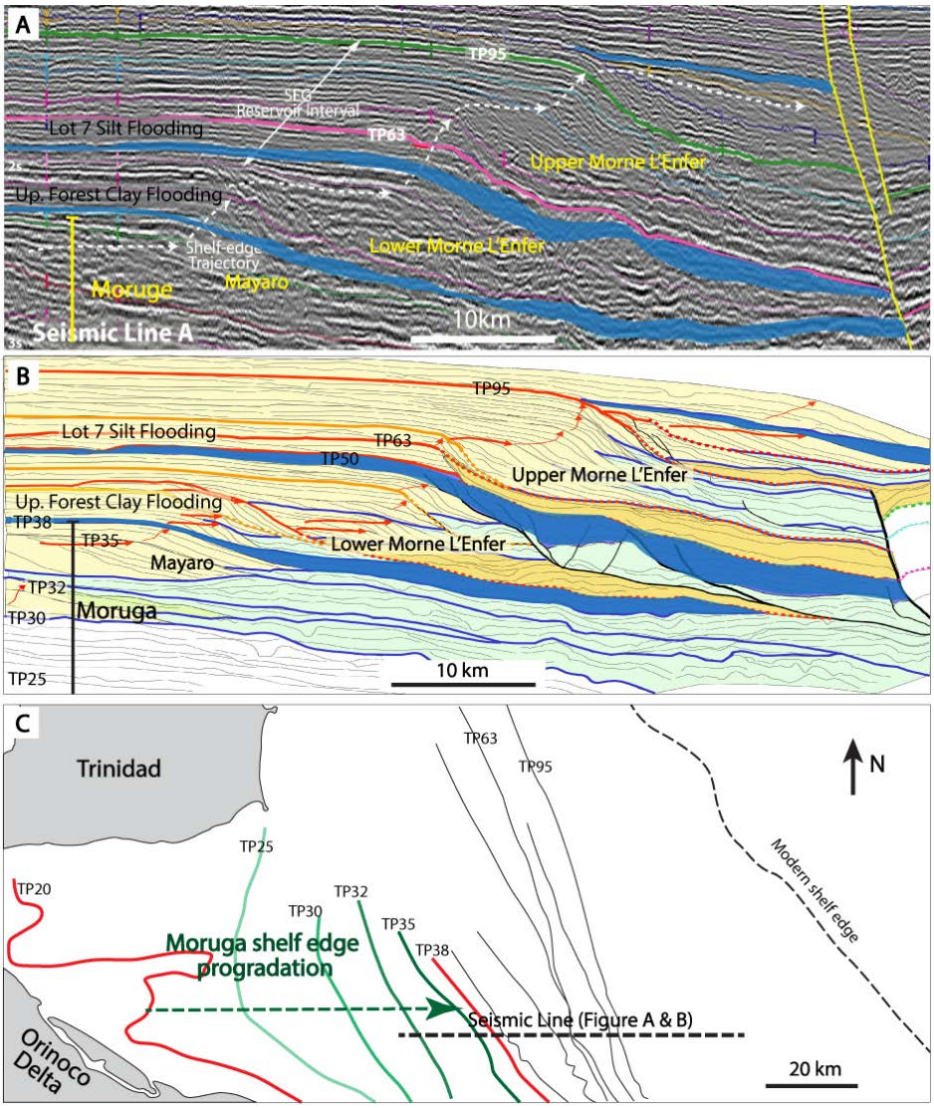

Figure 2.2: (A) and (B) Interpreted seismic data across the entire Orinoco shelf-margin prism indicates progradation and aggradation of shelf deltas into the offshore Columbus Basin (modified from Sydow et al., 2003; Dixon, 2005; Chen et al., 2018). The studied Moruga Wedge (TP20-TP38 Fig. 2.2B), bounded by Upper Forest Clay Flooding and Lower Forest Clay Flooding (not shown) surfaces, particularly the lower part displays rapid shelf-edge migration as indicated by the very low-angle, rising shelf-edge trajectory. (C) Approximate shelf-edge migration maximum of the paleo-Orinoco shelf margin during the Pliocene Moruga interval (colored lines). Note location of the seismic line in Fig. 2.2A and B, and the relatively long migration distance of the Moruga shelf edge.

GEOLOGICAL SETTING

The Late Miocene-Pliocene Orinoco shelf margin was built by rapid, mainly subsidence-generated aggradation (> 9 km in 4-5 My; Wood, 2000; Chen et al 2018) and significant basinward-stepping (>100 km in the same time interval; Dixon et al., 2005), achieved through repeated, cross-shelf transits of the Orinoco River and its large delta system. Outcrops on southern Trinidad as well as well log and seismic data (Fig. 2.2A and B) onshore and offshore in the Columbus Basin indicate that the 4-5 My stratigraphic interval is organized into four large-scale clastic wedges (three of which are shown in the seismic line of Fig. 2.2A and B) (Steel et al., 2007; Chen et al., 2018). The term 'clastic wedge', involving multiple formations, is used to denote that thick sand-prone intervals have a strongly progradational or basinward-stepping character but that they gradually split up and thin basinward into a mud-prone succession. The four main wedges are separated from each other by thick marine mudstones, representing periods of extensive (>100 km) landward flooding: (1) the Cruse wedge (late Miocene-earliest Pliocene) was the first influx of prograding Orinoco delta lobes to the southwest Trinidad area. It also reflects the initial Atlantic deepwater-margin outbuilding, and eventually displays a large collapsed (latest Miocene/earliest Pliocene) shelf edge at its eastern progradational termination on southern Trinidad outcrops (Chen et al., 2016). It also displays an early-stage, deepwater Atlantic slope succession with channel-levee systems (Vincent, 2012; Chen et al., 2016); (2) the Forest/Moruga/Mayaro clastic wedge (early-mid Pliocene and focus of this study), overlying the regionally developed marine mudstones of the Lower Forest Clay, is characterized by river- and tide-influenced deltaic deposits in its landward reaches, with the basinward equivalent wave-river dominated Moruga Formation and wave-dominated Mayaro delta lobes (Bowman, 2003; Peng et al., 2017). The Mayaro

Formation, excluded from the present study, contain a series of storm-wave dominated delta lobes within shelf-edge growth fault compartments (Figs 2.2 and 2.3) that reached basinward as far as the east coast of Trinidad (Sydow et al., 2003; Dixon, 2005; Dasgupta and Buatois, 2012; Bowman and Johnson, 2014), (3) the Lower Morne L'Enfer clastic wedge (Fig. 2.2A and B) (mid-late Pliocene), overlies the regionally developed mudstones of the Upper Forest Clay, and is characterized by river- and tide-dominated deltas and estuaries (Vincent, 2003; Osman, 2007; Chen et al., 2014), and (4) the Upper Morne L'Enfer/Palmiste wedge (Fig. 2.2A and B) (latest Pliocene-early Pleistocene) overlies the Lot 7 Silt and its regionally equivalent marine mudstones, and is characterized by river- and tide-dominated deltas and delta plain deposits (Fig. 2.2) (Chen et al., 2014).

The Moruga Formation

The studied Moruga Formation (Fig. 2.3A) lies in the middle to eastern reaches of the second major clastic wedge. In the study area, from the town of Moruga to the east coast of Trinidad, the outcropping Moruga Formation is subdivided into three subwedges (Fig. 2.3B): (1) the Gros Morne Siltstone and Gros Morne Sandstone members, (2) the St. Hilaire Siltstone and Trinity Hill Sandstone members, and (3) the Las Tablas Siltstone and Casa Cruz Sandstone members. The present study documents the upper two subwedges, a 1190 m thick succession that was built by multiple episodes of deltaic growth across the shelf with one deepwater, upper-slope segment in the St. Hilaire Siltstone Member. The lowest sub-wedge is only partly exposed and poorly accessible.

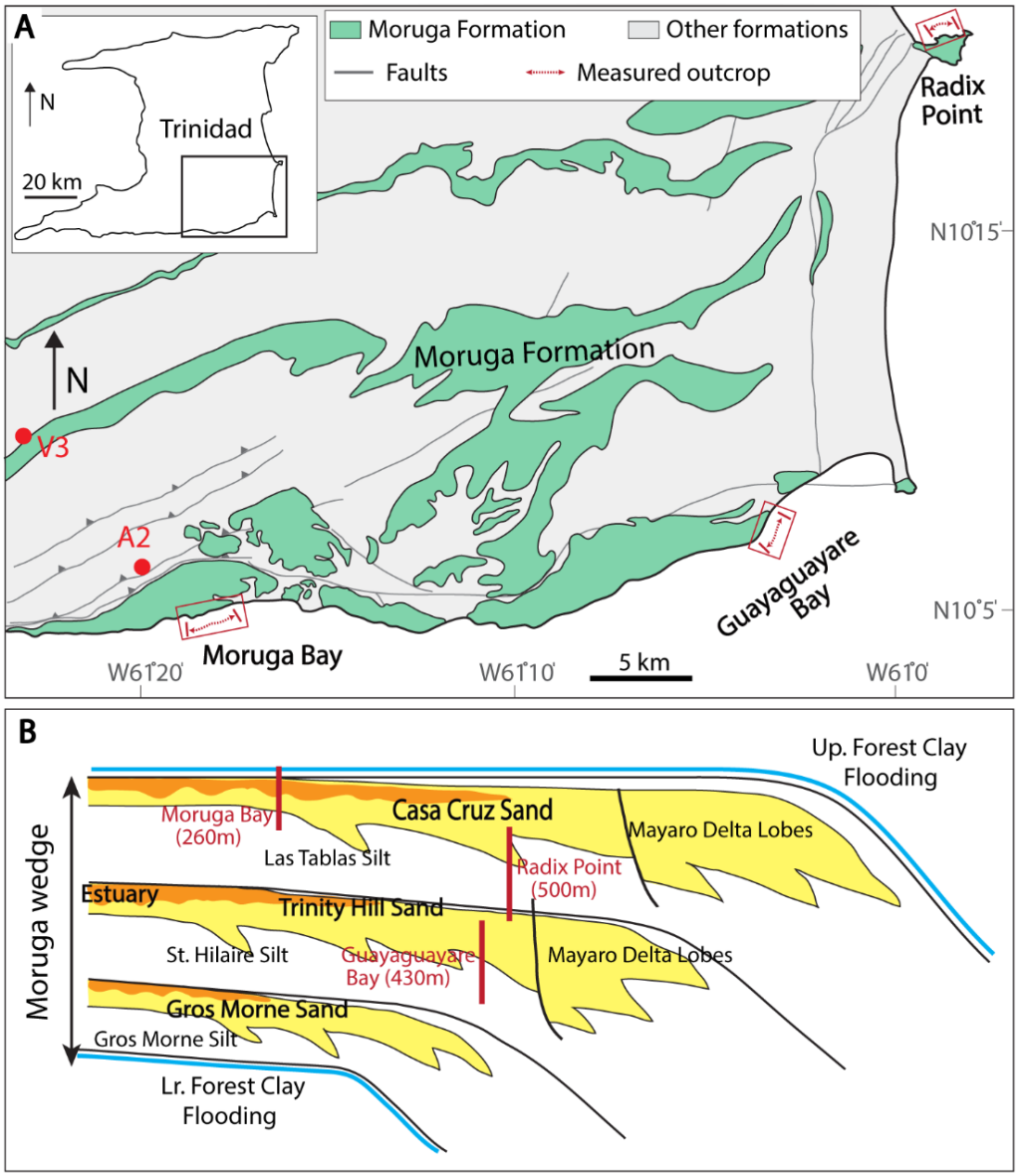

Figure 2.3: (A) Mapped distribution of the Moruga Formation on southeastern Trinidad (after Kugler, 1959) and locations of study areas with measured thickness. (B) The Pliocene Moruga Wedge stratigraphy illustrating three major deltaic growth stages (i.e., Gros Morne Sand, Trinity Hill Sand, and Casa Cruz Sand) separated by three muddy members, and the locations of measured sections on the shelf margin.

METHODOLOGY

Well-exposed outcrops within the Moruga Formation at Guayaguayare Bay, Moruga Bay, and Radix Point on south-eastern Trinidad (Fig. 2.3A) occur as documented in the Geological Map of Trinidad and Tobago (Kugler, 1959). These Moruga Formation strata were systematically measured and analyzed through a 1190 m composite stratigraphic section and with the use of photomosaics. The outcrop cliffs at Guayaguayare and Moruga Bays are oriented subparallel to the regional depositional dip. Some 140 m of the St. Hilaire Siltstone Member and 290 m of the Trinity Hill Sandstone Member (Fig. 2.3B) were measured at Guayaguayare Bay. At Radix Point, a total thickness of 500 m was measured, including the Trinity Hill Sandstone (40 m), the Las Tablas Siltstone (410m), and the Casa Cruz Sandstone (50 m) members (Fig. 2.3B). The upper Casa Cruz Sandstone Member crops out at Moruga Bay and is 260 m thick (Fig. 2.3B). Because of the progressive basinward (eastward) stepping of successive Gros Morne, Trinity Hills and Casa Cruz sandstone subwedges (Fig. 2.3B), and the variable W-E position of the measured sections (Fig. 2.3A), it is likely that the Guayaguayare and Radix Point measurement locations were outermost shelf sites, whereas the Moruga site lay farther westward. This determination was also partly guided by previous recognition of Mayaro representing a near shelf-edge location for time equivalent strata (Fig. 2.3B) (Bowman and Johnson, 2014). Although there may be minor gaps in the erected stratigraphic composite succession (Fig. 2.4), we have reasonable confidence in the resultant composite section because at each location the six component members of the Moruga Formation can be recognized.

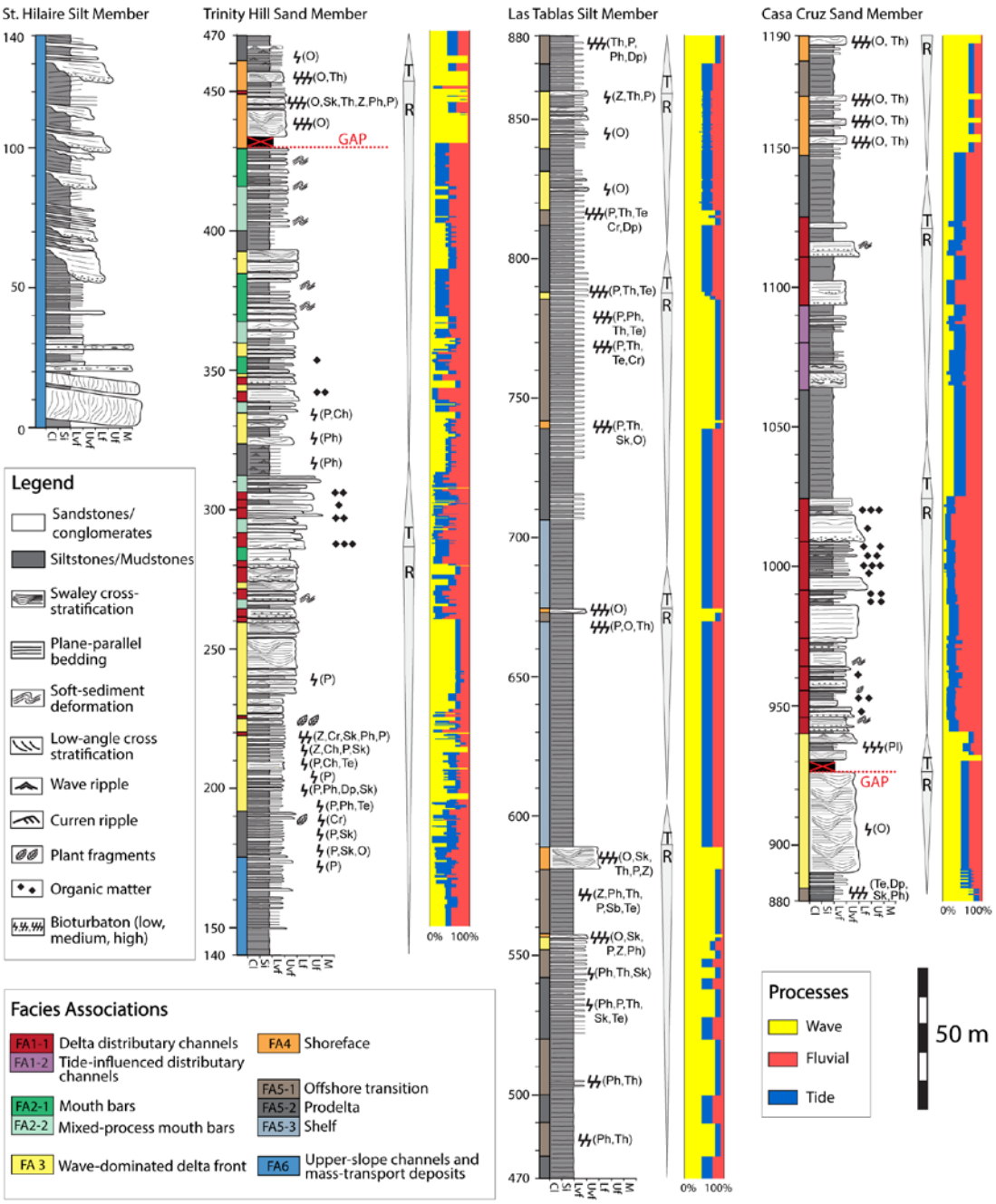

Figure 2.4: Composite sedimentary log reconstructed (facies associations and process histogram only for the shallow-water succession) for the 1190 m thick succession of the four studied members (top) of the Moruga Formation. Locations of the three stratigraphic intervals used to build the composite section are shown in Fig. 2.3B.

Facies variability was described at high resolution by recording bed thickness, grain size, sedimentary structures, organic matter/plant fragments, and trace fossils with Bioturbation Index (BI) (Taylor and Goldring, 1993). A sedimentary process histogram was generated using the field methodology of Rossi et al. (2017) whereby each measured bed or bedset was assigned three percentages, reflecting probability that it was influenced by waves, tides, or river currents, respectively.

FACIES ASSOCIATIONS AND DEPOSITIONAL ENVIRONMENTS

The studied Moruga clastic wedge (consisting of a series of shelf to deepwater clinoforms) (Fig. 2.3B) comprises six major facies associations, including five shallow-water ones (FA1-FA5) and one deep-water, uppermost-slope association (FA6) (Fig. 2.4). The facies of the outermost, growth-fault compartment of the Moruga wedge are described by Bowman and Johnson (2014), and not included here.

Facies Association 1: Channelized Sandstones

Facies Association 1 (FA1) consists of erosively based, channelized sandstones with a variety of infill types (Figs 2.5 and 2.6) that are characterized by fining-upward or blocky packages with mud rip-up clasts at their base. No bioturbation is observed. Some of these channels (Type A) commonly cap and truncate coarsening-upward successions that comprise heterolithic beds with wave ripples grading upwards to amalgamated swaley/hummocky (SCS/HCS) cross-stratified sandstones (FA3) (Fig. 2.5). The thickness of such channel fills is commonly 1 to 5 m when they occur on an outer shelf location (i.e., Trinity Hill Sand Member at Guayaguayare Bay) and 5 to 19 m when developed landwards on the mid shelf (i.e., Casa Cruz Sand Member at Moruga Bay). For the outer-shelf examples, the channel-fill deposits tend to be sandier than those on the mid shelf,

and are composed of low-angle cross-bedded to parallel-laminated sandstones (very fine to fine-grained) at the base with abundant mud clasts changing upward to heterolithic deposits including some HCS/SCS sandstones. In places, soft-sediment-deformed strata (Fig. 2.5C) occur below the channel-fill deposits. The mid-shelf channel-fill deposits consist of trough to low-angle cross bedded and parallel-laminated sandstones grading upwards to heterolithic beds with abundant organic matter. A second type of channel (Type B), generally 3 to 6 m thick on the outer shelf and 13 to 15 m thick on the mid shelf, is generally muddier than those described above and when occurring on the outer shelf also contains bidirectional cross beds, bidirectional current ripples, unidirectional cross beds, and some beds of HCS/SCS (Fig. 2.6). The mid-shelf examples of this type of channel fill comprise cross-bedded to parallel-laminated sandstones and heterolithic beds with flaser to wavy bedding and fluid-mud layers (Fig. 2.6C).

The sandier FA1 channels are interpreted as distributary channels (Zhang et al., 2017a) that supplied sediment to a storm wave-dominated delta front, because of the presence of abundant wave ripples and some hummocky cross strata, as well as their truncation down into upward-coarsening heterolithic delta-front units below. River and wave processes interacted as the driving delta distributary channels built out towards the pre-existing outer shelf area to encounter ever stronger open-ocean waves on this Atlantic margin (Porębski and Steel, 2006; Yoshida et al., 2007). The very sandy character and the presence of cross-bedded to parallel-laminated sandstones overlain by the HCS/SCS sandstones in these channels suggests that wave processes winnowed finer sediment and particularly reworked the upper part of the channel infill. The decreased depth/thickness of distributary channels from the mid shelf to the outer shelf suggest that channels became shallower basinwards (see also Olariu and Bhattacharya, 2006). The relatively

small channels (1-2 m thick) likely represent bifurcating terminal distributary channels (Olariu and Bhattacharya, 2006; Olariu et al., 2010; Li et al., 2018). By contrast, the muddier channel fills suggest an increased tidal signal (see also Zhang et al., 2016, for similar examples) and a mixed-influence of river-, wave- and tidal currents illustrated by intercalated beds of low-angle cross bedding to parallel lamination, HCS/SCS, bidirectional cross bedding, orderly unidirectional cross bedding, and bidirectional current ripples. The preservation of some channel bases in the succession may suggest a rapid subsidence and burial, probably within a coastal morphology protected from storm waves.

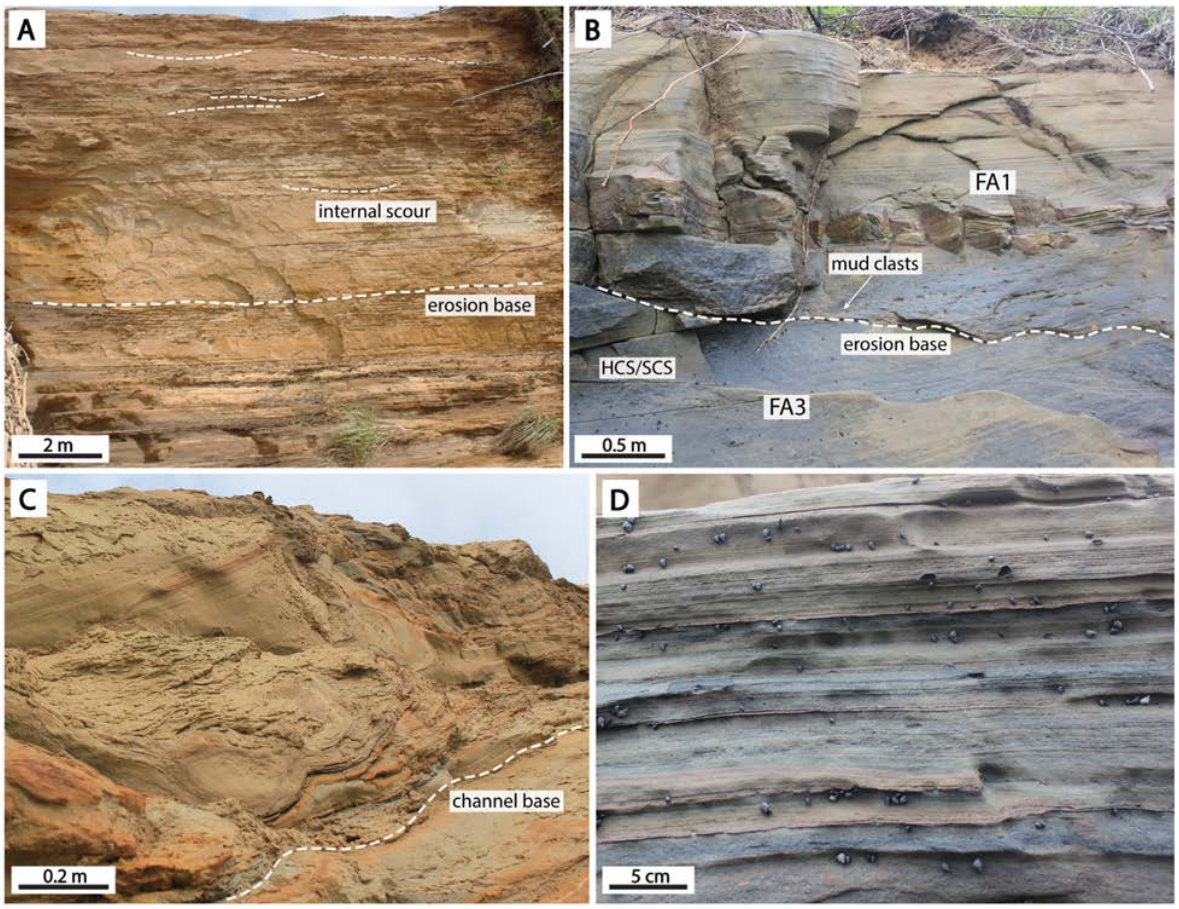

Figure 2.5: Channel-fill facies association (FA1) (Type A). (A) 6-m thick sharp-based, parallel-laminated sandstones with several internal scours. (B) Erosion-based, parallel-laminated sandstone unit with abundant mud clasts in its lower interval cutting down into the HCS/SCS sandstones of FA3. (C) 0.5 m thick deformed beds (up to 0.5 m) at the base of a large channel fill. (D) Parallel-laminated sandstones of channel fill; dark color due to organic matter.

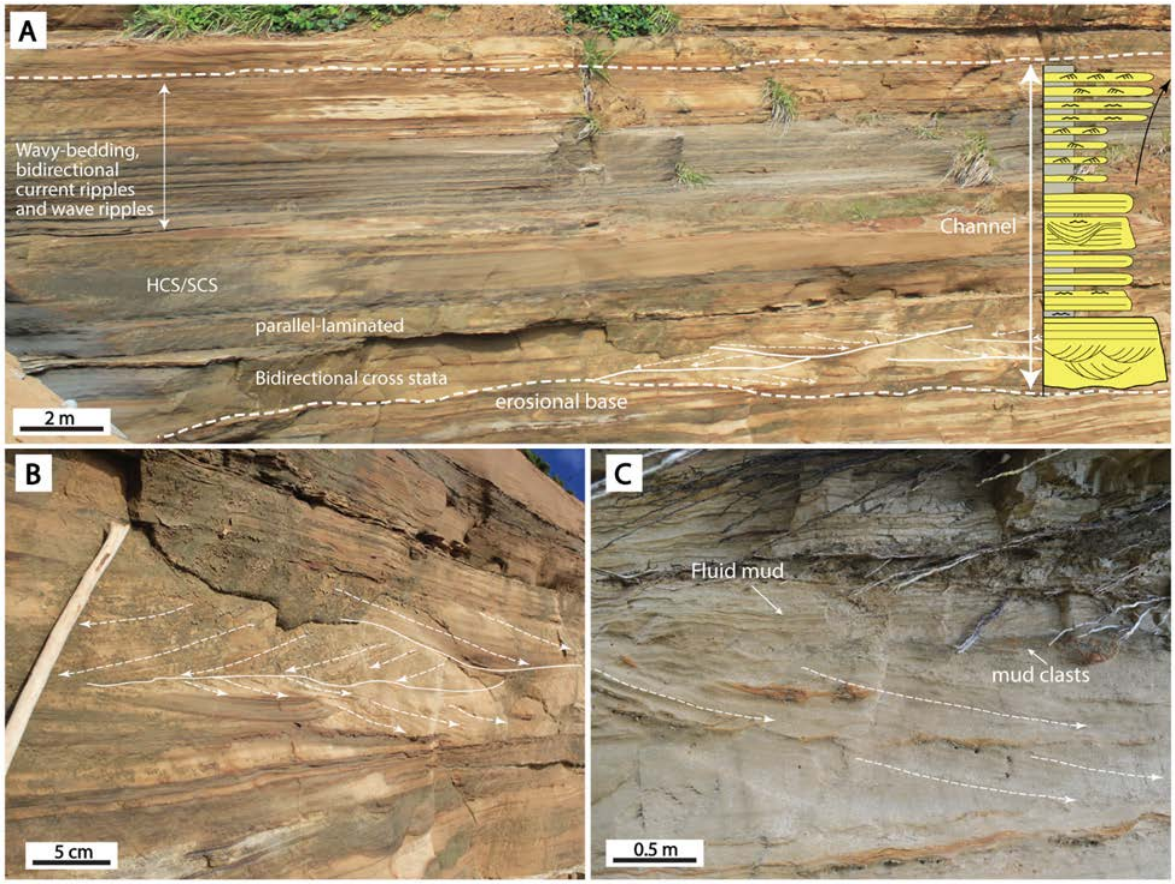

Figure 2.6: Channel-fill facies association (FA1) (Type B). (A) An erosional-based channel filled with bidirectional cross-bedded and parallel-laminated sandstones, as well as a unit of HCS/SCS sandstones. The upper part of the channel fill consists of coarsening-upward mixed-influenced thin-bedded strata with bidirectional current ripples and wave ripples. (B) Bidirectional cross-bedded sandstones at the base of channel fill. (C) Unidirectional cross-bedded sandstones and overlying interbedded sandstones and fluid-mud layers (wavy bedding) with mud clasts.

Facies Association 2: River-Dominated and Mixed-Process Delta Front

Facies Association 2 (FA2) comprises river-dominated delta front (FA2-1) (Fig. 2.7) and mixed-process delta front (FA2-2) (Fig. 2.8) that are characterized by stacked, sandier-upward and coarsening-upward successions (3-17m thick). Both FA2-1 and FA2-

2 show thin, interbedded very fine-grained sandstones and siltstones/mudstones in their lower part changing upwards to thick and amalgamated sandstone beds. Soft-sediment-deformed beds occur in places (Figs 2.7B and 2.8B). No bioturbation is observed. However, FA2-1 and FA2-2 display some difference in both lower and upper parts. The sandstone beds in the lower part of FA2-1 commonly have parallel- to current-rippled lamination (Fig. 2.7C) and include thin, normally graded beds (Fig. 2.7D) with abundant plant debris/organic matter. The sandstones in the upper part are parallel-laminated and low-angle cross bedded with relatively thick structureless sandstones (Fig. 2.7). In contrast, the thin sandstone layers in the lower parts of the FA2-2 show bidirectional current ripple-laminated (Fig. 2.8D) and wave ripple-laminated sandstones. The upper portion of FA2-2 exhibits HCS/SCS sandstone beds sharply overlying parallel-laminated sandstones (Fig. 2.8A and C).

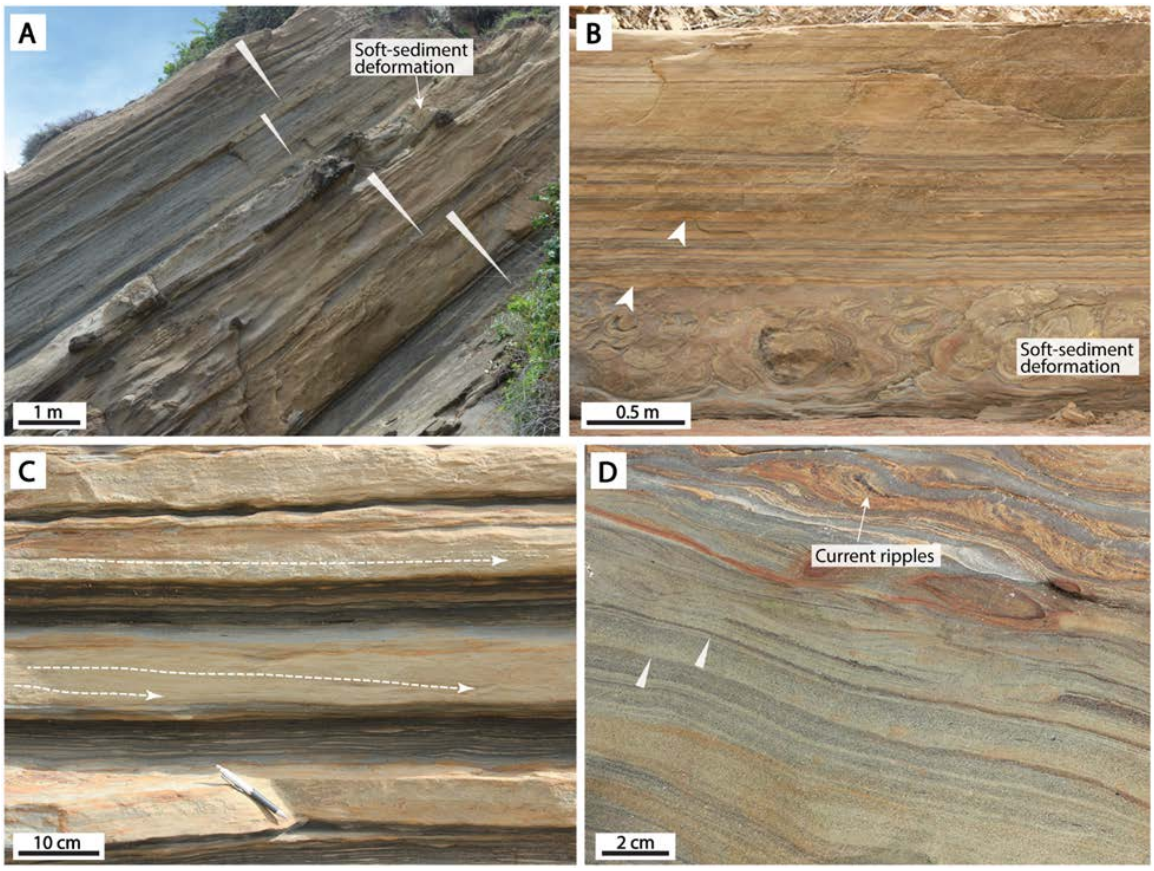

Figure 2.7: River-dominated delta front facies association (FA2-1). (A) Several stacked, coarsening-upward successions consisting of heterolithic beds grading upwards to parallel-laminated sandstones. (B) A coarsening-upward interval with soft-sediment-deformed bed on bottom. Note that the centimeters thick structureless sandstone beds (possible hyperpycnal flow beds) marked by white arrows. (C) Thin sandstone beds characterized by very low-angle cross-stratification or parallel lamination to unidirectional current ripples. (D) Normally graded sandstone beds rich in organic matter (possible hyperpycnites from river flooding) and unidirectional current ripples.

The coarsening- and thickening-upward successions are interpreted as distal, river-dominated delta front (FA2-1) (Olariu and Bhattacharya, 2006; Ahmed et al., 2014) and mix-process delta front (FA2-2) deposits (Ainsworth et al., 2016) because of their vertical bed arrangement and because they are sometimes truncated by distributary

channels. The soft-sediment-deformed beds are slumped deposits caused by rapid sediment loading and oversteepening on delta front (see also Steel et al., 2008). The abundant organic matter and plant debris together with lack of ichnofauna are consistent with the interpretation of a delta front that was directly fed by distributary channels. The parallel- to current-rippled sandstone intervals (Fig. 2.7C) and normally graded sandstone beds (Fig. 2.7D) in the lower FA2-1 are interpreted as river-fed turbidites that were deposited on the distal delta front (Ahmed et al., 2014). The thin sandstone beds with bidirectional current ripples and wave ripples in the lower portions of FA2-2 indicate reworking of some deposits in the distal delta front by tidal currents and storm waves. The upper and thicker sandstone intervals with HCS/SCS sandstone beds in FA2-2 suggest that the upper/proximal part of the distal delta front were reworked by storm waves intermittently. The preservation of the river-fed turbidite beds in distal delta front is probably due to rapid accumulation and to a sheltered coastal morphology that dampened the storm waves or lack of large storm waves during that time. Alternatively, storm waves tended to rework the upper and proximal delta front during lobe abandonment as fluvial discharge decreased or during subsequent transgression as water depth increased.

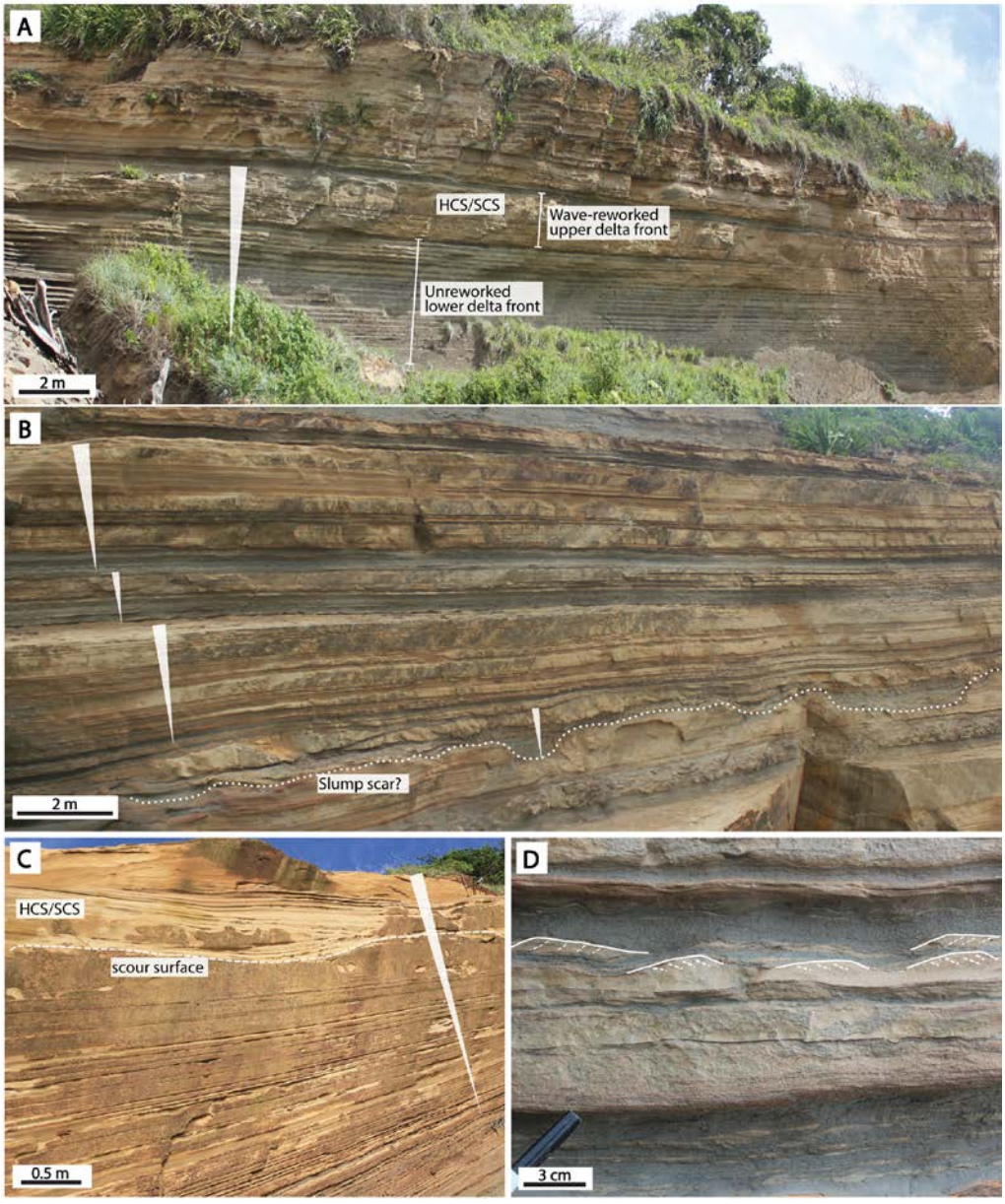

Figure 2.8: Mixed-process delta front facies association (FA2-2). (A) A coarsening-and thickening-upward succession in the delta front showing lateral wedging to the right with the unreworked lower part and wave-reworked upper part. (B) Several stacked, upward-thickening, mixed-process delta-front deposits. (C) A coarsening-upward succession with HCS/SCS sandstones in its upper part, indicating wave reworking. (D) Parallel-laminated sandstone bed overlain by bidirectional current-rippled sandstones.

Facies Association 3: Wave-dominated Delta Front

Facies Association 3 (FA3) is characterized by the stacking of multiple coarsening- and thickening–upward successions (5-30 m thick) (Fig. 2.9A) that are marine bioturbated and generally thicker than the delta front of FA2. The successions are entirely dominated by alternating thin beds of HCS sandstones (0.1-0.5 m thick) and muddy intervals (0.1-0.7 m thick) grading upwards to thick, amalgamated SCS sandstones (Fig. 2.9B and C). In places, fining-upward units (0.2-0.3 m thick) occur with sharp-based SCS sandstones changing upwards to wave-rippled sandstones, interbedded mudstones and wave-rippled sandstones capped by mudstones (Fig. 2.9D). Overall, bioturbation is rare (BI = 0 to 1) with the occurrence of *Ophiomorpha* (O), *Skolithos* (Sk), *Phycosiphon* (Ph), and *Planolites* (P).

FA3 is interpreted as wave-dominated delta-front deposits derived from a complete reworking of river mouth bars and delta front. The HCS and SCS were formed by oscillatory storm waves (Southard et al., 1990; Dumas et al., 2005) between storm wave base and fair-weather wave base with HCS occurring stratigraphically below SCS in the upward-coarsening shallow-marine succession (Leckie and Walker, 1982; Dumas and Arnott, 2006). The mudstone intervals with wave-rippled sandstones represent deposits developed under fair-weather or waning storm wave condition (Dumas and Arnott, 2006; Bowman and Johnson, 2014). The fining-upward facies succession of sharp-based SCS, wave ripples, mudstones with wave-ripples lenses, and ultimately to mudstones records an idealized storm bed developed during rising and waning stages of a storm event (Cheel, 1991; Peng et al., 2017). The low diversity and low abundance of trace fossils suggest ichnologically stressed environments influenced by nearby river mouths (MacEachern et al., 2005; Gani et al., 2007).

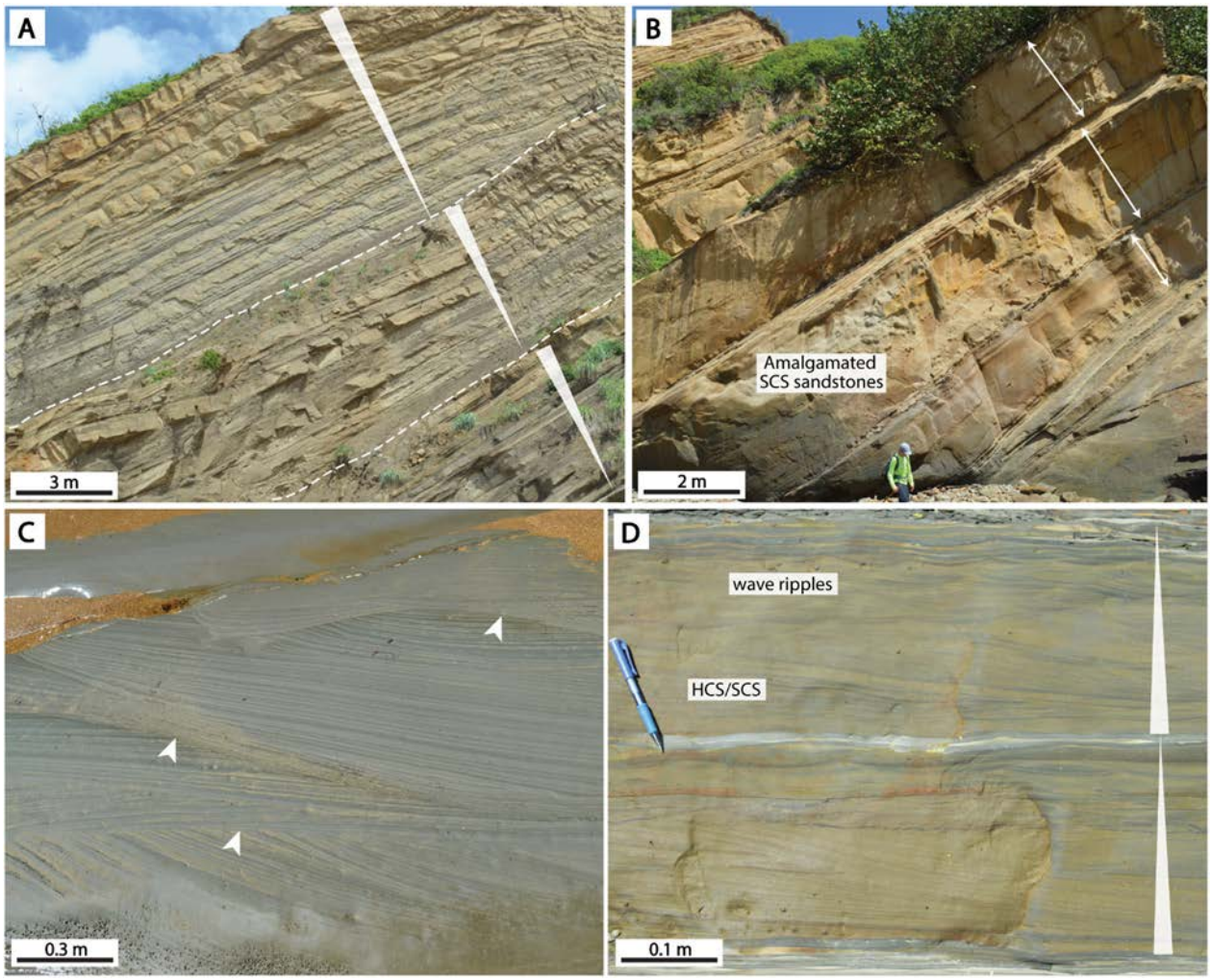

Figure 2.9: Wave-dominated delta-front facies association (FA3). (A) Repeated upward-coarsening and upward-thickening successions. (B) Stacked units of thick, amalgamated swaley cross-stratified sandstones (2-3 m) separated by thin muddy beds in the proximal wave-dominated delta front. (C) Amalgamated SCS sandstones illustrating scours surfaces (white arrows) and the internal undulating cross laminations. (D) Two fining-upward successions demonstrate erosional based SCS sandstones changing upwards to wave rippled sandstone capped by muddy intervals with some wave ripple lenses.

Facies Association 4: Shoreface

Facies Association 4 (FA4), similar to FA3, comprises coarsening-upward successions of thin sandstone beds interbedded with muddy intervals changing upwards into amalgamated SCS/ HCS to low-angle cross-bedded sandstones, but it is more sand-rich and intensely bioturbated (Fig. 2.10). The thin beds (up to 0.5 m thick) of sandstones are lower very fine-grained with non-amalgamated HCS sandstones and wave ripples in lower succession (Fig. 2.10D). In the upper succession, amalgamated HCS/SCS sandstones are up to 10 meters thick. The heterolithic intervals in the lower part and the entire upper part of FA4 exhibit high-diversity and high-abundance trace-fossil suite (BI = 3-6) including *Ophiomorpha* (O), *Thalassinoides* (Th), *Skolithos* (Sk), *Teichichnus* (Te), *Planolites* (P), *Chondrites* (Ch), *Phycosiphon* (Ph), *Fugichnia* (Fu), *Rosselia* (Ro), *Macaronichnus* (Ma), and *Diplocraterion* (D) (Fig. 2.10).

FA4 is interpreted as shoreface deposits (Hampson and Howell, 2005; Hampson et al., 2011). The interbedded mudstone/siltstone and HCS to wave-rippled sandstones in the lower succession represent distal shoreface, and the amalgamated SCS/HCS sandstones in the upper succession represent the proximal shoreface. The mudstones/siltstones were formed under fair-weather wave conditions and wave-rippled sandstones were deposited during waning storm waves. The lower amount of mud together with the intense bioturbation suggest FA 5 is non-deltaic shoreface that was less influenced by fresh-water river currents.

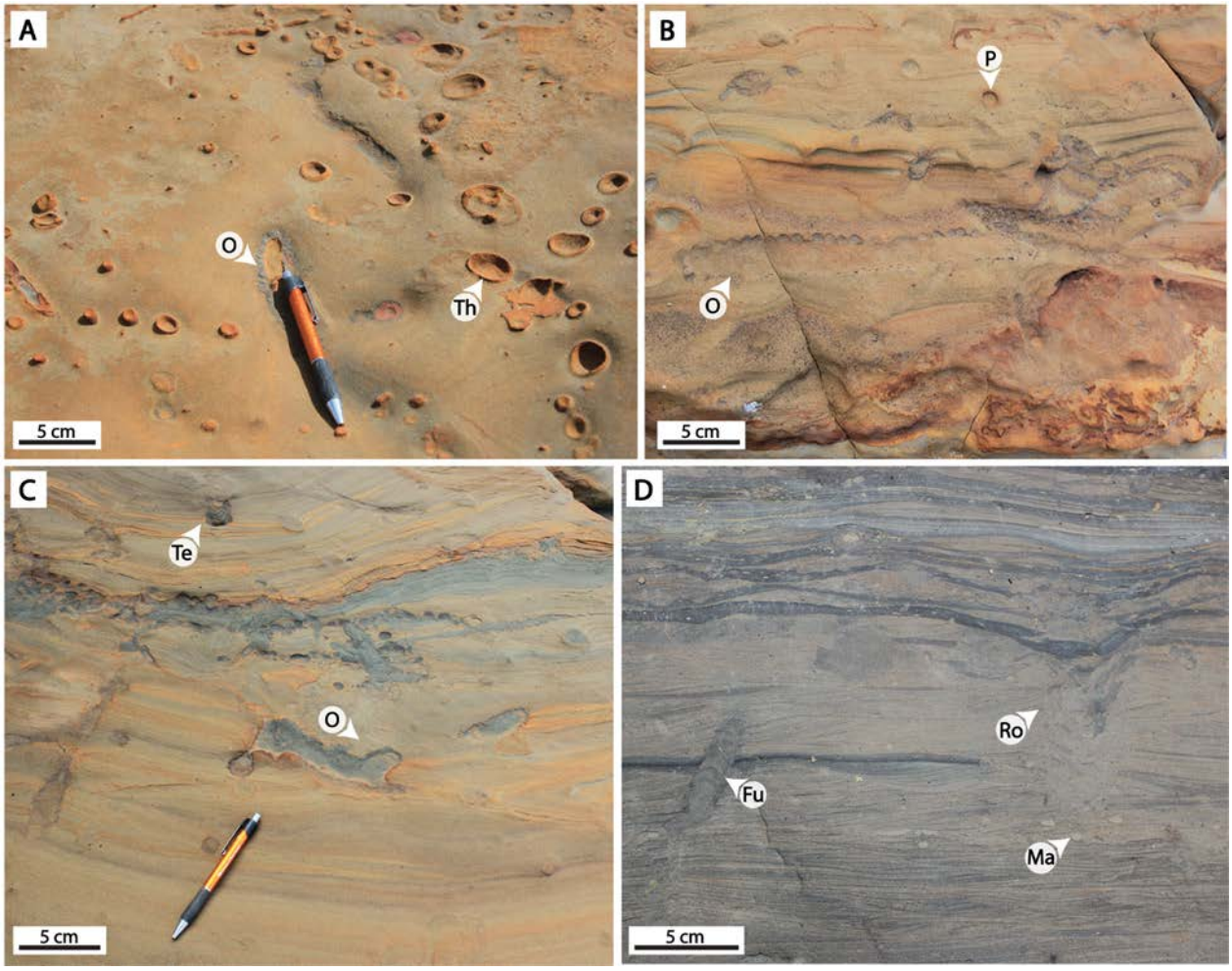

Figure 2.10: Shoreface facies association (FA4). (A-C) Well-developed trace fossils of *Ophiomorpha* (O) (pelleted walls), *Thalassinoides* (Th) (smooth-walled), *Teichichnus* (Te), and *Planolites* (P) in the thick, amalgamated SCS/HCS sandstones of proximal shoreface. (D) Distal shoreface showing thin beds of wave-rippled sandstones and the heterolithic intervals with bioturbation of *Fugichnia* (Fu), *Rosselia* (Ro), and *Macaronichnus* (Ma).

Facies Association 5: Prodelta, Offshore Transition, and Shelf

Facies Association 5 (FA5) comprises the muddy associations. FA5-1 is characterized by laminated mudstone/siltstone beds with thin, lower very fine-grained sandstones with wave ripples. Muddy, normally graded beds occur in places and are characterized by rippled sandstones grading upwards to siltstones (up to 5 cm thick) (Fig. 2.11A and B). Rare to no bioturbation is observed. FA5-2 comprises siltstones/mudstones with very thin HCS and wave-rippled sandstone beds (few centimeters). FA5-3 contains structureless to faintly laminated siltstones/mudstones with lenticular sandstones (Fig. 2.12 C and D). The siltstones/mudstones in both FA5-2 and FA5-3 are moderately to intensely bioturbated (BI=3-5) (Fig. 2.12).

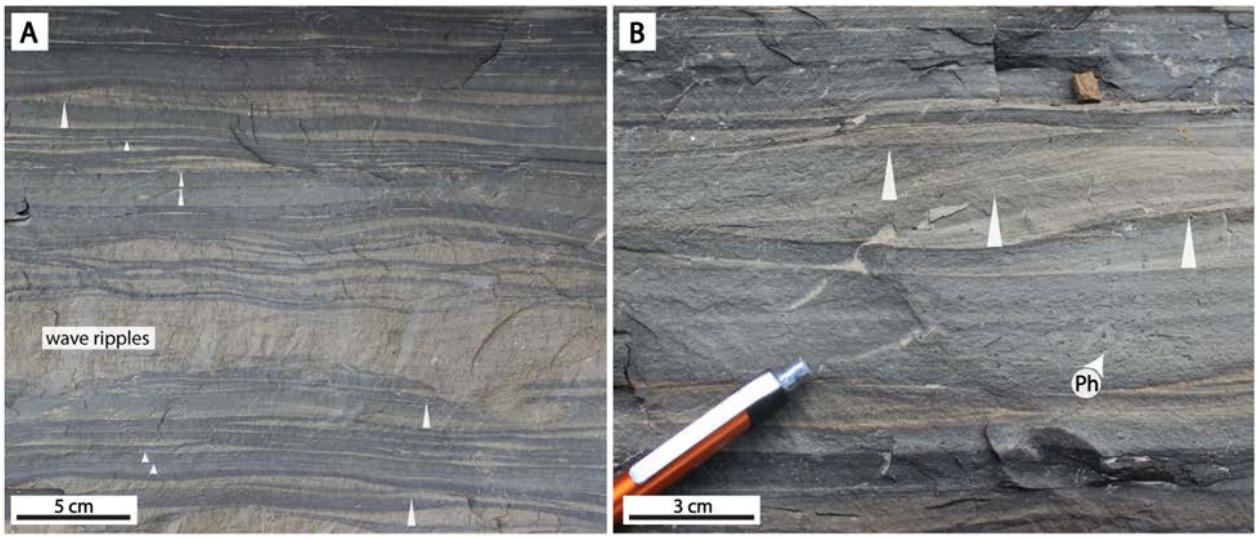

Figure 2.11: Prodelta facies association (FA5-1). (A) Thin, normally graded beds showing lower very fine-grained sandstones gradually or sharply overlain by siltstones. Note that they are associated with wave ripples. (B) Close-up view of the muddy, normally graded beds with sharp wave-scoured bases and rare bioturbation of *Phycosiphon* (Ph).

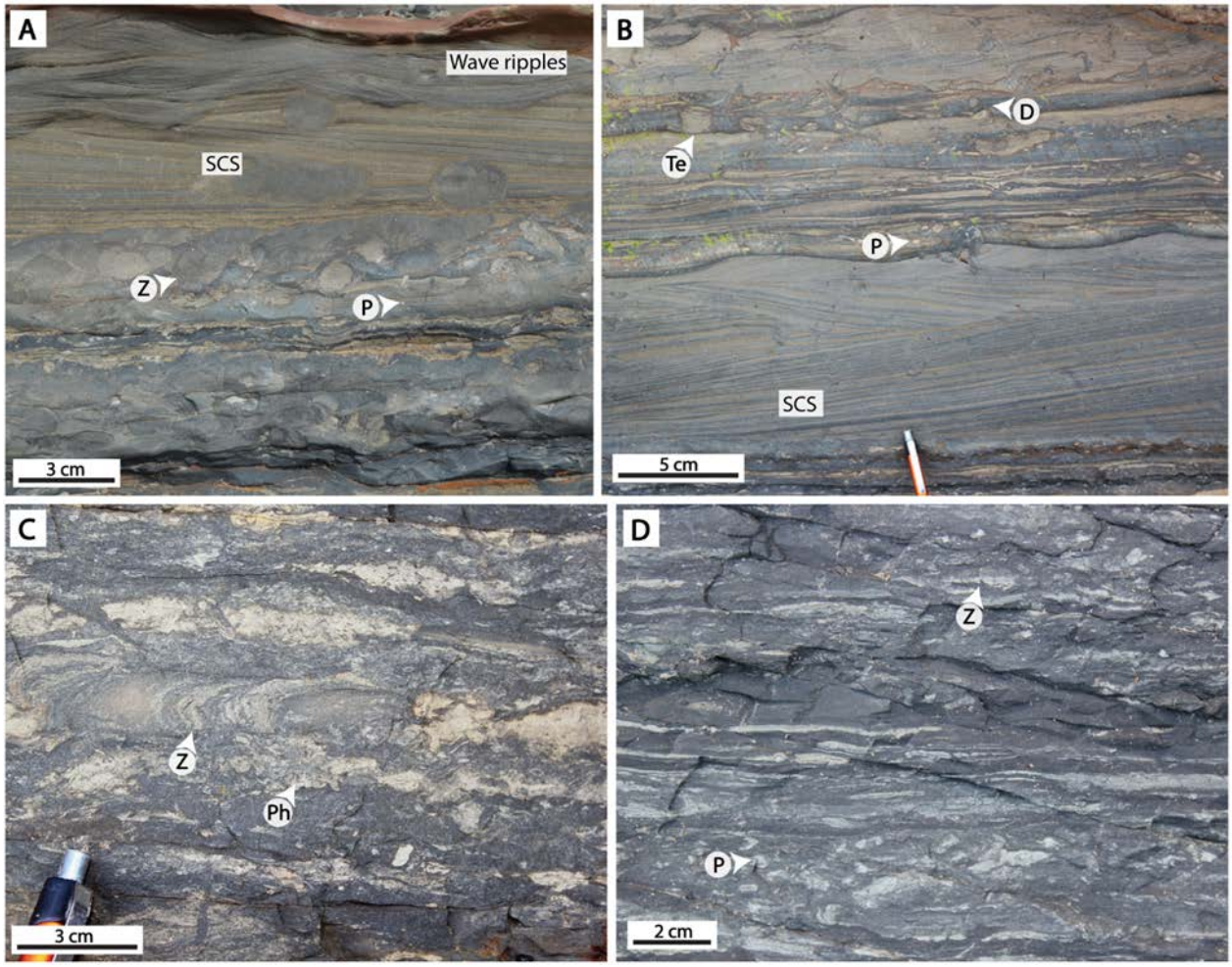

Figure 2.12: Offshore transition (FA5-2) and offshore shelf (FA5-3) facies association. (A) Thoroughly bioturbated (BI=5-6) siltstones/mudstones showing *Zoophycos* (Z), *Planolites* (P) and the overlying SCS to wave ripples. (B) The interbedded siltstones and wave-rippled sandstones were highly bioturbated with *Teichichnus* (Te), *Planolites* (P), and *Diplocraterion* (D.) (C) and (D) Structureless to faintly laminated siltstones/mudstones showing *Phycosiphon* (Ph), *Zoophycos* (Z), *Planolites* (P).

The muddy facies association is interpreted as prodelta (FA5-1), offshore transition (FA5-2), and shelf (FA5-3) (see also Hampson et al., 2011) deposits, respectively. The dominant finer-grained character of the sediment suggests a low-energy

setting. The thin sandstone beds with HCS or wave ripples in FA5-1 and FA5-2 indicate that the sea bottom was occasionally affected by storm waves above/near storm wave base. The interbedded siltstones/mudstones were deposited under fairweather condition. The muddy, normally graded beds are interpreted to represent products of wave-enhanced sediment-gravity flows (Macquaker et al., 2010; Plint, 2014) because they are commonly associated with wave ripples. The predominant siltstones/mudstones of FA5-3 represent deposition below the mean storm wave base. Rare bioturbation in the prodelta deposits suggest a stress condition due to close proximity of river sediment source, while the moderate to intense bioturbation in siltstones/mudstones in offshore transition to offshore shelf suggest a lack of river influence (MacEachern et al., 2005).

Facies Association 6: Upper-slope Channels and Mass-transport Deposits

Facies Association 6 (FA6) is characterized by a mudstone-dominated succession with various types of sediment gravity flow deposits, including rotated blocks of SCS/HCS sandstones (up to 10 m diameter), chaotic and poorly sorted blocks (up to 1 m diameter) and clasts (centimeters diameter) (Fig. 2.13A and D), convoluted heterolithic deposits (decimeter up to 1 m thick) (Fig. 2.13B), displaced and rotated blocks (5 to 10 m thick) (Fig. 2.13C), thick to thin normally graded sandstones (decimeter up to 2 m thick) (Fig. 2.13A and E). The displaced and disoriented/rotated blocks of heterolithic deposits have highly irregular bases, and are overlain by mudstones/siltstones, normally graded sandstones, and poorly sorted clasts with alternated convoluted beds (Fig. 2.13C). The disoriented heterolithic blocks show their internal strata dipping more steeply than the overlying and underlying strata towards the west (i.e., paleo-landward direction). No

bioturbation is observed except for *Ophiomorpha* in the displaced SCS/HCS sandstone. This association is described in detail in Chapter 3 in this dissertation.

FA6 is interpreted as deepwater channels (or gullies) and mass-transported deposits on the outermost shelf to upper slope (Peng et al., 2017). The disoriented SCS/HCS sandstone blocks represent mass-transport deposits that had collapsed from the storm wave-dominated delta front (FA 3) on the outer shelf to shelf edge. The displaced and rotated blocks of steeply dipping, heterolithic strata are interpreted to represent blocks that collapsed and slid out from the shelf edge or upper slope, and back-tilted towards the shelf (Peng et al., 2017). The beds of poorly sorted blocks and clasts are debrites formed by cohesive debris flows (Talling et al., 2012b), also likely derived from collapsed deposits at the shelf edge. The normally graded sandstones are deposits of turbidity currents. The highly irregular basal surfaces of the channels are more likely slump scars that attracted subsequently infilling of sediment gravity flows (i.e., debrites, turbidites, soft-sediment deformed deposits) (Peng et al., 2017).

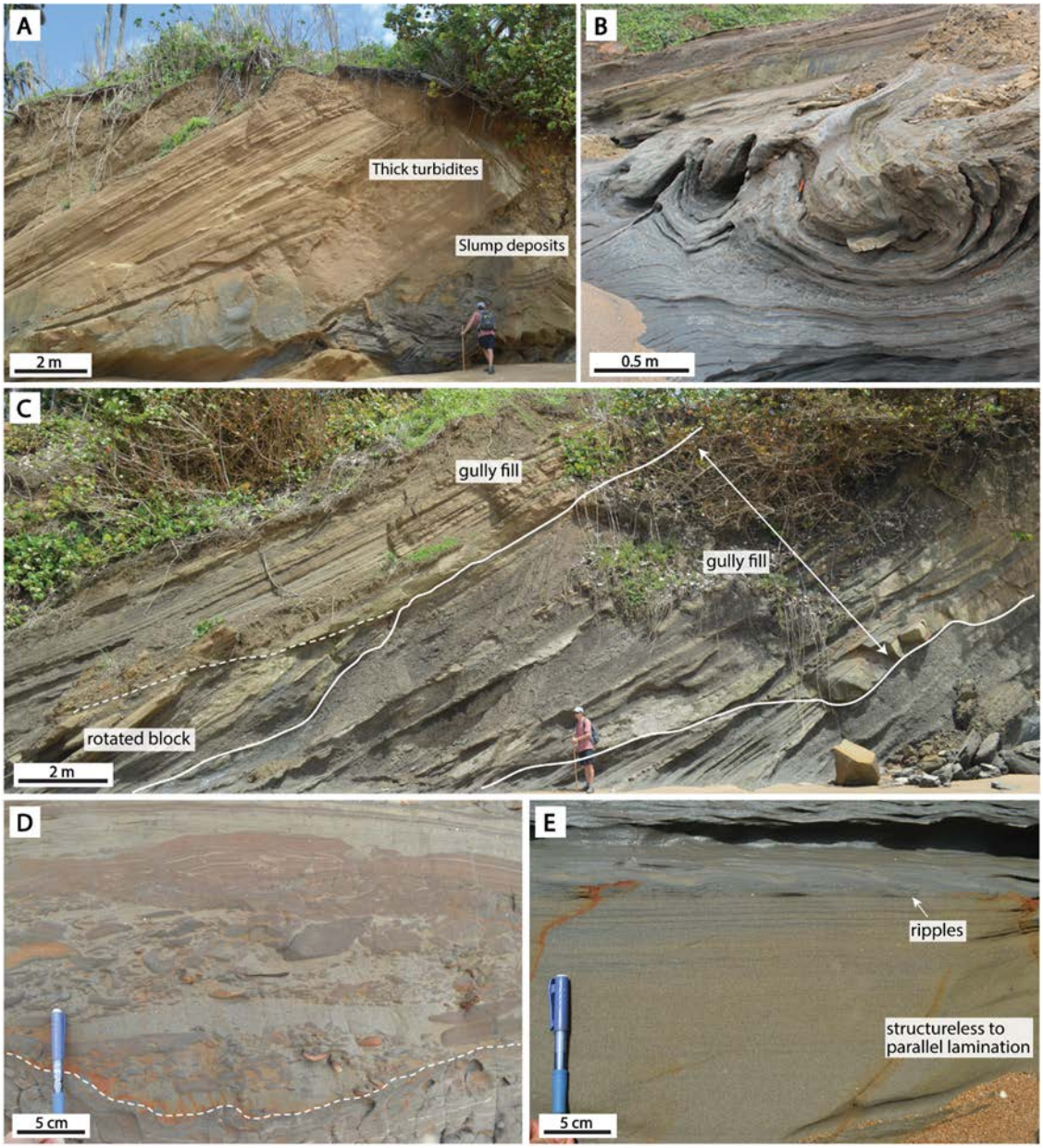

Figure 2.13: Upper-slope channel and mass-transport facies association (FA6). (A) Thick turbidites overlying the mass-transport deposits. (B) 1 m thick convoluted heterolithic bed. (C) Two muddy channel infills with the upper one containing a disoriented and rotated block at the base. (D) Debris-flow deposits comprising poorly sorted siltstone clasts in the sandy matrix. (E) Turbidites illustrating a normally graded bed with structureless to parallel lamination grading upwards to ripple lamination.

FACIES ARCHITECTURE AND PROCESS REGIME CHANGES

The studied succession displays three depositional successions (i.e., Gros Morne, St. Hilarie-Trinity Hill and Las Tablas-Casa Cruz subwedges) that are up to 250-300 m thick on the mid-shelf reaches near Moruga, and up to 500-600 m thick on the outer shelf reaches at Guayaguayare and Radix Point (Figs 2.2B and 2.14). The three sequences are bounded by flooding surfaces below the Gros Morne Siltstone, St. Hilaire Siltstone and Las Tablas Siltstone and are contained by major transgressive intervals, namely the Lower and Upper Forest Clay units (Fig. 2.14).

The regressive cycles commonly show a coarsening- and thickening-upward succession of delta front/shoreface with the delta front commonly truncated by channels (Figs 2.4 and 2.14). Most of the delta front is storm wave-dominated and is composed of sandstones with HCS/SCS and wave ripples on the outer shelf (Fig. 2.14). However, some river-fed turbidites in the river-dominated and mixed-process delta front were preserved on the mid-outer shelf (Fig. 2.14). The channels are generally very sandy with the preserved channel bases (cross-bedded to parallel-laminated sandstones with mud clasts lag) but show a wave-reworked upper channel infill (HCS/SCS sandstones) with mud winnowed away during the reworking processes. The transgressive cycles show fining-upward succession of mixed-process channels with increased tidal signals (fluid mud, bidirectional current ripples, mud drapes) and thick capping marine mudstones (Figs 2.4 and 2.14).

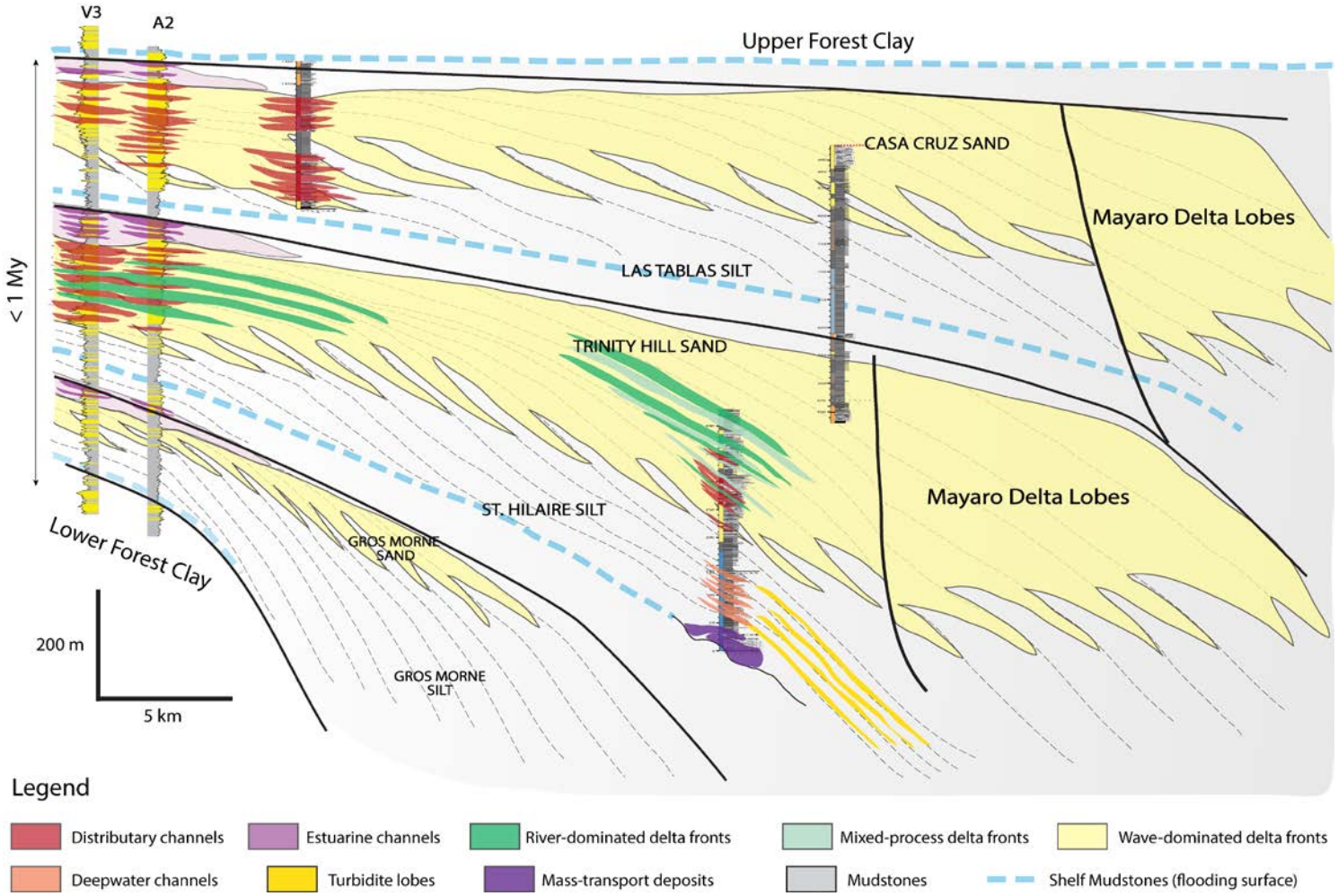

Figure 2.14: Stratigraphic framework based on measured sections and well logs. See text for details.

From the process histogram (Fig. 2.4), the regressive packages are dominated by increasing wave processes upwards with some minor river influence (Pw= 45%-55%; Pf= 25%-40%) in the lower parts (e.g., 180-260 m in Fig. 2.4), and then abruptly changed to fluvial dominance with some tidal influence (Pf= 48-50%; Pw= 23-25%) (e.g., 260-300 m in Fig. 2.4). During the transgressive packages, tidal processes clearly increased (Pt= 27-32%; Pw= 20-45%).

COMMENTS ON THE OVERALL LOW-ANGLE TRAJECTORY OF THE STRONGLY PROGRADATIONAL, EARLY MORUGA SHORELINE

The Pliocene Moruga clastic wedge, consisting of several shelf-margin clinoform sets (TP20-TP38), shows a relatively rapid migration of the shelf edge and slope basinwards during the overall margin growth from the seismic data (Fig. 2.2) (Dixon, 2005; Chen et al., 2018). The aggradational component of growth indicates a rising of relative sea level caused partly by high subsidence rate of the shelf margin (Sydow et al., 2003). This extraordinary subsidence rate is likely to have made it difficult to preserve evidence of eustatic sea-level fall even during the Pliocene icehouse period when eustatic sea level repeatedly fell by 60-80 m during intervals up to 100 ky (Sømme et al., 2009). The highly subsiding margin would have caused an overall rise of sea level. However, the low-angle trajectory of the progradational, Moruga shelf edge (Fig. 2.2) suggests that the very high sediment supply of the Orinoco counteracted and generally exceeded the relative sea-level rise, so that the deltas were capable of stepping forward and prograding to the shelf edge (Fig. 2.14) to accrete the shelf margin (Sydow et al., 2003; Zhang et al., 2017b). The very sand-rich character, especially of the Gros Morne and the Trinity Hill Sandstones, suggest high sediment supply and strong wave reworking. The unusual preservation of the lower parts of many ‘outer-shelf’ channels, despite generally strong

wave reworking, as well as stacked river-dominated or mixed-process delta front deposits in the Trinity Hill Sandstone testify to a high subsidence and sediment burial rate, and a protective coastal morphology, in order to get this degree of preservation of the fluvial supply signals despite the aggressive destruction of the delta front by the Early Atlantic, open coast storm waves. The more aggradational growth of the shelf margin and the higher-angle of the rising shelf-edge trajectory during the late development of the Moruga Formation strongly indicates that more sediments were stored on the shelf to form aggradational topsets.

CONCLUSIONS

The Early-mid Pliocene Orinoco shelf margin (Moruga Formation, Trinidad) exhibits a fairly, flat to low-angle rising shelf-edge trajectory with a relatively high progradation rate, but subsequently changes to moderate aggradational growth. The high progradation rate during the early development of the Moruga wedge was caused by extremely high sediment supply outpacing the relatively sea-level rise. During the late-stage development of the Moruga Formation, the shelf margin probably subsided more dramatically and shows an aggradational growth with increased storage of sediment on the shelf.

The studied outcrops of the Moruga Formation, particularly the accessible upper St. Hilaire-Trinity Hill and Las Tablas-Casa Cruz subwedges, provide insights to the facies and stratigraphic architecture of this rapid to moderately prograding portion of the Orinoco margin. As the highly supplied St. Hilaire-Trinity Hills deltas reached the shelf margin, the open-marine storm wave reworked but allowed and maintained strongly progradational sediment accumulation at the shelf edge, leading to periodic instability

shelf margin. The storm wave-dominated shelf-edge deltas collapsed at times, and formed a series of small upper-slope channels that attracted subsequent infilling by sediment gravity flows. During the later phase of aggradational growth of the shelf margin (i.e., Upper Trinity Hill, Las Tablas, and Casa Cruz members), thick coarsening-upward successions of storm wave-dominated delta fronts/shorefaces/mouth bars and overlying fluvial and mixed-influenced channels developed at the outer shelf. The presence of unreworked river- or mixed-process delta fronts and some preserved lower parts of channel fills suggest rapid burial with the help of a sheltered coastal morphology despite strong wave reworking on the open Atlantic coast.

Chapter 3: Transition from storm wave-dominated outer shelf to gullied upper slope: The mid-Pliocene Orinoco shelf margin, South Trinidad[1]

ABSTRACT

Shelf-edge deltas are a key depositional environment for accreting sediment onto shelf-margin clinoforms. The Moruga Formation, part of the paleo-Orinoco shelf-margin sedimentary prism of south-east Trinidad, provides new insight into the incremental growth of a Pliocene, storm wave-dominated shelf margin. Relatively little is known about the mechanisms of sand bypass from the shelf-break area of margins, and in particular from storm-wave dominated margins which are generally characterized by drifting of sand along strike until meeting a canyon or channel. The studied St. Hilaire Siltstone and Trinity Hill Sandstone succession is 260 m thick and demonstrates a continuous transition from gullied (with turbidites) uppermost slope upward to storm wave-dominated delta front on the outermost shelf. The basal upper-slope deposits are dominantly mass-transport deposited blocks, as well as associated turbidites and debrites with common soft-sediment-deformed strata. The overlying uppermost slope succession exhibits a spectacular set of gullies, which are separated by abundant slump-scar unconformities (tops of rotational slides), then filled with debris-flow conglomerates and sandy turbidite beds with interbedded mudstones. The top of the study succession, on the outer-shelf area, contains repeated upward-coarsening, sandstone-rich parasequences (2 to 15 m thick) with abundant hummocky and swaley cross-stratification, clear evidence of storm-swell and storm-wave dominated conditions. The observations suggest

[1] This chapter has been published as: Peng, Y., Steel, R.J., and Olariu, C., 2017, Transition from storm wave-dominated outer shelf to gullied upper slope: The mid-Pliocene Orinoco shelf margin, South Trinidad: Sedimentology, v. 64, p. 1511-1539. I was the primary author who conducted the research and drafted this paper with co-authors' help.

reconstruction of the unstable shelf margin as follows: (i) the aggradational storm wave-dominated, shelf-edge delta front became unstable and collapsed down the slope; (ii) the excavated scars of the shelf margin became gullied, but gradually healed (aggraded) by repeated infilling by debris flows and turbidites and then new gullying and further infilling; and (iii) renewed storm wave-dominated delta-front prograded out across the healed outer shelf, re-establishing the newly stabilized shelf margin. The Moruga Formation study, along with only a few others in the literature, confirms the sediment bypass ability of storm-wave dominated reaches of shelf edges, despite river-dominated deltas being, by far, the most efficient shelf-edge regime for sediment bypass at the shelf break.

INTRODUCTION

Shelf-margin delta growth is the primary way by which shelf margins prograde and sedimentary basins receive deep water sediments (Morton and Suter, 1996; Porębski and Steel, 2003). This is supported by the front reaches of large modern river deltas protruding the shelf edge for tens of kilometers (Olariu and Steel, 2009). The dominant process regime and therefore delta type at the shelf edge (i.e. river-dominated, wave-dominated or tide-dominated delta) is critical for shelf-margin growth. River-dominated shelf-edge deltas, with high sediment supply, have been shown to provide the most favorable scenario to drive the progradation of shorelines across the shelf to the shelf edge and beyond (Dixon et al., 2012b), where they may deliver significant volumes of sediment to the deep-water slope and basin floor. Such deep-water sediment delivery typically requires transit of the shelf deltas right to the shelf break either by strong river discharge (Carvajal and Steel, 2006), by sea-level fall and incision at the shelf edge

(Mellere et al., 2003), or by intersection with pre-existing slope conduits, such as slope channels or canyons incised into the shelf (Dasgupta and Buatois, 2015). This incision also sometimes results in partial collapse of the shelf margin (Steel et al., 2000; Petter and Steel, 2006; Covault and Graham, 2010; Fongngern et al., 2015). However, wave-dominated shelf-edge deltas (Deibert et al., 2003; Carvajal and Steel, 2009) or river-dominated shelf-edge deltas that have only modest supply or lack significant incision at the shelf edge (Plink-Björklund and Steel, 2008; Dixon et al., 2012b) may also contribute to construction of the shelf margin by draping sand-sheet aprons, or delta mouth bars onto the upper slope, although these do not often partition large sediment volumes to the basin floor (Plink-Björklund and Steel, 2008).

During the construction of shelf margins, sediment instability, slumping, and mass-transport events commonly occur, and they also play an important role in the shelf-margin growth and sediment transport to deep water (Moscardelli et al., 2006; Chen et al., 2016). Slides and slumps on the outermost shelf can remobilize sediment that was temporarily stored on the outer shelf and then redistribute it in the form of debris flows or by further transformation to turbidity currents with fragmentation during downslope transport (Mulder and Cochonat, 1996; Mulder and Alexander, 2001). Subsequent sedimentation in the collapse scars would infill or heal the slope depressions to allow renewed progradation. Such processes were documented previously in the river-dominated shelf-edge systems of eastern Spitzbergen (Nemec et al., 1988; Steel et al., 2000) and Tanqua Karoo Basin (Dixon et al., 2013; Laugier and Plink-Björklund, 2016). However, shelf-margin growth in front of wave-dominated shelf-edge segments is still little documented. Oblique wave action at the shelf edge most commonly drives sand along and parallel to the shoreline until captured by a canyon head, rather than allowing

immediate downdip delivery (Boyd et al., 2008; Carvajal and Steel, 2009), although there are also several reported cases of direct delivery (Jones et al., 2013; Gong et al., 2016).

The well-exposed outcrops of the Moruga Formation on Trinidad, a segment of the paleo-Orinoco Delta, exhibit a transition from gullied upper slope upward to storm wave-dominated delta front on the outermost shelf, and provides a unique opportunity to document the architecture of incremental growth on a well-exposed storm wave-dominated shelf edge that had become unstable. This study also provides insight into the sediment by-pass ability of a storm wave-dominated shelf edge and the initiation and infilling processes of slope gullies.

GEOLOGICAL SETTING

The study area is located on south-eastern Trinidad, at the junction of the east–west oriented East Venezuela–Columbus Foreland Basin constructed mainly by the late Miocene to present Orinoco River and its delta, and the north–south oriented Atlantic passive margin (Fig. 3.1A) (Mann et al., 2006; Escalona and Mann, 2011). As the Caribbean plate advanced to the east and south-east, the paleo-Orinoco River progressively shifted course eastward and infilled the East Venezuela Basin, onshore Southern Trinidad and offshore Columbus Basin (Fig. 3.1A) (Díaz de Gamero, 1996). The extremely high sediment supply from the Orinoco River (approximately 12,000 m of sediment were deposited in the Columbus Basin during the Pliocene and Pleistocene) (Wood, 2000) exceeded the shelf accommodation (Sydow et al., 2003), causing west to east migration of the paleoshelf-edge (progradation rate of 16 to 38 km/My) (Di Croce et al., 1999; Wood, 2000; Sydow et al., 2003; Carvajal et al., 2009) from onshore Eastern Venezuela to its present location 150 km off the modern Orinoco Delta, since the late

Miocene (Di Croce et al., 1999; Wood, 2000). Because of intense north–south compression as the Caribbean and South American plates met one another, Trinidad was deformed and uplifted through latest Pliocene and Pleistocene times (Kugler, 1959), providing an east–west depositional dip transect along the southern Trinidad coast through the entire shelf-margin sedimentary prism.

The migration of the Miocene–Pleistocene Orinoco River and Delta system from west to east has provided abundant sand reservoirs of both shallow-water and deep-water types along the axis of the East Venezuela Basin, and on the Trinidad paleo-Orinoco shelf and shelf-margin (Steel et al., 2007). Interpreted seismic and well log data of the offshore Columbus Basin show rapid progradation and aggradation of the shelf margin, including both shelf-edge deltas and associated deepwater slopes (Fig. 3.1B and C) (Sydow et al., 2003; Dixon, 2005). Outcrops along the south coast of Trinidad exhibit at least four major clastic wedges, or deltaic to deepwater growth stages (Steel et al., 2007) (Fig. 3.1D): (i) the late Miocene to early Pliocene Cruse Formation progradational episode (Kugler, 1959) was characterized by deep-water muddy slope deposits, turbidite-filled slope channels and overlying early Pliocene shelf-edge deltas, reached east as far as south central Trinidad, and is capped by the Lower Forest Clay transgressive flooding zone (Winter, 2006; Chen et al., 2016); (ii) the mid-Pliocene clastic wedge includes the Forest Formation of south-west Trinidad characterized by mixed river-influenced and tide-influenced delta lobes, and the basinward equivalent Moruga and Mayaro formations, a series of storm-wave dominated delta lobes that prograded as far as the east coast of Trinidad (Sydow et al., 2003; Dixon, 2005; Bowman and Johnson, 2014), and were capped by the Upper Forest Clay flooding zone; (iii) the mid-late Pliocene Lower Morne L'Enfer clastic wedge is characterized by river-dominated and tide-dominated

delta lobes and estuaries across southern Trinidad (Osman, 2007; Chen et al., 2014). After reaching offshore east Trinidad this wedge was capped by the well-documented Lot 7 Siltstone flooding zone; and (iv) the latest Pliocene Upper Morne L'Enfer/Palmiste Formation was characterized by tide-dominated deltas and a covering of coaly delta-plain deposits across all of southern Trinidad (Vincent, 2003; Chen et al., 2014).

The Moruga Formation, the second major clastic wedge that built across Trinidad, comprises three upward coarsening successions of storm wave-dominated delta front to shoreface deposits along the south coast of present-day Trinidad, as well as coeval deepwater slope deposits in the Columbus Channel and a laterally equivalent growth-fault compartment of wave-dominated deltas (Mayaro Formation) (Dixon, 2005; Dasgupta and Buatois, 2012; Bowman and Johnson, 2014) in the Columbus Basin areas cropping out along the south-eastern coast of Trinidad (Fig. 3.1D and E) (Leonard, 1983; Ali, 1995; Steel et al., 2007). The present study interval is 260 m thick, upward-coarsening topset segment of a single shelf-margin clinothem within the Moruga Formation growth stage. The upward-coarsening trend of the topset represents progradation of the Trinity Hills Sandstone Member out over the muddy St. Hilaire Siltstone Member reflecting the eastward and south-eastward progradation of the outermost paleo-Orinoco shelf across the muddy shelf edge to uppermost slope rollover. The study focuses on outcrops of gullies that occur on the outermost shelf and shelf-slope rollover, immediately seaward of the storm wave-dominated Trinity Hills Sandstone shelf-edge delta system.

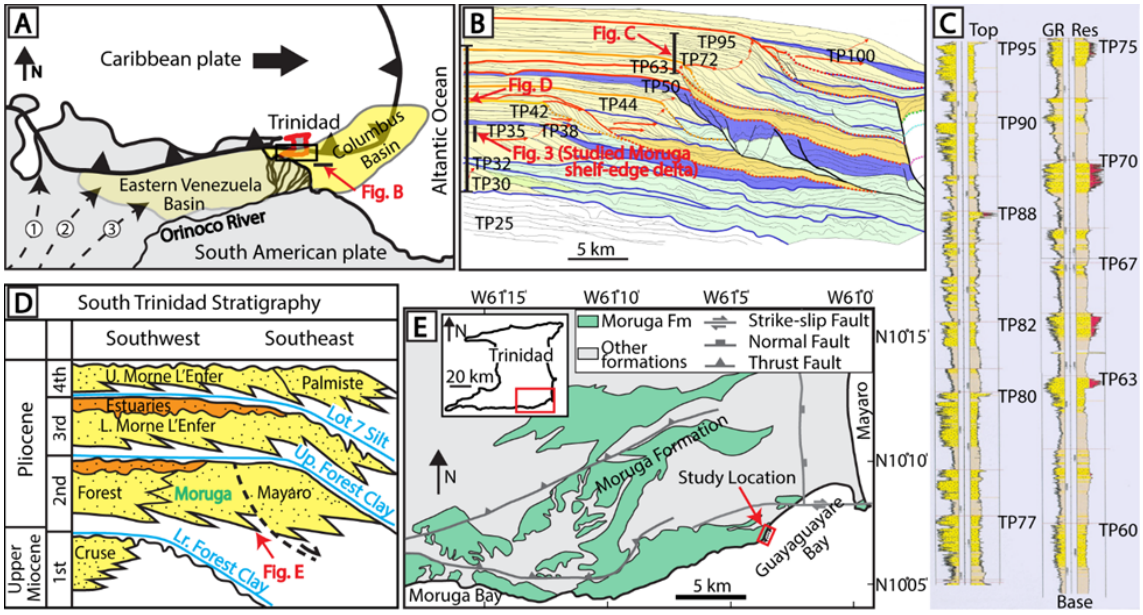

Figure 3.1: (A) Simplified Map illustrating that Trinidad is located in the foreland basin between the Caribbean plate and South American plate. The Paleo-Orinoco River delivered sediment and filled Eastern Venezuela Basin, onshore southern Trinidad, and offshore Columbus Basin. Previous changing courses of the paleo-Orinoco River from Paleocene to recent are illustrated by successive black dashed lines (numbered by 1 to 3) to the solid line from the west to the east (modified from Escalona and Mann, 2011). (B) Interpreted seismic data across the entire Orinoco shelf-margin prism exhibit progradation and aggradation of shelf deltas into the offshore Columbus Basin (from Dixon, 2005). Note that all deltaic units (TP95 down to TP30, in offshore stratigraphic terminology of Sydow et al., 2003) become shelf-edge deltas and rollover into deepwater slope deposits at the shelf break. The studied Moruga delta can also be seen to occupy a shelf edge position and occurs just below stratigraphic level TP35. (C) Composite well log in the offshore Columbus Basin [location in (B)] (Sydow et al., 2003) shows some 16 coarsening-upward units (each *ca* 200 m thick) indicating repeated stacking of regressive-transgressive Orinoco-Delta units, each becoming shelf-edge deltas on approach to the shelf-slope break. (D) Late Miocene–Pliocene shelf and shelf margin stratigraphy in the onshore Southern Basin of Trinidad in transition to offshore, illustrating four major deltaic growth stages separated by mud-prone flooding surfaces (modified from Steel et al., 2007). This same succession is much more growth faulted and thickened in the offshore Columbus Basin (Sydow et al., 2003) (E) Distribution of the Pliocene Moruga Formation and location of study area (after Kugler, 1959).

METHODOLOGY AND TERMINOLOGY

Well-exposed and continuous outcrops along a 2 km depositional-dip transect west of Guayaguayare Bay on south-eastern Trinidad were analyzed through the measurement of a 260 m thick stratigraphic section and with the use of photomosaics (Figs 3.2 and 3.3). Facies variability was described at a 0.1 m to 1.0 m resolution by recording bed thickness, grain size, sedimentary structures and trace fossils with Bioturbation Index (BI) (Taylor and Goldring, 1993). Paleocurrents were measured primarily from ripple lamination. The gullied upper-slope deposits that are the stratigraphic link between thickly developed, shelf-edge, wave-dominated delta deposits and muddy upper-slope, sediment gravity flow deposits were documented.

The term ‘slope gully’ is used here to refer to relatively small (up to a few tens of meters deep and tens to hundreds of meters wide), dip-oriented channel-like features, which are common on the upper portion of continental slopes (Twichell and Roberts, 1982; Chiocci, 1994; Pratson et al., 1994; Field et al., 1999; Lonergan et al., 2013). By comparison, slope channels are larger negative relief features (tens to a few hundreds of meters deep, 100 m to few tens of kilometers wide, and 10 to 3000 km in length) that are short-term or long-term conduits for sediment to be transported down the deepwater slope (Mutti, 1977; Stow and Mayall, 2000). Submarine canyons are very large V-shaped erosional conduits with vertical relief up to 1 km, widths ranging from several to more than 50 km, and lengths ranging from tens to several hundreds of kilometers (Galloway, 1998).

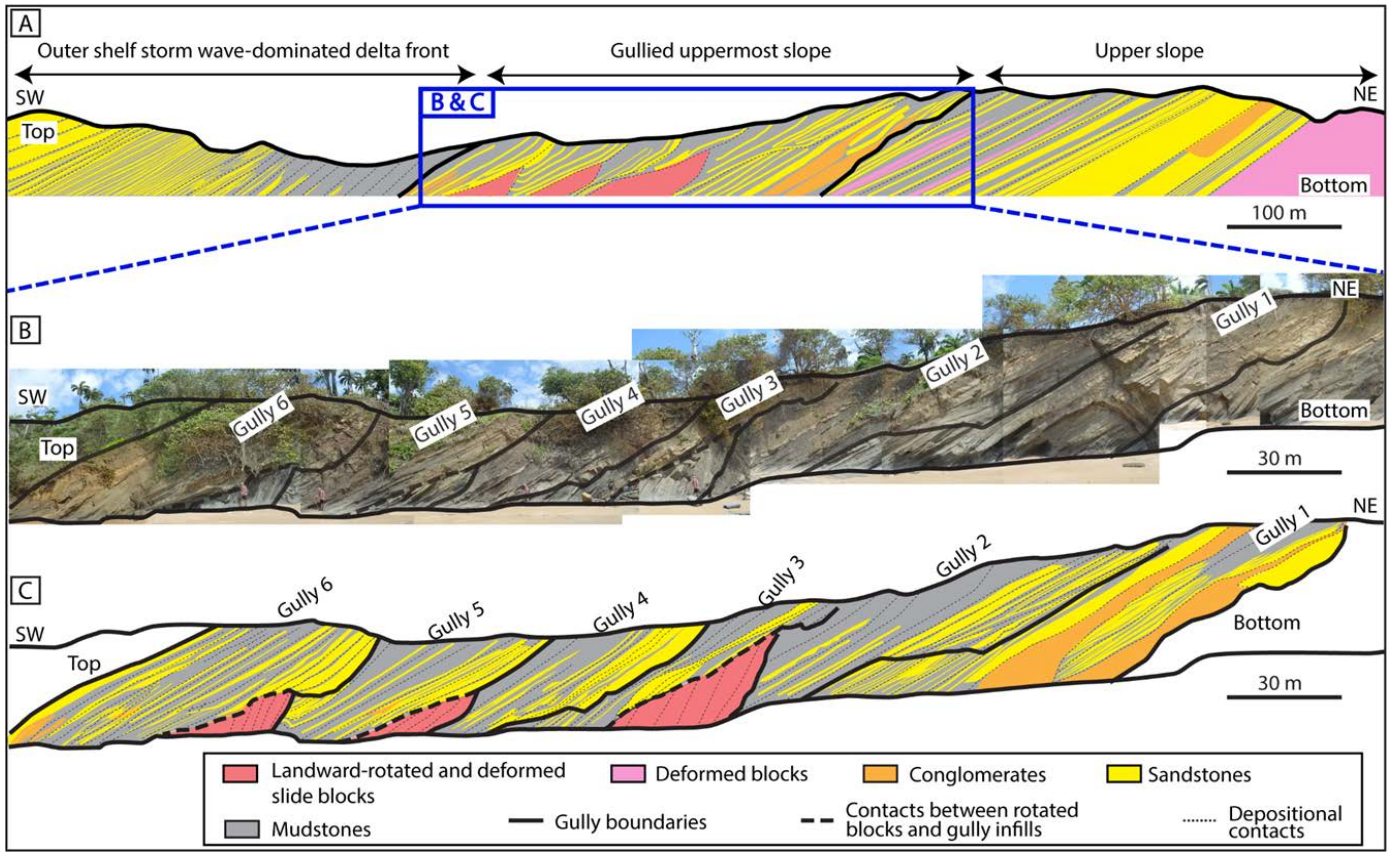

Figure 3.2: (A) Outcrop sketch of *ca* 260 m thick Moruga Formation succession displaying a transition from upper-slope deposits, through gullied upper-slope deposits to storm wave-dominated, upward-coarsening deposits of the outer shelf. For the location of the section see Figure 3.1. (B) and (C) Photomosaic and interpretation of gullied upper-slope succession (*ca* 80 m thick) illustrating the occurrence of landward-tilted, slide and deformed blocks with their internal strata dipping more steeply than underlying and overlying strata.

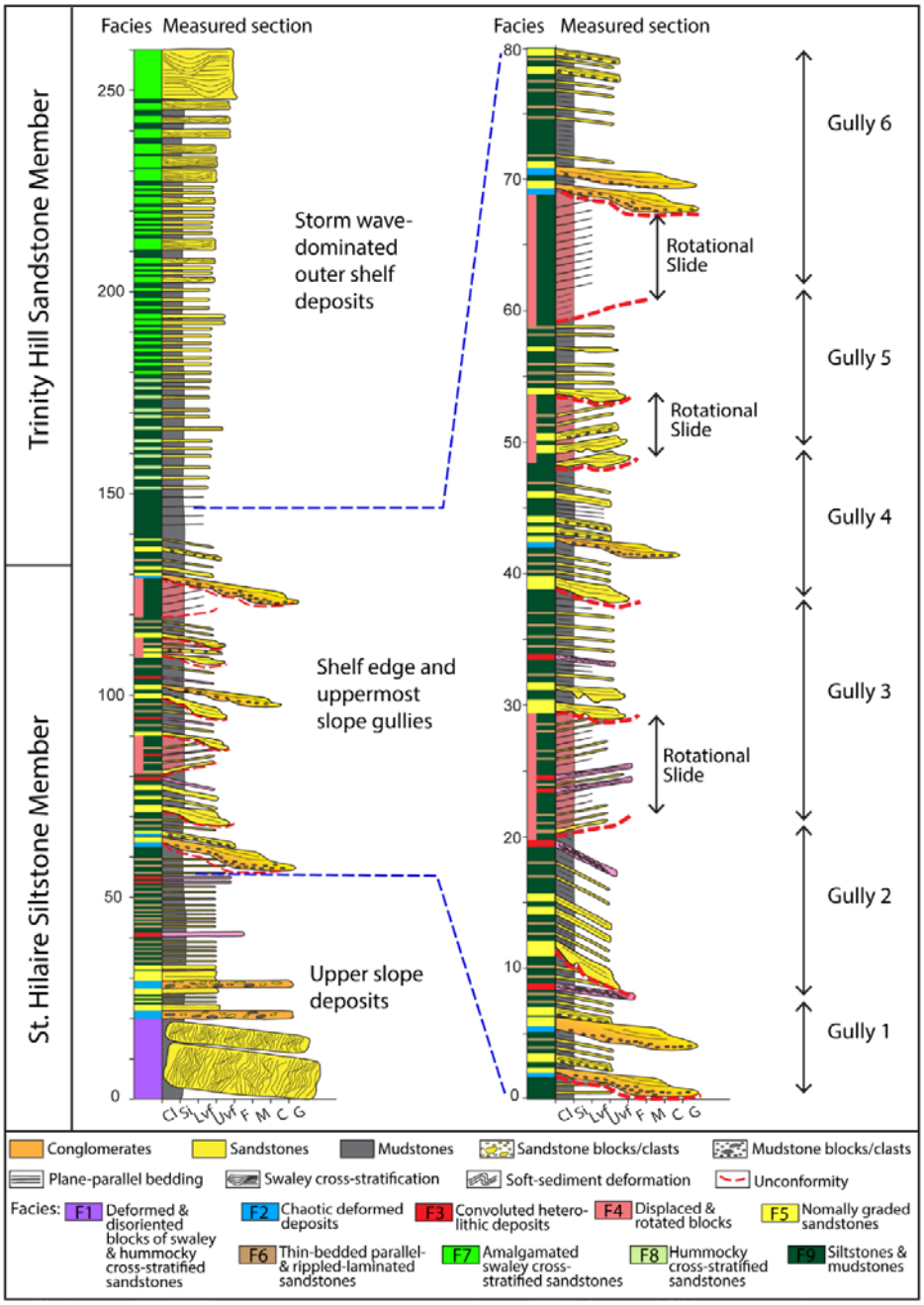

Figure 3.3: Sedimentary log of the 260 m thick succession of St. Hilaire Siltstone and Trinity Hill Sandstone Members (left), and the 80 m thick, collapsed and gullied section (right) west of Guayaguayare Bay. The red dash lines indicate the irregular erosion surfaces separating gully infills and rotated slide blocks.

SEDIMENTOLOGY AND FACIES

The studied succession within the Moruga Formation shows two main depositional environments from bottom to top: (i) upper slope to gullied upper slope, with various types of sediment gravity-flow deposits; and (ii) storm wave-dominated, sand-rich outer-shelf-deposits (Figs 3.2 and 3.3). Nine facies are distinguished within these depositional environments and summarized in Table 3.1.

Upper-slope to gullied uppermost-slope environment

The upper slope to gullied uppermost slope environment (i.e. 0 to 140 m in Fig. 3.3) exhibits six facies dominated by sediment gravity flow deposits. The gullies are bounded by frequent highly irregular erosion surfaces that have a relief of up to 10 m and occur within the interval 60 to 140 m in the studied succession (Figs 3.2 and 3.3). In places, disoriented blocks (facies F4) lie on the gully bases with their internal strata dipping more steeply than both the underlying and overlying strata.

Facies 1 (F1): Deformed and disoriented blocks of swaley cross-stratified and hummocky cross-stratified sandstones

Facies F1 occurs in the basal 20 m of the succession and contains large disoriented blocks (over 10 m diameter) of upper very fine-grained sandstones with undeformed amalgamated swaley cross-stratification and hummocky cross-stratification (SCS and HCS) (Fig. 3.4). The disorientation of the blocks is shown by their internal lamination being more steeply dipping (Fig. 3.4B and C) than the overlying strata. The individual swaley cross-stratified and hummocky cross-stratified bedforms in the sandstone blocks show a wavelength of 1 to 2 m and height of 10 to 20 cm. Abundant mudstone rip-up clasts are present on top of the irregular basal scour surfaces of

individual beds and laminasets (Fig. 3.4D and E). Slightly deformed heterolithic beds occur between the sandstone blocks (Fig. 3.4B). Bioturbation is sparse (BI = 0 to 1), and *Ophiomorpha* is observed in the sandstone blocks.

The disoriented blocks of swaley cross-stratified and hummocky cross-stratified sandstones are interpreted as mass transport deposits which had collapsed from the storm wave-dominated delta front on the outer shelf or shelf edge area onto the slope. The small swaley and hummocky bedforms suggest that storm events were frequent and the unidirectional component of the storm-wave currents was weak prior to collapse (Dumas et al., 2005). The irregular basal scour surfaces with mudstone clasts strongly suggest erosion by storm waves. The deformed heterolithic beds between sandstone blocks probably represent shear zones developed during the slumping process (Martinsen and Bakken, 1990). The described hummocky structures in the collapsed blocks could also conceivably, before collapse, have been supercritical flow deposits (Mulder et al., 2009; Lang and Winsemann, 2013; Cartigny et al., 2014). However, the rare occurrence of *Ophiomorpha* in the blocks indicates a stressed condition caused by high freshwater discharge and turbulence, high sedimentation rates, or large oceanic waves or swells in the shelf margin (Hampson and Howell, 2005; Dasgupta et al., 2016).

Table 3.1: Summary of the facies in the storm-wave dominated outer-shelf delta front to upper slope environment of the mid-Pliocene Orinoco delta.

	Facies	Grain-size & Bedding	Sedimentary structures	Depositional environment	Interpretation
1	Deformed and disoriented blocks of swaley & hummocky cross-stratified sandstones	Large blocks of upper-very-fine-grained sandstones (2 to >10 m diameter)	Steeply-dipping strata in blocks; amalgamated swaley cross-stratification	Upper slope	Collapsed from storm wave-dominated delta front near the shelf edge
2	Chaotic deformed deposits (Type A)	Blocks of upper-very-fine-grained sandstones and heterolithic strata (0.1-1.5 m diameter); 0.2-2.0 m thick	Chaotic clast-supported; subangular to subrounded clasts, muddy matrix	Upper slope	High-strength cohesive debris flows; Slump deposits of delta front and prodelta deposits on the outer shelf / shelf edge
	Chaotic deformed deposits (Type B)	Sandstone and siltstone clasts (1-20 cm long); 0.5-2.0 m thick	Ungraded, poorly sorted siltstone and sandstone clasts, sandstone matrix	Gullied upper slope	Low to moderate-strength cohesive debris flows; collapsed from prodelta and delta front
3	Convoluted heterolithic deposits	Lower-very-fine-grained sandstones and siltstones; 0.2-1.0 m thick	Convoluted bedding/lamination with mudstone intruding upwards	Upper slope	Downslope movement of unconsolidated sediment
4	Displaced and rotated blocks	Blocks of heterolithic beds (5-10 m thick)	Steeply-dipping strata; angular unconformities	Gullied upper slope	Back-tilted, rotational slides situated on bottom of slope gullies
5	Normally graded sandstones	Lower-very-fine-grained sandstones; 0.4-2.2 m thick	Normally-graded, sharp-based; structureless to parallel laminated; mud rip-up clasts on bottom	Upper slope; gullied upper slope	High-density turbidity currents
6	Thin-bedded parallel- & ripple-laminated sandstones	Lower-very-fine-grained sandstones; 2-6 cm thick	Parallel- and ripple-laminated sandstones; climbing ripples in places	Upper slope	Low-density turbidity currents
7	Amalgamated swaley cross-stratified (SCS) sandstones	Lower- to upper-very-fine-grained sandstones; up to 3 m thick	Flat-based, amalgamated; wave ripples on top in places; rare *Ophiomorpha*	Outer-shelf delta front	Storm-wave-reworked deposits
8	Hummocky cross-stratified (HCS) sandstones	Lower-very-fine-grained sandstones; up to 0.5 m thick	Flat-based; wave ripples; rare bioturbation	Outer-shelf delta front	Storm-wave-reworked deposits
9	Siltstones and mudstones	Siltstones and mudstones; 0.5-9.0 m thick	Massive/graded and laminated; occasionally bioturbated (*Chondrites*, *Planolites*)	Upper slope; gullied upper slope; outer-shelf delta front	Storm-wave-enhanced muddy sediment gravity flows; suspension of finer-grained sediment under low energy

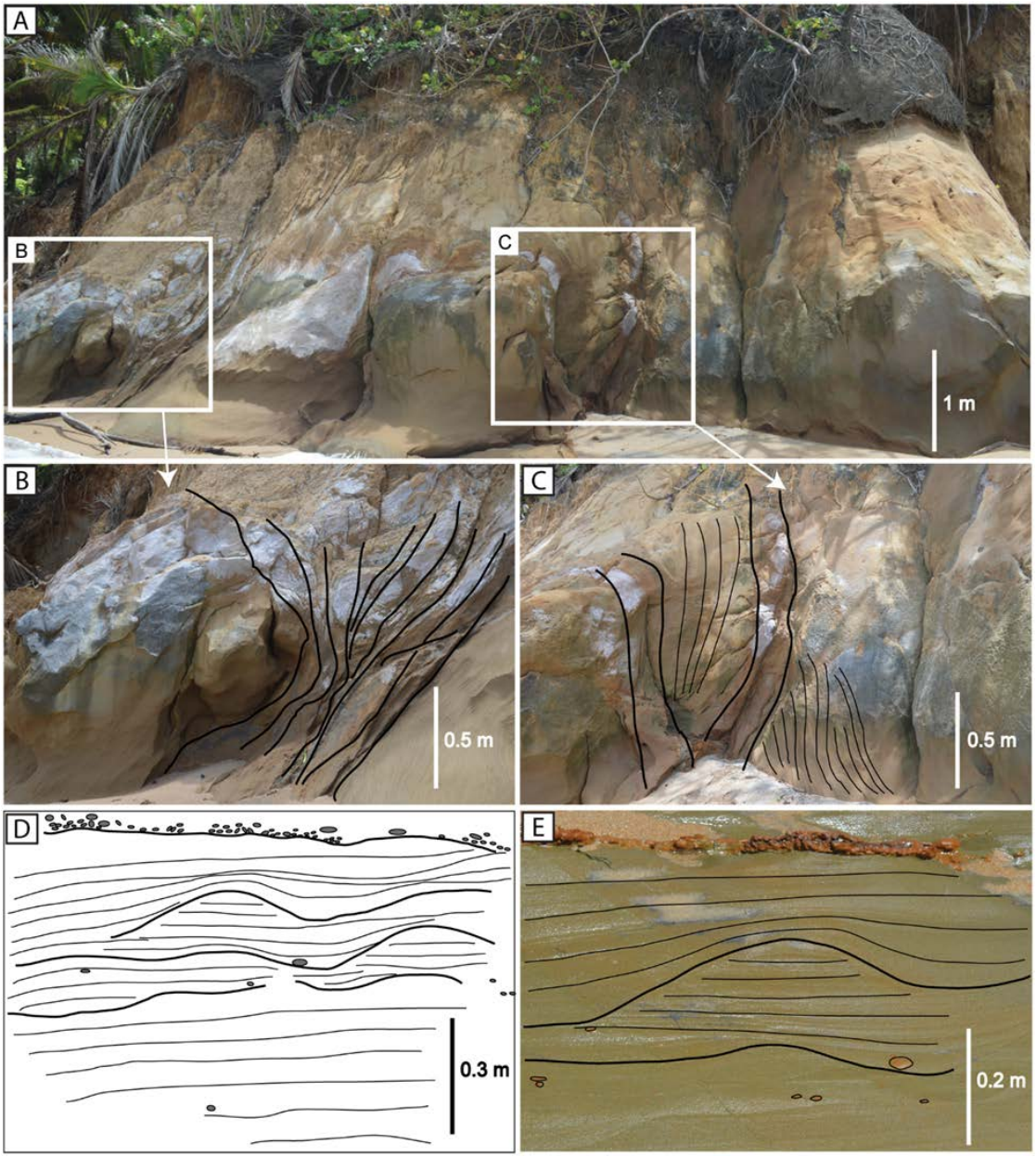

Figure 3.4: Characteristic features of Facies F1. (A) Large disoriented blocks of swaley cross-stratified and hummocky cross-stratified sandstones. Note that the overlying strata is not shown here. (B) The slightly deformed interbedded sandstone and mudstone beds between the two undeformed sandstone blocks. (C) The sub-vertical orientation of sandstone blocks. (D) and (E) Detail of swaley cross-stratified and hummocky cross-stratified sandstones with mudstone clasts overlying the scour surfaces.

Facies 2 (F2): Chaotic deformed deposits

Facies F2 is characterized by beds (0.5 to 2.0 m thick) with chaotic, poorly sorted sandstone and siltstone clasts (1.0 cm to 1.5 m diameter) supported by a sandy or muddy matrix (Fig. 3.5). Scoured and highly irregular basal surfaces are commonly observed. Two types of deposit are identified in the succession: (i) Type A beds with large and poorly sorted blocks (0.1 to 1.5 m diameter) within a mudstone matrix and preferentially occurring in the lower 20 to 30 m of the succession (Fig. 3.5A, B, and C); and (ii) Type B beds with smaller and better sorted clasts (1 to 20 cm diameter) in a very-fine-grained sandstone matrix occurring only in the middle of the succession (i.e. 60 to 140 m in Fig. 3.3) (Fig. 3.5D and E). The blocks of Type A beds comprise mudstones, interbedded sandstones and siltstones, and swaley cross-stratified sandstones with rare *Ophiomorpha* and *Thalassinoides* (Fig. 3.5A, B, and C). Type B beds are stratified intraformational conglomerates and contain smaller and well-rounded very fine-grained sandstone clasts (*ca* 20%) and larger sub-rounded siltstone clasts (*ca* 80%) in a structureless and muddy sandstone matrix (Fig. 3.5D and E). The muddy sandstone matrix is grey-colored and characterized by poorly sorted sands with abundant millimeter-scale mudstone clasts, and contains vertical pipes that are perpendicular to the original bedding in places (Fig. 3.5D and E). No bioturbation (BI = 0) is observed in the deposits.

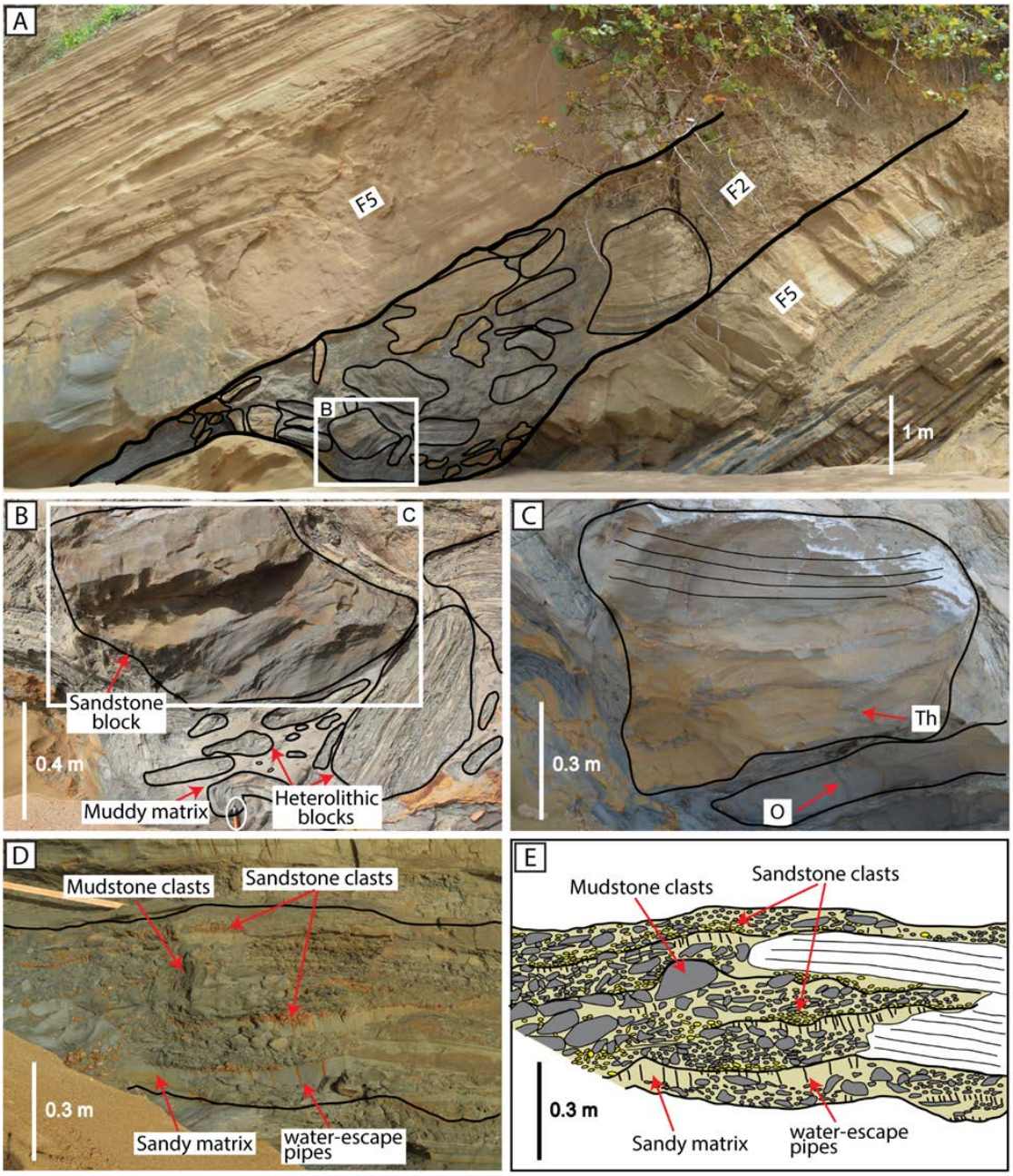

Figure 3.5: Chaotic deformed deposits (F2). (A) Irregularly based, large-scale chaotically deformed bed of F2 underlain and overlain by a thick sandstone bed (F5). (B) Sandstone and heterolithic blocks supported by muddy matrix with smaller dispersed mudstone clasts. (C) Possible swaley cross-stratified sandstone block with *Ophiomorpha* (O) and *Thalassinoides* (Th). (D) and (E) Stratified conglomerates of mudstone and sandstone clasts dispersing in structureless sandstone matrix in which pipes are well developed.

Because of their poor sorting and the matrix-rich character of beds, Type A and B beds are interpreted as debrites formed by *en masse* deposition from cohesive debris flows so as that the clasts do not segregate by differential settling (Talling et al., 2012a). Type A deposits occurring in the lower part of the succession are interpreted as high-strength cohesive debris-flow deposits which commonly occur on slope settings (Tripsanas et al., 2008; Piper and Normark, 2009; Talling et al., 2012b). Some authors (Dzulynski, 1963; Strachan, 2008; Oliveira et al., 2009) have also defined such beds as incoherent slumps because the indurated broken beds with original bedding were mixed with and incorporated mud from mass transport on the slope. The chaotic blocks of sandstone and heterolithic strata within the Type A debrites are attributed to slumped, down-slope movement of broken blocks, probably derived from the topographically higher shelf-edge area. The sandstone blocks with swaley cross-stratification and rare bioturbation probably originated from wave-influenced delta-front deposits on the outer shelf or shelf edge, whereas the heterolithic blocks were derived from the prodelta area. Cohesive debris flows of the Type A debrites tend not to mix efficiently with surrounding seawater. Type B deposits occur preferentially in the gullied upper-slope part of the succession and likely result from low to moderate-strength cohesive debris flows (Talling et al., 2012b). The muddy sandstones in the upper part of Type B beds suggests that there was some mixing with the ambient medium along the uppermost surface of beds to produce more dilute sediment suspensions of turbidity currents, in contrast with high-strength debris flows (Mulder and Alexander, 2001). The pipes in the Type B sandstones are water-escape structures created by over-pressured pore water flowing upward after deposition of the debris flows (Marr et al., 2001). The sub-angular siltstone clasts of the Type B debrites indicate transportation over short distance from the prodelta deposits or from locally collapsed gully margins. In contrast, the well-rounded and well-sorted

sandstone clasts within the Type B debrites may suggest transportation over longer distances from collapsed, delta front deposits. The clast-rich character of the low to moderate-strength cohesive debris-flow deposits suggests that they may have transported sediment over longer distances down the slope (Nelson et al., 1992; Schwab et al., 1996; Talling et al., 2010; Talling et al., 2012a). The highly irregular basal surface of facies F2 (Fig. 3.5A) is likely to represent antecedent topography rather than erosion caused by the debris flows, because hydroplaning in such subaqueous debris flows may lubricate the base of the flow, contributing to flow mobility downslope on the sea floor (Mohrig et al., 1998). However, the local erosion surfaces between the conglomerate beds were probably created by debris flows.

Facies 3 (F3): Convoluted heterolithic deposits

Facies F3 is characterized by deformed and convoluted heterolithic beds at a variety of scales (0.2 to 1.0 m thick) and is commonly underlain and overlain by undeformed beds (Fig. 3.6). Deformed beds of facies F3 are the most common in the lower parts of the succession and show a decrease in scale and degree of distortion upwards through the succession. The deposits are commonly loaded into underlying mudstones, and they demonstrate a pattern of broad synclines and sharp anticlines with random to roughly parallel fold axes verging towards the north-east (Fig. 3.6). Bioturbation is absent (BI = 0) in F3.

Facies F3 is the product of downslope movement that commonly occurs in unconsolidated sediment as a result of gravitational forces (Owen et al., 2011). The upward decrease in scale and degree of distortion indicate decreasing gradients from the upper slope towards the outer shelf. The downslope movement took place shortly after sediment deposition on unconsolidated cohesive muds, where differential density at the

interface of dense sediment deposited over less dense water-filled mud (Owen, 2003). The convoluted deposits are coherent as the original bedding is only partially disrupted, and are dominated by vertical displacements resulting from the gravitational force associated with reverse density systems and possible horizontal shear stress as they accumulated rapidly on the slope (Mills, 1983; Oliveira et al., 2011). The consistent inclination of fold axes that exhibit a non-random alignment provides evidence for slump movement down a north-eastward-dipping slope. The lack of bioturbation supports the stressed condition of the upper slope environment.

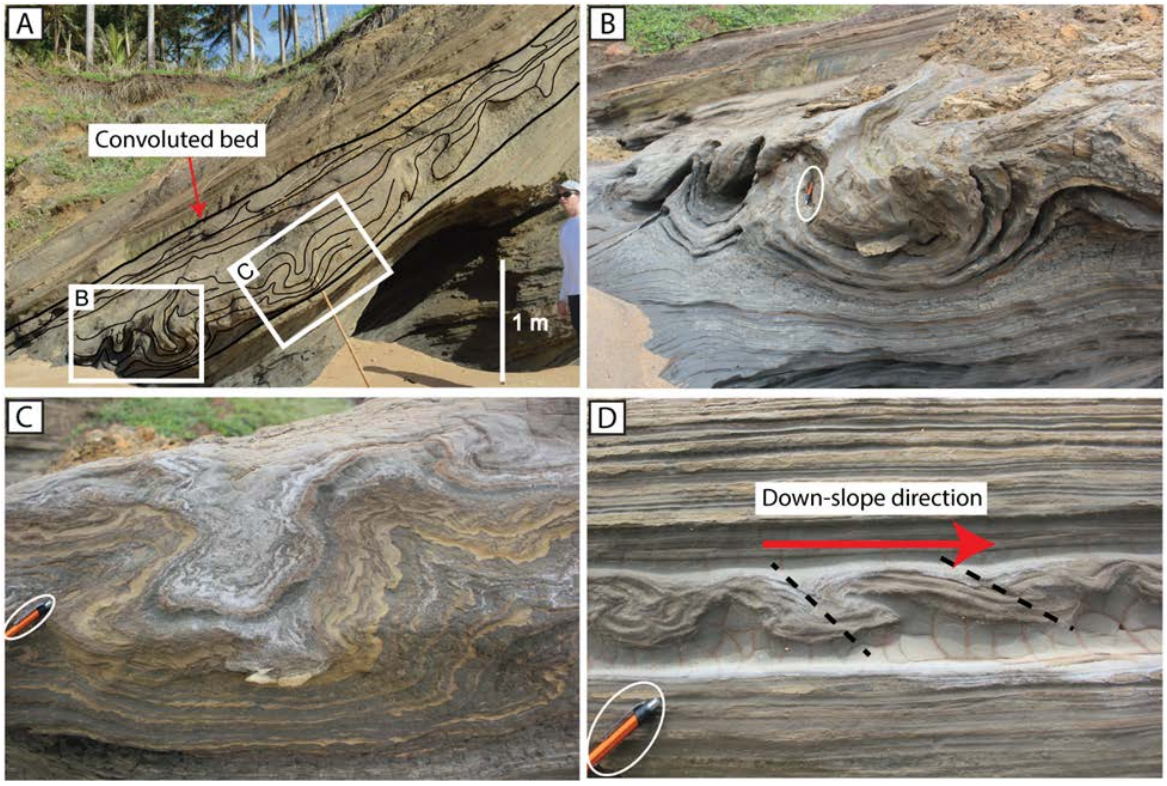

Figure 3.6: Varieties of convolute-laminated layers interbedded with undisturbed beds of lower very fine sandstone and siltstone. (A) 1 m thick convoluted bed bounded by undeformed heterolithic beds. (B) and (C) Detail of convolute bedding in figure (A). (D) One small-scale (10 cm thick) contorted heterolithic bed loaded into underlying mudstone.

Facies 4 (F4): Displaced and rotated blocks

Facies F4 is characterized by very large (5 to 10 m thick), disoriented blocks of heterolithic beds consistently lying with their internal strata dipping more steeply than both the underlying and overlying strata (Fig. 3.7). It is noticeable that the rotated strata commonly dip towards the west (i.e. paleo-landward, such that the blocks have rotated back into the slope), and the underlying strata display contorted beds in places (Fig. 3.7). The top and basal surfaces of the blocks are highly irregular and dip towards the north-east. The lower very fine-grained sandstone beds in the rotated block are internally deformed and loaded into the underlying mudstones (Fig. 3.7A). Scour surfaces (up to 1 m deep) occur in the blocks in places and are filled by interbedded sandstones and mudstones. Bioturbation is absent (BI = 0).

The disoriented blocks of heterolithic strata are interpreted to represent landward back-tilted blocks that slid out from slump scars and came to rest at the terminus of the slide track. The slide track then attracted sediment gravity flows, and became infilled as a gully. The highly irregular basal surface of each interpreted gully suggests that it developed as a slump scar rather than from sediment-gravity flow erosion (Mohrig et al., 1998). The north-easterly dip of the scour surfaces suggests that they were aligned down the slope, although two-dimensional and three-dimensional geometry of the surfaces is not demonstrated in the exposure. The steeply-dipping strata in the blocks below the gully bases are back-tilted toward the shelf because of listric rotation during their collapse down the slope, and the less steeply-dipping underlying and overlying strata represent the gully infills. The interbedded sandstones and mudstones with internal deformation, the lack of bioturbation, together with the landward backtilting strata in the blocks suggest that these blocks were probably derived from the shelf edge and upper slope where the slope was unstable (Deibert et al., 2003; Carvajal and Steel, 2009; Dixon

et al., 2012a). The scour surfaces in the blocks were probably formed by small-scale collapse due to sediment instability.

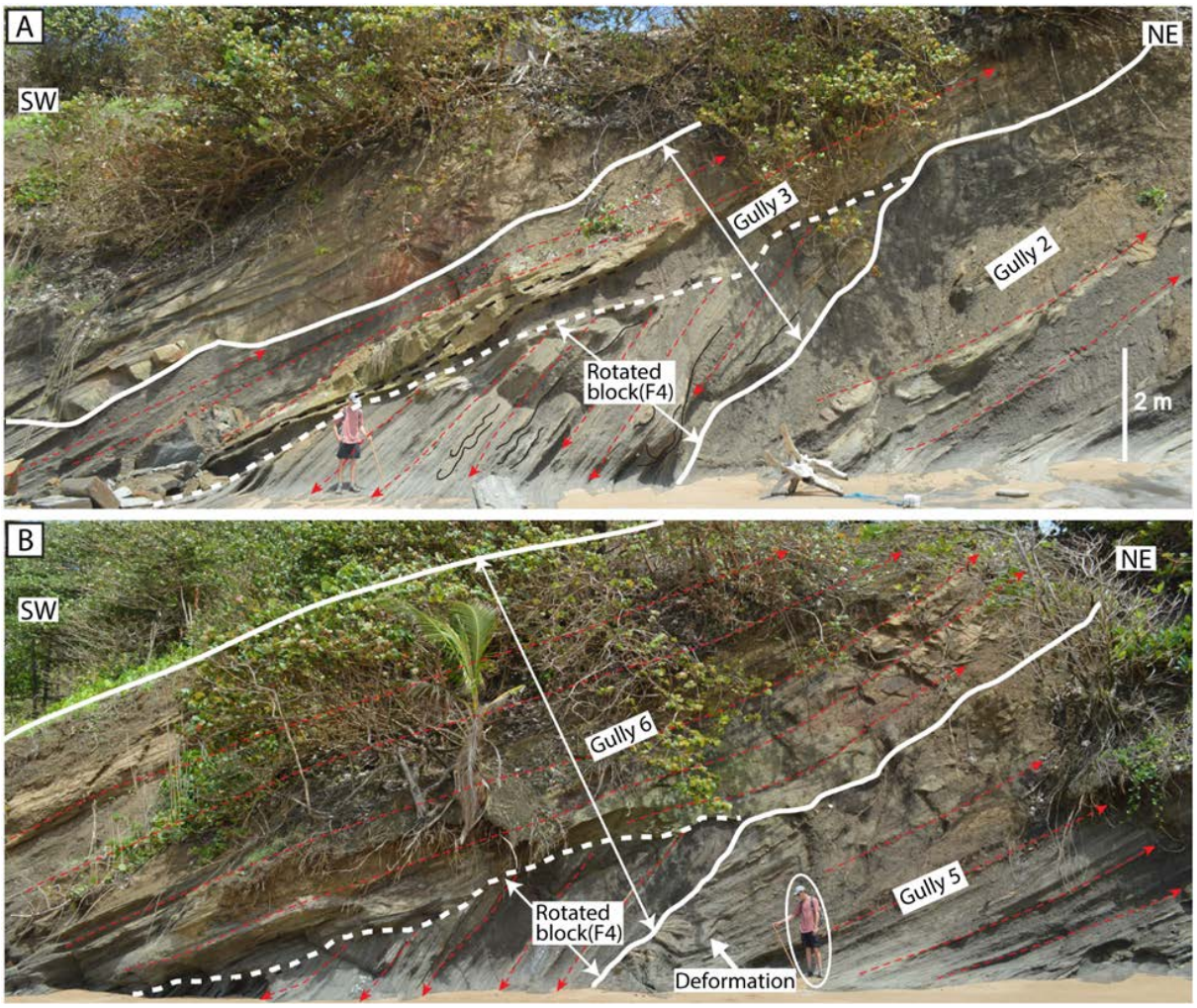

Figure 3.7: (A) Disoriented, steeply-dipping block underlain by the high irregular base of Gully 3 with the unconformably overlying gully-infill strata. The sandstone beds are internally deformed and loaded into the underlying mudstones in places. (B) The muddy and steeply-dipping block underlain by the slightly contorted strata of Gully 5 and overlain by the less steeply-dipping, infilled strata of Gully 6. White solid lines indicate gully boundaries, white dashed lines indicate contacts between rotated blocks and overlying gully infills, and red arrowed lines represent bedding planes with different dip directions.

Facies 5 (F5): Normally graded sandstones

Facies F5 (total thickness *ca* 30 m) is dominated by normally graded lower very fine-grained sandstone beds (0.4 to 2.2 m thick) that are structureless to parallel-laminated and ripple-laminated. Packages of F5 commonly alternate with slumped deposits (Fig. 3.8). The sandstone beds are sharp-based and erosional into the underlying muddy deposits (Fig. 3.8A and B). Mudstone rip-up clasts (millimetre to centimetre long) are distributed along discrete horizons in structureless sandstones rather than being chaotically dispersed (Fig. 3.8B). Thick sandstone beds (1.0 to 2.2 m thick) commonly occur in the lower part of the measured section (0 to 30 m in Fig. 3.3), and they are structureless and progressively grade upwards into parallel lamination which becomes convolute (Fig. 3.8B and C). In places, the sandstones exhibit a basal coarsening-up unit (i.e. parallel-laminated sandstones grade upward to structureless sandstones) overlain by a fining-up unit (i.e. structureless sandstones grade upward to parallel-laminated sandstones) (Fig. 3.8C). The relatively thin graded sandstone beds (0.4 to 1.0 m thick) (Fig. 3.8D to F) are well-developed in the middle measured section (50 to 100 m in Fig. 3.3). No bioturbation (BI = 0) is observed in these deposits.

The normally graded sandstones of F5 are interpreted as deposits of turbidity currents (i.e. turbidites). The beds include T_A and $T_{B\text{-}2}$ divisions of deposit-based classification of turbidites (Bouma et al., 1962; Talling et al., 2012b) and were deposited incrementally by high-density turbidity currents (Middleton and Hampton, 1973; Lowe, 1982; Kneller and Branney, 1995; Talling et al., 2012b). The erosional surfaces and mudstone rip-up clasts on the bottom of the sandstone beds indicate erosion and sediment bypass by strong turbidity currents with high velocity. The lowermost structureless sandstone (T_A) was probably deposited by a high-density turbidity current where sediment settled rapidly as sediment concentration increased and hindered settling

became dominant (Kneller, 1995; Kneller and Branney, 1995). The parallel laminated sandstones (T_{B-2}) above the structureless interval (T_A) represent the waning flow of high-density turbidity currents where turbulence in the high-concentration near-bed layers (i.e. traction carpet) was strongly dampened (Kuenen, 1966; Leclair and Arnott, 2005; Sumner et al., 2008). Thus, sediments were abruptly deposited and subsequent lateral shearing over a short distance produced parallel-lamination (Sumner et al., 2008). The occasional convolute laminations in parallel laminated sandstones (Fig. 3.8C) are attributed to dewatering caused by rapid deposition (Bouma et al., 1962; Talling et al., 2012b). The coarsening-upward and fining-upward sandstone beds suggest hyperpycnal flows in which the flows were sustained over long time intervals by increasing/waxing and decreasing/waning discharge (Mulder et al., 2003). The thicker turbidite sandstones which are structureless or contain parallel-lamination (1.0 to 2.2 m thick) are interpreted as deposits near the gully axis, and the thinner turbidite sandstones (0.4 to 1.0 m thick) with parallel-lamination interpreted to be more common near transitional areas towards the gully margins (Hirayama and Nakajima, 1977; Kneller and Branney, 1995).

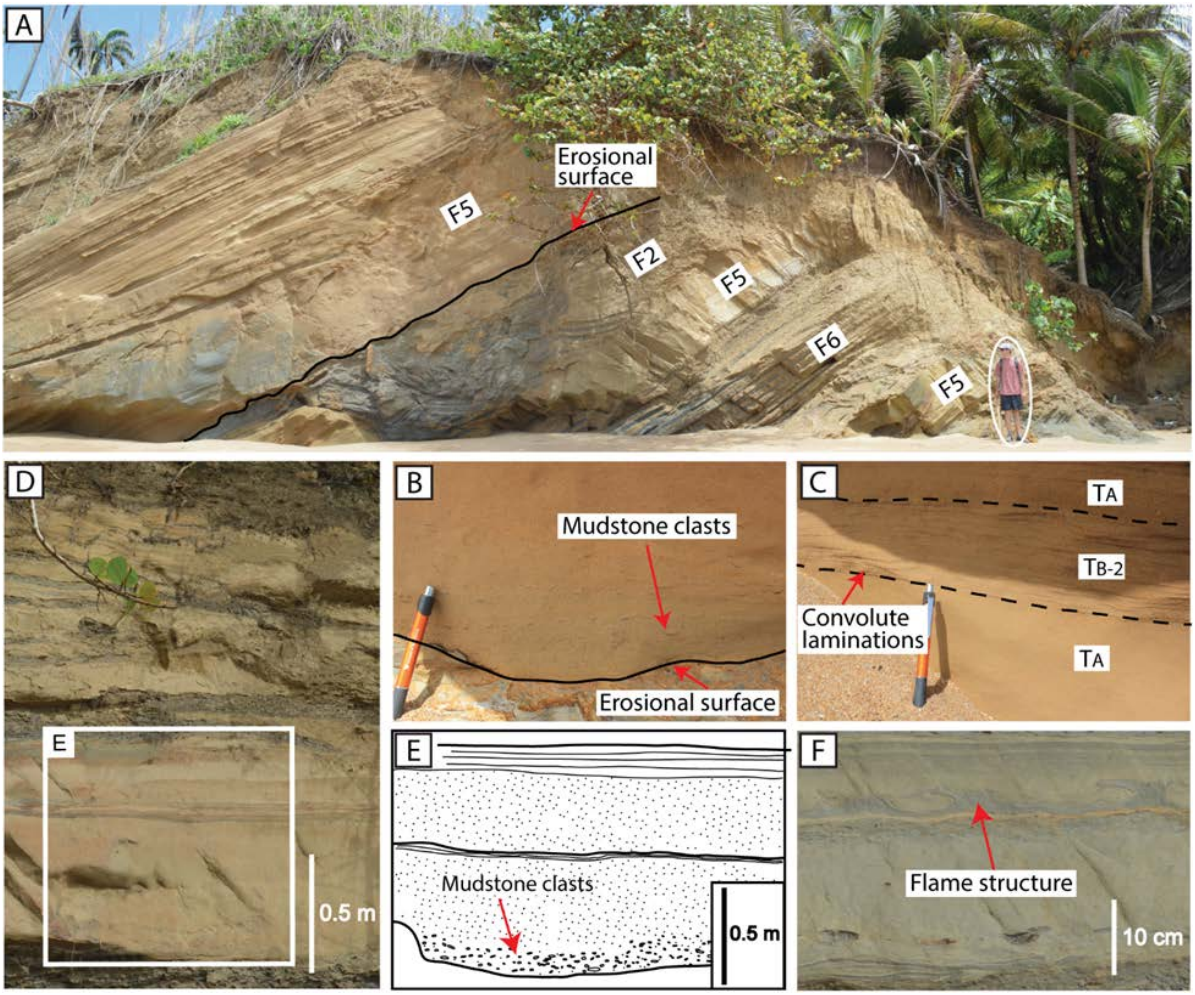

Figure 3.8: Characteristics of thick sandstone facies (F5) on the uppermost slope. (A) Thick sandstone beds are sharp-based and erosional into the underlying deposits, and they are commonly associated with facies F2 and F6. (B) Normally graded structureless sandstone bed with sharp-based erosional surface and floating mud clasts. (C) Sandstone bed exhibits coarsening-up (T_{B-2} to T_A) and fining-up (T_A to T_{B-2}) units. (D) and (E) Normal graded sandstone beds within upper slope gullies. (F) Stacked sandstone beds with flame structures and sandstone clasts.

Facies 6 (F6): Thin-bedded parallel-laminated and ripple-laminated sandstones

Facies F6 beds (total thickness *ca* 25 m) are characterized by thin-bedded lower very fine-grained sandstones (up to 20 cm thick) with parallel-laminations and ripple-laminations, commonly interbedded with siltstones and mudstones (Fig. 3.9). The sandstones are sharp-based and flat-based and display normal grading with parallel-lamination progressively changing upward into ripple lamination (Fig. 3.9C and D). Climbing-ripple cross-lamination is developed in places, displaying low climb angles (<15°) with partial erosion of ripple stoss sides (Fig. 3.9E to H). Paleocurrent direction estimated from rippled-laminated sandstones (NNE to ESE) are typically sub-parallel to the regional down-slope directions (east to north-east). No bioturbation (BI = 0) is observed.

The parallel-laminated and ripple-laminated sandstones are interpreted as deposits from low-density turbidity currents (Middleton and Hampton, 1973; Lowe, 1982; Kneller and Branney, 1995; Talling et al., 2012b), and they represent T_{B-1} and T_C intervals, respectively (Bouma et al., 1962; Talling et al., 2012b). The parallel-laminated sandstone beds are interpreted as T_{B-1} because: (i) they are finer-grained than those in facies F5; (ii) they occur commonly below the ripple-laminated sandstones (T_C); and (iii) their thickness is less than 40 cm, as noted for low-density turbidites in the literature (Sadler, 1982; Talling, 2001; Sylvester, 2007; Talling et al., 2007). The ripple-laminated sandstones (T_C) record deposition from low sediment fallout rates from suspension by dilute and fully turbulent flows (Baas, 1999). The presence of climbing ripples indicates that the rates of suspended-load fallout were relatively high, and that the bedload transport rates were relatively low (Allen, 1970). The low climb angles of the ripples and partial stoss side erosion suggest that they are subcritical climbing ripples that were caused by lower suspended-load fallout rates and higher bedload transport rates than

those of supercritical climbing ripples (Allen, 1973; Jobe et al., 2012). The thin low-density turbidites (up to 20 cm thick) with flat bases were probably deposited by waning turbidity currents on the upper slope areas.

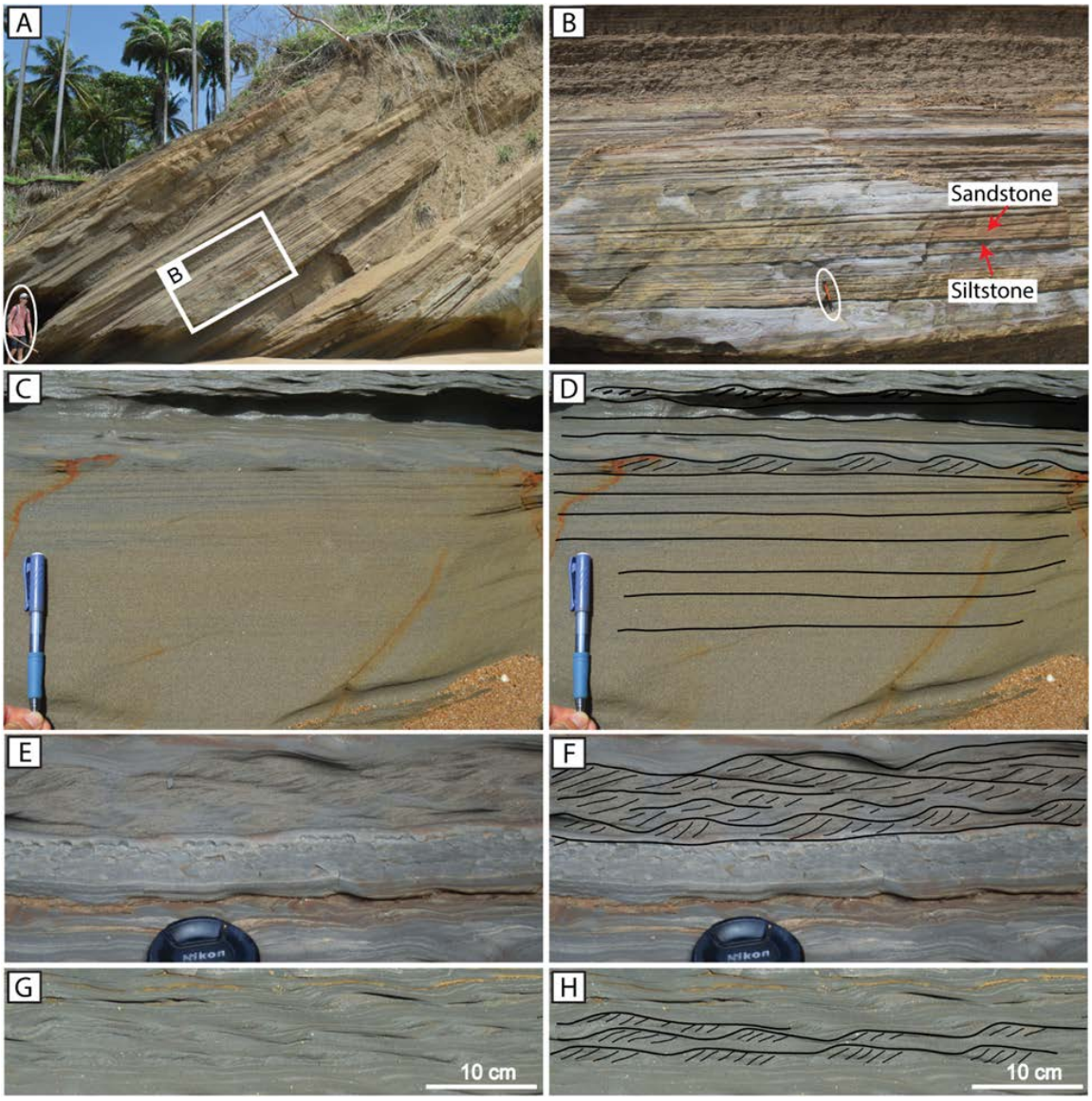

Figure 3.9: Characteristics of thin-bedded parallel- and ripple-laminated sandstones (F6). (A) and (B) Parallel-laminated sandstones interbedded with siltstones. (C) and (D) A normal graded bed with parallel-lamination grading into ripple-lamination. (E), (F), (G) and (H) Low-angle climbing ripples.

Upper Slope Facies Summary

The upper slope to gullied uppermost slope environment preserved a variety of sediment gravity flow deposits. The upper slope environment was dominated by muddy and sandy turbidites, debrites and blocks collapsed from the outer shelf (Figs 3.2 and 3.3). The overlying, gullied uppermost slope succession is mudstone-dominated and displays six sediment-gravity-flow-filled gullies, three of which rest on rotated slide blocks with a capping of debris-flow conglomerates and turbidite beds (Figs 3.2B-C and 3.3). The highly irregular erosion surfaces are interpreted as slump scars (i.e. the excavated track of the slides) which attracted subsequent infilling by sediment gravity flows. The abundance of turbidites, debrites, slumped blocks and other soft-sediment deformed units (Facies F1 to F6) all suggest that the lower part of the study succession, was situated in the upper-slope environment. In particular, the very large collapse blocks of consolidated hummocky and swaley cross-stratified sandstones (Facies F1) strongly support that the setting was below the shelf edge and not landward of the shelf edge. The lack of bioturbation in these facies, except for the collapsed blocks from the outer shelf, further supports the interpretation of upper slope environment.

Outer shelf environment

The upper part of the study succession (140 to 260 m in Fig. 3.3), interpreted as outer shelf environment, is characterized by muddy deposits grading upward into repeated upward-coarsening and upward-thickening packages of sandstones (Fig. 3.10A).

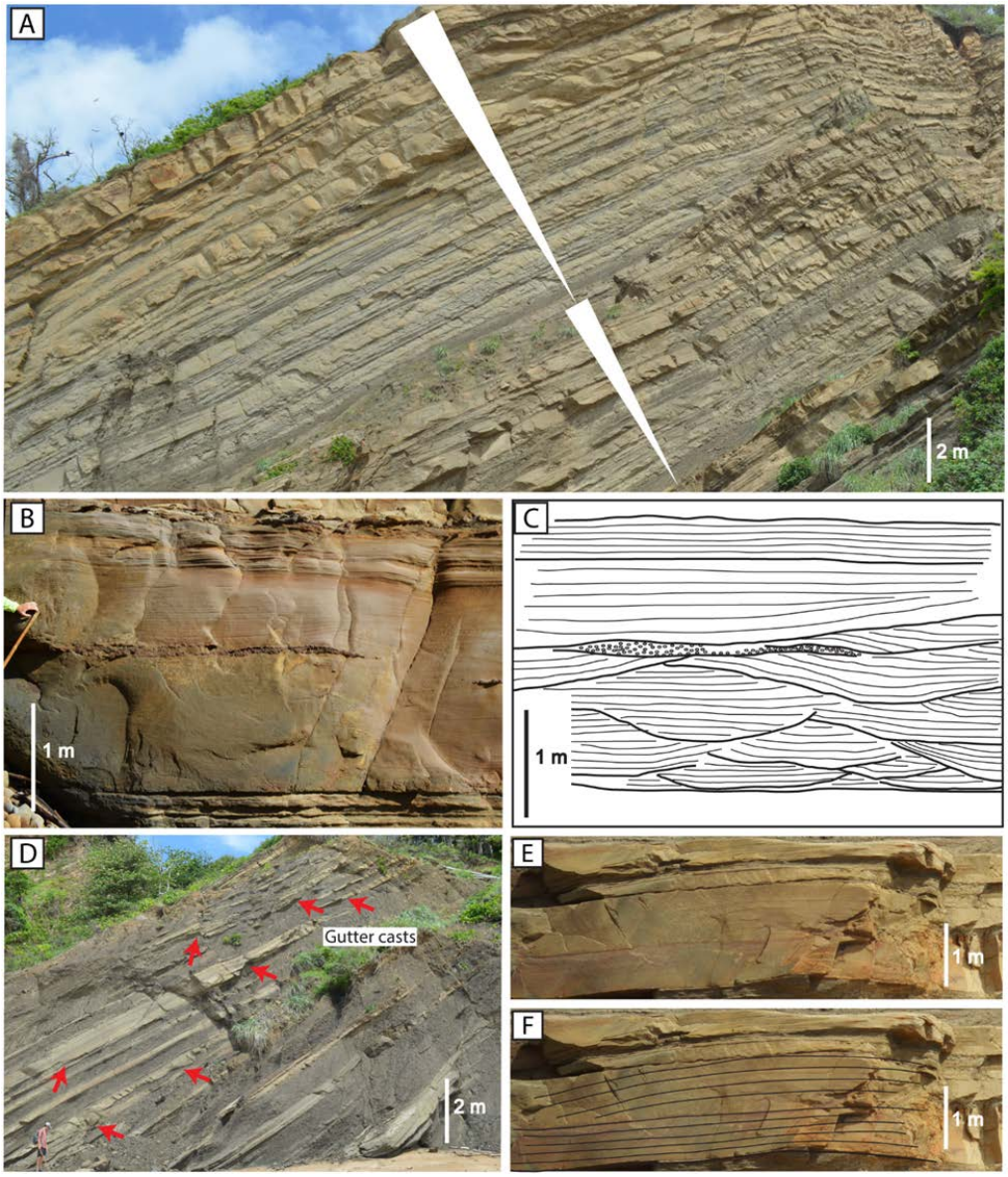

Figure 3.10: (A) The delta-front environment is characterized by repeated upward-coarsening and upward-thickening motifs (1 to 3 m thick). (B) and (C) Photograph and sketch of amalgamated swaley cross-stratified sandstone sets (F7) illustrating scour surfaces mantled with mudstone clasts and overlying undulating lamination gradually changing to upward-flattening lamination. (D) The underlying muddy prodelta deposits, transitional between the overlying delta front and underlying gullied upper slope, contain sets of isolated to amalgamated, sand-filled gutter casts. (E) and (F) Single hummocky cross-stratified sandstone bed (F8) displaying parallel lamination and slightly upward-arching lamination.

Facies 7 (F7): Amalgamated swaley cross-stratified (SCS) sandstones

Facies F7 comprises thick units of lower to upper very fine-grained sandstones (containing cosets of cross-strata up to 3 m thick), characterized by amalgamated sets of low-angle cross-strata (Fig. 3.10A to C) with sharp tops and bases bounded by mudstones. The thickness of the swaley cross-stratified sandstone units increases upward in the succession, and mudstone bed thickness decreases correspondingly. Individual sandstone laminasets are bounded by low-angle (up to 30° dip) erosional surfaces with internal laminae approximately parallel to the lower bounding surfaces and gradually passing upward into flat laminae (Fig. 3.10B and C). The scours are 1 to 10 m wide and 10 to 40 cm deep, and are commonly mantled with well-rounded mudstone clasts. Sets commonly show long wavelength (up to 10 m long) concave laminations that overlie a flat to undulose basal scour surface with an upper symmetrical-ripple laminated zone (5 to 20 cm thick). Plant fragments occur in places, and bioturbation is scarce (BI = 0 to 1) with occurrence of *Ophiomorpha*.

The swaley cross-stratified (SCS) sandstones represent high energy storm-wave reworking of sand deposits between storm-wave base and fair-weather-wave base. The deposits were generated by combined flows that most probably had a strong oscillatory component (during the storms) with a weak unidirectional component (Southard et al., 1990; Dumas et al., 2005; Dumas and Arnott, 2006). The preferential preservation of erosional swales over constructional hummocks is because of deposition in relatively shallow water where the scouring is frequent and the aggradation rate is low (Dumas and Arnott, 2006). The symmetrical ripples are wave ripples either formed by wave reworking during the waning stage of a storm or later fair-weather conditions (Bowman and Johnson, 2014). The sequence of sharp-based SCS with mudstone clasts to wave-rippled beds on top records rising and waning stages of a storm event as follows: (i)

during the rising phase of the storm, sediment is suspended and the muddy sea floor is eroded to form the erosional surface; (ii) as the storm starts to wane, initial parallel-laminated sand is deposited under powerful combined flow conditions; (iii) as the storm continues to wane, sediment settling forms SCS, eventually mantled by small wave ripples (Cheel, 1991; Cheel and Leckie, 1993; Plint, 2010). The rare bioturbation and occasional plant fragments suggest a stressed condition due to close proximity to a river as the sediment source (MacEachern et al., 2005; Buatois et al., 2012) with additional factors such as oceanic swells (Dasgupta et al., 2016), and therefore the facies is interpreted as storm-wave reworked proximal delta front.

Facies 8 (F8): Hummocky cross-stratified (HCS) sandstones

Facies F8 consists of lower very fine-grained sandstones (10 to 50 cm thick) commonly overlying mudstones (10 to 70 cm thick), and they typically occur in the muddy succession (i.e. 140 to 180 m in Fig. 3.3). The bases of sandstone beds are irregular and sharp as isolated gutter casts (10 to 80 cm deep and 3 to 15 m wide) that become amalgamated in places (Fig. 3.10D), and they grade upward into flat and sharp bases (Fig. 3.10E and F). The sandstones are characterized by a thin unit of parallel lamination progressively grading upward to concave-upward laminations (Fig. 3.10E and F). The internal stratification within the sandstone beds is very low angle (less than 15°) and defines concave-convex geometries with wavelengths of 3 to 5 m. Overall the bioturbation in the HCS sandstone beds is rare (BI = 0 to 2) with the occurrence of *Ophiomorpha*, *Skolithos*, *Zoophycos*, *Phycosiphon* and *Planolites* in places.

The convex-upward lamination style in this facies is characteristic of hummocky cross-stratification (HCS) displaying geometric similarity to swaley cross-stratification (SCS) but generally occurring below SCS in an upward coarsening shallow-marine

succession (Leckie and Walker, 1982; Duke, 1985). The gutter casts represent erosion of the substrate caused by storm waves. The HCS is generated by storm-wave currents under combined flows with a strong oscillatory component and a weak unidirectional component between storm-wave base and fair-weather-wave base (Dumas et al., 2005; Dumas and Arnott, 2006; Plint, 2010). The preferential preservation of hummocks rather than swales indicates that the sediment aggradation rates were sufficiently high to accrete sediment vertically (Dumas and Arnott, 2006). The scarcity of trace fossils and significant thickness of associated mudstones (10 to 70 cm thick) suggest that they were storm-wave reworked distal delta front deposits.

Facies 9 (F9): Siltstones and mudstones

Facies F9 consists of dark grey, structureless/graded to laminated siltstone and mudstone beds (forming units 0.5 cm to 9.0 m thick) and occurs throughout the study succession (Fig. 3.11). In the upper third of the measured section (Fig. 3.3), inversely to normally graded beds of siltstones and mudstones are observed in places, and they commonly overlie rippled sandstones with sharp erosional bases (Fig. 3.11B). The cross laminae of the ripples are tangential towards the lower set boundary and dip at variable angles in opposite directions (Fig. 3.11B). The bioturbation is rare with an assemblage of *Chondrites* and *Planolites* (BI = 0 to 1) in the siltstones and mudstones (Fig. 3.11C). Siltstone and mudstone beds in other parts of the section described here are faintly laminated to structureless and lack bioturbation (BI = 0).

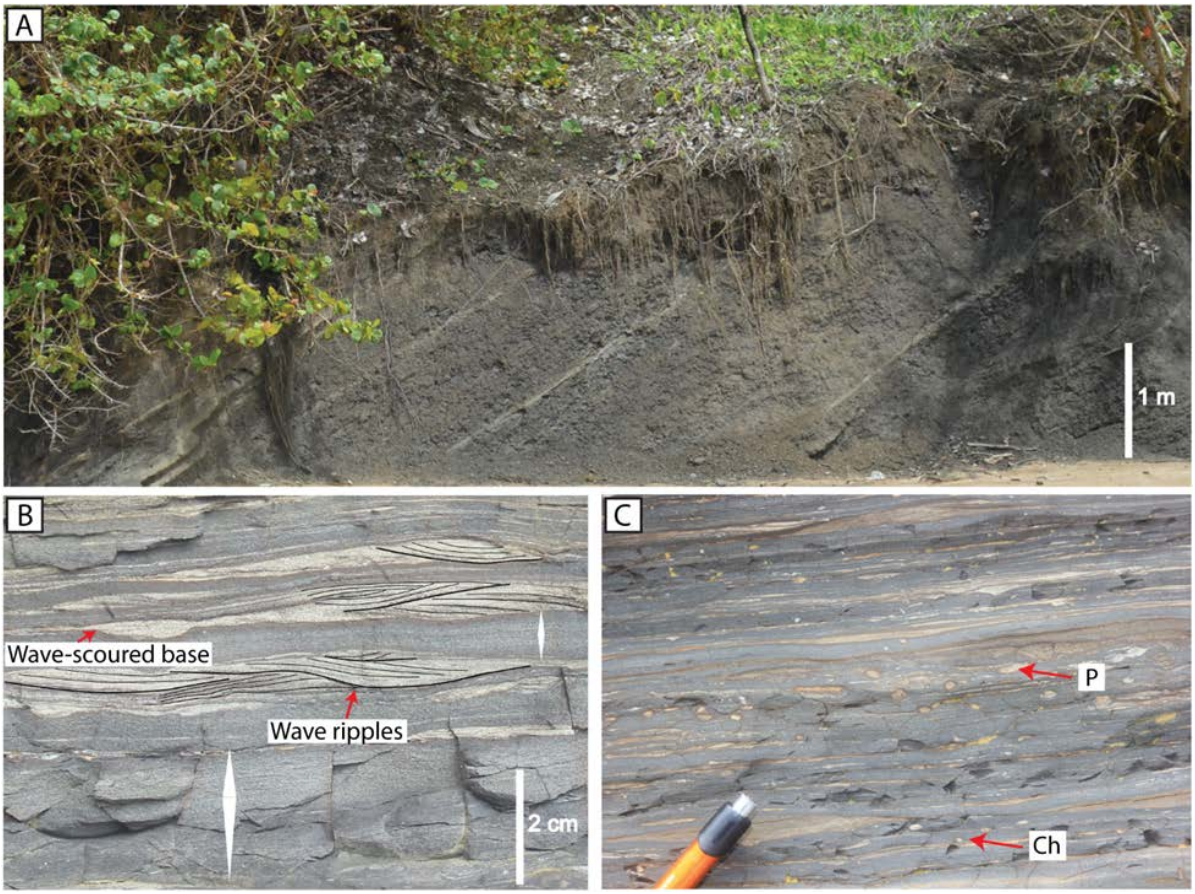

Figure 3.11: Characteristics of siltstones and mudstones (F9). (A) Thick dark-grey laminated mudstones. (B) Inversely to normally graded beds of siltstones and mudstones overlying the lenticular and wave-rippled sandstones with sharp wave-scoured bases. (C) Bioturbated mudstone beds showing *Chondrites* (Ch) and *Planolites* (P) trace fossils.

The siltstone and mudstone beds in the upper third of the measured section (Fig. 3.3) were deposited in a delta front and prodelta setting. The oppositely dipping ripple laminae with variable dip angles are interpreted as wave ripples (de Raaf et al., 1977). The sharp erosional bases to the rippled sets represent storm-wave-generated scoured surfaces on which the wave ripples were subsequently deposited. The overlying inversely to normally graded siltstones and mudstones are interpreted as the products of storm-wave-enhanced muddy sediment gravity flows given the fact that the muddy beds are

commonly associated with wave ripples (Bhattacharya and MacEachern, 2009; Macquaker et al., 2010; Plint, 2014). Alternatively, the inversely to normally graded siltstones and mudstones can also be turbidites (mud density flows) (McCave and Jones, 1988; Talling et al., 2012b) or hyperpycnal flow deposits (Mulder et al., 2003). The low-diversity and low abundance trace fossil assemblage in the laminated siltstone and mudstone beds suggests a rapidly deposited muddy deposit (Bhattacharya and MacEachern, 2009) and/or a stressed-shelf environment indicating the proximity to delta distributary mouths (MacEachern et al., 2005; MacEachern and Bann, 2008). The structureless and unburrowed mudstones in the lower section (i.e. 0 to 140 m in Fig. 3.3) suggest rapid deposition of cohesive muddy debris flow (Mulder and Alexander, 2001). The parallel-laminated mudstones in the upper slope environment indicate deposition under low-energy conditions.

Outer Shelf Facies Summary

The outer shelf environment exhibits muddy prodelta deposits grading upward into sandy delta-front deposits dominated by hummocky cross-stratified and swaley cross-stratified sandstones. The coarsening-upward succession, coupled with rare bioturbation represents the progradation of storm wave-dominated delta front on individual deltaic lobes. The isolated hummocky cross-stratified sandstone beds gradually changing upward to amalgamated swaley cross-stratified sandstone beds indicate increased storm-wave influence upward in the delta front. Despite the common absence of distributary channels cutting down into delta front strata, the interpretation of storm wave-dominated shelf-edge delta rather than a simple, non-deltaic outer shelf is also supported by the sand-prone character of the succession and the clear upward-coarsening

character of the 200 m thick units, implying marked progradation of the shelf edge (Fig. 3.1B and C) (Sydow et al., 2003; Dixon, 2005).

DEPOSITIONAL ENVIRONMENT AND PALEOGEOGRAPHY

The deposits of the mid-Pliocene Moruga Formation as described above exhibit a range of depositional systems from sand-rich, outer-shelf and shelf-edge wave-dominated delta lobes of the Trinity Hills Sandstone (Facies F7 to F9) transitioning downward to the St. Hilaire Siltstone that is dominated by very large slide blocks and intervening irregular gullies filled with mudstone and sandstone sediment-gravity flow deposits. At the base of the study succession there is a large, chaotically infilled area with mass transport deposits, all within an upper slope setting (Facies F1 to F6) (Fig. 3.12). A great thickness of muddy St. Hilaire Siltstone (>200 m thick), which represents deepwater slope deposits, occurs below the study area but is only rarely exposed.

Although the wave-dominated deltas on the outer shelf are likely to have had a lower number of coeval distributary channels than those in river-dominated deltas (Bhattacharya and Giosan, 2003), the high sediment supply of the paleo-Orinoco River would have enabled the delivery of large volumes of sand to the delta front. The open Atlantic storm waves and swells subsequently reworked sands into laterally extensive delta lobes and strandplains close to the shelf edge (Fig. 3.12). Evidence from nearby well data (Sydow et al., 2003) suggests that the outer shelf sandstone belts commonly accumulated thicknesses up to 200 m on the outermost and deepest parts of the shelf. The location of the study site was probably adjacent to one of the delta distributary mouths because marine bioturbation is not well-developed (Facies F7, F8 and F9).

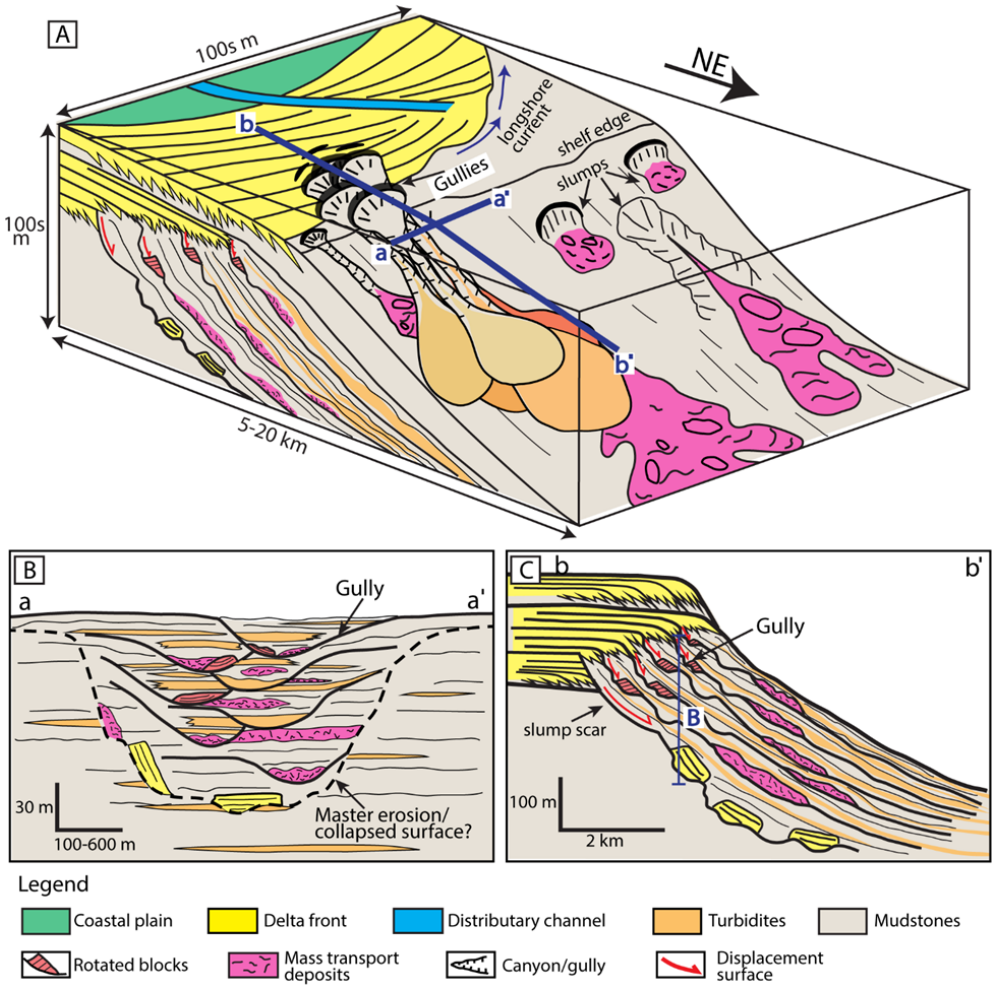

Figure 3.12: (A) Schematic three-dimensional block diagram of the interpreted paleo-geomorphology and depositional environments in the mid-Pliocene Orinoco Delta (Moruga Formation). Slope gullies extended back onto storm wave-dominated delta front on the outer shelf, captured longshore-drifted sands, and transported sands to the deep water. Turbidites in the amalgamated gullies are shown by a range of orange color to illustrate that they are derived from different episodes of gully infilling processes. (B) Cross-section view along the depositional strike illustrating stacked gullies filled with a variety of mass-transport and sediment gravity flow deposits. The dashed line indicates a possible master collapsed surface which constrains the development of amalgamated gullies. (C) Cross-section view along the depositional dip illustrating the collapsed scar of shelf margin with the overlying sets of slope gullies and renewed delta front deposits. Note that the rotational slides in the gullies are preserved near the base of each slump scar.

As the basinward-dipping gradient of the shelf-margin clinoform increased, slumping and mass wasting processes became dominant, leading to the generation of turbidity currents and debris flows on the slope (Mayall et al., 1992; Porębski and Steel, 2003). High sediment supply, together with storms and river floods, caused sets of gullies to be initiated on the upper slope by slope failure processes and eventually to be filled with debris-flow and sandy turbidite deposits (Fig. 3.12). Sandy sediment may also have been captured from the shelf-edge sandbelts through sets of gullies and delivered directly to the deepwater settings (Puig et al., 2003; Marchès et al., 2007). The stacked character of the gullies and common paleocurrent direction (north-east) measured from gully infill deposits indicate the gullies were probably constrained by an underlying larger conduit such as a master erosion/collapsed surface, fault, or canyon (Coleman et al., 1983; Surlyk, 1987; Sylvester et al., 2012). However, it is not possible to draw further conclusions about any such larger conduit due to limited data (see also Dasgupta and Buatois, 2015).

MODEL FOR STRATIGRAPHIC EVOLUTION OF AN UNSTABLE, WAVE-DOMINATED SHELF-MARGIN

Stage I: Storm wave-dominated shelf-edge delta aggradation and collapse

Marked aggradation of Orinoco delta lobes at the shelf edge (Wood, 2000; Chen et al., 2016), is likely to have produced a potentially unstable shelf margin (Fig. 3.13A and B). The deformed blocks of swaley cross-stratified and hummocky cross-stratified sandstones in the basal studied succession (Figs 3.2 and 3.3) confirm that they were deposited and had become consolidated before the collapse event due to the delta aggradation. Several mechanisms can cause the instability of the shelf margin, such as overloading due to either high sedimentation rates (Laugier and Plink-Björklund, 2016),

over-steepening in the distal parts of shelf-edge deltas, strong storms, or earthquakes (Moscardelli and Wood, 2008; Romero-Otero et al., 2010). The overloading of the shelf edge in this study is favored for the following reasons: (i) large volumes of sediment were supplied by the delta distributaries to the delta front, and they became subsequently reworked by storm waves and trapped at the shelf edge leading to overloading; and (ii) the repeated collapse and infill episodes of gullies as well as continued progradation (also see stage II) indicates that sediment supply was extremely high. The local collapse of the shelf edge and uppermost slope at this time resulted in a very rugose upper-slope morphology, also because smaller slope collapses were initiated elsewhere on the slope (Figs 3.12 and 3.13).

Stage II: Intermittent healing of a deforming shelf edge and slope: local slope collapse caused repeated and widespread back-tilted, rotation of strata and subsequent formation of slide-scar gullies; gullies become infilled

The continued progradation of the delta began to heal the collapsed and excavated shelf margin by delivering sediment from the outer shelf to the upper slope (Fig. 3.14C to E). The turbidites and slump units in the lower part of the succession (i.e. level 20 to 60 m in Figs 3.2 and 3.3) contributed to the early infill of the initial collapses on the uppermost slope (Fig. 3.3). The continued and repeated collapse of the shelf edge to upper-slope region (i.e. the level at 60 to 140 m in Figs 3.2 and 3.3) suggests that the shelf margin was still unstable (Moscardelli and Wood, 2008; Romero-Otero et al., 2010), and that mass wasting was frequent leaving slump scars and downslope removal of strata (Callot et al., 2009; Ito, 2013). The outcrop evidence of this is the development of at least six phases of collapse and accompanying landward rotation and backtilting of strata (Figs 3.2 and 3.3), seen by an angular unconformity between many of the rotated blocks and the flat-lying overlying infill strata (Figs 3.2 and 3.3). The disruption of the

slope by each of these events probably created low-lying topographic conduits or gullies, into which new sediment as turbidites and debris flows was eventually channelled. The resedimentation and sediment draping into each slump scar, was generated from either turbidites captured from the shelf-edge delta lobes by frequent storm or flooding events or turbidites and debrites derived from the slope failure processes themselves. Deposition in the gullies eventually terminated in slope lobes. The healing process of the shelf margin was eventually completed after multiple phases of collapse, gully generation and infill (Fig. 3.13E).

Stage III: Continued shelf-edge progradation across the stable rebuilt shelf margin

The repetitive processes of gully formation and infilling ultimately healed the unstable and excavated slope, allowing the stable shelf margin to grow further forward (Fig. 3.13F). Packages of hummocky and amalgamated swaley cross-stratified sandstone beds (F7 and F8) in the upper part of the succession (i.e. 140 to 260 m in Fig. 3.3; Trinity Hill Sandstone Member) display an overall coarsening-upward and thickening-upward trend indicative of a progradation of the storm wave-reworked delta front in the outer shelf environment.

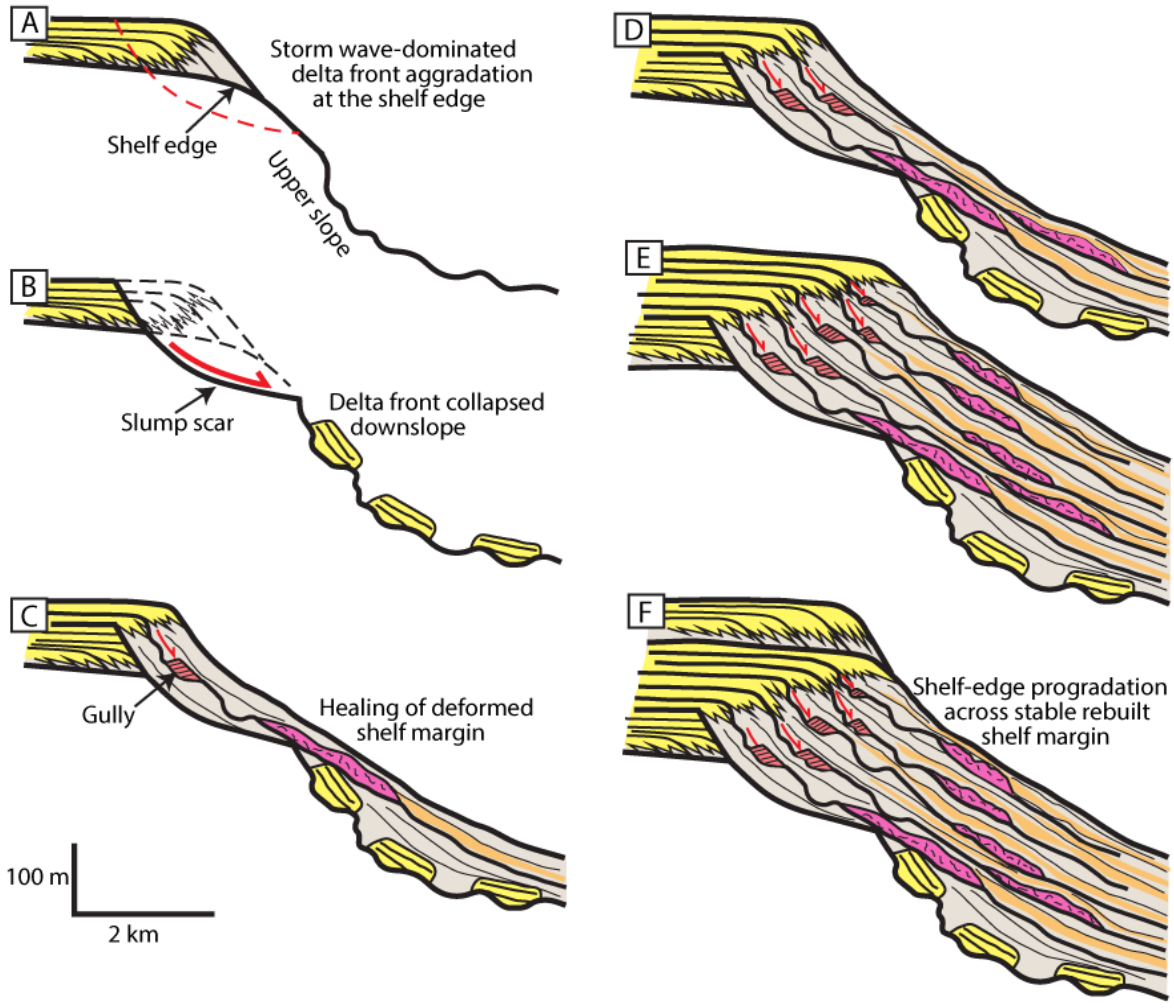

Figure 3.13: Two-dimensional schematic cross-sections demonstrating stratigraphic evolution stages of the shelf-margin growth (Stages I, II and III) associated with the deltaic shelf-edge system. (A) and (B) Stage I: storm wave-dominated delta front aggraded to produce an unstable shelf margin that subsequently collapsed down the slope. (C) to (E) Stage II: intermittent healing of the deforming shelf margin by local collapse, rotational blocks, and gully formation and infilling. (F) Stage III: renewed, storm-wave dominated delta front prograded out across the re-established, stabilized shelf margin. Note that the legend is the same as in Figure 3.12.

DISCUSSION

Comparison with other shelf margins

The unusual aspect of the Moruga Formation compared with other shelf margins is the occurrence of multiple stacked or amalgamated gullies at the shelf edge and uppermost slope within the study area. The amalgamated gullies that incised the outer shelf were able to capture and funnel the sediment from the shelf basinward to the deep-water setting. A series of previously documented shelf margins, including Clinoform 17 of the Eocene margin of western Spitsbergen (Uroza and Steel, 2008), the Oligocene Frio Formation in the Gulf of Mexico (Olariu et al., 2013), the Pliocene–Pleistocene Mayaro Formation of the Orinoco Delta (Bowman and Johnson, 2014; Dasgupta and Buatois, 2015), the Pleistocene Fuji-Einstein system in the northeastern Gulf of Mexico (Sylvester et al., 2012), the Kookfontein Formation in the Tanqua Karoo Basin (Dixon et al., 2013; Laugier and Plink-Björklund, 2016), the Cretaceous deltas of eastern Spitsbergen (Nemec et al., 1988) and the Miocene Cruse Formation of the Orinoco Delta (Chen et al., 2016), exhibit a variety of sediment instability features in front of wave- or river-dominated shelf-edge deltas and are summarized in Figure 3.14 in terms of their degree of shelf-margin instability and gully/channel formation and evolution.

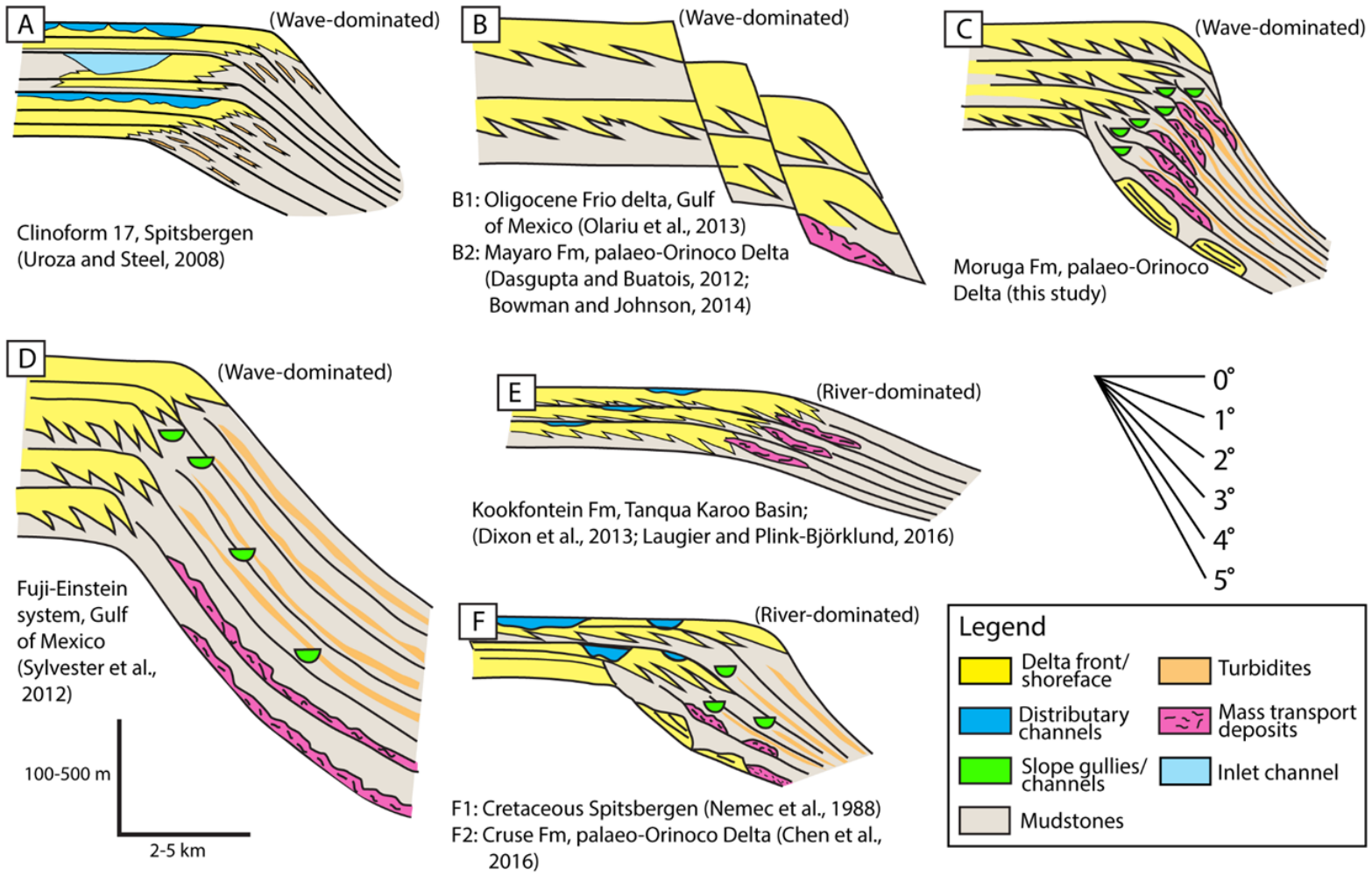

Figure 3.14: Schematic comparison of six types of shelf margins with a variety of sediment instability features from outcrop and subsurface studies. Details are discussed in the text.

The Clinoform 17 of western Spitsbergen (Uroza and Steel, 2008) shows little sediment instability with a storm wave-dominated delta front at the shelf edge and thin sets of tempestites (storm beds) without gullies or channels formed on the upper slope. The lack of deformation has been attributed to the relatively low sediment supply of the Spitsbergen delta system as well as wave-dominated process regime during a rising relative sea level (Porębski and Steel, 2006; Carvajal et al., 2009). In examples of the Frio Formation of the Gulf of Mexico (Olariu et al., 2013; Olariu and Olariu, 2015) and Mayaro Formation of the Orinoco Delta (Bowman and Johnson, 2014), relatively small-scale instability occurs in the form of local growth faults within the wave-dominated shelf-edge deltas as a result of high flux of sediment supply. The stacked gullies of the Moruga clinothem show that slope gullies/channels can develop in front of wave-dominated shelf-edge delta when the sediment supply is sufficiently high to cause collapses. Such amalgamated gullies may possibly evolve to a larger conduit, which is exhibited by the Fuji-Einstein system in the northern Gulf of Mexico (Sylvester et al., 2012). In the Fuji-Einstein system, the channels began to amalgamate to form a larger conduit that links shallow-water, wave-dominated shelf-edge delta and deep-water channel and canyon systems, which enabled the delivery of sediment to the deeper-water settings. In contrast to the Fuji-Einstein channel-levée system, the Moruga gullies described herein are characterized by more erosional rather than aggradational architecture (Clark and Pickering, 1996) and they represent embryonic stage of channel development before evolving to a sinuous graded slope channel.

The Kookfontein clinothems of the Tanqua Karoo Basin (Dixon et al., 2013; Laugier and Plink-Björklund, 2016) show sediment failures of mouth-bar deposits from terminal distributary channels and re-establishment of shelf-edge deltas. The relatively high sediment supply by distributary channels together with low gradient (0.5° to 0.75°)

led to sediment overloading at the shelf edge and subsequent collapse to the upper slope (Oliveira et al., 2011; Laugier and Plink-Björklund, 2016). The Kookfontein example represents initial stage of slope channel formation in front of river-dominated deltas caused by collapse rather than hyperpycal flows such as in the Spitsbergen clinothems described by Plink-Bjorklund et al. (2001). The exposures of the Cretaceous Spitsbergen (Nemec et al., 1988) and Miocene Cruse Formation of the Orinoco delta (Chen et al., 2016) demonstrate large-scale slope failure events followed by renewed, progradation of river-dominated shelf-edge deltas and subsequent channels on the shelf edge or upper slope. These clinothems probably represent larger and more established conduit systems on the slope.

Facies of slope gullies compared with slope channels and reservoir implications

Facies in slope gullies are poorly known although previous workers have used high-quality seismic data and seabed-imaging techniques to study the morphology of deep-water gullies (Surlyk, 1987; Chiocci and Normark, 1992; Field et al., 1999; Spinelli and Field, 2001; Surpless et al., 2009; Chiocci and Casalbore, 2011; Sylvester et al., 2012; Lonergan et al., 2013; Prélat et al., 2015). Compared to the well-documented sinuous, aggradational slope channels which contain a variety of architectural elements (i.e. lateral accretion packages, nested mounds, outer-bank bars and levées) (Clark and Pickering, 1996; Abreu et al., 2003; Hubbard et al., 2009; Nakajima et al., 2009), the slope gullies are more likely to be straight and show more erosional features (for example, scours and slump scars) with fewer architectural elements, but they are filled in with a similar spectrum of sediment gravity flow deposits including slides, slumps, debris-flow deposits, and high-density and low-density turbidites. The Moruga gullies are identified by local angular unconformities between the background slope deposits and

gully-infill deposits. In places, back-tilted (landward) rotational blocks occur above local gully bases, and they are derived from shelf-edge and upper-slope collapse and subsequently lie in the distal reaches of slump scars. Slope gullies (i.e. chutes of up to 3 m thick and 50 to 100 m wide) were also documented in the Eocene clinothems of the Central Basin (Spitsbergen), and they were filled with fine or medium-grained turbidites that are linked to hyperpycnal flows from distal distributary channel and mouth bar systems (Plink-Björklund et al., 2001) rather than collapses described herein.

Upper slope gullies in front of wave-dominated shorelines are common in deltas that reach the shelf edge under a strong wave regime, such as along the Gulf of Mexico (Beaubouef and Friedmann, 2000; Sylvester et al., 2012), Rhone (Maillet et al., 2006) and Orinoco shelf edges (Dasgupta and Buatois, 2015). Wave-dominated delta and strandplain systems form high-quality reservoirs of laterally continuous belts of sandstones aligned sub-parallel to the paleoshorelines (Galloway and Hobday, 1983). As the wave-dominated deltas prograde to the shelf edge, the associated increase of accommodation would produce thick and strike-elongate sandbodies which are high-quality reservoirs (Porębski and Steel, 2003; Sydow et al., 2003; Steel et al., 2007). However, the occurrence of slope gullies extending back onto the outer shelf may disrupt the continuity of such reservoirs. Slope gullies filled with heterolithic facies (Figs 3.2 and 3.7) would constitute poor reservoirs and may form barriers to fluid flow. However, thick intervals of high-density turbidites in slope gullies (Fig. 3.8) could be good reservoir facies that form flow paths to locations beyond the shelf edge; they would have to be sealed by slope mudstones on their tops and margins in order to form stratigraphic traps.

CONCLUSIONS

The mid-Pliocene Orinoco shelf margin (Moruga Formation near Guayaguayare Bay) demonstrates a range of depositional systems from a muddy, sediment-gravity flow-dominated, upper slope to gullied uppermost slope succession (St. Hilaire Siltstone) rapidly transitioning upward to sand-rich, outer-shelf and shelf-edge wave-dominated delta lobes (Trinity Hills Sandstone).The 140 m thick sediment gravity flow and soft-sediment deformation facies at the base of the documented succession are interpreted as deposits on the uppermost slope rather than those caused by shelf delta-front instability, because the very large collapse blocks of consolidated hummocky and swaley cross-stratified sandstones strongly support that the setting was below the shelf edge rather than landward of the shelf edge. Local episodes of slope collapse are recognized in outcrop by angular unconformities separating landward-tilted strata evacuated from slope slump scars, from overlying flat or gently tilted gully-infill strata. The slope gullies created on top of the slump scars were filled with debrites and turbidites captured from the outer shelf.The study interval of the Moruga Formation provides insight to the growth mechanism of an unstable shelf margin in front of a storm wave-dominated delta system (paleo-Orinoco), as outlined by three sequential stages in shelf margin development: (i) the highly aggradational storm wave-dominated, shelf-edge delta front became unstable and collapsed near the shelf edge; (ii) the collapsed and excavated scars of the shelf margin gradually healed by subsequent repetitive aggradational episodes of gully formation and infilling; and (iii) the storm wave-dominated delta system prograded out across the healed and re-established shelf edge and slope, allowing renewed forward growth of the newly stabilized shelf margin. Storm wave-dominated shelf edges are often characterized by limited sand delivery immediately across the adjacent slope break, because of dominance of longshore, strike-feeding of sediment. However, amalgamated

gullies can form conduits that extend back onto the shelf edge to capture longshore drifting sand, thus providing the potential to deliver large volumes of sand across the upper slope to deep-water settings.

Chapter 4: Mixed-energy process interactions read from a compound-clinoform delta (paleo-Orinoco Delta, Trinidad): preservation of river and tide signals by mud-induced wave damping[2]

ABSTRACT

A segment of the Pliocene Orinoco Delta on Trinidad preserved a progradational compound clinoform that reveals detailed interaction of river, wave, and tide processes with fluid mud at a scale of tens of meters to centimeters in the deposits. Based on sedimentary structures, grain size, bioturbation, and organic-matter content, each measured bed or bed set was assigned a probability percentage of having been dominated by a particular process and process probabilistic histograms were generated. Characteristic river signals in these deposits are rare, and are represented by outsized grain sizes, normally to inversely graded beds, and abundant organic matter, though organic matter can also be derived from vegetated supratidal areas without fluvial influence. Wave and storm-wave signals are recorded by symmetrical ripples, hummocky-swaley cross stratification, and a diverse ichnofauna. Tidal signals are represented by stacked, orderly cross-bedded sandstones with mud drapes, abundant mudstone layers, bidirectional ripple laminae, spring-neap tidal bundles, and a restricted ichnofauna. The study gave the following results: (i) at the scale of regressive parasequences (30-50 m), the intensity of preserved wave signals increased from the prodelta towards the outer delta-front platform and decreased to the inner delta-front platform, whereas there was a reciprocal trend in the intensity of tidal signals; the fluvial signals are generally not strong, but sometimes they become irregularly stronger towards

[2] This chapter has been published as: Peng, Y., Steel, R.J., Rossi, V.M., Olariu, C., 2018. Mixed-energy Process Interactions Read from a Compound-clinoform Delta (paleo–orinoco Delta, Trinidad): Preservation of River and Tide Signals By Mud-induced Wave Damping. Journal of Sedimentary Research 88, 75-90. I was the primary author who conducted the research and drafted this paper with co-authors' help.

the upper levels of a parasequence, (ii) at the scale of individual spring-neap tidal bundles (centimeter to decimeter), thick tidal rippled sandstones with thin to partially eroded fluid-mud layers were deposited during spring tides, and thin tidal rippled sandstones or silt laminae with thick fluid-mud layers were deposited during neap tides on the middle-inner delta-front platform; storm waves reworked the deposits mainly on the outer delta-front platform. The observations suggest that the abundant fluid mud (transported by the wave-driven littoral Guyana Current from the Amazon river mouth) on the delta-front platform caused wave damping and the preferred preservation of river and tidal signals on the middle-inner delta-front platform and distal subaerial delta.

INTRODUCTION

Modern delta systems commonly exhibit compound clinoforms that consist of a subaerial clinoform and subaqueous clinoform with topset-foreset-bottomset morphology (tens of meters in relief) (Fig. 4.1A) (e.g., Pirmez et al., 1998; Driscoll and Karner, 1999; Kuehl et al., 2005; Swenson et al., 2005). The subaerial and subaqueous delta clinoforms are genetically and morphologically linked, and they are separated by a broad subaqueous platform as their bottomset and topset, respectively (e.g., Cattaneo et al., 2003; Swenson et al., 2005; Helland-Hansen and Hampson, 2009; Walsh and Nittrouer, 2009; Patruno et al., 2015a). The subaerial delta clinoforms comprise delta plain, delta-front slope, and delta-front platform (or subaqueous clinoform), and the subaqueous delta clinoforms consist of delta-front platform, prodelta slope, and prodelta bottomset contiguous with the shelf (Fig. 4.1A). The topset-foreset rollover of the subaerial clinoforms is in proximity to the shoreline (e.g., Ta et al., 2002; Correggiari et al., 2005) occurring at water depths of less than 5 m, whereas the subaqueous clinoform rollover lies at a variable distance

(kilometers to tens of kilometers) offshore from the shoreline (Pirmez et al., 1998; Swenson et al., 2005) at water depths of up to 60 m (Patruno et al., 2015a).

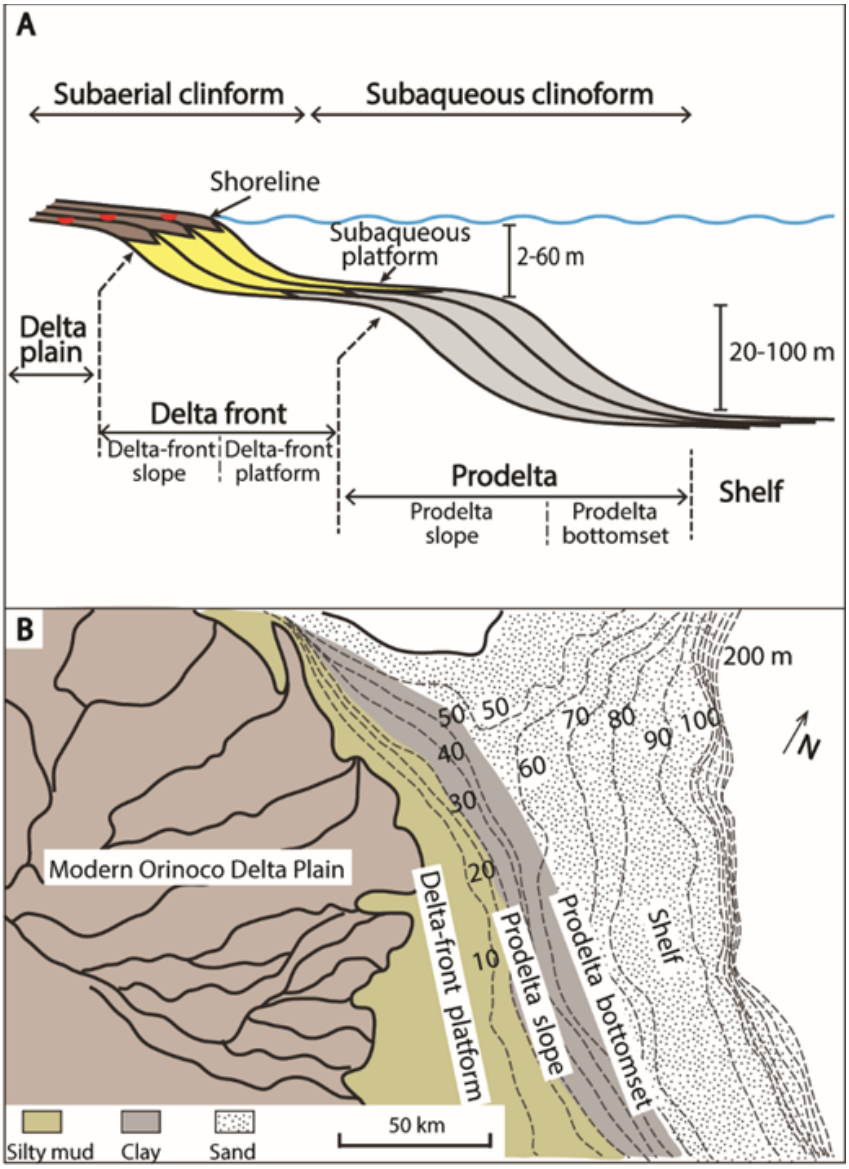

Figure 4.1: (A) Schematic cross section of a deltaic compound clinoform comprising subaerial and subaqueous clinoforms (modified after Helland-Hansen and Hampson, 2009; Patruno et al., 2015a) associated with deltaic subenvironments. (B) Map view of the modern Orinoco delta and shelf with bathymetry and sediment distribution (modified after Warne et al., 2002).

The interplay of fluvial input with shallow marine hydrodynamics (i.e., tides, waves, and currents) controls the sediment dispersal and spatial separation of the subaerial and subaqueous clinoforms (Swenson et al., 2005; Walsh and Nittrouer, 2009). Subaerial clinoforms are mainly affected by fluvial discharge, whereas subaqueous clinoforms are formed by combined basinal processes (tides, waves, and currents) (Pirmez et al., 1998; Driscoll and Karner, 1999; Swenson et al., 2005; Rossi et al., 2016). Some deltas exhibit only a single clinoform when they discharge in low-energy marine (e.g., the Mississippi River delta) or lake settings. The compound clinoforms are well developed in modern muddy deltas situated in energetic marine environments, such as the Amazon (Kuehl et al., 1986; Nittrouer et al., 1986), the Ganges-Brahmaputra (Kuehl et al., 1997; Michels et al., 1998; Kuehl et al., 2005), the Yangtze (Hori et al., 2001; Liu et al., 2006), and the Fly River Delta (Walsh et al., 2004).

The modern Orinoco delta, as one of these examples, also displays compound clinoform geometry with the subaqueous clinoform rollover at water depths of 10 m and 10-50 km seaward from the coast (Fig. 4.1B) (Warne et al., 2002), and it is principally affected by waves, tides, and the northwest-directed Guyana Littoral Current. The Guyana Current transports suspended sediments derived from the Amazon River by fluid-mud banks migrating in the littoral zone (5 m to 20 m water depth or less) along the northeast coast of South America (Allison et al., 2000). The mud banks migrate alongshore by constant reworking of their trailing edges and transport of mud towards their leading edges by waves, during which process large volumes of fluid mud are held in suspension (Allison and Lee, 2004; Anthony et al., 2014). The Orinoco delta receives at least as much muddy sediments from the Amazon as comes from the Orinoco River itself (Eisma et al., 1978; Meade, 1994), and this additional mud promotes shoreline progradation during the Holocene rising to highstand of sea level (Aslan et al., 2003).

Although examples of modern subaqueous delta clinoforms or compound clinoforms have been increasingly documented, ancient examples have been documented only rarely (e.g., Hampson, 2010; Vakarelov et al., 2012; Patruno et al., 2015b; Rossi and Steel, 2016; Hampson and Premwichein, 2017), as the complexity of this process mixing is still understudied. In this study, a muddy compound clinoform of a tide-dominated, wave-influenced delta is described in outcrops where there occurs the distal part of a subaerial delta and the proximal to distal subaqueous delta in a clean, well-exposed, continuous stratigraphic segment of the Pliocene Orinoco Delta within the lower Telemaque Sandstone Member of the Manzanilla Formation on Trinidad. In addition, the outcrop demonstrates high-resolution and high-frequency variations of tide-, wave-, and river-generated facies at both large (i.e., tens of meters), medium (meter) and small (decimeter to centimeter) scales. The mixing of interacting river, wave, and tide processes in this succession is documented using a new quantitative methodology for highlighting process mixing to better understand how the processes interacted on a compound clinoform of the Orinoco Delta. Additionally, the role of the abundant fluid-mud deposits in the study succession is evaluated in terms of how the mud, coming partly from the impinging Guyana Littoral Current system, impacted wave, tide, and river processes during construction of the muddy Manzanilla compound clinoform.

GEOLOGICAL SETTING

Trinidad lies in a plate-boundary zone of significant Neogene structural deformation caused by the Caribbean plate moving eastward and colliding with the South American plate. Intermittent tectonic activity across Trinidad, while the late Miocene-Pliocene sedimentary succession was accumulating, caused southward thrusting and uplift of the Northern Range and probably of the Central Range (Tyson et al., 1991; Babb

and Mann, 1999), producing an incomplete separation of the Northern and Southern sub-basins across which the northeastward- to eastward-directed Orinoco delta system moved (Fig. 4.2) (Tyson et al., 1991; Díaz de Gamero, 1996; Escalona and Mann, 2011).

The Southern Basin (south of the Central Range) was filled by four large-scale clastic wedges as the late Miocene-Pliocene Orinoco Delta system migrated from west to east across Trinidad (Fig. 4.2) (Steel et al., 2007; Chen et al., 2018). These four phases of the late Miocene-Pliocene growth of the Orinoco shelf margin are: (1) the late Miocene to early Pliocene "Cruse" wedge, characterized in outcrop by partially collapsed shelf-edge deltas and deep-water slope and channel-levee systems (Vincent, 2012; Chen et al., 2016) reached as far as southwest Trinidad; (2) the early- to mid-Pliocene "Forest/Moruga/Mayaro" wedge, characterized by mixed-energy river- and tide-influenced deposits in its landward reaches (Forest Formation), and the basinward-equivalent wave-dominated Moruga (Bowman, 2003; Peng et al., 2017) and Mayaro formations, a series of storm-wave-dominated delta lobes that prograded as far as the east coast of Trinidad (Sydow et al., 2003; Dixon, 2005; Dasgupta and Buatois, 2012; Bowman and Johnson, 2014); (3) the mid-late Pliocene "Lower Morne L'Enfer" wedge, characterized by river- and tide-dominated deltas and estuaries in the landward reaches (Lower Morne L'Enfer Formation) (Vincent, 2003; Osman, 2007; Chen et al., 2014), and (4) the latest Pliocene to early Pleistocene "Upper Morne L'Enfer/Palmiste" wedge, characterized by extensive channelized and coal-bearing delta-plain deposits (Chen et al., 2014). The Northern Basin, during the late Miocene-Pliocene, was filled by deepwater turbidites and muddy slope deposits (San Jose Siltstone; Fig. 4.2) as well as younger river- and tide-dominated delta deposits of the Manzanilla and Springvale formations (Huggins, 2007) derived from a northern branch of the paleo-Orinoco River, with some

contributions of coarse-grained sediments from the uplifted Northern Range source (Woodside, 1981).

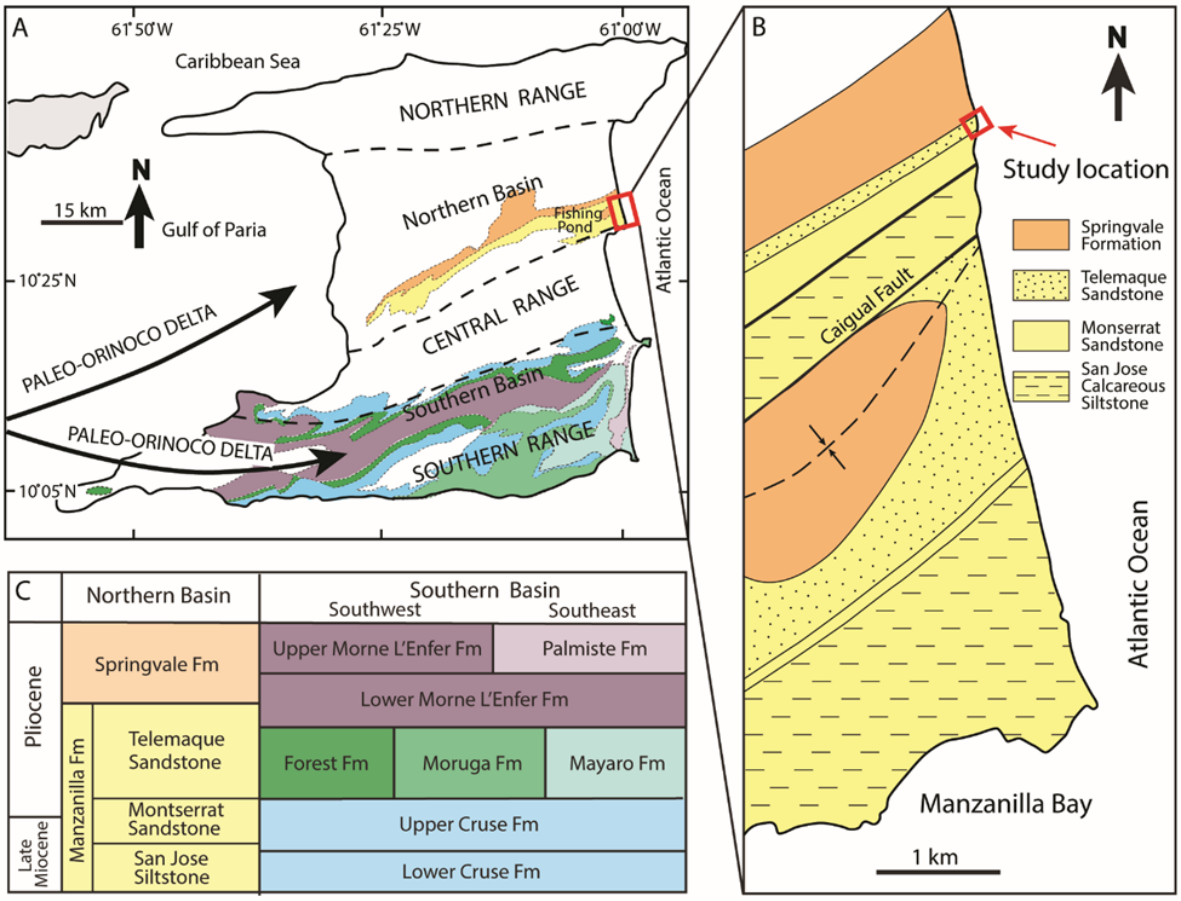

Figure 4.2: (A) Geologic map showing how the late Miocene-Pliocene Orinoco deltaic deposits are currently distributed in the Northern and Southern Basins of Trinidad. Particularly the Northern Range and to a lesser extent the Central Range had some syndepositional relief, whereas the Southern Range is mainly latest Pliocene and younger. (B) The studied succession of the Manzanilla Formation (lower part of Telemaque Sandstone Member) is located on the east coast of Trinidad. (C) Stratigraphic column for the Manzanilla Formation and tentative correlation to the formations of the Southern Basin, from the late Miocene to Pliocene.

The Manzanilla Formation crops out well on the eastern coast of Trinidad, and can be subdivided into the San Jose Siltstone Member, the Montserrat Sandstone Member, and the Telemaque Sandstone Member (Fig. 4.2) (Kugler, 1959). Because this segment of the paleo-Orinoco delta prograded between the Northern Range and embryonic Central Range, the Manzanilla Formation was probably somewhat protected from strong waves of the Atlantic Ocean and thus was dominated by river and tidal processes. The studied interval is a 125-m-thick succession from the mid-Pliocene Telemaque Sandstone Member, and represents a part of the paleo-Orinoco Delta that showed eastward progradation as a deltaic compound clinoform which exhibited an unusually well-preserved mix of tide, wave, and river signals. Although it is obvious that most of Trinidad since the late Miocene was constructed from the paleo-Orinoco system, the various scales of upward coarsening and thickening seen in the study succession strongly suggest the type of progradation that would be expected from forward and lateral movement of delta lobes. Previous large-scale study of the Manzanilla Formation (e.g., Huggins, 2007) also suggested a tide-influenced delta front and distributary channels in the context of the paleo-Orinoco delta.

METHODOLOGY

We follow the new field methodology of Rossi et al. (2017) whereby each measured bed or set was assigned three percentages, reflecting the probability that it was influenced by waves, tides, or river currents respectively, as judged against an extensive literature review of previous work including ancient and modern deposits, and experimental studies. The evaluation was done in this way because some sedimentary structures are reported as capable of being generated by more than one process. Process probabilistic histograms were generated by connecting percentage values of beds from

bottom to top in the study succession. The minor limitation of this method is a reliance on the original literature studies, which can occasionally be subjective and biased (Rossi et al., 2017). However, the methodology does provide a more accurate way to document temporal and spatial changes in process variability. In this study, the higher probability of a specific process (river currents, waves, or tides) is reflected by the following characteristics: (i) river signals in beds are illustrated by outsize grain sizes, structureless or normally graded beds, abundant organic-matter content, and rare or no ichnofauna, (ii) wave and storm-wave signals include symmetrical ripples (de Raaf et al., 1977) and hummocky-swaley cross stratification commonly associated with diverse ichnofauna, (iii) tidal signals are stacked, orderly cross-bedded sandstone sets with mud drapes, abundant mud layers, bidirectional ripple laminae, and spring-neap tidal bundles with restricted ichnofauna species.

The studied section contains a significant amount of mudstones. Fluid-mud and hemipelagic-mud deposits were distinguished and marked in the measured sedimentary log to reveal the interacting relationship between fluid mud and other depositional processes. Fluid mud refers to a mobile subaqueous suspension of muddy sediments (i.e., clay- and silt-size particles), and is formed rapidly by flocculation, commonly in estuarine circulation trapping high suspended-sediment concentration (more than 10 gL^{-1}) in the mixing zone of fresh and salt water (Kirby and Parker, 1983; Uncles et al., 2006; Ichaso and Dalrymple, 2009). Characteristics of fluid-mud deposits are thick layered (commonly more than 0.5 cm thick after compaction) (Dalrymple et al., 2003), homogeneous and structureless, unbioturbated, regular or irregular and squishy in shape (Fig. 4.3A-C). Some fluid-mud deposits can be thinner (a few millimeters) if they are deposited from the distal part of the fluid-mud zone or resuspended by waves and deposited later by tides during slack-water periods. In contrast, hemipelagic-mud deposits

are formed by accumulation by slow, particle-by-particle settling from suspension (sediment concentration less than 0.1 gL^{-1}), and are characterized by relatively thin mudstone layers (1-2 mm thick) (McCave, 1971), with internal lamination, and bioturbation (Fig. 4.3D-F). The hemipelagic-mud deposits in this study are generally darker colored than the fluid-mud deposits, probably because they contain more organic matter (Fig. 4.3).

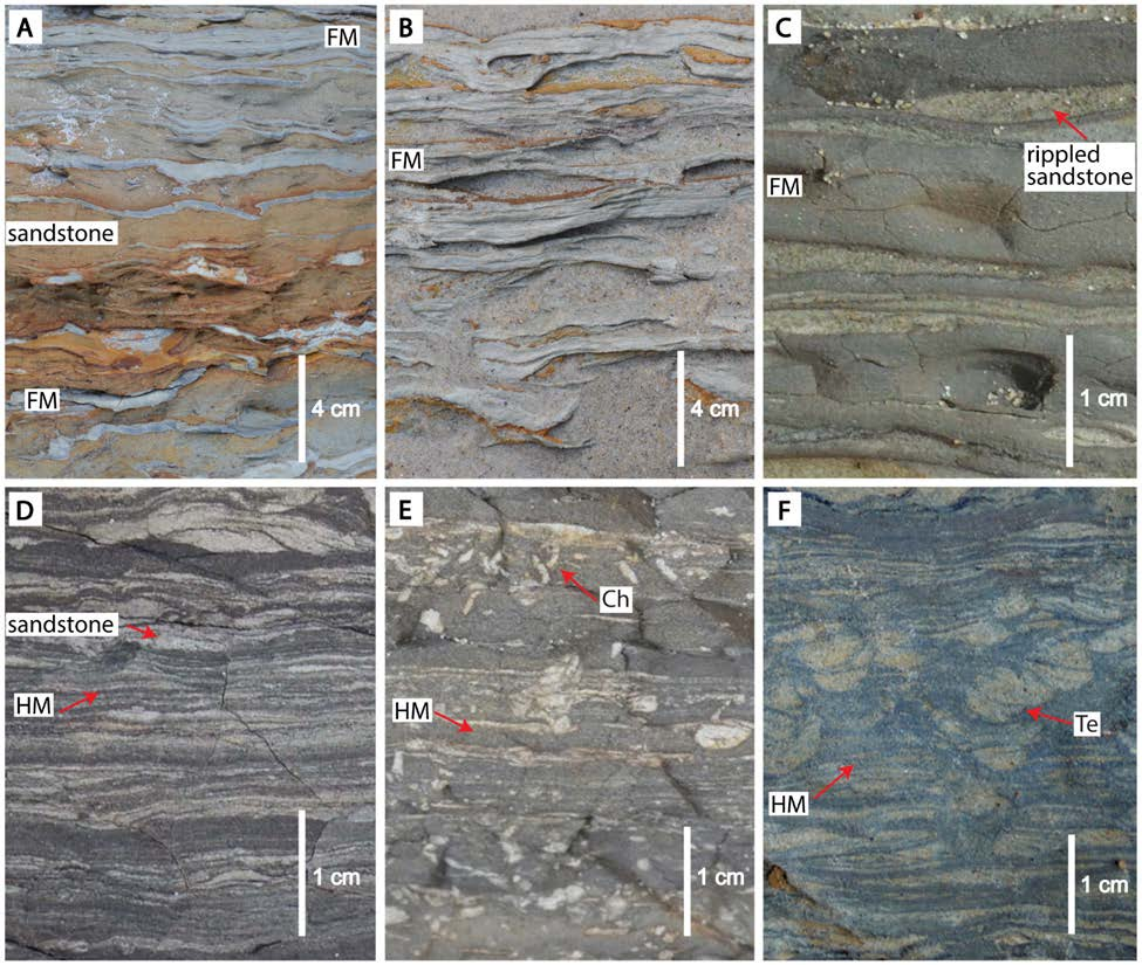

Figure 4.3: Characteristics of the fluid-mud (FM) and hemipelagic-mud (HM) deposits. (A) Squishy, chunky and light-colored fluid-mud layers forming a network around sandstone lenses. The fluid-mud deposits are structureless. (B) Light-colored fluid-mud layers lacking bioturbation. Note that the sandstones are covered with modern sands. (C) Thick, fluid-mud deposits interbedded with thin rippled sandstones showing no bioturbation. (D) Thin, dark-colored hemipelagic-mud layers with internal lamination interbedded with thin sandstone beds. (E) Parallel-laminated hemipelagic-mud deposits with occurrence of *Chondrites* (Ch). (F) Interbedded hemipelagic-mud deposits and rippled sandstones with abundant *Teichichnus* (Te).

OVERALL DEPOSITIONAL ENVIRONMENT

The studied outcrop (125 m thick) comprises three generally coarsening-to-fining-upward (CUFU) units (30 to 50 m thick) with the uppermost unit abruptly overlain by cross-stratified sandstones (3 to 5 m thick) (Fig. 4.4). The lower two CUFU units are relatively muddy, whereas the upper CUFU is sandier, showing a slight increase in sand/mud ratio (Fig. 4.4). The uppermost cross-stratified sandstone units (Figs. 4.4 and 4.5A) are sharp based, and consist mainly of fine-grained sandstones with bidirectional cross-laminated sets dipping in basinward (80°) and landward (260°) directions. Deformed beds of sandstones occur in places, and mud clasts are distributed along some of the foresets and on irregular basal surfaces. The succession below the cross-stratified sandstones is characterized by interbedded thick mudstones and thin beds of upper-very-fine-grained sandstones with lenticular, wavy, and flaser lamination. The sandstones display bidirectional asymmetrical ripples, rhythmic alternations between mudstones and parallel- to rippled-sandstones (Fig. 4.5), hummocky-swaley cross stratification, symmetrical ripples (Fig. 4.6), plane-parallel lamination, inverse and normal grading, and unidirectional asymmetrical ripples (Fig. 4.7). Organic matter is observed either as coaly siltstone or disseminated fragments in sandstone and mudstone beds. The whole succession shows a general low-diversity and moderately abundant trace-fossil suite with an occasional interval of high-diversity and/or high-abundance suite including *Planolites* (Pl), *Chondrites* (Ch), *Teichichnus* (Te), *Phycosiphon* (Ph), *Thalassinoides* (Th), *Skolithos* (Sk), and *Ophiomorpha* (Oph).

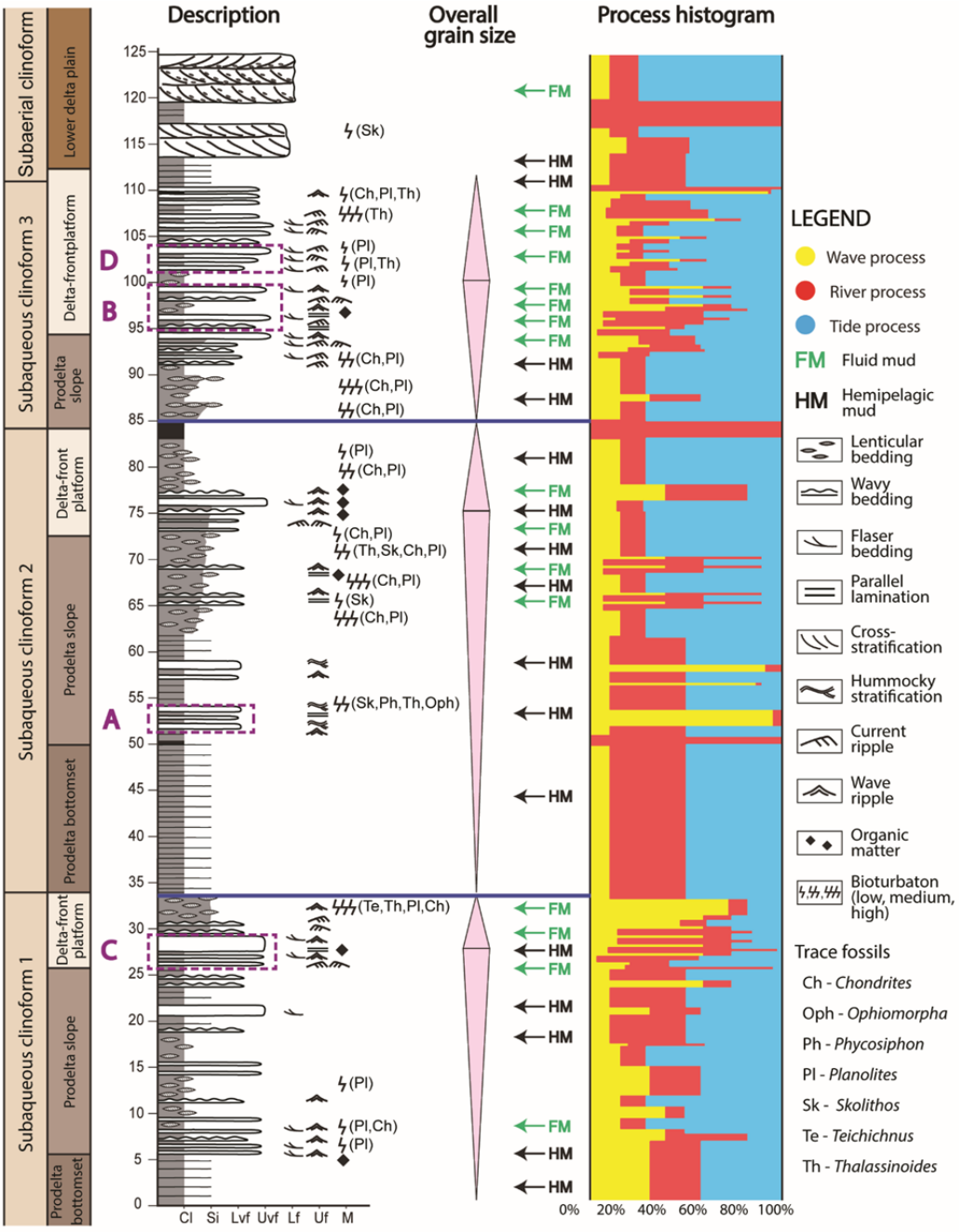

Figure 4.4: The 125-m-thick, studied stratigraphic succession of Telemaque Sandstone, Manzanilla Formation, and the interpreted depositional environments and processes. The positions of fluid-mud (FM) and hemipelagic-mud (HM) deposits are marked along the succession. Note that dashed boxes of A to D indicate stratigraphic positions of studied small-scale, measured sections in Figure 4.9.

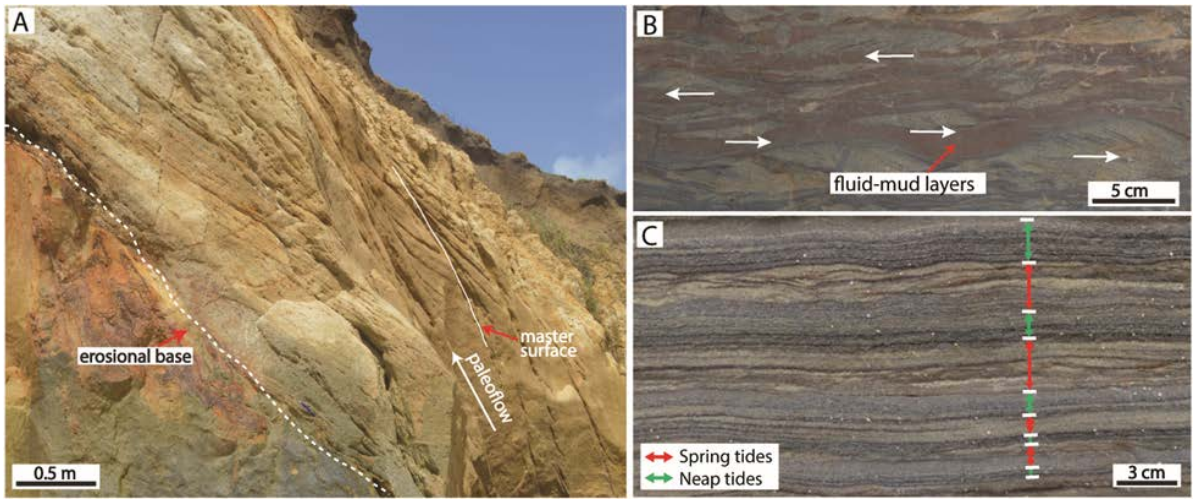

Figure 4.5: Tidal sedimentary structures in the study succession. (A) Sets of cross-bedded sandstones (dunes) with erosional, channelized bases. (B) Tidal bidirectional asymmetrical-ripple laminae associated with relatively thick and continuous fluid-mud layers. White arrows indicate ripple migration directions. (C) Alternations of thick-bedded and thin-bedded sand packages with abundant organic-matter drapes forming spring and neap tidal bundles.

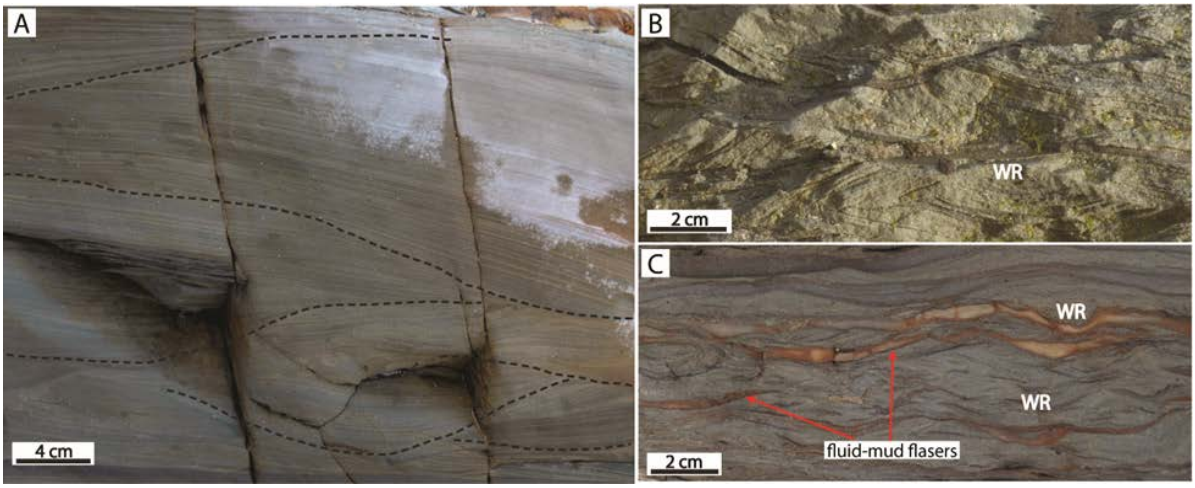

Figure 4.6: Wave (storm waves or waning storm waves) sedimentary structures in the study succession. (A) Hummocky-swaley cross stratification with wave-scoured bases. (B) Wave-ripple cross-lamination (WR) showing occasional chevron-type and offshooting and draping structures, as also described by de Raaf et al. (1977). (C) Wave ripples with mud flasers.

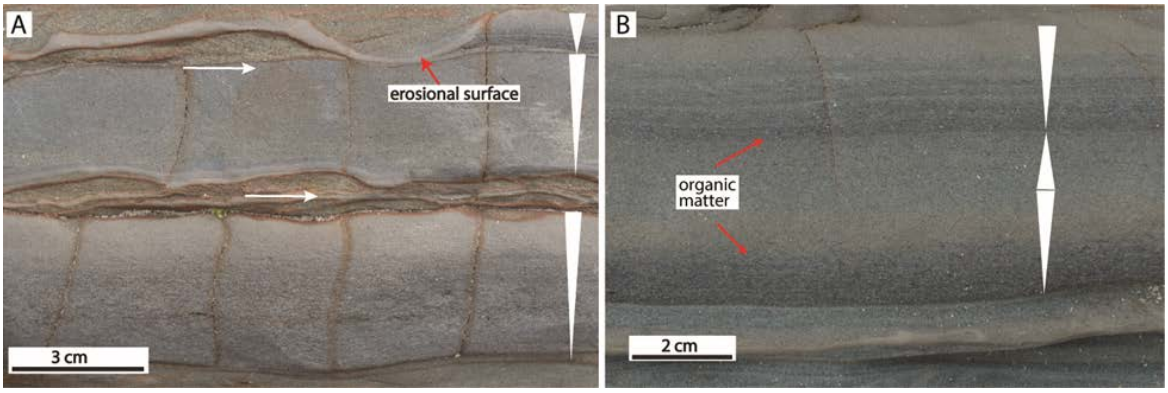

Figure 4.7: Fluvial sedimentary structures in the study succession. (A) Inversely graded sandstone beds with capping asymmetrical ripples and some fluid-mud deposits that are scoured in places. White arrow indicates ripple migration direction. Note that the vertical lines are modern fractures. (B) Inversely and inversely-to-normally graded sandstone beds with dark organic matter.

Each CUFU interval passes from interbedded mudstones and siltstones (millimeters to centimeters thick) upwards to interbedded mudstones and upper-very-fine-grained sandstones (millimeters to centimeters thick). The symmetrical ripples or hummocky-swaley cross stratification show an irregular increase upwards in the coarsening-upward parts of the units towards the coarsest sandstone interval and then a decrease upwards through the fining-upward parts if present (Fig. 4.4). Bidirectional asymmetrical ripples and abundant mud layers have a converse relationship; their abundance decreases upwards to the coarsest sandstone intervals and then increases upwards, respectively. In places, inverse and normal grading and unidirectional asymmetrical ripples occur in sandstone beds (Fig. 4.7). Fluid-mud layers tend to occur mainly in the middle to upper parts of units, notably near the transition between the coarsening-upward and fining-upward parts of units (Fig. 4.4). The fluid-mud deposits are associated with both symmetrical and bidirectional asymmetrical ripples, but they tend to be relatively thick and continuous in between sandy layers with bidirectional

asymmetrical ripples (Fig. 4.5B) and commonly thin and broken as mud flasers in between symmetrical ripples (Fig. 4.6B and C).

The described 125-m-thick succession is interpreted to represent the distal parts of a prograding delta with compound clinoforms. The deltaic stratigraphy comprises two stacked subaqueous clinoforms (i.e., 0-85 m in Fig. 4.4) and an upper, third subaqueous clinoform overridden by the distal part of a subaerial clinoform (i.e., 85-125 m in Fig. 4.4); see also the depositional reconstruction diagram in Figure 4.8. Each subaqueous clinoform (CUFU) shows a coarsening-upward succession from the muddy prodelta to the sandier prodelta slope and outer delta-front platform, and a fining-upward succession from the outer to inner delta-front platform (Goodbred and Saito, 2012) (Fig. 4.4). The lower two muddy CUFU units represent the distal clinoforms of subaqueous deltas. It is suggested that as the subaqueous delta prograded, storm waves became dominant and therefore reworked the distal river-mouth bars or tidal bars and transported sediments to the outer delta-front platform and prodelta slope (Fig. 4.8A). The upper part of the succession (85-125 m) represents the most landward subaqueous clinoform overlain by the distal part of subaerial clinoform (lower delta plain) with tidal channels filled with bidirectional cross-bedded sandstones (Fig. 4.8C). The progradation of the deltaic succession was driven by relative sea-level fall or increased sediment supply during relative sea-level rise. In support of the latter, a relative sea-level rise or increased subsidence may have been necessary to preserve the subaqueous delta from being intensely incised and reworked by the tidal distributary channels (Goodbred et al., 2003; Storms et al., 2005). Alternatively, the subaerial to subtidal channels overlying the subaqueous delta could also have been caused simply by the lateral migration of distributary channels (Dalrymple et al., 2003).

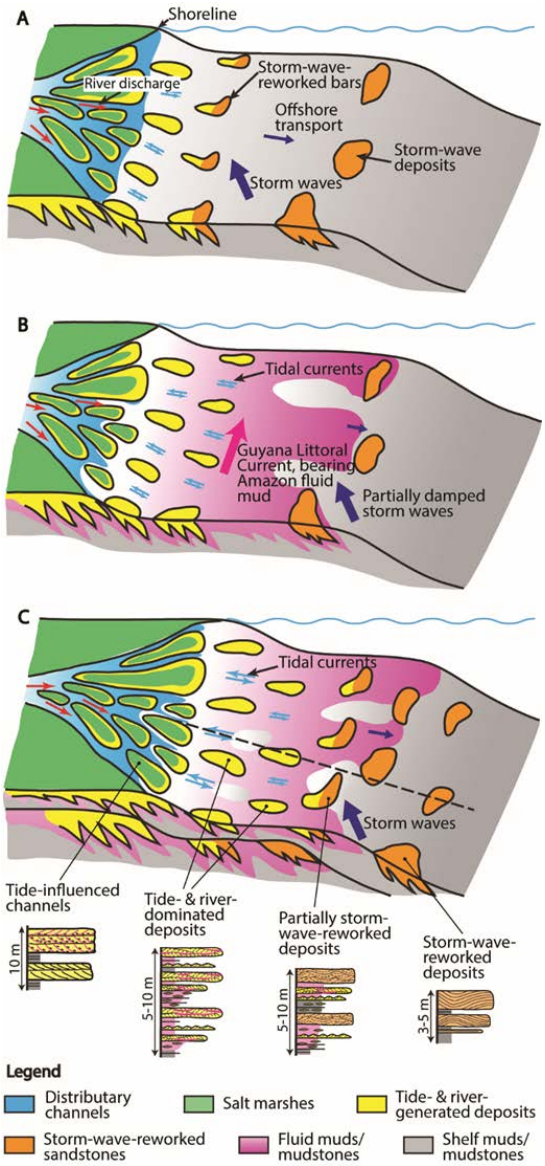

Figure 4.8: (A) Storm waves reworked distal parts of river mouth bars or tidal bars on the inner delta-front platform and transported sediments basinwards onto the outer delta platform to the delta-front slope. (B) Fluid mud was transported and dispersed onto the Orinoco delta-front platform by the Guyana Littoral Current, and this mud damped the subsequent storm waves. (C) Final-stage depositional environments illustrating the prograding subaerial and subaqueous delta clinoform with storm-wave-reworked deposits on the outer delta-front platform and delta-front slope and tide- and river-generated deposits on the middle-inner delta-front platform. The black dashed line indicates the possible location of the described succession.

The mixture of tide-, wave-, or storm-wave-generated sedimentary structures with occasional river-generated deposits indicates an interaction of tide, wave, and river processes influencing the compound delta system at tens-of-meters scales. Bidirectional ripples, abundant mud layers, spring-neap tidal bundles, and stacked, orderly cross-bedded sandstones with mud drapes together with restricted ichnofauna species (Fig. 4.5) result from tidal-process domination (Nio and Yang, 1991; Willis, 2005; Gani et al., 2007; Steel et al., 2012). Symmetrical wave ripples and hummocky-swaley cross stratification (Fig. 4.6), commonly with diverse ichnofauna, suggest wave-dominated processes (de Raaf et al., 1977; MacEachern et al., 2005; Dumas and Arnott, 2006; Gani et al., 2007). Inversely and normally graded beds together with abundant organic-matter content (Fig. 4.7) are associated with river process and may have originated during flooding from nearby distributary channels (Mulder et al., 2003; Olariu and Bhattacharya, 2006; Olariu et al., 2010; Ahmed et al., 2014). Alternatively, the organic matter can have been produced by erosion of fringing supratidal salt marsh as a result of channel switching (Dalrymple et al., 1991).

The frequency of preserved wave signals increased from the prodelta through the prodelta slope towards the outer delta-front platform deposits and then decreased to the inner delta-front platform deposits, whereas the frequency of tide signals had a broadly reciprocal relationship to the wave signals (Fig. 4.4). The fluvial signals were not strong (rare normally to inversely graded beds and unidirectional asymmetrical ripples), but sometimes became stronger (more frequent) towards the upper levels of the succession. The coarsest sandstone interval in each subaqueous delta is interpreted to correspond with stronger wave energy on the uppermost part of the prodelta slope towards the rollover point (Hori et al., 2001; Ta et al., 2005), where wave energy decreased both seaward and landward because of increased water depth and frictional dissipation of shoaling waves,

respectively. The fluid mud was transported and distributed mainly on the delta-front platform as wave energy waned, with a minor proportion on the prodelta slope dispersed by the offshore-directed storm waves (Figs. 4 and 4.8). The presence of significant volumes of fluid mud is another factor that would have caused attenuation of the subsequent storm waves on the outer delta-front platform to inner delta-front platform (Figs. 4.4 and 4.8) (Wells and Coleman, 1981), thereby allowing river- and tide-generated structures to be better preserved on the delta-front platform (Figs. 4.4 and 4.8). A main result from this Pliocene Orinoco delta study is that fluvial and tidal signals were enhanced on the delta-front platform due to the wave damping by the influx of littoral fluid mud from the Amazon Delta transported by the Guyana Current.

DEPOSITIONAL-PROCESS INTERACTION DURING NEAP-SPRING TIDAL CYCLES

At the small scale (decimeter to centimeter), four segments (2 to 5 m thick) were chosen for detailed description from the distal to the proximal setting on the subaqueous delta clinoform, and they not only demonstrate high-frequency interaction of waves, tides, and river currents but also reveal how these processes interacted with fluid mud.

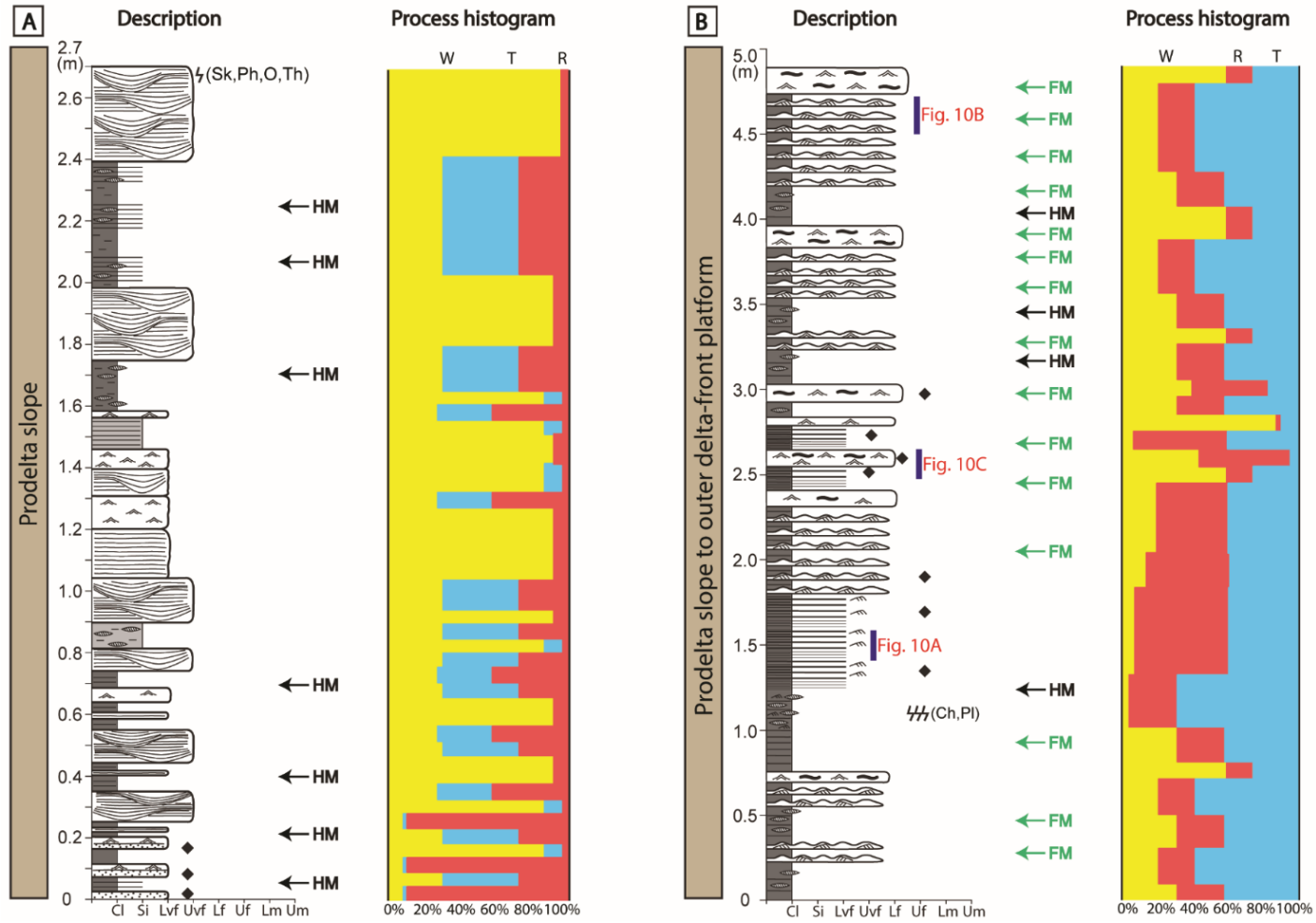

Figure 4.9: caption below.

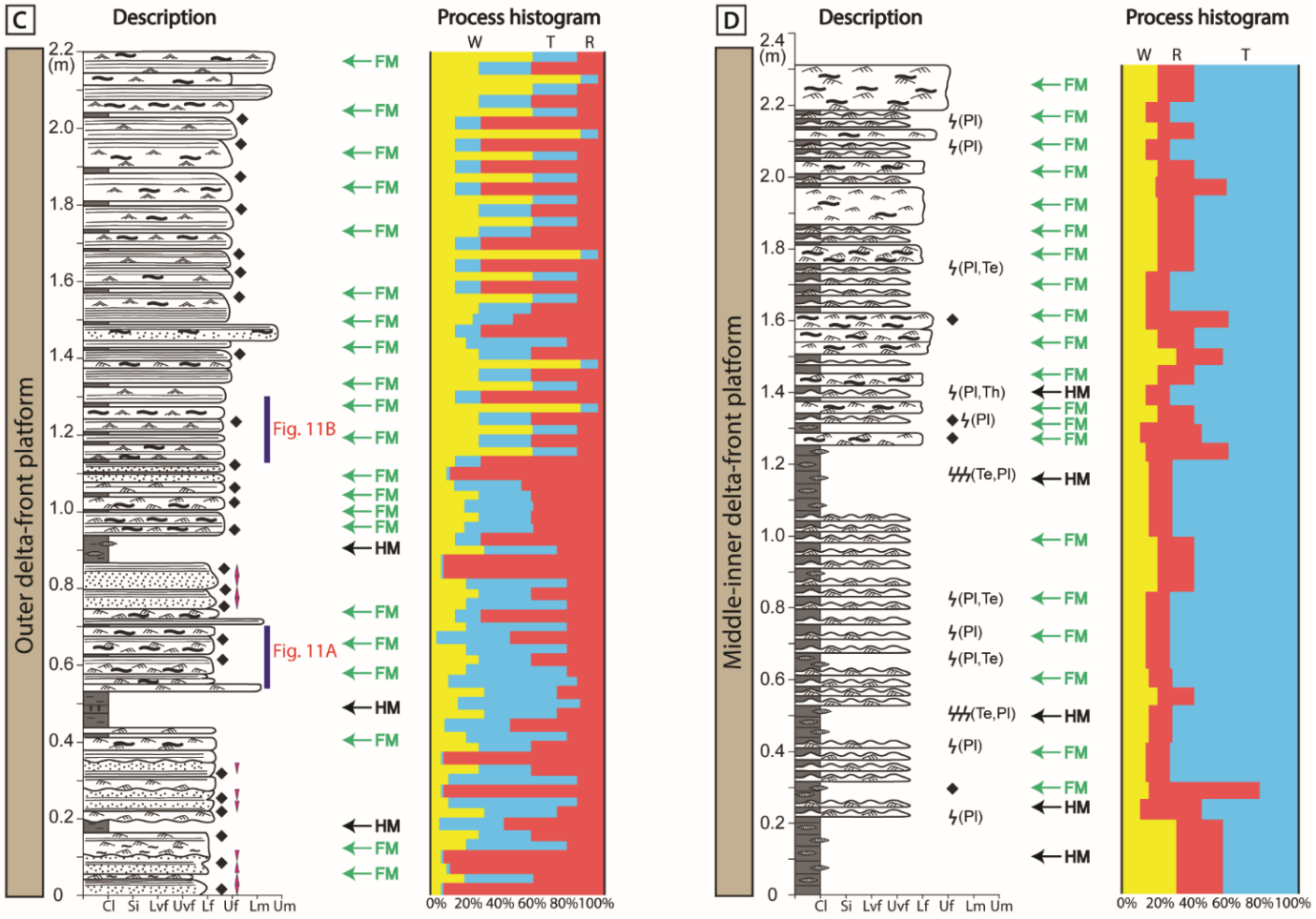

Figure 4.9: (A-D) Details of small-scale, measured stratigraphic sections, interpreted environments, and process changes. Detailed descriptions and interpretations are in the text. The legend is the same as in Figure 4.4. Note that the scale for each segment is different.

Segment A (2.7 m thick, Fig. 4.9A) is characterized by muddy intervals (2-40 cm thick) alternating with stacked sets of fine-grained sandstones (2-30 cm thick) that show hummocky-swaley cross stratification, parallel lamination, symmetrical ripples, and organic-matter-rich normally graded beds. The mudstone beds are parallel-laminated with occasional lenticular sandstones and sparse low-diversity trace fossils including *Planolites* (Pl) and *Teichichnus* (Te). No fluid-mud deposit is observed in segment A. Overall the bioturbation in the hummocky and swaley cross-stratified sandstone beds is rare, with some occurrence of *Skolithos* (Sk), *Phycosiphon* (Ph), *Ophiomorpha* (Oph), and *Thalassinoides* (Th) in places.

Segment B (4.9 m thick, Fig. 4.9B) is composed of interbedded mudstones (mainly fluid-mud deposits) and fine-grained sandstones with flaser, wavy, and lenticular bedding, and it demonstrates a coarsening-upward trend by increasing sandstone/mudstone ratio and sandstone thickness. Alternation of muddy and sandy intervals is observed at decimeter scale (Fig. 4.9B). Muddy intervals (13-70 cm thick) consist mainly of organic-rich heterolithics (Fig. 4.10A) and fluid-mud-dominated intervals (centimeter-scale sets) (Fig. 4.10B). The organic-rich heterolithics are characterized by alternating thick (1.5-2.5 cm thick) beds of parallel-laminated to occasionally current-rippled sandstones and thin (0.5-1.5 cm thick) beds of parallel-laminated siltstones with organic-matter drapes and a few fluid-mud deposits (Fig. 4.10A). In the fluid-mud-dominated intervals, the mudstone-dominated heterolithics comprise thick fluid-mud layers (up to 1 cm thick) and silty laminae or small bidirectional asymmetric ripples (0.2 cm thick), and the sandstone-dominated heterolithics consist of well-developed, bidirectional, asymmetrical sandy ripples (up to 0.6 cm thick) with sharp bases and relatively thin fluid-mud layers (0.1 to 0.3 cm) with erosional tops (Fig. 4.10B). Sandy intervals (6-15 cm thick) are symmetrical-rippled

sandstones (1-2 cm thick) with mud clasts and flasers (Fig. 4.10C). Erosionally overlying and underlying the sandy intervals are heterolithics comprising parallel-laminated sandstone beds and fluid-mud deposits with organic-matter drapes (Fig. 4.10C). The fluid-mud layers show soft-sediment deformation at the top, and they contain carbonaceous detritus locally. Bioturbation is rare, with occurrence of *Planolites* (Pl) and *Chondrites* (Ch) in the mudstone beds.

Segment C is 2.2 m thick (Fig. 4.9C) and consists of thin mudstones (0.5 to 1 cm thick) interbedded with fine-grained sandstones (1-7 cm thick). The sandstone beds or bed sets tend to "bundle" thick and thin (Figs. 4.9C and 4.11). In the lower part of segment C, the thicker intervals (3-4.5 cm thick) show sets of unidirectional to bidirectional asymmetrical ripples, whereas the thinner intervals (1.5-3 cm thick) are characterized by parallel laminations with organic-matter double mud drapes (Figs. 4.9C and 4.11A). In the upper part of segment C, thicker sandstone intervals (7-8 cm thick) are erosionally based, showing bundled sets of micro-swaley to parallel-laminated sandstones with mud flasers and interbedded with thinner, parallel-laminated sandstones (3-4 cm thick) with organic-matter drapes (Figs. 4.9C and 4.11B). Fluid-mud deposits occur as thin layers with deformed or erosional tops when associated with bidirectional asymmetrical ripples (Fig. 4.11A). By contrast, the fluid-mud deposits are preserved as mud flasers and clasts in the micro-swaley sandstones (Fig. 4.11B). The parallel-laminated sandstones with organic-matter drapes generally lack fluid-mud deposits in segment C (Fig. 4.11). In places, inverse or inverse-normal grading and unidirectional asymmetrical ripples are observed, and bioturbation is absent in segment C (Fig. 4.9C).

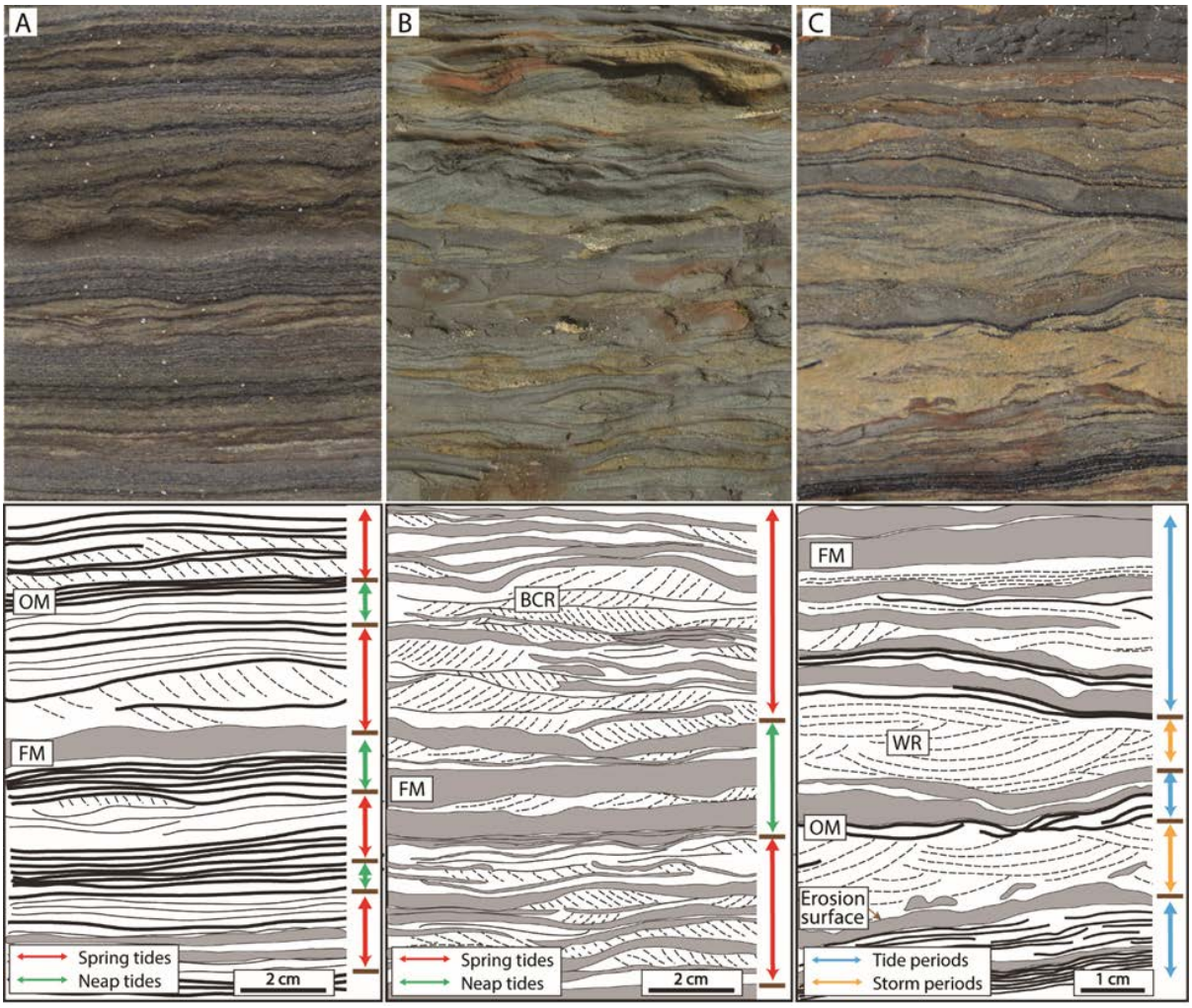

Figure 4.10: (A) Alternating thicker-bedded and thinner-bedded intervals forming spring and neap tidal bundles with abundant organic-matter drapes (OM; indicated by black bold lines) and a few fluid-mud (FM) deposits in the muddy intervals. (B) Alternation of asymmetrical bidirectional current-rippled (BCR) sandstone sets with thick and continuous fluid-mud layers. (C) Intercalated wave-rippled sandstone (WR) beds with erosional bases and fluid-mud clasts and tide-generated heterolithic beds (interbedded sandstones and fluid-mud layers with organic-matter drapes).

Segment D (2.3 m thick, Fig. 4.9D) also displays a similar coarsening-upward trend of facies but is sandier and coarser grained than segment B. This segment consists of interbedded mudstones (mostly fluid-mud deposits) and fine-grained sandstones with

lenticular and wavy bedding in the lower part, and it gradually changes upwards into wavy and flaser bedding (Fig. 4.9D). In places, centimeter-scale cyclic variations in layer thickness are observed. Bidirectional asymmetrical ripples are recognized throughout the segment, and organic matter is richly present in places (Fig. 4.9D). Bioturbation is commonly of low diversity and low abundance, and ichnofauna species are restricted to *Planolites* (Pl), *Teichichnus* (Te), and *Thalassinoides* (Th).

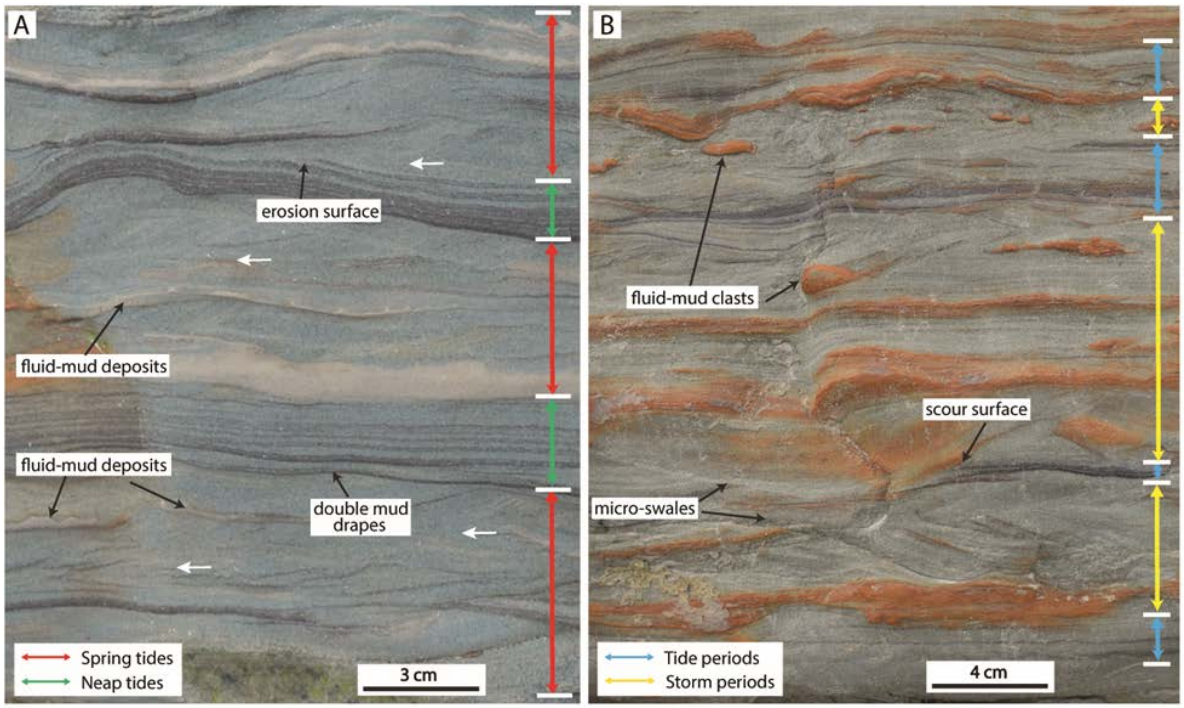

Figure 4.11: (A) Alternating thicker-bedded and thinner-bedded sandy packages forming spring and neap tidal bundles. The thicker intervals contain unidirectional to bidirectional asymmetrical ripples and continuous top-eroded fluid-mud layers with some organic-matter drapes. The thinner intervals are parallel-laminated with double mud drapes that are rich in organic matter. White arrows indicate ripple migration directions. (B) Micro-swaley storm-wave strata intercalated with tidal deposits of parallel-laminated sandstones with organic-matter drapes. The micro-swaley-stratified sandstones are sharp based with fluid-mud clasts and flasers.

Segment A is interpreted to represent deposition during an alternation of storm and inter-storm conditions on the prodelta slope (Figs. 4.1, 4.8, and 4.12), and it displays decimeter-scale storm-wave influence alternating with slight tidal and fluvial influence (Fig. 4.9A). During storm conditions, waves penetrated and reworked deposits into hummocky and swaley cross-stratified sandstones, whereas tidal and fluvial influence was well preserved during inter-storm periods (Vakarelov et al., 2012; Wei et al., 2016). The lack of fluid-mud deposits suggests that the hummocky and swaley cross-stratified sandstones were deposited seaward of the fluid-mud zones (i.e., delta-front platform and proximal prodelta slope) on the prodelta slope (Figs. 4.1, 4.8, and 4.12). Alternatively, segment A could also have been sited basinward of a mud-deficient area, as in this setting there are spatial and temporal variation in suspended muddy sediment concentration nearshore (Anthony and Dolique, 2004). The low-diversity trace fossils in the muddy intervals suggest a stressed environment influenced by tides and river currents (MacEachern et al., 2005; Gani et al., 2007).

Segment B is interpreted as deposits in the transition zone from the prodelta slope to the outer delta-front platform (Figs. 4.1, 4.8, and 4.12), and it exhibits centimeters to decimeters scale alternations of tidal influence with occasional wave and minor fluvial influence (Fig. 4.9B). In the muddy intervals, both the organic-rich heterolithics (Fig. 4.10A) and fluid-mud-dominated heterolithics with bidirectional current ripples represent spring-neap tidal bundles (Nio and Yang, 1991). The thick beds (with occasional current ripples) of organic-rich heterolithics were produced by currents with stronger shear stress during spring tides, and the thin, parallel-laminated beds with abundant organic-matter drapes were deposited by weaker currents during neap tides (Fig. 4.10A) (Dalrymple et al., 1991; Williams, 1991). The lesser amount of fluid-mud deposits in the organic-rich heterolithics probably indicates that fluvial influence was significant and the water

column contained abundant river-derived organic matter, and/or that most of fluid mud was farther landwards on the delta-front platform. The mudstone-dominated heterolithics with thicker fluid-mud layers and smaller bidirectional current ripples are interpreted as deposited during neap tides when the current velocity and corresponding shear stress decreased and the near-bottom suspended-sediment concentration increased; the sandstone-dominated heterolithics exhibiting thinner fluid-mud layers and larger bidirectional current ripples with sharp contacts were produced by spring tides as the velocity and shear stress increased and caused erosion of the previously deposited mud beds and deposition of thicker sand beds (Fig. 4.10B) (Jaeger and Nittrouer, 1995). The sandy intervals characterized by symmetrical-rippled lamination resulted from periods of wave dominance (de Raaf et al., 1977). The scoured surfaces underlying the wave-rippled sandstone beds and the mud clasts and flasers suggest that storm waves eroded the muddy beds and reworked the sandy beds (Fig. 4.10C). The wave ripples are interpreted as produced by waning storm waves, since most fair-weather waves would be damped by the fluid mud and only relatively strong storm waves could have reworked the sediments. The adjacent parallel-laminated sandstones and fluid-mud layers with organic-matter drapes are interpreted as tidal deposits, as the storm waves waned and tides became dominant. The deformed fluid-mud layers with locally concentrated carbonaceous detritus further support deposition by tides during the slack-water periods.

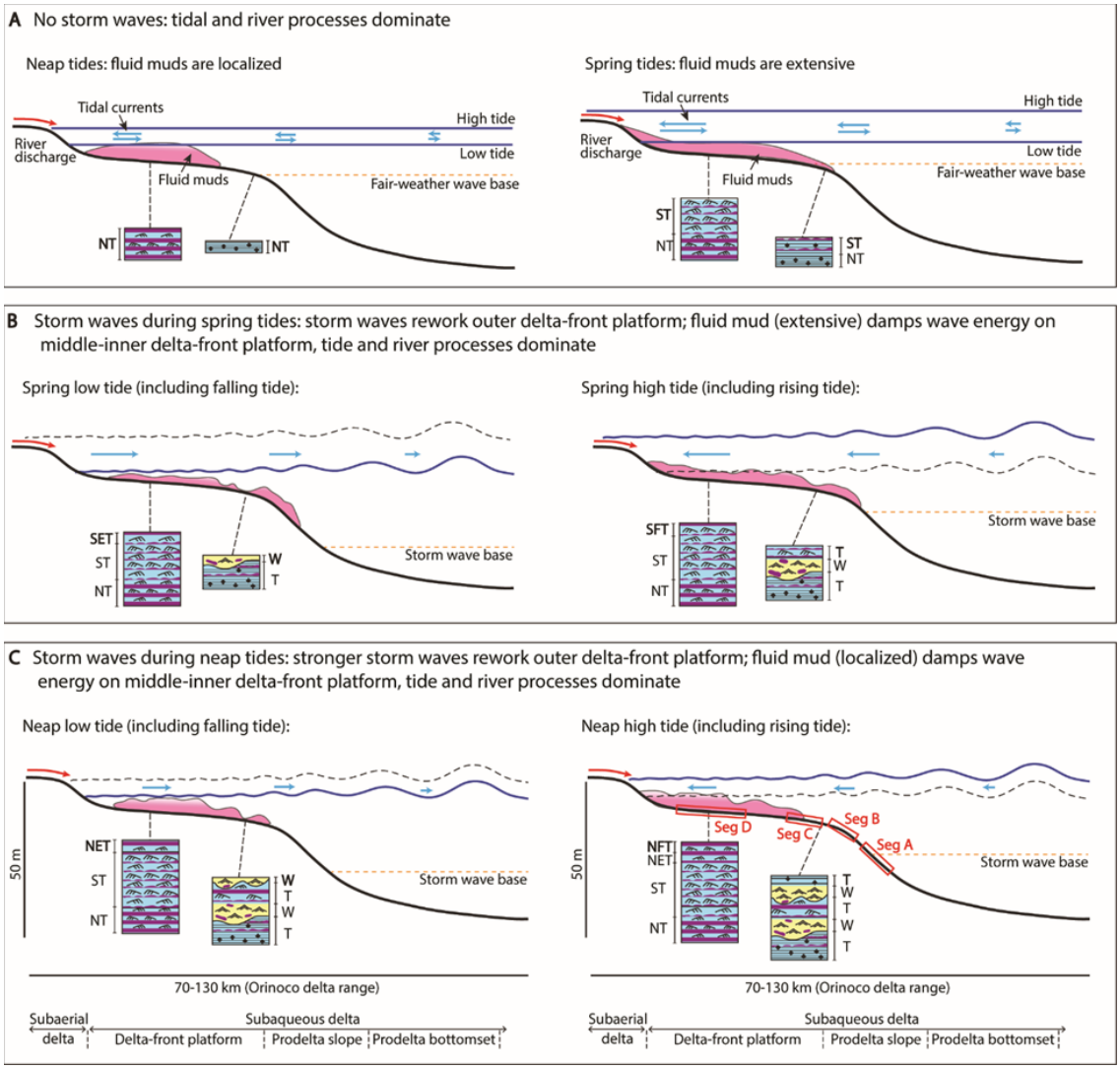

Figure 4.12: Schematic diagram showing how fluid mud likely impacted the wave, tide, and river processes and the resultant deposits during spring-neap tides and storm-interstorm periods. Note that purple lines indicate fluid-mud layers and mud flasers, and the lengths of the blue arrows are scaled to the tidal-current speeds. (A) Spring (ST) and neap (NT) tidal processes and deposits during interstorm or fair-weather condition. (B-C) Storm waves (W) and deposits during spring and neap tides, respectively. Storm waves were damped by the fluid mud on the delta-front platform, so that river and tide deposits were preferentially preserved on the middle-inner delta-front platform. Note that SET and SFT indicate spring ebb-tide deposit and spring flood-tide deposit, and NET and NFT indicate neap ebb-tide deposit and neap flood-tide deposit. The inferred locations for segments A-D are marked on the delta clinoform. See detailed descriptions and interpretations in text.

Segment C is interpreted to represent deposits on the outer delta-front platform (Figs. 4.1, 4.8, and 4.12), and it illustrates interacting tidal and fluvial dominance in the lower part, gradually changing upwards into stronger wave and fluvial dominance with minor tidal influence (Fig. 4.9C). The decimeter- to centimeter-scale cyclic alternation of groups of thicker and thinner sandstone sets is interpreted as spring-neap tidal cycles which show wave influence progressively dominating towards the outer delta-front platform (upper part of segment C). In the lower part of segment C, thicker intervals of unidirectional to bidirectional asymmetrical ripples were deposited during spring tides because of stronger tidal currents, and thinner intervals of parallel laminations with organic-matter-rich double mud drapes were deposited by weaker tidal currents during neap tides (Fig. 4.11A) (Nio and Yang, 1991). In the upper part of segment C, the erosional-based, micro-swaley to parallel-laminated sandstones with mud flasers are interpreted as storm-wave deposits (Dashtgard et al., 2012), and the parallel-laminated sandstones with organic-matter drapes are tidal deposits (Fig. 4.11B). The tidal deposits tend to be scoured by subsequent storm waves causing less preservation potential, although some parts were not completely eroded in this interval. River influence is relatively consistent through segment C and is mainly shown by abundant organic matter. The lack of bioturbation is consistent with continuous fluvial influence in segment C. The thin fluid-mud layers with deformed and erosional tops in the spring-tide deposits record rapid deposition of sands over unconsolidated fluid-mud beds and erosion of the consolidated fluid-mud layers by relatively strong spring tidal currents, respectively. The fluid-mud clasts and flasers in the micro-swaley strata reflect erosion of storm waves. The lack of fluid-mud deposits in the parallel-laminated sandstones with organic-matter drapes indicates that the depositional location is more seaward of the fluid-mud zone,

particularly during the neap tides, when fluid mud is distributed more locally because of small tidal range (Fig. 4.12).

Segment D is interpreted to represent deposits on the middle-inner delta-front platform (Figs. 4.1, 4.8, and 4.12), and it illustrates dominant tidal influence and minor fluvial influence with suppressed wave influence (Fig. 4.9D). The prevalent interbedded fluid-mud deposits and bidirectional asymmetrical-rippled sandstones indicate that tidal processes were dominant throughout segment D and wave influence was insignificant. The organic matter in some sandstone and mudstone beds suggests minor fluvial influence. Compared with segment B, segment D is located landwards of the outer delta-front platform, where wave energy has been dissipated because of the energy-attenuating fluid mud and shoaling effect. When wave energy was damped, in turn, the tidal and river signals were enhanced.

This Manzanilla zone of the paleo-Orinoco Delta thus demonstrate interaction of tides, waves, and minor river currents with added impact of fluid mud during spring-neap tidal cycles and storm-interstorm cycles (evidenced by segments A-D) at decimeter and centimeter scale (Fig. 4.12). During fair-weather or interstorm conditions, the subaqueous delta was dominated mainly by tidal processes with some river influence (Fig. 4.12A). Fluid mud on the delta-front platform tended to be localized during neap tides and spread more extensively during spring tides (Fig. 4.12A). Correspondingly, neap tidal deposits show thin bidirectional current-rippled sandstones or silt laminae with thicker fluid-mud deposits, and spring tidal deposits display thick bidirectional current-rippled sandstones with thinner and partially eroded fluid-mud layers on the delta-front platform (Fig. 4.12) (Jaeger and Nittrouer, 1995). At locations seaward of the fluid-mud zone, very thin to no fluid mud occurs and only organic-matter drapes were deposited during slack-water periods (Fig. 4.12A). When storm waves occurred, the waves most likely eroded and

reworked the outer delta-front platform, particularly during low tides because of relatively low water depth (Fig. 4.12B and C). The middle to inner delta-front platform was mainly tide-dominated due to the fluid mud that damped the wave energy and the shoaling effect of waves (Fig. 4.12B and C). As storm waves waned, tidal structures became well preserved and tide-generated deposits draped the storm-wave-generated deposits (Fig. 4.12B and C).

DISCUSSION

Cohesive fluid mud facilitating deltaic compound clinoforms

The described stratal succession represents the progradation and stacking of deltaic compound clinoforms that trapped large volumes of littoral fluid mud, in fact a total of 40 m of fluid-mud deposits, half of the muddy succession (Figs. 4.4 and 4.8). We suggest that the fluid mud was likely derived from the Amazon River and brought by the northwest-directed Guyana Current to the Pliocene Orinoco littoral zone in huge quantities. The Amazonian fluid-mud deposits in this study are generally light colored compared to the hemipelagic-mud deposits, which contain more organic matter. Amazon organic matter is likely to have been winnowed out during the lengthy journey of the Guyana Current from the Amazon area. The Amazon River is known to have been established between the middle to the late Miocene (Figueiredo et al., 2009). In addition, the studied succession with delta-scale subaqueous clinoforms was probably deposited during rising to highstand of sea level so that the subaqueous delta was preserved from being intensely incised and reworked by distributary channels. Such sea-level rise to highstand condition in the Pliocene, similar to the late Holocene sea-level highstand, created a broad shelf and accommodation promoting the coastal migration of muddy

sediments, given that the Amazon River likely bypassed most of its sediment load across the shelf and out into deepwater during low sea level.

The fluid mud, located mainly on the subaqueous platform, appears to have had a cohesive role in stabilizing the shoreline and prograding both the subaerial and subaqueous deltaic segments. In mud-dominated coasts, fine-grained sediments are maintained in suspension as they are transported shoreward by strong tide or wave action (Gratiot et al., 2007; Winterwerp et al., 2007). In turn, wave energy is attenuated and suspended sediments are deposited rapidly due to reduced shear stress (Wells and Roberts, 1980). As fluid mud on the delta-front platform moves to the intertidal zone, it can become shore-attached and cause subaerial delta accretion and progradation (Figs. 4.8 and 4.12), similar to the processes documented along the French Guiana coast (Allison and Lee, 2004; Gratiot et al., 2007). The modern western coast of Louisiana (Wells and Roberts, 1980; Roberts et al., 1989; Allison et al., 2005; Draut et al., 2005) and the southwestern coast of India (Mallik et al., 1988; Mathew and Baba, 1995) exhibit similarities to both the modern Amazon-Orinoco coast and the Manzanilla Formation of the paleo-Orinoco Delta in that both of them receive large quantities of fine-grained sediments (i.e., mainly silts and clays) from adjacent, upstream, large river deltas that trigger shoreline progradation. Meanwhile, the offshore-directed fluid mud carried by storm waves can feed the subaqueous delta, leading to aggradation and progradation of the subaqueous clinoform (Figs. 4.8 and 4.12) (Cacchione et al., 1995; Kineke et al., 1996; Michels et al., 1998). For sand-dominated shorelines, waves typically erode, resuspend, and redeposit sands, leading to dynamically changing shorelines (Komar, 1998).

The wave-borne fluid mud of the Guyana Current impinged the Pliocene Orinoco littoral zone, and had a major impact on delta-front sedimentation by protecting the

shoreline from more wave reworking. The wave-energy damping resulted in preservation of more river- and tide-associated deposits. Additionally, the extra-large supply of mud delivered from the Amazon caused the studied succession to be much more mud rich than it otherwise would be, and it led to rapid subaerial and subaqueous delta accretion and progradation probably during intervals of rising and highstand of sea level.

Comparison with other sedimentary basins

The deltaic compound clinoforms in the Manzanilla Formation are similar to modern tide-dominated delta systems, such as the Ganges-Brahmaputra (Kuehl et al., 2005), the Mekong (Ta et al., 2002), the Yangtze (Hori et al., 2002), and the Gulf of Papua (Harris et al., 1993; Dalrymple et al., 2003; Walsh et al., 2004), in that they demonstrate a coarsening-upward subaqueous clinothem overlain by a fining-upward subaerial clinothem. The coarsening-upward subaqueous succession extends from the prodelta through prodelta slope to the outer delta-front platform, and they are more influenced by fair-weather waves, storm waves and other ocean currents. The sedimentary facies in the succession are alternating mud and sand deposits with wave ripples, hummocky-swaley cross stratification (this study), normally graded sandy and silty beds (tempestites by storms) (e.g., the Ganges-Brahmaputra), and frequent sharp-based scour surfaces (e.g., the Yangtze) (Hori et al., 2002). The subaqueous delta deposits are often bioturbated, such as the Gulf of Papua (Walsh et al., 2004) and this study. The fining-upward succession is from the outer delta-front platform through mid-inner delta-front platform to the subaerial delta plain. The sedimentary facies on the delta-front platform are interbedded sand and mud deposits that are formed under the strong influence of tides, such as the Amazon (Jaeger and Nittrouer, 1995) and the Manzanilla Formation of the Pliocene Orinoco Delta. The subaqueous platform of the

Manzanilla Formation shows bidirectional current-rippled sandstones interbedded with abundant fluid-mud deposits particularly on the middle-inner part, and interbedded thin fluid-mud layers and erosionally based sandstones with wave ripples and small swales on the outer part. The subaerial delta plain (containing distributary channels) includes the lower delta plain, influenced by tides and other marine processes and upper delta plain, dominated by fluvial processes. The studied section of the Manzanilla Formation shows only the lower delta plain with tidal channels filled with tidal bars (Figs. 4.4 and 4.8).

The muddy compound clinoforms are commonly formed in high-energy marine settings, particularly in tide-dominated and modestly wave-influenced settings with relatively high sediment supply (more than 10^8 metric tons yr^{-1}) (Walsh and Nittrouer, 2009). The large tidal range and the resultant strong tidal currents enabled the separation between the subaerial delta clinoform and subaqueous delta clinoform (Walsh and Nittrouer, 2009). The soft gel-like fluid mud in the muddy environments plays a very important role in effectively attenuating the incoming waves and causing the delta to preserve more tidal signatures. As waves become significantly strong, the muddy sediments temporarily stored on the subaqueous clinoform can become wave-reworked. In the Gulf of Papua subaqeous clinoform, interbedded sands and muds or thick homogeneous muds (more than 10 cm) are preserved on the inner subaqueous platform during the weak NW monsoon, and they are remobilized to the outer subaqueous platform and the prodelta slope during the strong SE tradewind season (Walsh et al., 2004). It is possible that the muddy sediments damp the incoming waves of the NW monsoon, leading to seasonal mud storage on the inner subaqueous platform. Systems with small sediment supply discharged into energetic oceanographic environments (i.e., large waves or currents) (e.g., the Eel and Columbia) or with relatively large sediment supply into low-energy oceanographic environments (i.e., small waves, tides, or currents)

(e.g., the Po and the Mississippi) will not build a subaqueous clinoform, because they either efficiently disperse the fine-grained sediments into the ocean or rapidly deposit near the river mouth.

CONCLUSIONS

The studied interval of the Manzanilla Formation (lower Telemaque Sandstone) on Trinidad represents progradation of a deltaic compound-clinoform system that exhibits two subaqueous clinoforms and an upper subaqueous clinoform to distal subaerial clinoform with tide-influenced channels. The delta was strongly influenced by an energy mix of waves, tides, and river currents with the added impact of fluid mud at variable scales. At large-clinoform scale (meters to tens of meters scale), storm waves became dominant and reworked the distal river mouth bars and tidal bars, and transported sediments to the outer delta-front platform and prodelta slope as the subaqueous delta prograded. The fluid mud was distributed mainly on the delta-front platform with a minor proportion on the prodelta slope. At the scale of a spring-neap tidal bundle (decimeter scale), thick bidirectional current-rippled sandstones with thin and partially eroded fluid-mud layers tended to be deposited during spring tides and thin bidirectional current-rippled sandstones or silt laminae with thick fluid-mud deposits deposited during neap tides on the middle-inner delta-front platform. Storm waves occurred in both spring tides and neap tides. Despite the presence of the fluid mud, strong storm waves eroded the fluid-mud deposits and reworked the sand deposits on the outer delta-front platform, and therefore storm-wave ripples are preserved and intercalated with tidal deposits. Fluid mud, probably brought in huge quantities to the paleo-Orinoco littoral zone by the Guyana Current from the mouth of the Amazon delta, impacted mainly the delta-front platform and damped the storm wave energy. This led to preferred preservation of river

and tide signals on the delta-front platform of the subaqueous delta and the distal subaerial delta. The large added volumes of fluid mud stabilized the shoreline from wave reworking and rapidly prograded the compound clinoform of the delta.

Chapter 5: Amazon fluid mud impact on tide- and wave-dominated Pliocene lobes of the Orinoco Delta[3]

ABSTRACT

The modern Orinoco Delta is a major sink for the world's largest alongshore (littoral) mud dispersal system; it receives some 10^8 tons/yr from the Amazon river delta. The influence of these huge volumes of Amazon mud on the paleo-Orinoco Delta succession is now investigated for the first time. Abundant fluid-mud deposits are preserved in outcrops from the Pliocene Orinoco Delta deposits (Lower Morne L'Enfer, Manzanilla and Mayaro formations on Trinidad) with different styles in tide-dominated, in tide-dominated and wave-influenced, and in storm wave-dominated delta lobes. Fluid-mud deposits in sandy parasequences (10-20 m thick) of the Lower Morne L'Enfer Formation change from thin layers amalgamating to form mud bedsets (up to 4cm) or draping across ripple laminae in the lower part, to thick layers (up to 10 cm) occasionally with deformed and load structures at their top, in the upper part. The Manzanilla Formation parasequences (30-40 m thick) exhibit coarsening-to-fining-upward (CUFU) facies successions with fluid-mud deposits located mainly in the middle to upper parts of the parasequences, near the transition between the CU and FU parts of the units. Most of the fluid-mud layers are interbedded with bi-directional, current rippled-sandstones, whereas minor mud layers are associated with erosion-based sandstones with small-scale swaley strata and bi-directional symmetrical ripples. The Mayaro Formation parasequences (5-15 m thick) are characterized by alternating fluid-mud intervals and sets of hummocky cross-stratified sandstones (HCS) passing upward into amalgamated

[3] This chapter has been submitted as: Peng, Y., Steel, R.J., and Olariu, C., Amazon fluid mud impact on tide- and wave-dominated Pliocene lobes of the Orinoco Delta. I was the primary author who conducted the research and drafted this manuscript with co-authors' help.

swaley cross-stratified (SCS) sandstones. The fluid-mud intervals have flat or irregular tops occasionally overlain by amalgamated SCS sandstones with fluid-mud clasts.

Very thick (1-1.5 m) fluid-mud intervals occur in places in both tide- and wave-dominated strata and these are probably large muddy bedforms similar to mud banks that migrate currently along the modern Amazon-Orinoco coast. The outcrop analysis strongly suggests that the fluid-mud banks, as they approached the Orinoco delta-front area, were handled differently depending on whether the delta-front lobes were wave- or tide-dominated. Tide-dominated delta lobes tended to trap the muds near the shoreline and on the subaqueous delta-front platform in water depth less than 10 m with only minor volumes escaping offshore. In contrast, storm wave-dominated delta lobes had a more dynamic impact on the approaching mudbanks. Mud accumulated in the shallow water tend to be eroded and re-deposited into deeper water near the storm wave base (15-50 m water depth).

The volumes of Pliocene Amazon mud transported along the innermost shelf and arriving on the Orinoco Delta were likely influenced by high-amplitude, Pliocene glacio-eustatic sea level fluctuations. During sea-level fall and lowstand periods, increased volumes of Amazon mud would have bypassed to the deep water and thus decreased mud volumes drifted and became incorporated in the Orinoco delta front. In contrast, sea-level rise and highstand periods would have promoted increased volumes of Amazon mud both on the shelf and onto the Orinoco, similar to the Holocene and modern muddy system.

INTRODUCTION

The modern Orinoco Delta is one of the major sinks for Amazon-derived mud (Fig. 5.1A) (Eisma et al., 1978; Eisma et al., 1991; Warne et al., 2002; Aslan et al., 2003). Research suggests that 36-68% (4.3-8.3 $\times 10^8$ tons) of the yearly Amazon mud supply

(Kuehl et al., 1986) are deposited on the Amazon shelf off the river mouth, 20% are being transported along the coast either in suspension (1.5×10^8 tons) or in the form of migrating mud banks (1×10^8 tons), and 20% are deposited in the Orinoco Delta and Gulf of Paria (2.5×10^8 tons), with the remainder small amount deposited on the Guianas coast (French Guiana, Suriname, and Guyana) or transported off the shelf (Eisma et al., 1978; Wells and Coleman, 1978; Eisma et al., 1991) This huge supply of Amazon mud is a significant additional sediment source to the Orinoco Delta; it accounts for at least half of the muddy sediment deposited on the Orinoco Delta (Eisma and Van der Marel, 1971; Eisma et al., 1978). Although there have been several studies on the Guianas coast, little has been done on the Orinoco delta front except for Aslan et al. (2003) who documented mudcapes derived from the Amazon system accumulated along the western Orinoco Delta in the late Holocene. There has been no previous work on ancient Amazon mud within the Orinoco Delta stratigraphy.

Mud dispersal is mainly controlled by interplay of muddy sediment supply and basinal processes (tides, waves, and currents) (Walsh and Nittrouer, 2009) that result in mud distribution to variable locations on shelves as muddy coasts, nearshore/inner-shelf mud belts, mid- and outer-shelf mud belts (McCave, 1972; Hanebuth et al., 2015). Eustatic sea-level falls and rises can drive regressive and transgressive transits of shorelines, between the innermost and the outermost reaches of the pre-existing shelf, and therefore decrease and increase shelf width and accommodation for muddy sediment on the shelf. In the meantime, coastal and shallow marine processes may correspondingly shift as sea level changes. The marine processes and eustatic sea-level changes play important roles on the muddy systems and remain understudied.

The objectives of this work are (1) to provide well exposed outcrop examples of how Amazon-derived fluid-mud layers are recognized and characterized in both tide-

and wave-dominated settings, (2) to show how littoral fluid mud tended to accumulate on the subaqueous platform of strongly tide-influenced delta lobes, whereas on wave-dominated lobes the mud was commonly eroded and reworked farther out into deeper settings, and (3) to suggest that the glacial-interglacial, Pliocene sea-level changes (10s of Ky duration) are likely to have affected the overall increased or decreased volumes of mud incorporated into the Orinoco during falling-stage, lowstand, transgressive, and highstand sea-level intervals.

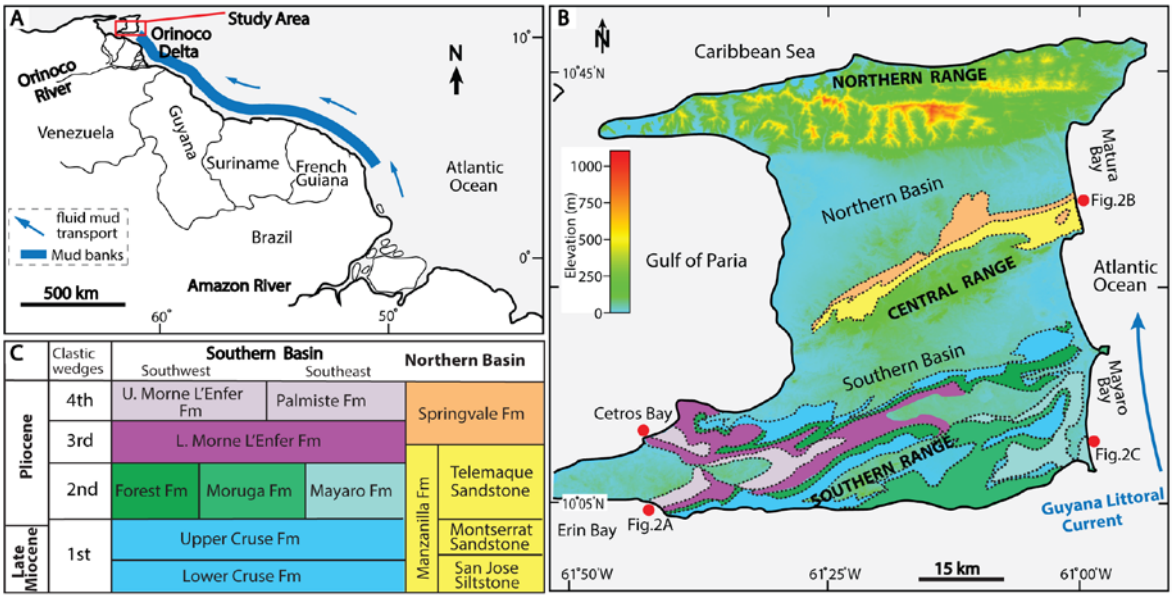

Figure 5.1: (A) Sketch map of the 1600-km muddy Amazon-Orinoco coast in South America.The blue bold line indicates the zone of mud banks and the blue arrows indicate fluid mud transport direction. (B) Geologic map of Trinidad showing the late Miocene-Pliocene Orinoco deltaic to deep-water deposits in the Northern and Southern Basins of Trinidad. The island of Trinidad was plotted with the DEM elevation to emphasize the main mountain ranges using the NASA's Shuttle Radar Topography Mission (SRTM) Version 3.0 data. Red dots indicate the locations of all studied outcrops which includes locations of the three selected successions in Figure 5.2A-C. (C)Stratigraphic column for the four clastic wedges and tentative correlation between the formations of the Northern and Southern Basins.

BACKGROUND

Fluid mud formation

The Amazon-Orinoco coastline in south America is the world's largest (1600 km) migrating muddy systems (Fig. 5.1A), and it shows a morphodynamic interaction with the shoreline along which it drifts. Tremendous volumes of fluid mud (10-400 g/l) (Allison et al., 1995b) that consist of mostly silt and clay are formed as the Amazon fresh water and saline Atlantic Ocean water meet (estuarine circulation) in a turbidity-maximum area due to mud coagulation and flocculation (Gibbs and Konwar, 1986) in an area 100-200 km seaward of the Amazon River mouth (Nittrouer and DeMaster, 1986; Trowbridge and Kineke, 1994; Kineke et al., 1996). The nearbed suspended fluid mud (up to 7 m thick) covers an area about 5700 km^2 during falling and low river discharge and about 10,000 km^2 during rising and high discharge on the inner and middle shelf northwest of the Amazon river mouth (Kineke and Sternberg, 1995). The cross-shelf extent of fluid mud is greater during rising and high discharge, and reaches the outer topset and upper foreset of the subaqueous clinoform at a water depth of more than 35 m compared to the period of falling and low discharge (i.e., 15 m water depth on the mid-outer topset) (Kineke and Sternberg, 1995). Thick mud layers (up to 1.5 m; containing about 1.5×10^8 tons sediment) were deposited rapidly from the fluid-mud suspension before remobilization to the northwest (Allison et al., 1995b).

Fluid mud transport and deposition

The transport and deposition of the Amazon mud are mainly attributed to the trade-wind-generated waves (Wells and Coleman, 1978; Eisma et al., 1991; Allison et al., 1995b; Allison et al., 2000; Gratiot et al., 2007). The fluid mud is transported from the Amazon River northwestward until shoreface-attached mud banks progressively form

near Capo Cassipore (350 km northwest of the Amazon River) (Fig. 5.1A) (Allison et al., 2000). The mud banks (up to 5 m thick, 10-60 km long, 10-20 km wide) subsequently migrate alongshore to the northwest in the littoral zone (5 m to 20 m water depth) by constant wave reworking of their trailing edges and transport of mud towards their leading edges, causing large volumes of fluid mud to be held in suspension (Eisma et al., 1991; Allison and Lee, 2004; Augustinus, 2004; Gardel and Gratiot, 2005; Gratiot et al., 2007; Anthony et al., 2010). The muddy shoreface progradation and erosion along the coast are associated with the migration of mud banks and interbanks caused by long-term (10s to 100s yrs) variations of the trade winds (i.e., shifts in wind direction and changes in mean wind velocity) (Eisma et al., 1991; Allison et al., 1995a). The development of coastal-plain accretion and cheniers in between represent episodes (10^3 yr scale) of mudcape and shoreface progradation, and shoreface retreat by intense erosion (Brinkman and Pons, 1968; Augustinus et al., 1989).

The paleo-Orinoco sink: regional setting

It is believed that the Orinoco Delta is likely to have been receiving Amazon mud since the late Miocene, as the Amazon River is known to have been established as a large river with its main Andean sediment input from middle to late Miocene (Figueiredo et al., 2009). During the late Miocene-Pleistocene, glacial-interglacial eustatic sea-level fluctuations were able to drive both Amazon and Orinoco deltaic sediment-supply systems back and forth across the shelf at short time scales (10s to 100 ky) (Porębski and Steel, 2006). Four main clastic wedges were formed by the repetitive transits of the paleo-Orinoco Delta system in the Southern and Northern Basins of Trinidad (Fig. 5.1B and C) (Steel et al., 2007): (i) the late Miocene to early Pliocene Cruse Formation (shelf-edge deltas and slope-channel systems) reached its shelf edge in southeast Trinidad

(Winter, 2006; Vincent, 2012; Chen et al., 2016), (ii) the early-mid Pliocene Forest-Moruga-Mayaro formations (landward to basinward equivalents; river- to wave-dominated shelf to shelf-edge deltas) prograded to the corresponding shelf edge in southeast Trinidad (Bowman, 2003; Bowman and Johnson, 2014; Peng et al., 2017), (iii) the mid-late Pliocene Lower Morne L'Enfer Formation (river- and tide-dominated deltas and estuaries) (Vincent, 2003; Osman, 2007; Chen et al., 2014) and (iv) the latest Pliocene to early Pleistocene Upper Morne L'Enfer-Palmiste Formation (delta-plain deposits and tide-dominated deltas) representing the landward reaches on the inner shelf (Vincent, 2003; Chen et al., 2014). The coeval deposits in the Northern Basin of Trinidad are deep-water turbidites and muddy slope deposits (San Jose Siltstone) and younger river- and tide-dominated, wave-influenced delta deposits (Manzanilla and Springvale formations) (Huggins, 2007; Peng et al., 2018) with some contribution of coarse-grain sediments from the uplifted Northern Range source (Fig. 5.1). The second and third of these Orinoco clastic wedges have been examined for delta lobe-fluid mud interactions in the present work.

DATA AND METHODOLOGY

The studied outcrops are from the Lower Morne L'Enfer Formation at Erin Bay and Cedros Bay, Manzanilla Formation at Matura Bay, and Mayaro Formation at Mayaro Bay on the coast of Trinidad (Fig. 5.1). Three deltaic successions were selected and described in detail (Fig. 5.2) as they represent tide-dominated delta lobes (20 m thick) on an inner shelf setting (Chen et al., 2014), tide-dominated and wave-influenced delta lobes (80 m thick) on a mid-outer shelf setting (Peng et al., 2018), and storm wave-dominated lobes (15 m thick) on a shelf edge setting (Bowman and Johnson, 2014), respectively (Fig. 5.2). Other outcrops with additional characteristics that indicate supplementary

depositional processes were photographed and included in this study. All the three deltaic successions contain abundant mudstone beds or layers that are thick (up to more than 0.5 cm thick), homogeneous and structureless, and unbioturbated (Fig. 5.3). Some the mudstone layers are dark colored and contain organic matter (Fig. 5.3). The mudstones are interpreted as fluid-mud deposits (Ichaso and Dalrymple, 2009; Peng et al., 2018), which are the focus of this study. Interaction between the invasive fluid mud and the associated host facies was described at a cm to dm scale by recording bed thickness, grain size, sedimentary structures, and trace fossils. Fluid-mud layers that display a range of sedimentation and preservation styles (Table 5.1) are further grouped in tide- and wave-dominated settings based on their associations with sedimentary structures in sandstones. Other mudstones are relatively thin (a few millimeters thick) layers with internal lamination and bioturbation and are interpreted as hemipelagic-mud deposits (here in the Orinoco outcrops referred to as terrestrial-derived mud that settled from suspension under a relatively low sediment concentration).

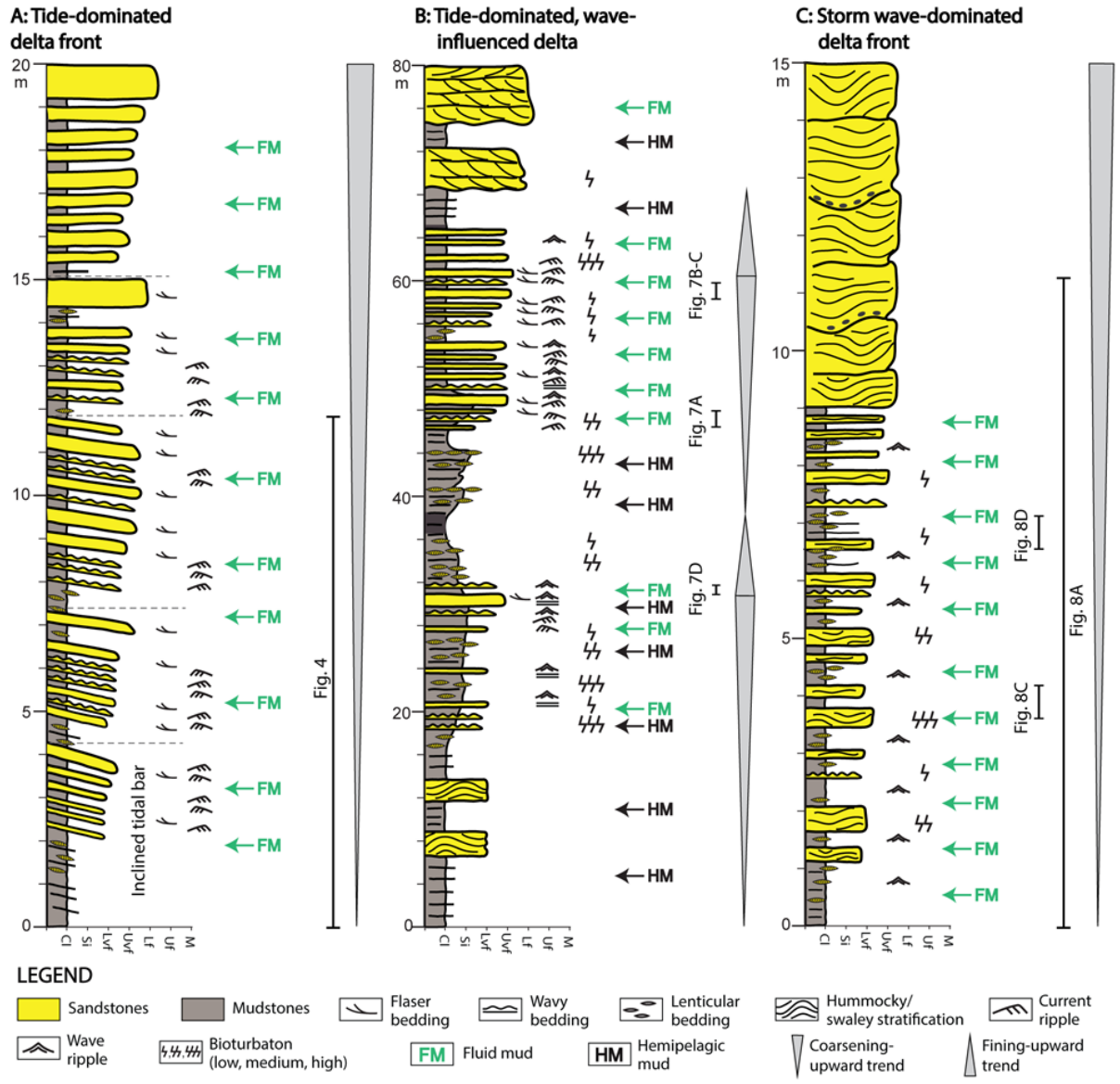

Figure 5.2: The three stratigraphic successions with fluid-mud (FM) and hemipelagic-mud (HM) deposits marked along the successions. Note that the vertical scale is different for each section. (A) A tide-dominated delta front (from the Lower Morne L'Enfer Fm.) consisting of several slightly inclined tidal bars with a coarsening-upward trend. (B) A tide-dominated and wave-influenced delta (from the Manzanilla Fm.) shows two coarsening-to-fining-upward units/parasequences. (C) A storm wave-dominated delta front (from the Mayaro Fm.) with hummocky and swaley cross-stratified sandstones in the upper part and fluid-mud intervals interbedded with lenticular wave ripples in the lower part.

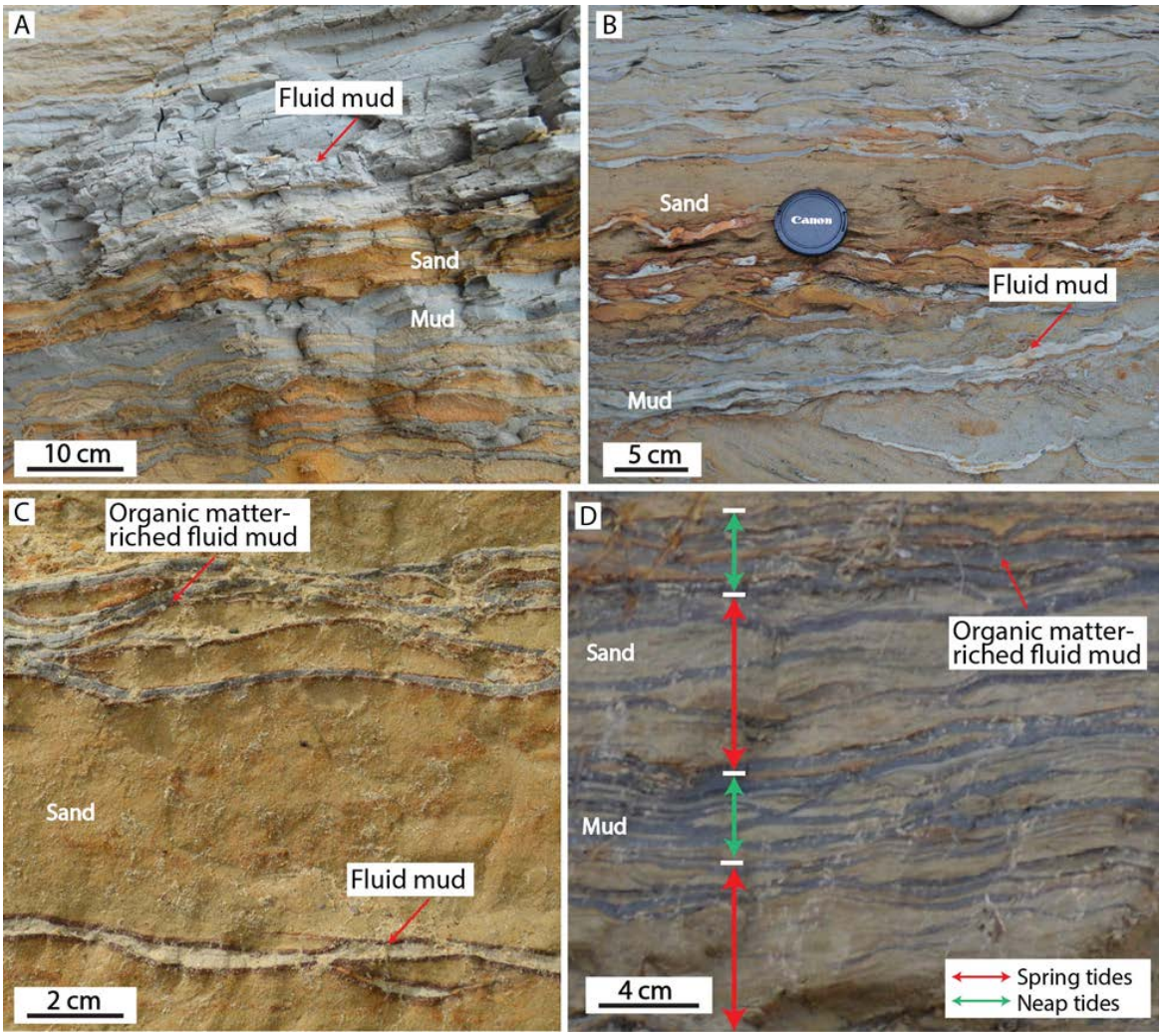

Figure 5.3: (A-B) Thick, light-colored fluid-mud layers (red arrows) interbedded with current-rippled sandstones (from Lower Morne L'Enfer Fm. and Manzanilla Fm., respectively). (C) Dark-colored fluid-mud layers with organic matter and light-colored fluid-mud layers (from Lower Morne L'Enfer Fm.). (D) Organic matter-enriched fluid-mud layers form networks between rippled sandstones (from Lower Morne L'Enfer Fm.). The alternating thicker and thinner heterolithic beds form spring and neap tidal bundles.

Table 5.1: Summary of the mudstone facies with variable sedimentation and preservation styles in the Pliocene Orinoco Delta.

Mudstone type	Dominant process	Mudstone thickness	Mudstone structure and bed geometry	Associated sandstone sedimentary structures	Other observations	Photos/figures as references
Thick, deformed mudstone	Tide	1-10 cm	Structureless; Squishy, continuous	Thick, structureless	Non-bioturbated	Fig. 5A-B, Fig. 9A
Thick, underformed mudstone	Tide	0.4-1.5 cm	Structureless; Wavy, continuous	Structureless, bidirectional current ripples	Rich in organic-matter in places; Non-bioturbated	Fig. 3B-D, Fig. 7A-C, Fig. 9B
Very thin mudstone	Tide	0.1-0.5 cm	Structureless; Very thin layers amalgamate to thicker bedsets; drape along ripple laminae	Thin sand lenticulars; parallel-laminated to current-rippled	Non-bioturbated	Fig. 5C-D, Fig. 9C
Discontinuous mudstone flaser	Wave	0.2-0.6 cm	Structureless; Broken/discontinuous mud flasers	Small-scale swales; wave ripples; mud clasts	Non-bioturbated	Fig. 7D, Fig. 9D
Mudstone interval with irregular top	Wave	0.2-1 cm	Structureless; Wavy, continuous	Erosionally overlain by HCS/SCS	Non-bioturbated	Fig. 8B-E, Fig. 9E
Thick wavy mudstone interval	Wave	0.5-1 cm	Structureless; Wavy, continuous	Wave ripples	Rarely- to Non-bioturbated	Fig. 8D and F, Fig. 9F

FLUID MUD INTERACTION WITH A TIDE-DOMINATED DELTA FRONT

The Lower Morne L'Enfer Formation contains some tide-dominated delta lobes that were somewhat protected from open ocean waves in the Gulf of Paria area of SW Trinidad (Chen et al., 2014). The studied delta lobes comprise repeated cycles of mainly rippled-laminated and cross-bedded, coarsening-upward delta-front deposits overlain by distributary channels (Fig. 5.4A-C) with minor, capping estuary deposits (Fig. 5.4D) (Chen et al., 2014). The delta lobes also contain significant volumes of mud deposits (≥20% of the delta front). Evidence for tide influence on the delta front includes stacked, orderly cross-bedded sandstones with mud drapes, pervasive heterolithic beds showing occasional spring-neap bundles, and restricted ichnofauna (Fig. 5.4); in the muddier prodelta strata there are unusually well preserved tidal rhythmites. The mudstone layers occur associated with delta-front sandstones and have a wide range of layer characteristics (Figs. 5.2A and 5.5). Mudstones in the upper part of coarsening-upward

successions are very thick (1-10 cm) but vary laterally and show soft deformation due to loading from overlying sand beds (Fig. 5.5A and B). Most of the mudstone layers (0.5-1.5 cm thick) are undeformed, and they are interbedded and form networks with structureless to ripple-laminated sandstone beds (Fig. 5.3C and D). In the lower parts of the delta-front successions, the mudstones become very thin (1-5 mm thick), and they either amalgamate to form thicker mud bedsets (up to 4 cm) (Fig. 5.5C and D) or drape along ripple laminae (Fig. 5.5C). In places, the mudstones are dark-colored and rich in organic matter (Fig. 5.3D).

The Morne L'Enfer example is interpreted as a tide-dominated sandy delta front that received abundant sediment from active distributary channels (Chen et al., 2014) and also moderate amounts of mud from the Amazon-derived mudbelts coming into the Gulf of Paria. The heterolithic strata on the delta front were deposited from river and tidal currents with the mud deposited during tidal slack-water periods. The mudstones with variable characteristics (Fig. 5.5) are interpreted as fluid-mud deposits. The upward change from thin to very thick and deformed fluid-mud deposits reflects an upward increase in suspended-sediment concentration (SSC) from the lower delta front to the upper delta front. The very thick and deformed fluid-mud layers (Fig. 5.5A and B) are interpreted as deposited under conditions of very high SSC values (10 g L^{-1} - 500 of g L^{-1}) (Mackay and Dalrymple, 2011) in the upper delta front (Fig. 5.6). The deformation or load structures at the top of the fluid-mud deposits correspond to rapid deposition of sands onto the fluid-mud layers with high water content and high pore pressure (Sills and Elder, 1986; Mackay and Dalrymple, 2011). The relatively thick fluid-mud layers are interpreted to have formed under flows of intermediate SSC (>10 g L^{-1}). The very thin fluid-mud layers (Fig. 5.5C and D) are interpreted as flows with a relatively low SSC (1 g L^{-1} - 10s of g L^{-1}) (Baas et al., 2009; Mackay and Dalrymple, 2011) on the lower delta

front. The light-colored, fluid-mud deposits are likely Amazon derived. Wave-generated longshore currents during long-distance travel would have tended to suspend and winnow away the finer-grained sediment and the organic matter. The dark-colored, organic matter-enriched fluid-mud layers probably indicate a nearby river derivation (i.e., the paleo-Orinoco River), although they can also have come from erosion of the trailing-edge mangrove fringe on the updrift mud banks (Allison and Lee, 2004).

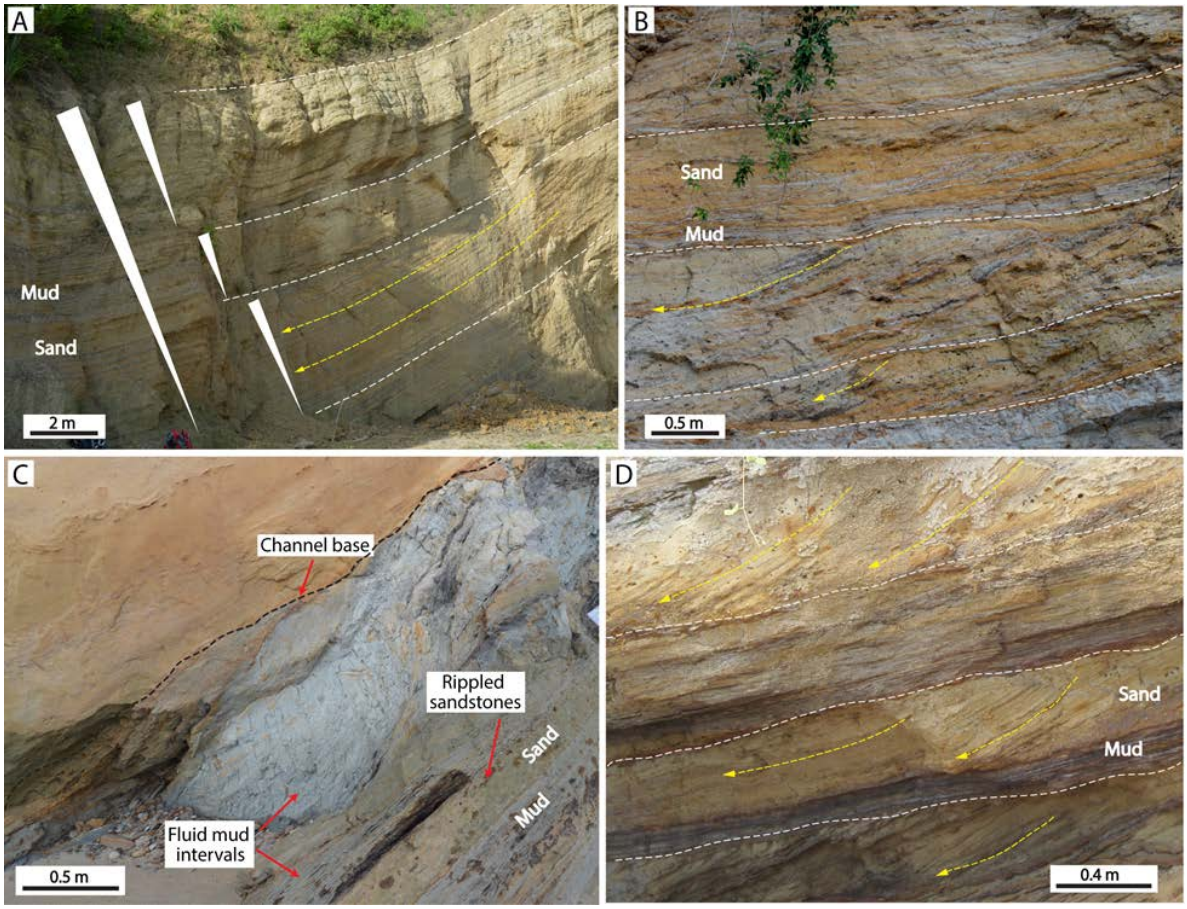

Figure 5.4: Tide-dominated sedimentary structures in the Lower Morne L'Enfer Fm. (A) A coarsening-upward tide-dominated delta front consisting of several low-angle inclined beds interpreted as tidal bars. (B) A tidal channel containing tidal bars characterized by sets of cross-bedded sandstones with mud clasts and fluid-mud layers. (C) An erosional channel base truncating the heterolithic delta front with a very thick (1 m) fluid-mud interval. (D) Tide-dominated estuarine channels containing several cross-bedded tidal bars with mud drapes. Note that white dashed lines indicate boundaries of tidal bars, and yellow dashed lines indicate dip direction of the accretion surfaces.

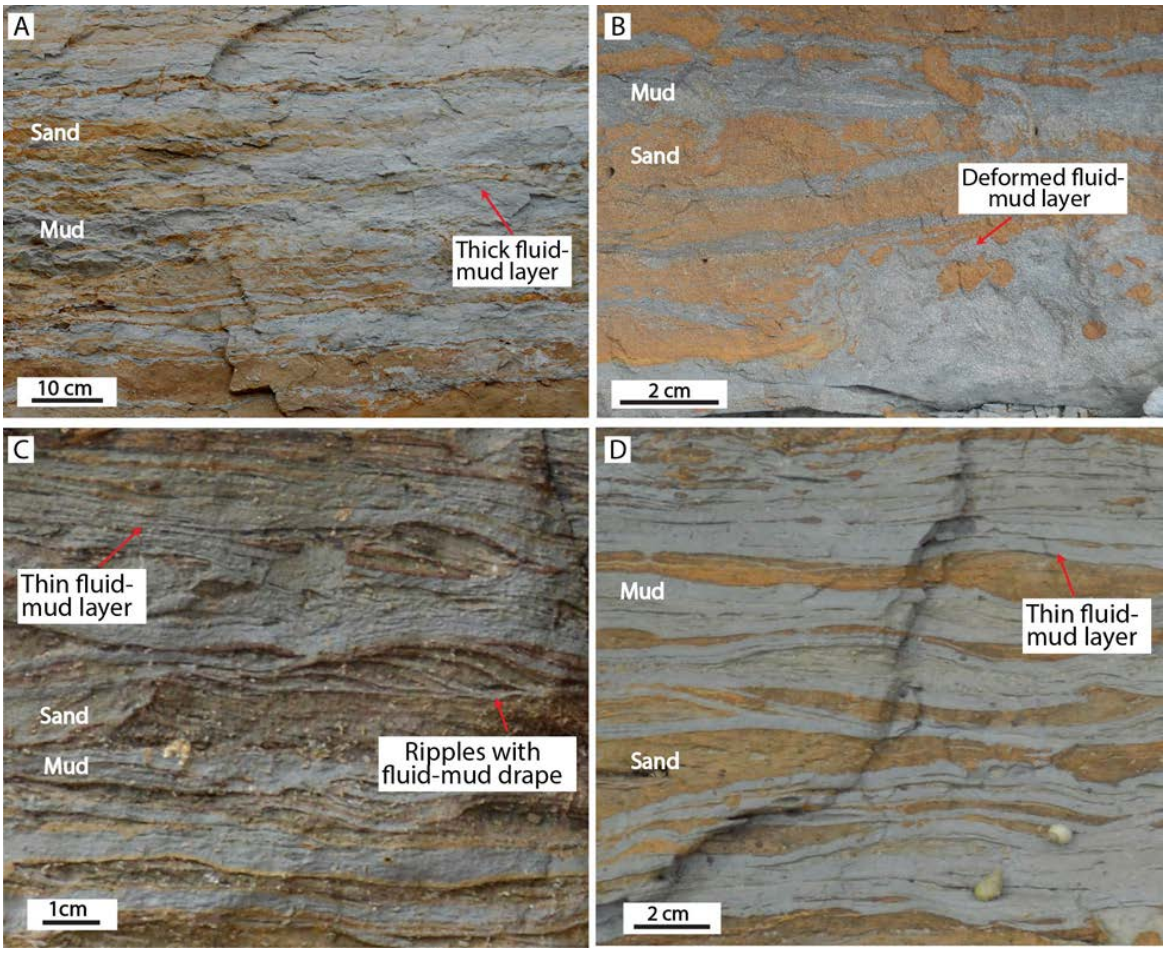

Figure 5.5: (A) Very thick (1-10 cm) fluid-mud layers showing lateral inconsistent thickness and uncontinuity. (B) Thick (1-3 cm), deformed fluid-mud layers interbedded with structureless sandstones. (C) Thin (1-5 mm) fluid-mud layers amalgamate to thick beds and drape along ripple laminae. (D) Fluid-mud intervals composed of very thin (1-5 mm) fluid-mud layers.

FLUID MUD INTERACTION WITH A TIDE-DOMINATED, WAVE-INFLUENCED DELTA FRONT

The study segment (80 m thick) of the Manzanilla Formation is a tide-dominated, wave-influenced deltaic system that was open to ocean waves but partially protected by the modest relief of an Atlantic headland of the Central Trinidad Range (Peng et al., 2018). Two coarsening-to-fining-upward (CUFU) units containing abundant mud deposits (30-40% of delta front) (Fig. 5.2B) are documented here. Most of the succession

in the Manzanilla Formation consists of sandy distributary channel and tide-dominated delta front systems (Fig. 5.6A and B) (Huggins, 2007) characterized by extensive bi-directional asymmetrical ripples, tidal rhythmites, and spring-neap tidal bundles with restricted ichnofauna. The wave influence in the study succession, recorded by hummocky and swaley cross-stratification, small-scale swales, or bi-directional symmetrical ripples (Fig. 5.6C and D), occurs primarily in the lower to the middle parts and occasionally in the upper parts of the CUFU units (Fig. 5.2B). The majority of mud deposits are thick (1-1.5 cm) and structureless occurring near the transition of the coarsening to fining of the CUFU units (Fig. 5.2B). Other mudstones are thin (1-2 mm thick) and laminated with intense bioturbation (Figs. 5.2B and 5.7A). The thick mud layers are commonly continuous and predominantly interbedded with bi-directional current ripples (Fig. 5.7A-C). In places, the mud deposits are associated with small-scale swales and bi-directional symmetrical ripples as broken mud layers/flasers (Fig. 5.7D).

The Manzanilla example with CUFU units is interpreted to represent a prograding muddy delta system with compound clinoforms (i.e., shoreline and subaqueous clinoforms) that received large amounts of Amazon fluid mud (Peng et al., 2018). The lower CUFU unit represents a distal subaqueous clinoform showing a coarsening-upward succession from the muddy prodelta bottomset to the sandier prodelta slope and outer delta-front platform, and a fining-upward succession from the outer to inner delta-front platform. The upper CUFU unit demonstrates the most landward part of the subaqueous clinoform overlain by the distal part the subaerial clinoform (lower delta plain) with tidal channels. The wave-generated structures in the lower unit indicate that storm waves are dominant on the prodelta slope to the outer delta-front platform (Peng et al., 2018). The majority of thick mud deposits near the transition between the CU and FU units are interpreted as fluid mud that were distributed mainly on the delta-front platform, whereas

the thin mud layers in the rest of the succession represent hemipelagic mud deposits. The continuous fluid-mud layers associated with bi-directional current ripples in the middle to upper part of the units were deposited during slack-water periods of tidal cycles on the delta-front platform (Fig. 5.7A-C). In contrast, the broken fluid-mud layers/flasers associated with small-scale swales and symmetrical ripples represent the mud layers eroded by storm wave process (Fig. 5.7D). Waves transported Amazon-derived fine-grained sediment northwestward along the shoreline and maintained them in suspension, whereas the tidal process during slack-water periods allowed settling of the suspended sediment as fluid-mud layers. This explains why most of the fluid-mud deposits in this case are associated with sedimentary structures generated by tides.

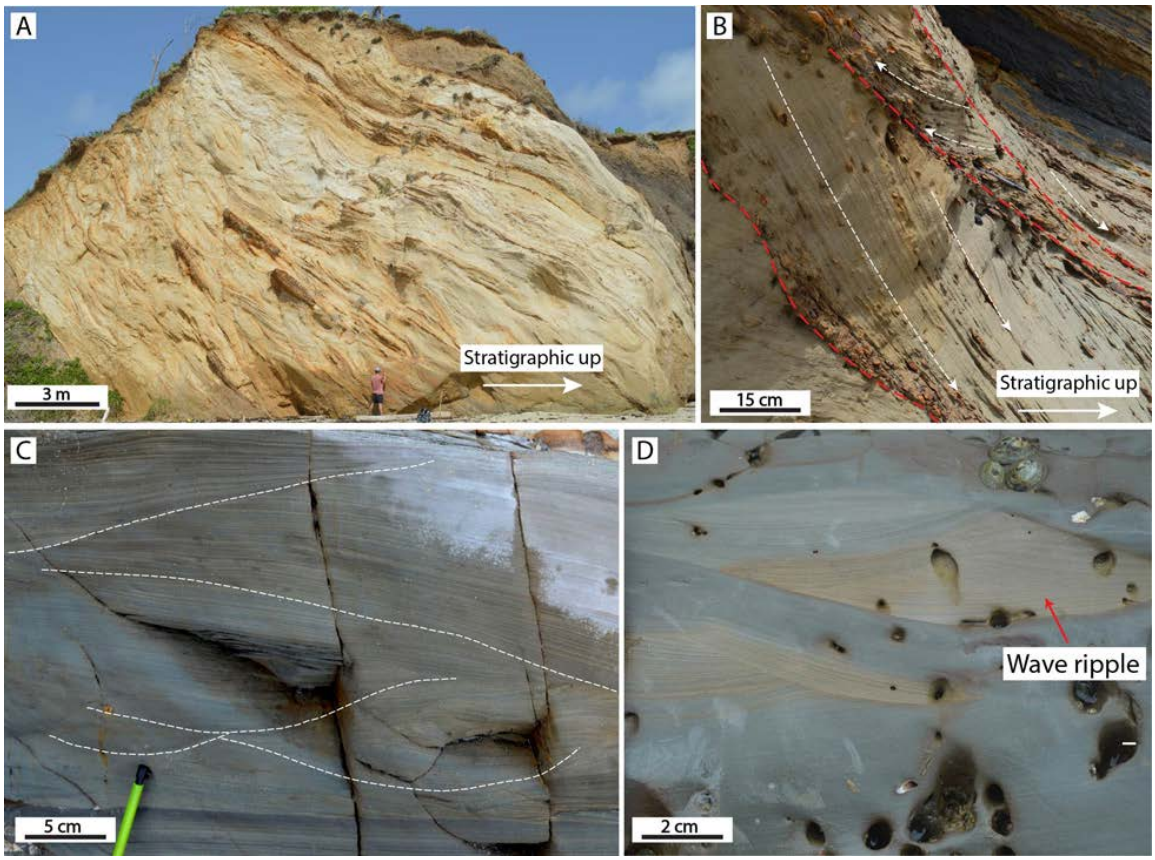

Figure 5.6: Tide-dominated and wave-influenced sedimentary structures in the Manzanilla Formation. (A) One example of a tidal distributary channel containing compound dunes that overlie the studied succession. (B) Bi-directional cross-bedded sandstones with mud clasts. (C) Hummocky and swaley cross-bedded sandstones. (D) Wave rippled-sandstones.

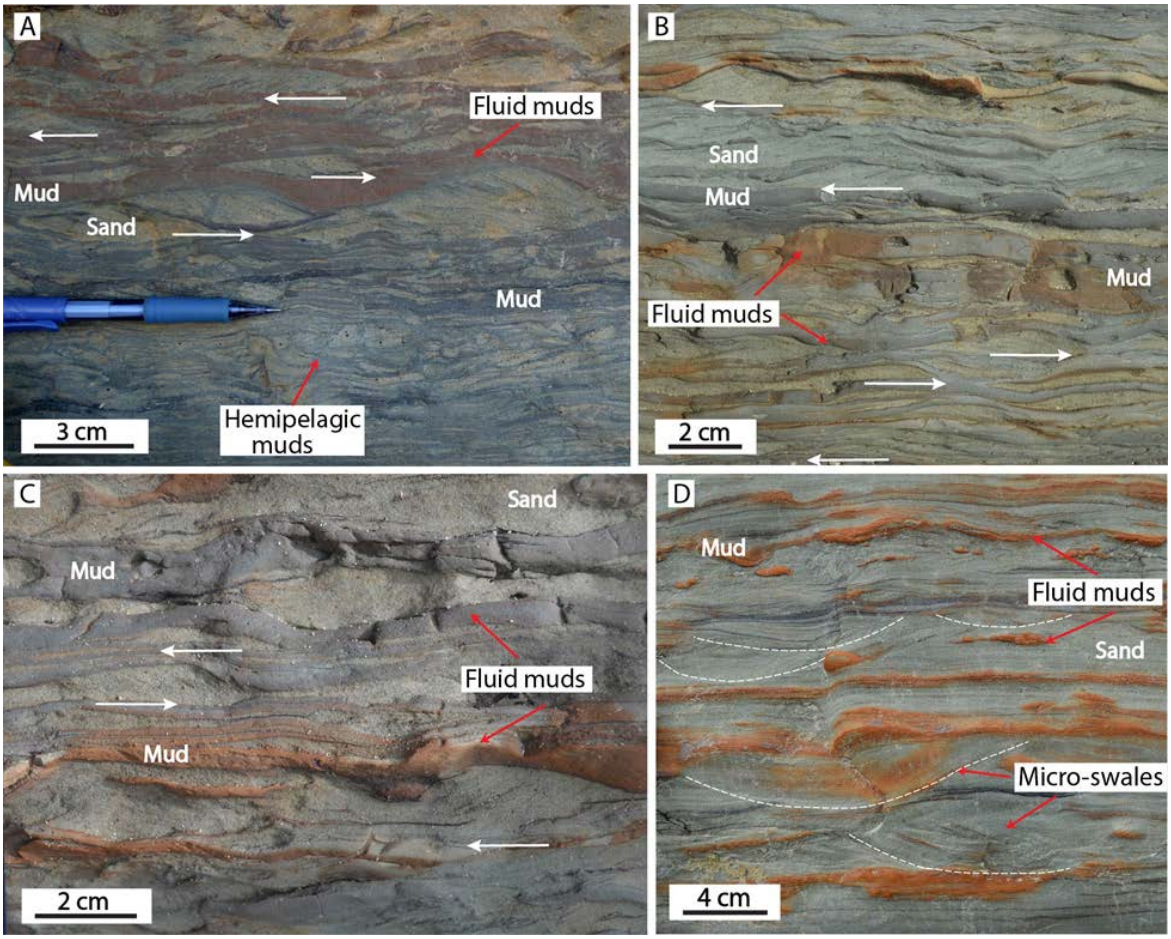

Figure 5.7: (A) Thick, unbioturbated fluid-mud layers interbedded with bi-directional current ripples in the upper part, and thin hemipelagic-mud layers with bioturbation in the lower part. (B) and (C) Thick fluid-mud layers interbedded with bi-directional current ripples. (D) Micro-swaley cross-stratified sandstones with fluid mud flasers. Note that white arrows indicate ripple migration directions.

FLUID MUD INTERACTION WITH STORM WAVE-DOMINATED DELTA FRONT

The study interval of the Mayaro Formation delta lobes, eastern Trinidad, was one of an open ocean, wave-dominated coast (Bowman and Johnson, 2014). It is characterized by multiple stacked 5 to 15 m thick parasequences of storm-wave dominated delta-front deposits (Bowman, 2003; Dixon, 2005; Bowman and Johnson,

2014) with mud deposits (up to 10% of the delta front) (Fig. 5.2C). The parasequences commonly demonstrate a gradual coarsening-upward trend with alternating mud intervals (5cm to 1.5m thick) and hummocky cross-stratified (HCS) sandstone cosets passing upwards to amalgamated swaley cross-stratified (SCS) sandstones (Figs. 5.2C and 5.8A). The mud intervals consist of dominant thick (0.2 to 1 cm) and structureless mud layer and lenticular sandstones (Fig. 5.8B-F). The tops of the mud intervals are relatively flat (Fig. 5.8A-C) or very irregular (Fig. 5.8D and E), and they are overlain by HCS/SCS sandstones occasionally with some mud clasts along the laminae (Fig. 5.8B and D). An idealized fining-upward succession (10-20 cm thick) in which the thick mud deposits occur, shows the following features from bottom to top: (i) sharp-based HCS/SCS sandstones with/without mud clasts, (ii) small-scale swaley-stratified sandstones, (iii) sandy wave ripples (1-2 cm amplitude) interbedded with thin mud layers (< 0.5 cm) (i.e., wavy bedding), and (iv) thick (0.5 to 1 cm) mud layers with small wave ripples (up to 0.5 cm amplitude) (Fig. 5.8D and F). Occasionally there is a coarsening-upward trend exhibited by interbedded mud layers and rippled sandstones, passing upward to HCS/SCS sandstones (Fig. 5.8C). In places, very thick mud intervals (1 to 1.5 m thick) containing small hummocks (dm-scale wavelength) are directly overlain by amalgamated SCS sandstones (Fig. 5.8B). Bioturbation is overall scarce (BI = 0-1) with rare occurrence of *Ophiomorpha*, *Skolithos* and *Thalassinoides*.

The Mayaro Formation is interpreted to represent a storm wave-dominated delta front (Bowman and Johnson, 2014) that reveal the interaction of mud layers and storm wave-generated deposits and some of the dynamics of mud-bank transport. The mud intervals with thick and structureless mud layers described above are interpreted as fluid-mud intervals. The flat to irregular tops of fluid-mud intervals and the overlying HCS/SCS sandstones with mud clasts suggest that storm waves eroded the upper delta

front, then transported and deposited sediment offshore near storm wave base (Dumas and Arnott, 2006). The fining-upward facies succession from storm-generated sandstones to fluid-mud capping is interpreted as deposition under waning/decelerating conditions of storm-wave events (Fig. 5.8). Storm waves eroded the underlying fluid-mud intervals and suspended this sediment during the rising phase of storms. As storm waves waned, sediment settled under oscillatory flow conditions to produce HCS/SCS sandstones, small-scale swaley-stratified sandstones, wave-rippled sandstones interbedded with fluid-mud layers, eventually mantled by thicker fluid-mud layers. The very thick (up to 1.5 m) mud intervals (Fig. 5.8B) probably represent relict mud banks that migrated along the Amazon-Orinoco muddy coast. The preservation of such mud banks in the Pliocene stratigraphy of the Orinoco Delta may be partially due to the unusually high subsidence rates on the Orinoco shelf margin (Wood, 2000). This is consistent with studies of modern mud dynamics where mud banks are well documented to have migrated for great distances on the inner shelf at depths of 0-20 m along the Amazon-Orinoco coast by Guyana Littoral Currents (Allison and Lee, 2004; Anthony et al., 2010). The Mayaro example above possibly represents the dynamic erosion of mud banks near the shelf edge, where the open-marine storm waves are very strong.

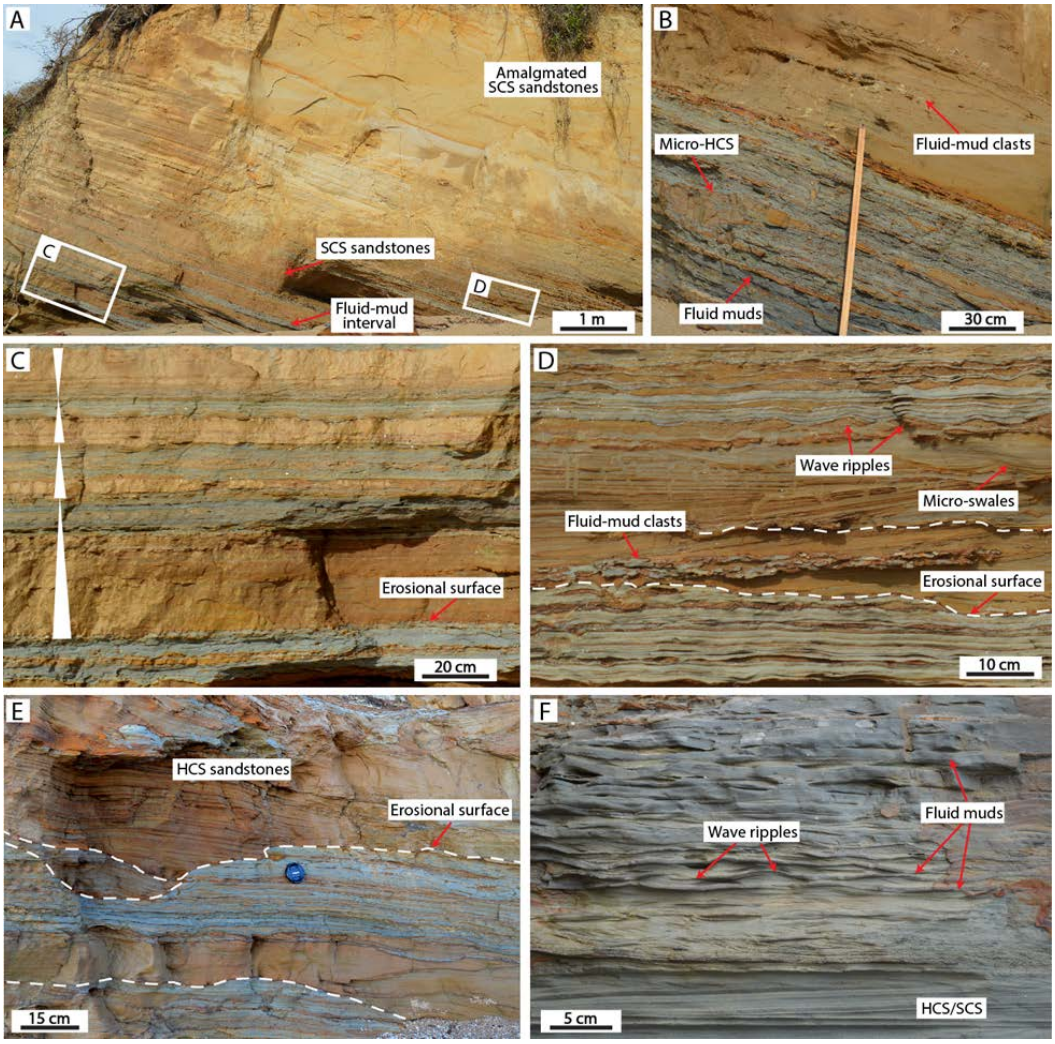

Figure 5.8: Storm wave-dominated sedimentary structures associated fluid-mud deposits in the Mayaro Fm. (A) A coarsening-upward succession showing alternating thin beds of hummocky cross-stratified (HCS) sandstones and fluid-mud-dominated intervals gradually changing upwards to a thick, amalgamated swaley cross-stratified (SCS) sandstone bed. (B) 1 m thick fluid-mud-dominated interval with micro-HCS sandstones and overlying amalgamated SCS sandstones. (C) Several fining-upward intervals and an overlying coarsening-upward interval. (D) Erosional based SCS sandstones changing upwards through micro-swaley cross-stratified sandstones, to interbedded wave-rippled sandstones and fluid-mud layers. (E) HCS sandstones are sharp-based and erosional into the underlying fluid-mud deposits. (F) HCS/SCS sandstones changing upwards through the interbedded wave-rippled sandstones and thin layers of fluid mud, to thicker fluid-mud layers with very small wave ripples.

FLUID MUD CHARACTERISTICS IN TIDE AND WAVE-DOMINATED SETTINGS

Fluid-mud deposits show variable but distinctive characteristics in tide- vs. wave-dominated delta fronts, grouped in 6 types of deposits (A to F; Fig. 5.9). In the tide-dominated delta fronts, three types of fluid-mud deposits (A, B and C) are identified based on thickness, presence/absence of deformation, association with variable sandstone sedimentary structures, and they are described in the order of deposition under decreasing SSC. Type A fluid-mud deposits are very thick (1-10 cm) and show laterally varying thickness in places (Fig. 5.9A). The fluid mud-layers are commonly deformed (squishy geometry) and interbedded with structureless sandstones (Fig. 5.9A). Type B fluid-mud deposits are relatively thick (0.5-1.5 cm) and undeformed, and they form networks around unidirectional or bidirectional current-rippled sandstones (Fig. 5.9B). In places the fluid-mud layers are erosionally overlain by current-rippled sandstones as fluid-mud flasers (Fig. 5.9B). Type C fluid-mud deposits are very thin (0.1-0.5 cm thick) and undeformed, and they either amalgamate to form thicker beds or drape along ripple laminae (Fig. 5.9C). In contrast, the fluid-mud deposits in the wave-dominated delta fronts (D, E and F) exhibit evidence of erosion, reworking and re-deposition into slightly deeper water settings suggested by association with wave ripples and HCS/SCS sandstones. Type D fluid-mud deposits occur as fluid-mud clasts dispersed in the small swaley-stratified sandstones and represent the shallowest location that was reworked by small or damped storm waves (Peng et al., 2018) (Fig. 5.9D). Type E fluid-mud deposits are fluid-mud intervals with lenticular sandstones that show very irregular erosional surfaces overlain by HCS/SCS sandstones (Fig. 5.9E), and they were located deeper than type D fluid-mud deposits. Type F fluid-mud deposits occur in the upper part of fining-upward successions that from bottom to top show (i) sharp-based HCS/SCS sandstones with mud clasts, (ii) small-scale SCS sandstones, (iii) sandy wave ripples with thin layers

(< 0.5 cm) of fluid mud, and (iv) thick (0.5 to 1 cm) fluid-mud layers with small wave ripples (Fig. 5.9F). This type of fluid-mud succession represents deposits of waning storm waves, and they probably occurred at the deepest location (near storm wave base) among all the deposits described in this study.

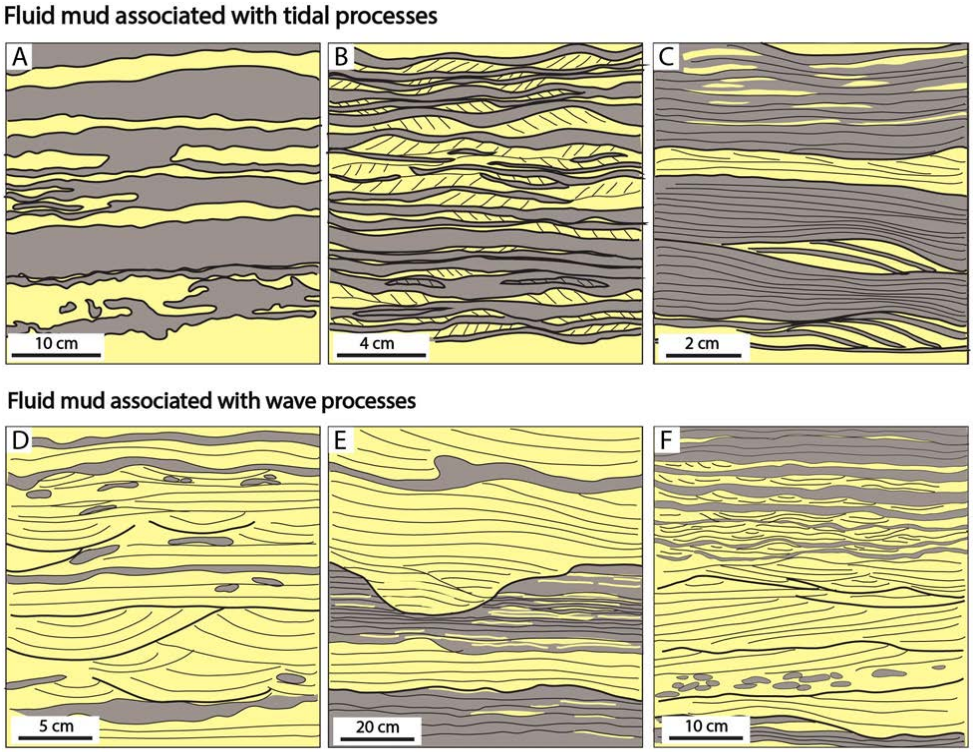

Figure 5.9: Schematic illustrations showing six types of fluid-mud deposits associated with sandstones in tide-dominated delta fronts (A-C) and wave-dominated delta fronts (D-F). (A) Centimeters thick fluid-mud layers with thin discontinuous sandstone beds (from Fig. 5.2A). (B) Wavy bedding with bidirectional current ripples (from Fig. 5.7B). (C) Millimeters thick laminated fluid-mud deposits and lenticular sandstones (from Fig. 5.5C and D). (D) Fluid-mud flasers/clasts associated with wave ripples and small swales (from Fig. 5.7D). (E) Irregular-based HCS sandstones truncating fluid-mud intervals (from Fig. 5.8E). (F) A fining-up succession changes from sharp-based HCS/SCS sandstones with fluid-mud clasts, through small-scale SCS and wave ripples interbedded with thin fluid-mud layers, to thick fluid-mud intervals (from Fig. 5.8D). The legend is the same as in Figure 5.2.

DISCUSSION

Contrasts between storm-wave and tidal current handling of fluid mud

The Pliocene Orinoco Delta is likely to have had both tide- and wave-dominated delta lobes, as in the modern Orinoco Delta (Fig. 5.10). The Pliocene stratigraphy herein shows how tidal and wave processes in these delta fronts handled fluid mud differently. The tide-dominated delta front examples from the Morne L'Enfer and Manzanilla formations demonstrate that the Amazon fluid mud was mainly trapped and deposited within the delta front (Fig. 5.10A). The Amazon fluid mud was likely mixed with the Orinoco mud, particularly on the delta front (Figs. 5.2 and 5.10A). The fluid mud that accumulated on the delta front dampened storm waves, and only strong storm waves were able to propagate far landward (Peng et al., 2018). Occasionally, offshore-directed wave currents transported fluid mud farther offshore onto the prodelta area. In contrast, fluid-mud deposits were rarely preserved and observed in most storm wave-dominated delta fronts in the Moruga Formation (Peng et al., 2017) and Mayaro Formation. The described segment of the Mayaro Formation is one of the few successions that preserved fluid-mud deposits and represents erosion and re-deposition of muddy sediment offshore by storm waves (Fig. 5.10B). Both the tide- and wave-dominated delta fronts exhibit fluid-mud intervals over 1 m thick, probably reflecting muddy bedforms similar to the mud banks currently migrating along the modern Amazon-Orinoco coast (Allison et al., 2000; Allison and Lee, 2004; Anthony et al., 2010). The tide- and wave-dominated deltaic shorelines described here could have coexisted during any state of eustatic sea level, and similar processes to those described above would have occurred, irrespective of changes in the overall mud volumes available, between sea-level highstand and lowstand.

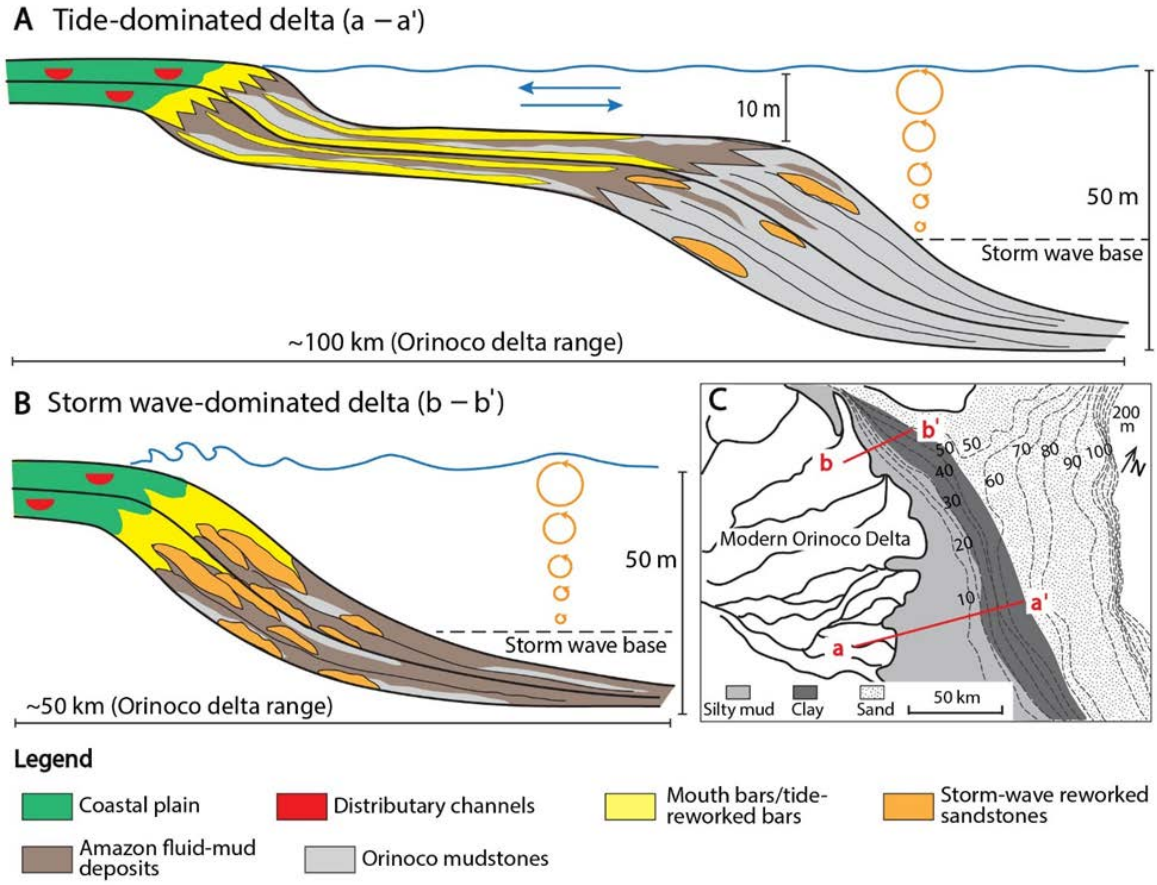

Figure 5.10: Schematic diagrams showing the possible distribution of the fluid-mud deposits in the tide-dominated (A) and wave-dominated (B) delta fronts developed based on outcrop stratigraphic measured sections (see Fig. 5.2) and associated sedimentary structures in the individual tide- and wave-dominated settings (see Fig. 5.9). (C) Map view of the modern Orinoco delta with tide- and wave-dominated deltaic shorelines and possible corresponding locations for each delta profile 10A and 10B (modified from Warne et al., 2002). See text for the details.

Influence of Pliocene glacial-interglacial, sea level changes on fluid mud volumes incorporated into the paleo-Orinoco Delta

The NW transport of the Amazon fine-grained sediment during the Pliocene is likely to have been influenced by high-amplitude, icehouse glacial-interglacial sea-level fluctuations (10s to 100 ky). Falling and lowstand of sea level would have driven deltas

from the innermost shelf to the shelf edge, whereas rise and highstand of sea level would have shifted deltas landward (Fig. 5.11). The repeated deltaic transits back and forth across the Orinoco shelf that built each clastic wedge of the paleo-Orinoco stratigraphy would have received varying Amazon mud volumes with varied volumes as sea level changed (Fig. 5.12). The paleo-Orinoco delta lobes that contain variable proportions of fluid mud at different cross-shelf locations would therefore allow an estimate of the relative abundance of fluid mud delivered to the Orinoco at variable sea level stands.

During falling and lowstand of sea level during glacial periods, the northwestward drift of mud would have gradually decreased (a bigger percentage of the mud budget going over the Amazon shelf edge). This would have made progressively less mud available to the Orinoco system, assuming the Orinoco and Amazon delta systems were broadly in-sync during ca. 30-40 Ky of falling eustatic sea level, and would have caused the Orinoco Delta to receive minimum Amazon mud while it was situated at the shelf edge (Fig. 5.11A-C and 5.12C). The rarely observed fluid-mud deposits in the shelf-edge Moruga and Mayaro delta lobes suggests that less mud reached the Orinoco system or was preserved during the Pliocene sea-level lowstand. Moreover, a prolonged period at the shelf edge, perhaps more than half of the 100 Ky cycle (Burgess and Hovius, 1998; Muto and Steel, 2002; Steel et al., 2008), implies much reduced volumes of Amazon mud during the major part of the sea-level cycle. The likely reason for this is that (1) much of the discharging Amazon sediment during falling and lowstand of sea level would have been captured by the shelf-incised canyon and delivered to the deep water (see Lopez, 2001; 10-70ky, 120-180 ky, 250-300 ky B.P. glacial periods) (Fig. 5.12B) as the Amazon river and delta gradually migrated towards the shelf edge; (2) gradually decreased accommodation on the shelf during sea-level fall would more likely have caused mud transport to the slope; and (3) even the Amazon fluid mud that managed to reach north as

far as the Orinoco delta during sea-level lowstand would have been confronted by the open-marine, high-energy storm waves at the shelf edge and therefore reworked into deeper settings (Peng et al., 2017) (see also 5.1).

In contrast, during rising eustatic sea level and coastal transgression, the maximum volume of mud is likely to have been received on the Orinoco system while it was sited on the inner Orinoco shelf (Fig. 5.11D and 5.12C), since delta lobes and estuaries would have moved landwards causing a widening of the shelf, similar to the modern setting. The Manzanilla and Morne L'Enfer formations at their studied locations represent deltas situated on the inner- to mid-shelf during sea-level highstand in the Pliocene. The fact that greater abundance of fluid-mud deposits is now observed in the Manzanilla and Morne L'Enfer delta lobes tends to confirm that highstand of sea level promoted the largest volumes of fluid mud transported and accumulated on the paleo-Orinoco Delta. This scenario is also supported by the occurrence of only hemipelagic sediment deposited (i.e., 0-10 ky, 70-120 ky, 180-250 ky B.P.) in the Amazon deep-water fan (Fig. 5.12B) during the interglacial periods (Lopez, 2001) as sea-level rise and highstand greatly reduced supply of sediment to the deep water (Piper and Normark, 2001).

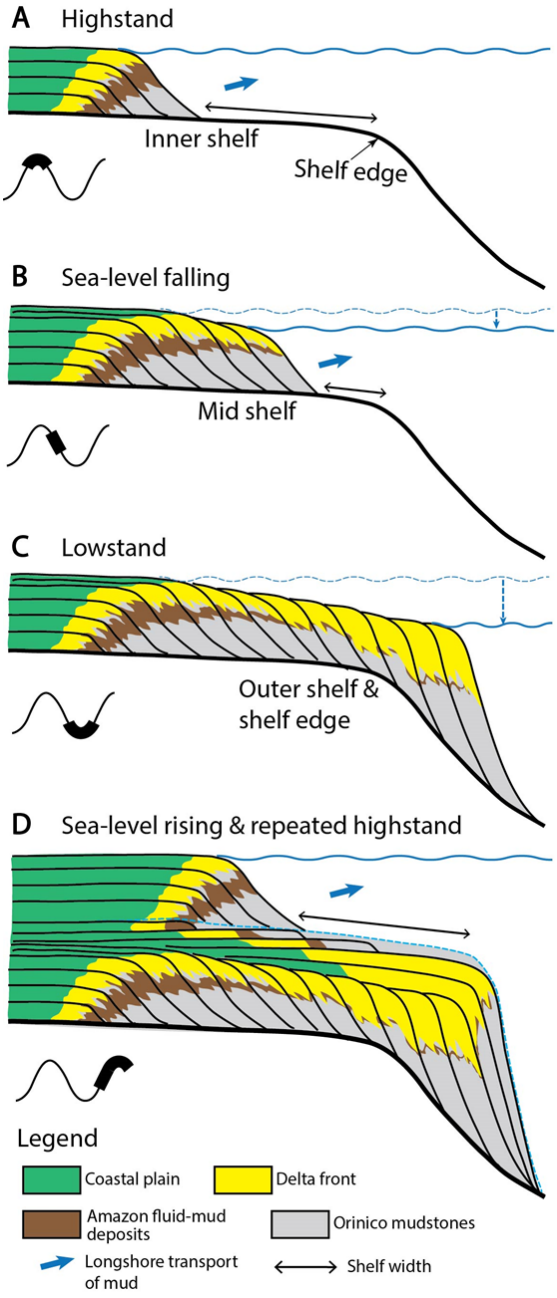

Figure 5.11: Two-dimensional schematic cross-sections of the paleo-Orinoco Delta demonstrating the influence of glacial-interglacial sea-level changes to the incorporated fluid-mud volumes. Note that the gradual decrease in the Amazon fluid-mud volumes (illustrated by thinning of brown-colored zone) as the Orinoco Delta move basinwards during sea-level falling and lowstand.

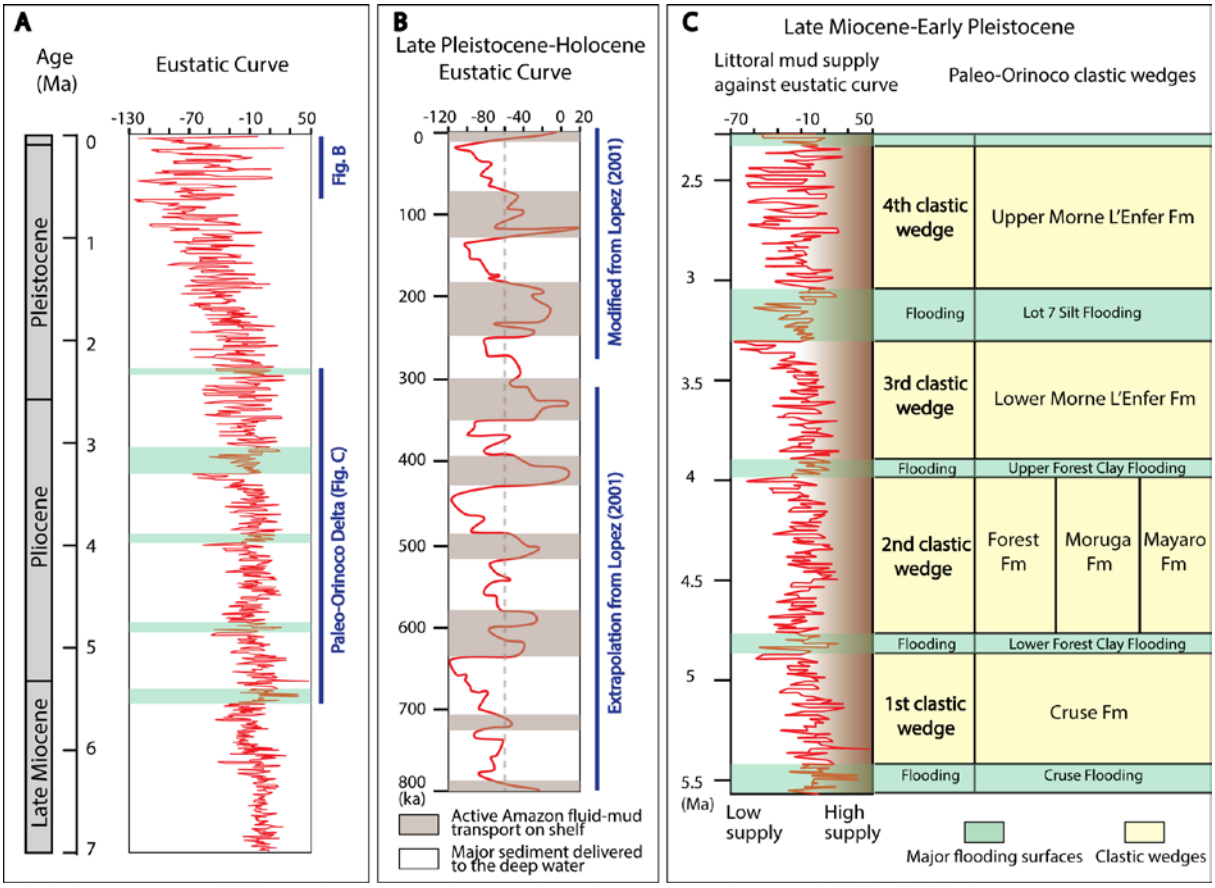

Figure 5.12: (A) Geologic time scale of the late Miocene to the present and eustatic sea-level variability from Miller et al. (2005) with marked paleo-Orinoco clastic wedges separated by major flooding surfaces (modified after Chen et al., 2018). (B) The last 800 kyr sea-level curve indirectly suggests the roughly ~50-70 ky interglacial-glacial periodicity of predominant longshore transport of the Amazon sediment during high sea levels and primarily deep-water delivery of the Amazon sediment during low sea levels (modified from Lopez, 2001). (C) Proposed model of gradually increase or decrease of volumes of the Amazon mud transport and incorporation in the Orinoco delta corresponding with eustatic sea-level rising to highstand and falling to lowstand, respectively.

Comparison with other mud dispersal systems on shelves

Three distinctive and representative mud dispersal systems (i.e., the Amazon-Orinoco coast, the Po-Adriatic shelf, and the Eel River shelf) can be compared in terms of their sediment supply, transport and deposition mechanisms, and depositional locations on the shelf as sea level changed. Mud in these systems is accumulated in the energetic environments by high wave and current activity (Rine and Ginsburg, 1985; Macquaker and Bohacs, 2007; Schieber et al., 2007). Both modern muddy systems and their ancient records are used to evaluate the influence of the sea-level changes on the mud dispersal systems through geologic time.

The modern Amazon-Orinoco muddy system provides examples of muddy coasts and nearshore to inner-shelf mud belts on the wide shelf during rising and highstand of sea level (Fig. 5.13A). In addition, the studied Manzanilla and Morne L'Enfer formations with abundant Amazon-derived fluid mud in the paleo-Orinoco Delta support an enhanced mud delivery condition during sea-level rise to highstand in the Pliocene. During falling and lowstand of sea level, with the Amazon-Orinoco shoreline progressively approaching the shelf edge, much of the Amazon mud sediment would have been directly captured by the shelf-incised canyon head (Lopez, 2001) with a gradually reduced amount of muddy sediment advected on the narrow shelf towards the Orinoco. The rarely observed fluid-mud deposits in the Moruga and Mayaro formations (see also Bowman and Johnson, 2014; Peng et al., 2017) also suggest that less mud reached or was preserved the paleo-Orinoco system during sea-level lowstand.

The late-Holocene mud clinoform (up to 35 m thick) on the western side of the Po-Adriatic shelf represents a highstand mud wedge that extends from the Po Delta (30 m water depth) in the north to several hundreds of kilometers down-flow to offshore Gargano area (100 m water depth) to the south (Fig. 5.13B) (Cattaneo et al., 2003;

Cattaneo et al., 2007; Pellegrini et al., 2015). The Po-Adriatic shelf, in comparison with the Amazon-Orinoco coast and the Eel shelf that face the open oceans, is located in an epicontinental sea that typically experiences less energetic oceanographic storm-wave conditions. About half of the Po River flood sediment is deposited in the Po delta (Palinkas and Nittrouer, 2007), and the remaining sediment from the Po prodelta is reworked and transported downdrift by storm waves or bottom currents (Cattaneo et al., 2007; Palinkas and Nittrouer, 2007). The development of the late-Holocene mud clinoform indicates that the drowning and widening Adriatic shelf enhanced shore-parallel mud advection during rising to highstand of sea level (Cattaneo et al., 2003; Cattaneo et al., 2007; Amorosi et al., 2016). However, during sea-level fall and lowstand phases in the late Pleistocene, the Po River prograded and intercepted most of the Apennine rivers to become a mega-river flowing into the central and south Adriatic as the shelf was progressively exposed (Fig. 5.13B) (Amorosi et al., 2016; Pellegrini et al., 2017). Therefore, most of the western shelf became gradually starved because most sediment was delivered to the deep water (Amorosi et al., 2016) and reduced shelf width hampered longshore dispersal (Fig. 5.13B).

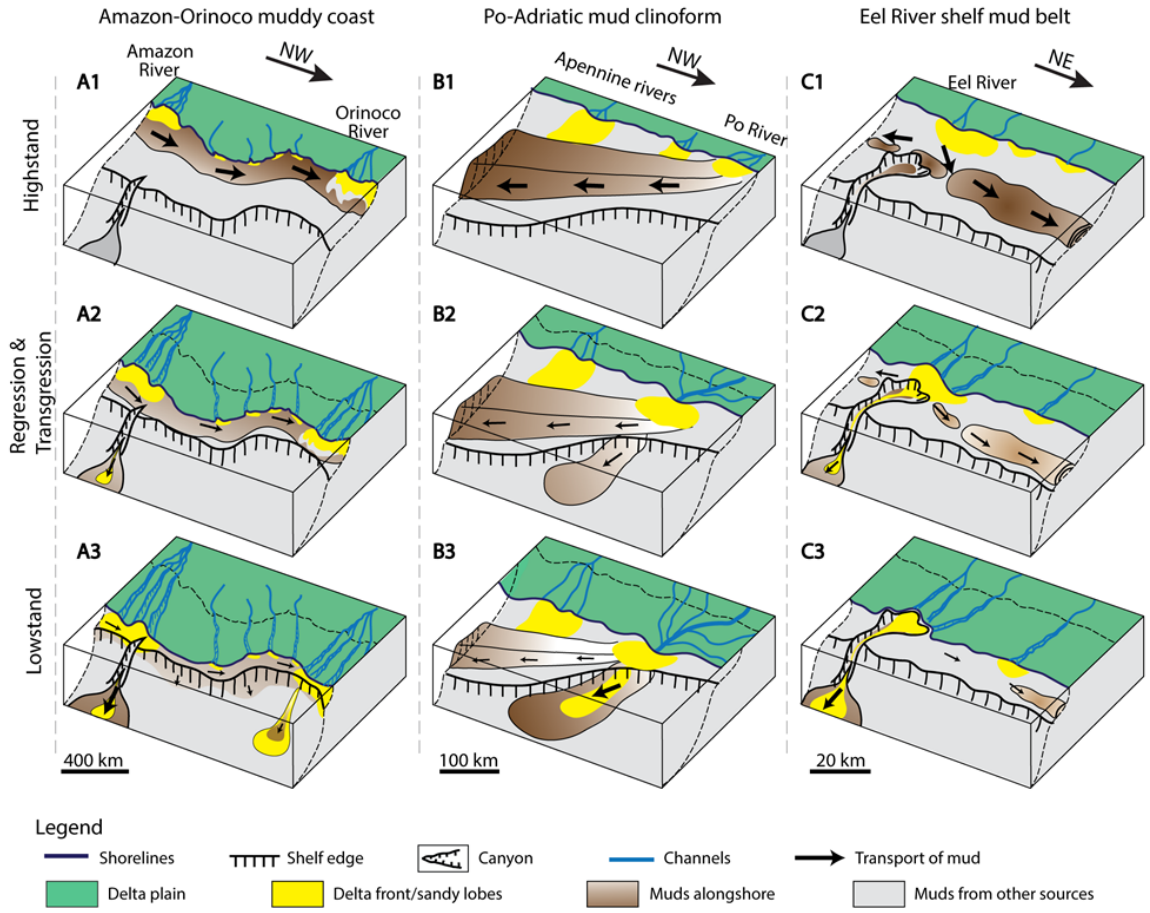

Figure 5.13: Schematic three-dimensional block diagrams illustrating the Amazon-Orinoco muddy coast (A1-3) (modified from Lopez, 2001; Warne et al., 2002), the Po-Adriatic mud clinoform (B1-3) (modified from Amorosi et al., 2016), and the Eel River shelf mud belt offshore California (C1-3) (modified from Sommerfield and Nittrouer, 1999; Burger et al., 2001; Burger et al., 2002; Puig et al., 2003) during eustatic sea-level fluctuations. The shore-parallel transport of mud in the three systems are likely influenced by eustatic sea level by gradually increasing or decreasing mud volumes on the shelf and to the sink, despite the mud transport mechanisms being different.

Mud sedimentation patterns on the Eel shelf shift dramatically in response to sea-level fluctuations. The modern mud accumulation on the Eel shelf represents mud dispersal during sea-level highstand (Fig. 5.13C). In contrast with the open-marine

Amazon-Orinoco shelf (80-300 km in width), the Eel shelf is relatively narrow (15-20 km in width) but relatively energetic with periodically significant storms which influence fluvial sediment supply and mud accumulation on the shelf (Sommerfield and Nittrouer, 1999; Traykovski et al., 2000). The storm waves transport or disperse river sediment predominantly northwards (sometime southwards) and seawards as fluid mud (Fig. 13C) (Sommerfield and Nittrouer, 1999), and distribute this mud on the mid- to outer-shelf (50-150 m water depth) (Sommerfield and Nittrouer, 1999; Wheatcroft and Borgeld, 2000). Similar to the Amazon-Orinoco and Po-Adriatic systems, the alongshelf mud dispersal is also likely to occur during transgressive and highstand phases with enough accommodation for shallow marine mud dispersal processes. The late-Pleistocene Eel shelf would have represented a lowstand phase, in which southwest-oriented fluvial channels incised the subaerially exposed shelf (130 m below present sea level) and discharged most sediment towards the Eel Canyon (Fig. 5.13C) (Burger et al., 2001; Burger et al., 2002) with less sediment available on the shelf.

CONCLUSIONS

Outcrop examples from the Morne L'Enfer, Manzanilla, and Mayaro delta lobes of the Orinoco paleo-delta system show distinctive fluid-mud characteristics in their tide- and wave-dominated delta fronts. In the tide-dominated delta fronts, fluid-mud deposits range from very thick and deformed layers to very thin layers that amalgamated to thicker beds or drape along ripple laminae. The sedimentary structures in sandstones associated with the fluid-mud deposits are structureless to bidirectional current ripples that were generated by tidal processes. The fluid-mud deposits in the wave-dominated delta fronts are preserved as broken fluid-mud flasers/clasts, intervals erosionally overlain by

HCS/SCS sandstones, or layers interbedded with wave ripples in the upper part of the waning storm-wave deposits.

The variable characteristics in the fluid-mud deposits and associated sandstones illustrate how tide- vs. wave-dominated delta fronts handled the impact of Amazon fluid mud that arrived by Guyana current littoral drift. The tide-dominated delta lobes were more likely to trap muddy sediment near the shoreline and on the subaqueous delta platform in paleo-water depth less than 10 to 20 m. In contrast, the storm wave-dominated delta lobes handled the fluid mud dynamically; the open marine storm waves tended to erode and re-suspend the fluid mud in shallow water, and re-deposit it into deeper water near storm wave base (15-50 m water depth).

Amazon mud transport and thus the impinging of the Amazon mud into the front of the paleo-Orinoco Delta were also influenced by high-amplitude, glacio-eustatic sea-level changes as supported by the Pliocene Orinoco outcrops. Amazon deltaic regressions, during glacial fall and lowstands of sea level, would have caused a systematic reduction of shelf width and most of the Amazon sediment budget bypassed the shelf edge into the deep-water basin. Therefore, greatly reduced volumes of Amazon fluid mud would have been available to drift northwards along the Guianas coastline for incorporation into the Orinoco delta front. In contrast, during sea-level rise and highstand of interglacial periods, much of the muddy sediment budget from the Amazon river would have been directed northwestwards along the shelf, and thus the Amazon mud dispersal system was active all the way to the Orinoco at this time.

References

Abreu, V., Sullivan, M., Pirmez, C., Mohrig, D., 2003. Lateral accretion packages (LAPs): an important reservoir element in deep water sinuous channels. Marine and Petroleum Geology 20, 631-648.

Ahmed, S., Bhattacharya, J.P., Garza, D.E., Li, Y., 2014. Facies architecture and stratigraphic evolution of a river-dominated delta front, Turonian Ferron Sandstone, Utah, USA. Journal of Sedimentary Research 84, 97-121.

Ainsworth, R.B., Vakarelov, B.K., MacEachern, J.A., Nanson, R.A., Lane, T.I., Rarity, F., Dashtgard, S.E., 2016. Process-Driven Architectural Variability In Mouth-Bar Deposits: A Case Study From A Mixed-Process Mouth-Bar Complex, Drumheller, Alberta, Canada. Journal of Sedimentary Research 86, 512-541.

Ainsworth, R.B., Vakarelov, B.K., Nanson, R.A., 2011. Dynamic spatial and temporal prediction of changes in depositional processes on clastic shorelines: Toward improved subsurface uncertainty reduction and management. AAPG bulletin 95, 267-297.

Ali, W., 1995. Reconnisance Field work south and south east coast –Trinidad, 3rd GSTT Conference and 14th Caribbean Geological Conference, Trinidad.

Allen, J.R.L., 1970. A quantitative model of climbing ripples and their cross-laminated deposits. Sedimentology 14, 5-26.

Allen, J.R.L., 1973. A classification of climbing-ripple cross-lamination. Journal of the Geological Society 129, 537-541.

Allison, M., Nittrouer, C., Faria, L., 1995a. Rates and mechanisms of shoreface progradation and retreat downdrift of the Amazon river mouth. Marine Geology 125, 373-392.

Allison, M., Nittrouer, C., Kineke, G., 1995b. Seasonal sediment storage on mudflats adjacent to the Amazon River. Marine Geology 125, 303-328.

Allison, M.A., Lee, M.T., 2004. Sediment exchange between Amazon mudbanks and shore-fringing mangroves in French Guiana. Marine Geology 208, 169-190.

Allison, M.A., Lee, M.T., Ogston, A.S., Aller, R.C., 2000. Origin of Amazon mudbanks along the northeastern coast of South America. Marine Geology 163, 241-256.

Allison, M.A., Sheremet, A., Goñi, M.A., Stone, G.W., 2005. Storm layer deposition on the Mississippi–Atchafalaya subaqueous delta generated by Hurricane Lili in 2002. Continental Shelf Research 25, 2213-2232.

Amorosi, A., Maselli, V., Trincardi, F., 2016. Onshore to offshore anatomy of a late Quaternary source-to-sink system (Po Plain–Adriatic Sea, Italy). Earth-Science Reviews 153, 212-237.

Anthony, E.J., Dolique, F., 2004. The influence of Amazon-derived mud banks on the morphology of sandy headland-bound beaches in Cayenne, French Guiana: a short-to long-term perspective. Marine Geology 208, 249-264.

Anthony, E.J., Gardel, A., Gratiot, N., 2014. Fluvial sediment supply, mud banks, cheniers and the morphodynamics of the coast of South America between the Amazon and Orinoco river mouths, in: Martini, I.P., Wanless, H.R. (Eds.),

Sedimentary Coastal Zones from High to Low Latitudes: Similarities and Differences, Geological Society of London, Special Publication 388, pp. 533-560.
Anthony, E.J., Gardel, A., Gratiot, N., Proisy, C., Allison, M.A., Dolique, F., Fromard, F., 2010. The Amazon-influenced muddy coast of South America: A review of mud-bank–shoreline interactions. Earth-Science Reviews 103, 99-121.
Aslan, A., White, W.A., Warne, A.G., Guevara, E.H., 2003. Holocene evolution of the western Orinoco Delta, Venezuela. Geological Society of America, Bulletin 115, 479-498.
Augustinus, P., Hazelhoff, L., Kroon, A., 1989. The chenier coast of Suriname: modern and geological development. Marine Geology 90, 269-281.
Augustinus, P.G., 2004. The influence of the trade winds on the coastal development of the Guianas at various scale levels: a synthesis. Marine Geology 208, 145-151.
Baas, J.H., 1999. An empirical model for the development and equilibrium morphology of current ripples in fine sand. Sedimentology 46, 123-138.
Baas, J.H., Best, J.L., Peakall, J., Wang, M., 2009. A phase diagram for turbulent, transitional, and laminar clay suspension flows. Journal of Sedimentary Research 79, 162-183.
Babb, S., Mann, P., 1999. Structural and sedimentary development of a neogene transpressional plate boundary between the caribbean and South America plates in Trinidad and the Gulf of paria, in: Mann, P. (Ed.), Sedimentary Basins of the World. Elsevier, pp. 495-557.
Beaubouef, R., Friedmann, S., 2000. High resolution seismic/sequence stratigraphic framework for the evolution of Pleistocene intra slope basins, western Gulf of Mexico: depositional models and reservoir analogs, Deep-water reservoirs of the world: Gulf Coast Section SEPM 20th Annual Research Conference. SEPM, pp. 40-60.
Bhattacharya, J.P., Giosan, L., 2003. Wave-influenced deltas: geomorphological implications for facies reconstruction. Sedimentology 50, 187-210.
Bhattacharya, J.P., MacEachern, J.A., 2009. Hyperpycnal Rivers and Prodeltaic Shelves in the Cretaceous Seaway of North America. Journal of Sedimentary Research 79, 184-209.
Bouma, A.H., Kuenen, P.H., Shepard, F.P., 1962. Sedimentology of some flysch deposits: a graphic approach to facies interpretation. Elsevier Amsterdam.
Bowman, A.P., 2003. Sequence stratigraphy and reservoir characterization in the Columbus Basin, Trinidad. Imperial College London, Ph.D. dissertation, p. 530.
Bowman, A.P., Johnson, H.D., 2014. Storm-dominated shelf-edge delta successions in a high accommodation setting: The palaeo-Orinoco Delta (Mayaro Formation), Columbus Basin, South-East Trinidad. Sedimentology 61, 792-835.
Boyd, R., Dalrymple, R., Zaitlin, B., 1992. Classification of clastic coastal depositional environments. Sedimentary Geology 80, 139-150.
Boyd, R., Ruming, K., Goodwin, I., Sandstrom, M., Schröder-Adams, C., 2008. Highstand transport of coastal sand to the deep ocean: a case study from Fraser Island, southeast Australia. Geology 36, 15-18.

Brinkman, R., Pons, L., 1968. A pedo-geomorphological classification and map of the Holocene sediments in the coastal plain of the three Guianas. Soil Survey Institute Wageningen, the Netherlands.
Buatois, L.A., Santiago, N., Herrera, M., PLINK-BJÖRKLUND, P., Steel, R., Espin, M., Parra, K., 2012. Sedimentological and ichnological signatures of changes in wave, river and tidal influence along a Neogene tropical deltaic shoreline. Sedimentology 59, 1568-1612.
Burger, R.L., Fulthorpe, C.S., Austin, J.A., 2001. Late Pleistocene channel incisions in the southern Eel River Basin, northern California: implications for tectonic vs. eustatic influences on shelf sedimentation patterns. Marine Geology 177, 317-330.
Burger, R.L., Fulthorpe, C.S., Austin, J.A., Gulick, S.P., 2002. Lower Pleistocene to present structural deformation and sequence stratigraphy of the continental shelf, offshore Eel River Basin, northern California. Marine Geology 185, 249-281.
Burgess, P.M., Hovius, N., 1998. Rates of delta progradation during highstands: consequences for timing of deposition in deep-marine systems. Journal of the Geological Society 155, 217-222.
Cacchione, D., Drake, D., Kayen, R., Sternberg, R., Kineke, G., Tate, G., 1995. Measurements in the bottom boundary layer on the Amazon subaqueous delta. Marine Geology 125, 235-257.
Callot, P., Odonne, F., Debroas, E.J., Maillard, A., Dhont, D., Basile, C., Hoareau, G., 2009. Three-dimensional architecture of submarine slide surfaces and associated soft-sediment deformation in the Lutetian Sobrarbe deltaic complex (Ainsa, Spanish Pyrenees). Sedimentology 56, 1226-1249.
Cartigny, M.J., Ventra, D., Postma, G., Den Berg, J.H., 2014. Morphodynamics and sedimentary structures of bedforms under supercritical-flow conditions: New insights from flume experiments. Sedimentology 61, 712-748.
Carvajal, C., Steel, R., 2009. Shelf-edge architecture and bypass of sand to deep water: influence of shelf-edge processes, sea level, and sediment supply. Journal of Sedimentary Research 79, 652-672.
Carvajal, C., Steel, R., Petter, A., 2009. Sediment supply: the main driver of shelf-margin growth. Earth-Science Reviews 96, 221-248.
Carvajal, C.R., Steel, R.J., 2006. Thick turbidite successions from supply-dominated shelves during sea-level highstand. Geology 34, 665-668.
Cattaneo, A., Correggiari, A., Langone, L., Trincardi, F., 2003. The late-Holocene Gargano subaqueous delta, Adriatic shelf: sediment pathways and supply fluctuations. Marine Geology 193, 61-91.
Cattaneo, A., Trincardi, F., Asioli, A., Correggiari, A., 2007. The Western Adriatic shelf clinoform: energy-limited bottomset. Continental Shelf Research 27, 506-525.
Cheel, R.J., 1991. Grain fabric in hummocky cross-stratified storm beds: genetic implications. Journal of Sedimentary Research 61, 102-110.
Cheel, R.J., Leckie, D.A., 1993. Hummocky cross-stratification. Sedimentology Review: Oxford, U.K., Blackwell Scientific Publications 31, 103-122.

Chen, S., Steel, R., Olariu, C., Li, S., 2018. Growth of the paleo-Orinoco shelf-margin prism: Process regimes, delta evolution, and sediment budget beyond the shelf edge. GSA Bulletin 130, 35-63.
Chen, S., Steel, R.J., Dixon, J., Osman, A., 2014. Facies and architecture of a tide-dominated segment of the Late Pliocene Orinoco Delta (Morne L'Enfer Formation) SW Trinidad. Marine and Petroleum Geology 57, 208-232.
Chen, S., Steel, R.J., Olariu, C., 2016. Upper-slope to shelf-edge delta architecture, Miocene Cruse Formation, Orinoco shelf margin, Trinidad. Journal of Sedimentary Research 86, 87-106.
Chiocci, F., 1994. Very High-Resolution Seismics as a Tool for Sequence Stratigraphy Applied to Outcrop Scale--Examples from Eastern Tyrrhenian Margin Holocene/Pleistocene Deposits. AAPG bulletin 78, 378-395.
Chiocci, F.L., Casalbore, D., 2011. Submarine gullies on Italian upper slopes and their relationship with volcanic activity revisited 20 years after Bill Normark's pioneering work. Geosphere 7, 1284-1293.
Chiocci, F.L., Normark, W.R., 1992. Effect of sea-level variation on upper-slope depositional processes offshore of Tiber delta, Tyrrhenian Sea, Italy. Marine Geology 104, 109-122.
Clark, J.D., Pickering, K.T., 1996. Architectural elements and growth patterns of submarine channels: application to hydrocarbon exploration. AAPG bulletin 80, 194-220.
Coleman, J.M., Prior, D.B., Lindsay, J.F., 1983. Deltaic influences on shelf edge instability processes, The shelf break: critical interface on continental margins (Eds Stanley, D. J., and Moore, G. T.): Society of Economic Paleontologists and Mineralogists Special Publication, pp. 121-137.
Coleman, J.M., Wright, L., 1975. Modern river deltas: variability of processes and sand bodies.
Correggiari, A., Cattaneo, A., Trincardi, F., 2005. The modern Po Delta system: lobe switching and asymmetric prodelta growth. Marine Geology 222, 49-74.
Covault, J.A., Graham, S.A., 2010. Submarine fans at all sea-level stands: tectono-morphologic and climatic controls on terrigenous sediment delivery to the deep sea. Geology 38, 939-942.
Dalrymple, R.W., Baker, E.K., Harris, P.T., Hughes, M.G., 2003. Sedimentology and stratigraphy of a tide-dominated, foreland-basin delta (Fly River, Papua New Guinea), in: Sidi, F.H., Nummedal, D., Imbert, P., Darman, H., Posamentier, H.W. (Eds.), Tropical Deltas of Southeast Asia-Sedimentology, Stratigraphy, and Petroleum Geology, SEPM, Special Publication 76, pp. 147-173.
Dalrymple, R.W., Choi, K., 2007. Morphologic and facies trends through the fluvial–marine transition in tide-dominated depositional systems: a schematic framework for environmental and sequence-stratigraphic interpretation. Earth-Science Reviews 81, 135-174.
Dalrymple, R.W., Makino, Y., Zaitlin, B.A., 1991. Temporal and spatial patterns of rhythmite deposition on mud flats in the macrotidal Cobequid Bay-Salmon River

estuary, Bay of Fundy, Canada, in: Smith, D.G., Reinson, G.E., Zaitlin, B.A., Rahmani, R.A. (Eds.), Clastic Tidal Sedimentology: Canadian Society of Petroleum Geologists, Memoir 16, pp. 137-160.

Dasgupta, S., Buatois, L.A., 2012. Unusual occurrence and stratigraphic significance of the Glossifungites ichnofacies in a submarine paleo-canyon—Example from a Pliocene shelf-edge delta, Southeast Trinidad. Sedimentary Geology 269, 69-77.

Dasgupta, S., Buatois, L.A., 2015. High-frequency stacking pattern and stages of canyon/gully evolution across a forced regressive shelf-edge delta-front. Marine and Petroleum Geology 68, 40-53.

Dasgupta, S., Buatois, L.A., Mángano, M.G., 2016. Living On the Edge: Evaluating the Impact of Stress Factors On Animal–Sediment Interactions In Subenvironments of A Shelf-Margin Delta, the Mayaro Formation, Trinidad. Journal of Sedimentary Research 86, 1034-1066.

Dashtgard, S.E., MacEachern, J.A., Frey, S.E., Gingras, M.K., 2012. Tidal effects on the shoreface: Towards a conceptual framework. Sedimentary Geology 279, 42-61.

de Raaf, J.F.M., Boersma, J.R., van Gelder, A., 1977. Wave-generated structures and sequences from a shallow marine succession, Lower Carboniferous, County Cork, Ireland. Sedimentology 24, 451-483.

Deibert, J., Benda, T., Løseth, T., Schellpeper, M., Steel, R., 2003. Eocene clinoform growth in front of a storm-wave-dominated shelf, Central Basin, Spitsbergen: no significant sand delivery to deepwater areas. Journal of Sedimentary Research 73, 546-558.

Di Croce, J., Bally, A., Vail, P., 1999. Sequence stratigraphy of the eastern Venezuelan basin. Sedimentary Basins of the World 4, 419-476.

Díaz de Gamero, M.L., 1996. The changing course of the Orinoco River during the Neogene: a review. Palaeogeography, Palaeoclimatology, Palaeoecology 123, 385-402.

Dixon, J.F., Steel, R.J., Olariu, C., 2012a. River-dominated, shelf-edge deltas: delivery of sand across the shelf break in the absence of slope incision. Sedimentology 59, 1133-1157.

Dixon, J.F., Steel, R.J., Olariu, C., 2012b. Shelf-Edge Delta Regime As A Predictor of Deep-Water Deposition. Journal of Sedimentary Research 82, 681-687.

Dixon, J.F., Steel, R.J., Olariu, C., 2013. A Model for Cutting and Healing of Deltaic Mouth Bars At the Shelf Edge: Mechanism for Basin-Margin Accretion. Journal of Sedimentary Research 83, 284-299.

Dixon, R.J., 2005. Fieldtrip to examine outcrops of the Mayaro Formation, Mayaro Beach, SE Trinidad, Guide to Selected Geological Localities on Trinidad and Tobago, Geological Society of Trinidad and Tobago, p. 39.

Draut, A.E., Kineke, G.C., Huh, O.K., Grymes, J.M., Westphal, K.A., Moeller, C.C., 2005. Coastal mudflat accretion under energetic conditions, Louisiana chenier-plain coast, USA. Marine Geology 214, 27-47.

Driscoll, N.W., Karner, G.D., 1999. Three-dimensional quantitative modeling of clinoform development. Marine Geology 154, 383-398.

Duke, W.L., 1985. Hummocky cross-stratification, tropical hurricanes, and intense winter storms. Sedimentology 32, 167-194.
Dumas, S., Arnott, R., 2006. Origin of hummocky and swaley cross-stratification—the controlling influence of unidirectional current strength and aggradation rate. Geology 34, 1073-1076.
Dumas, S., Arnott, R., Southard, J.B., 2005. Experiments on oscillatory-flow and combined-flow bed forms: implications for interpreting parts of the shallow-marine sedimentary record. Journal of Sedimentary Research 75, 501-513.
Dzulynski, S., 1963. Directional structures in flysch. Studia Geologica Polonica 12, 136.
Eisma, D., Augustinus, P., Alexander, C., 1991. Recent and subrecent changes in the dispersal of Amazon mud. Netherlands Journal of Sea Research 28, 181-192.
Eisma, D., Van der Gaast, S., Martin, J., Thomas, A., 1978. Suspended matter and bottom deposits of the Orinoco delta: turbidity, mineralogy and elementary composition. Netherlands Journal of Sea Research 12, 224-251.
Eisma, D., Van der Marel, H., 1971. Marine muds along the Guyana coast and their origin from the Amazon Basin. Contributions to Mineralogy and Petrology 31, 321-334.
Escalona, A., Mann, P., 2011. Tectonics, basin subsidence mechanisms, and paleogeography of the Caribbean-South American plate boundary zone. Marine and Petroleum Geology 28, 8-39.
Field, M., Gardner, J., Prior, D., 1999. Geometry and significance of stacked gullies on the northern California slope. Marine Geology 154, 271-286.
Figueiredo, J., Hoorn, C., Van der Ven, P., Soares, E., 2009. Late Miocene onset of the Amazon River and the Amazon deep-sea fan: Evidence from the Foz do Amazonas Basin. Geology 37, 619-622.
Fongngern, R., Olariu, C., Steel, R.J., Krézsek, C., 2015. Clinoform growth in a Miocene, Para-tethyan deep lake basin: thin topsets, irregular foresets and thick bottomsets. Basin Research 28, 770-795.
Galloway, W., Hobday, D., 1983. Terrigenous Clastic Depositional Settings: Applications to Petroleum, Coal, and Uranium Exploration. Springer Verlag, New York.
Galloway, W.E., 1975. Process framework for describing the morphologic and stratigraphic evolution of deltaic depositional systems.
Galloway, W.E., 1998. Siliciclastic slope and base-of-slope depositional systems: component facies, stratigraphic architecture, and classification. AAPG bulletin 82, 569-595.
Gani, M.R., Bhattacharya, J.P., 2007. Basic Building Blocks and Process Variability of a Cretaceous Delta: Internal Facies Architecture Reveals a More Dynamic Interaction of River, Wave, and Tidal Processes Than Is Indicated by External Shape. Journal of Sedimentary Research 77, 284-302.
Gani, M.R., Bhattacharya, J.P., MacEachern, J.A., 2007. Using ichnology to determine relative influence of waves, storms, tides, and rivers in deltaic deposits: examples from Cretaceous Western Interior Seaway, USA, in: MacEachern, J.A., Bann,

K.L., Gingras, M.K., Pemberton, S.G. (Eds.), Applied Ichnology, SEPM, Short Course Notes 52, pp. 209-225.
Gardel, A., Gratiot, N., 2005. A Satellite Image–Based Method for Estimating Rates of Mud Bank Migration, French Guiana, South America. Journal of Coastal Research, 720-728.
Gibbs, R.J., Konwar, L., 1986. Coagulation and settling of Amazon River suspended sediment. Continental Shelf Research 6, 127-149.
Gong, C., Steel, R.J., Wang, Y., Lin, C., Olariu, C., 2016. Grain size and transport regime at shelf edge as fundamental controls on delivery of shelf-edge sands to deepwater. Earth-Science Reviews 157, 32-60.
Goodbred, S.L., Kuehl, S.A., Steckler, M.S., Sarker, M.H., 2003. Controls on facies distribution and stratigraphic preservation in the Ganges–Brahmaputra delta sequence. Sedimentary Geology 155, 301-316.
Goodbred, S.L.J., Saito, Y., 2012. Tide-dominated deltas, in: Davis, R.A.J., Dalrymple, R.W. (Eds.), Principles of Tidal Sedimentology. Berlin, Springer, pp. 129-149.
Gratiot, N., Gardel, A., Anthony, E.J., 2007. Trade-wind waves and mud dynamics on the French Guiana coast, South America: input from ERA-40 wave data and field investigations. Marine Geology 236, 15-26.
Hampson, G., Steel, R., Burgess, P., Dalrymple, R., 2008. Recent advances in models of shallow-marine stratigraphy: Introduction and perspectives. Recent advances in models of shallow-marine stratigraphy: SEPM Special Publication 90, 3-12.
Hampson, G.J., 2010. Sediment dispersal and quantitative stratigraphic architecture across an ancient shelf. Sedimentology 57, 96-141.
Hampson, G.J., Gani, M.R., Sharman, K.E., Irfan, N., Bracken, B., 2011. Along-strike and down-dip variations in shallow-marine sequence stratigraphic architecture: Upper Cretaceous Star Point Sandstone, Wasatch Plateau, Central Utah, USA. Journal of Sedimentary Research 81, 159-184.
Hampson, G.J., Howell, J.A., 2005. Sedimentologic and geomorphic characterization of ancient wave-dominated deltaic shorelines: Upper Cretaceous Blackhawk Formation, Book Cliffs, Utah, USA. In: River Deltas-Concepts, Models and Examples (Ed. by L. Giosan & J.P. Bhattacharya), SEPM Spec. Publ. 83, 133-154.
Hampson, G.J., Premwichein, K., 2017. Sedimentologic character of ancient muddy subaqueous-deltaic clinoforms: Down Cliff Clay Member, Bridport Sand Formation, Wessex Basin, U.K. Journal of Sedimentary Research 87, 951-966.
Hanebuth, T.J., Lantzsch, H., Nizou, J., 2015. Mud depocenters on continental shelves—appearance, initiation times, and growth dynamics. Geo-Marine Letters 35, 487-503.
Harris, P., Baker, E., Cole, A., Short, S., 1993. A preliminary study of sedimentation in the tidally dominated Fly River Delta, Gulf of Papua. Continental Shelf Research 13, 441-472.
Helland-Hansen, W., Hampson, G., 2009. Trajectory analysis: concepts and applications. Basin Research 21, 454-483.

Hirayama, J., Nakajima, T., 1977. Analytical study of turbidites, Otadai Formation, Boso Peninsula, Japan. Sedimentology 24, 747-779.
Hori, K., Saito, Y., Zhao, Q., Cheng, X., Wang, P., Sato, Y., Li, C., 2001. Sedimentary facies and Holocene progradation rates of the Changjiang (Yangtze) delta, China. Geomorphology 41, 233-248.
Hori, K., Saito, Y., Zhao, Q., Wang, P., 2002. Architecture and evolution of the tide-dominated Changjiang (Yangtze) River delta, China. Sedimentary Geology 146, 249-264.
Hubbard, S.M., de Ruig, M.J., Graham, S.A., 2009. Confined channel-levee complex development in an elongate depo-center: deep-water Tertiary strata of the Austrian Molasse basin. Marine and Petroleum Geology 26, 85-112.
Huggins, G.V., 2007. The facies architecture of the Manzanilla Formation, Trinidad and Tobago. University of Texas at Austin, Unpublished MS thesis, p. 81.
Ichaso, A.A., Dalrymple, R.W., 2009. Tide- and wave-generated fluid mud deposits in the Tilje Formation (Jurassic), offshore Norway. Geology 37, 539-542.
Ito, M., 2013. The role of slump scars in slope channel initiation: A case study from the Miocene Jatiluhur Formation in the Bogor Trough, West Java. Journal of Asian Earth Sciences 73, 68-86.
Jaeger, J.M., Nittrouer, C.A., 1995. Tidal controls on the formation of fine-scale sedimentary strata near the Amazon River mouth. Marine Geology 125, 259-281.
Jobe, Z.R., Lowe, D.R., Morris, W.R., 2012. Climbing-ripple successions in turbidite systems: depositional environments, sedimentation rates and accumulation times. Sedimentology 59, 867-898.
Jones, G.E., Hodgson, D.M., Flint, S.S., 2013. Contrast in the process response of stacked clinothems to the shelf-slope rollover. Geosphere 9, 299-316.
Kineke, G., Sternberg, R., 1995. Distribution of fluid muds on the Amazon continental shelf. Marine Geology 125, 193-233.
Kineke, G., Sternberg, R., Trowbridge, J., Geyer, W., 1996. Fluid-mud processes on the Amazon continental shelf. Continental Shelf Research 16, 667-696.
Kirby, R., Parker, W., 1983. Distribution and behavior of fine sediment in the Severn Estuary and Inner Bristol Channel, UK. Canadian Journal of Fisheries and Aquatic Sciences 40, s83-s95.
Kneller, B., 1995. Beyond the turbidite paradigm: physical models for deposition of turbidites and their implications for reservoir prediction. Geological Society, London, Special Publications 94, 31-49.
Kneller, B.C., Branney, M.J., 1995. Sustained high-density turbidity currents and the deposition of thick massive sands. Sedimentology 42, 607-616.
Komar, P.D., 1998. Beach Processes and Sedimentation. Prentice Hall, New Jersey.
Kuehl, S.A., Allison, M.A., Goodbred, S.L., Kudrass, H., 2005. The Ganges-Brahmaputra Delta, in: Gioson, L., Bhattacharya, J.P. (Eds.), River Deltas-Concepts, Models and Examples, SEPM, Special Publication 83, pp. 413-434.
Kuehl, S.A., DeMaster, D.J., Nittrouer, C.A., 1986. Nature of sediment accumulation on the Amazon continental shelf. Continental Shelf Research 6, 209-225.

Kuehl, S.A., Levy, B.M., Moore, W.S., Allison, M.A., 1997. Subaqueous delta of the Ganges-Brahmaputra river system. Marine Geology 144, 81-96.
Kuenen, P.H., 1966. Experimental turbidite lamination in a circular flume. The Journal of Geology 74, 523-545.
Kugler, H., 1959. Geological Maps of Trinidad–1: 50,000 and Spot Maps at Various Scales. Petroleum Association of Trinidad, Port of Spain.
Lang, J., Winsemann, J., 2013. Lateral and vertical facies relationships of bedforms deposited by aggrading supercritical flows: from cyclic steps to humpback dunes. Sedimentary Geology 296, 36-54.
Laugier, F.J., Plink-Björklund, P., 2016. Defining the shelf edge and the three-dimensional shelf-edge to slope facies variability in shelf-edge deltas. Sedimentology 63, 1280-1320.
Leckie, D.A., Walker, R.G., 1982. Storm-and tide-dominated shorelines in Cretaceous Moosebar-Lower Gates interval--outcrop equivalents of Deep Basin gas trap in western Canada. AAPG bulletin 66, 138-157.
Leclair, S.F., Arnott, R.W.C., 2005. Parallel lamination formed by high-density turbidity currents. Journal of Sedimentary Research 75, 1-5.
Leonard, R., 1983. Geology and hydrocarbon accumulations, Columbus Basin, offshore Trinidad. AAPG bulletin 67, 1081-1093.
Li, Y., Bhattacharya, J.P., Ahmed, S., Garza, D., 2018. Re-evaluating the Paleogeography of the River-dominated and Wave-influenced Ferron Notom Delta, Southern Central Utah: an Integration of Detailed Facies-architecture and Paleocurrent Analysis. Journal of Sedimentary Research 88, 214-240.
Liu, J.P., Li, A.C., Xu, K.H., Velozzi, D.M., Yang, Z.S., Milliman, J.D., DeMaster, D.J., 2006. Sedimentary features of the Yangtze River-derived along-shelf clinoform deposit in the East China Sea. Continental Shelf Research 26, 2141-2156.
Lonergan, L., Jamin, N.H., Jackson, C.A.-L., Johnson, H.D., 2013. U-shaped slope gully systems and sediment waves on the passive margin of Gabon (West Africa). Marine Geology 337, 80-97.
Lopez, M., 2001. Architecture and depositional pattern of the Quaternary deep-sea fan of the Amazon. Marine and Petroleum Geology 18, 479-486.
Lowe, D.R., 1982. Sediment gravity flows; II, Depositional models with special reference to the deposits of high-density turbidity currents. Journal of Sedimentary Research 52, 279.
MacEachern, J., Bann, K., 2008. The role of ichnology in refining shallow marine facies models. Recent Advances in Models of siliciclastic shallow-marine stratigraphy (Eds G. J. Hampson, R. J. Steel, P. M. Burgess, and R. W. Dalrymple), SEPM, Special Publication 90, 73-116.
MacEachern, J.A., Bann, K.L., Bhattacharya, J.P., Howell, C.D., 2005. Ichnology of deltas: organism responses to the dynamic interplay of rivers, waves, storms, and tides, in: Gioson, L., Bhattacharya, J.P. (Eds.), River Deltas-Concepts, Models, and Examples, SEPM, Special Publication 83, pp. 49-85.

Mackay, D.A., Dalrymple, R.W., 2011. Dynamic mud deposition in a tidal environment: the record of fluid-mud deposition in the Cretaceous Bluesky Formation, Alberta, Canada. Journal of Sedimentary Research 81, 901-920.
Macquaker, J.H., Bentley, S.J., Bohacs, K.M., 2010. Wave-enhanced sediment-gravity flows and mud dispersal across continental shelves: Reappraising sediment transport processes operating in ancient mudstone successions. Geology 38, 947-950.
Macquaker, J.H., Bohacs, K.M., 2007. On the accumulation of mud. science 318, 1734-1735.
Maillet, G.M., Vella, C., Berné, S., Friend, P.L., Amos, C.L., Fleury, T.J., Normand, A., 2006. Morphological changes and sedimentary processes induced by the December 2003 flood event at the present mouth of the Grand Rhône River (southern France). Marine Geology 234, 159-177.
Mallik, T., Mukherji, K., Ramachandran, K., 1988. Sedimentology of the Kerala mud banks (fluid muds?). Marine Geology 80, 99-118.
Mann, P., Escalona, A., Castillo, M.V., 2006. Regional geologic and tectonic setting of the Maracaibo supergiant basin, western Venezuela. AAPG bulletin 90, 445-477.
Marchès, E., Mulder, T., Cremer, M., Bonnel, C., Hanquiez, V., Gonthier, E., Lecroart, P., 2007. Contourite drift construction influenced by capture of Mediterranean Outflow Water deep-sea current by the Portimão submarine canyon (Gulf of Cadiz, South Portugal). Marine Geology 242, 247-260.
Marr, J.G., Harff, P.A., Shanmugam, G., Parker, G., 2001. Experiments on subaqueous sandy gravity flows: the role of clay and water content in flow dynamics and depositional structures. Geological Society of America Bulletin 113, 1377-1386.
Martinsen, O.J., Bakken, B., 1990. Extensional and compressional zones in slumps and slides in the Namurian of County Clare, Ireland. Journal of the Geological Society 147, 153-164.
Mathew, J., Baba, M., 1995. Mudbanks of the southwest coast of India. II: Wave-mud interactions. Journal of Coastal Research, 179-187.
Mayall, M.J., Yeilding, C.A., Oldroyd, J.D., Pulham, A.J., Sakurai, S., 1992. Facies in a shelf-edge delta; an example from the subsurface of the Gulf of Mexico, middle Pliocene, Mississippi Canyon, Block 109. AAPG bulletin 76, 435-448.
McCave, I., 1971. Wave effectiveness at the sea bed and its relationship to bed-forms and deposition of mud. Journal of Sedimentary Petrology 41, 89-96.
McCave, I., 1972. Transport and escape of fine-grained sediment from shelf areas, in: Swift, D.J.P., Duane, D., O., P. (Eds.), Shelf Sediment transport, Dowden Hutchinson and Ross, Stroudsburg, PA, pp. 225-248.
McCave, I., Jones, K., 1988. Deposition of ungraded muds from high-density non-turbulent turbidity currents. Nature 333, 250-252.
Meade, R.H., 1994. Suspended sediments of the modern Amazon and Orinoco rivers. Quaternary International 21, 29-39.
Mellere, D., Breda, A., Steel, R., 2003. Fluvially-incised shelf-edge deltas and linkage to upper-slope channels (Central Tertiary Basin, Spitsbergen). Global significance

and future exploration potential (Eds H. H. Roberts, N. C. Rosen, R. F. Fillon and J. B. Anderson), Gulf Coast Section-SEPM Special Publication 23, 231-266.
Michels, K., Kudrass, H., Hübscher, C., Suckow, A., Wiedicke, M., 1998. The submarine delta of the Ganges–Brahmaputra: cyclone-dominated sedimentation patterns. Marine Geology 149, 133-154.
Middleton, G.V., Hampton, M.A., 1973. Sediment gravity flows: mechanics of flow and deposition, Turbidites and deep-water sedimentation (Eds G. V. Middleton and A. H. Bouma). SEPM Short Course, Anaheim, pp. 1-38.
Miller, K.G., Kominz, M.A., Browning, J.V., Wright, J.D., Mountain, G.S., Katz, M.E., Sugarman, P.J., Cramer, B.S., Christie-Blick, N., Pekar, S.F., 2005. The Phanerozoic record of global sea-level change. science 310, 1293-1298.
Mills, P.C., 1983. Genesis and diagnostic value of soft-sediment deformation structures—a review. Sedimentary Geology 35, 83-104.
Mohrig, D., Ellis, C., Parker, G., Whipple, K.X., Hondzo, M., 1998. Hydroplaning of subaqueous debris flows. Geological Society of America Bulletin 110, 387-394.
Morton, R.A., Suter, J.R., 1996. Sequence stratigraphy and composition of late Quaternary shelf-margin deltas, northern Gulf of Mexico, AAPG bulletin, pp. 505-530.
Moscardelli, L., Wood, L., 2008. New classification system for mass transport complexes in offshore Trinidad. Basin Research 20, 73-98.
Moscardelli, L., Wood, L., Mann, P., 2006. Mass-transport complexes and associated processes in the offshore area of Trinidad and Venezuela. AAPG bulletin 90, 1059-1088.
Mulder, T., Alexander, J., 2001. The physical character of subaqueous sedimentary density flows and their deposits. Sedimentology 48, 269-299.
Mulder, T., Cochonat, P., 1996. Classification of offshore mass movements. Journal of Sedimentary Research 66, 43-57.
Mulder, T., Gonthier, E., Lecroart, P., Hanquiez, V., Marches, E., Voisset, M., 2009. Sediment failures and flows in the Gulf of Cadiz (eastern Atlantic). Marine and Petroleum Geology 26, 660-672.
Mulder, T., Syvitski, J.P.M., Migeon, S., Faugères, J.-C., Savoye, B., 2003. Marine hyperpycnal flows: initiation, behavior and related deposits. A review. Marine and Petroleum Geology 20, 861-882.
Muto, T., Steel, R.J., 2002. In defense of shelf-edge delta development during falling and lowstand of relative sea level. The Journal of Geology 110, 421-436.
Mutti, E., 1977. Distinctive thin-bedded turbidite facies and related depositional environments in the Eocene Hecho Group (South-central Pyrenees, Spain). Sedimentology 24, 107-131.
Nakajima, T., Peakall, J., McCaffrey, W.D., Paton, D.A., Thompson, P.J., 2009. Outer-bank bars: a new intra-channel architectural element within sinuous submarine slope channels. Journal of Sedimentary Research 79, 872-886.

Nelson, C.H., Twichell, D.C., Schwab, W.C., Lee, H.J., Kenyon, N.H., 1992. Upper Pleistocene turbidite sand beds and chaotic silt beds in the channelized, distal, outer-fan lobes of the Mississippi fan. Geology 20, 693-696.

Nemec, W., Steel, R., Gjelberg, J., Collinson, J., Prestholm, E., Oxnevad, I., 1988. Anatomy of collapsed and re-established delta front in Lower Cretaceous of eastern Spitsbergen: gravitational sliding and sedimentation processes. AAPG bulletin 72, 454-476.

Nio, S.D., Yang, C.S., 1991. Diagnostic attributes of clastic tidal deposits: a review, in: Smith, D.G., Reinson, G.E., Zaitlin, B.A., Rahmani, R.A. (Eds.), Clastic Tidal Sedimentology: Canadian Society of Petrolem Geologists, Memoir 16, pp. 3-27.

Nittrouer, C.A., DeMaster, D.J., 1986. Sedimentary processes on the Amazon continental shelf: past, present and future research. Continental Shelf Research 6, 5-30.

Nittrouer, C.A., Kuehl, S.A., DeMaster, D.J., Kowsmann, R.O., 1986. The deltaic nature of Amazon shelf sedimentation. Geological Society of America, Bulletin 97, 444-458.

Olariu, C., 2014. Autogenic process change in modern deltas: lessons for the ancient. From Depositional Systems to Sedimentary Successions on the Norwegian Continental Margin (Special Publication 46 of the IAS) 46, 149-166.

Olariu, C., Bhattacharya, J.P., 2006. Terminal distributary channels and delta front architecture of river-dominated delta systems. Journal of Sedimentary Research 76, 212-233.

Olariu, C., Steel, R.J., 2009. Influence of point-source sediment-supply on modern shelf-slope morphology: implications for interpretation of ancient shelf margins. Basin Research 21, 484-501.

Olariu, C., Steel, R.J., Petter, A.L., 2010. Delta-front hyperpycnal bed geometry and implications for reservoir modeling: Cretaceous Panther Tongue delta, Book Cliffs, Utah. American Association of Petroleum Geologists, Bulletin 94, 819-845.

Olariu, M.I., Hammes, U., Ambrose, W.A., 2013. Depositional architecture of growth-fault related wave-dominated shelf edge deltas of the Oligocene Frio Formation in Corpus Christi Bay, Texas. Marine and Petroleum Geology 48, 423-440.

Olariu, M.I., Olariu, C., 2015. Ubiquity of Wave-Dominated Deltas In Outer-Shelf Growth-Faulted Compartments. Journal of Sedimentary Research 85, 768-779.

Oliveira, C.M., Hodgson, D.M., Flint, S.S., 2009. Aseismic controls on in situ soft-sediment deformation processes and products in submarine slope deposits of the Karoo Basin, South Africa. Sedimentology 56, 1201-1225.

Oliveira, C.M., Hodgson, D.M., Flint, S.S., 2011. Distribution of soft-sediment deformation structures in clinoform successions of the Permian Ecca Group, Karoo Basin, South Africa. Sedimentary Geology 235, 314-330.

Osman, A., 2007. Deltaic to Estuarine Regime Change on Proximal Paleo-Orinoco Shelf: Morne L'Enfer Formation, South Trinidad. University of Texas at Austin, Unpublished MS thesis, p. 93.

Owen, G., 2003. Load structures: gravity-driven sediment mobilization in the shallow subsurface. Geological Society, London, Special Publications 216, 21-34.
Owen, G., Moretti, M., Alfaro, P., 2011. Recognising triggers for soft-sediment deformation: current understanding and future directions. Sedimentary Geology 235, 133-140.
Palinkas, C., Nittrouer, C., 2007. Modern sediment accumulation on the Po shelf, Adriatic Sea. Continental Shelf Research 27, 489-505.
Patruno, S., Hampson, G.J., Jackson, C.A., 2015a. Quantitative characterisation of deltaic and subaqueous clinoforms. Earth-Science Reviews 142, 79-119.
Patruno, S., Hampson, G.J., Jackson, C.A.L., Dreyer, T., 2015b. Clinoform geometry, geomorphology, facies character and stratigraphic architecture of a sand-rich subaqueous delta: Jurassic Sognefjord Formation, offshore Norway. Sedimentology 62, 350-388.
Pellegrini, C., Maselli, V., Cattaneo, A., Piva, A., Ceregato, A., Trincardi, F., 2015. Anatomy of a compound delta from the post-glacial transgressive record in the Adriatic Sea. Marine Geology 362, 43-59.
Pellegrini, C., Maselli, V., Gamberi, F., Asioli, A., Bohacs, K.M., Drexler, T.M., Trincardi, F., 2017. How to make a 350-m-thick lowstand systems tract in 17,000 years: The Late Pleistocene Po River (Italy) lowstand wedge. Geology 45, 327-330.
Peng, Y., Steel, R.J., Olariu, C., 2017. Transition from storm wave-dominated outer shelf to gullied upper slope: The mid-Pliocene Orinoco shelf margin, South Trinidad. Sedimentology 64, 1511-1539.
Peng, Y., Steel, R.J., Rossi, V.M., Olariu, C., 2018. Mixed-energy Process Interactions Read from a Compound-clinoform Delta (paleo–orinoco Delta, Trinidad): Preservation of River and Tide Signals By Mud-induced Wave Damping. Journal of Sedimentary Research 88, 75-90.
Petter, A.L., Steel, R.J., 2006. Hyperpycnal flow variability and slope organization on an Eocene shelf margin, Central Basin, Spitsbergen. AAPG bulletin 90, 1451-1472.
Piper, D.J., Normark, W.R., 2001. Sandy fans--from Amazon to Hueneme and beyond. AAPG bulletin 85, 1407-1438.
Piper, D.J., Normark, W.R., 2009. Processes that initiate turbidity currents and their influence on turbidites: a marine geology perspective. Journal of Sedimentary Research 79, 347-362.
Pirmez, C., Pratson, L.F., Steckler, M.S., 1998. Clinoform development by advection-diffusion of suspended sediment: modeling and comparison to natural systems. Journal of Geophysical Research 103, 24,141-124,157.
Plink-Björklund, P., Mellere, D., Steel, R.J., 2001. Turbidite variability and architecture of sand-prone, deep-water slopes: Eocene clinoforms in the Central Basin, Spitsbergen. Journal of Sedimentary Research 71, 895-912.
Plink-Björklund, P., Steel, R., 2008. Type II Shelf Margin, Høgsnyta, Norway: An Attached Slope-turbidite System, Atlas of Deep-Water Outcrops: AAPG Studies

in Geology 56 (Eds T. H. Nilsen, R. D. Shew, G. S. Steffens, and J. R. Studlick). AAPG and Shell Exploration & Production, Tulsa, pp. 282-286.
Plint, A., 2010. Wave-and storm-dominated shoreline and shallow-marine systems, Facies models 4 (Eds R. W. Dalrymple and N. P. James). Geological Association of Canada, St. John's, pp. 167-201.
Plint, G.A., 2014. Mud dispersal across a Cretaceous prodelta: storm-generated, wave-enhanced sediment gravity flows inferred from mudstone microtexture and microfacies. Sedimentology 61, 609-647.
Porębski, S.J., Steel, R.J., 2003. Shelf-margin deltas: their stratigraphic significance and relation to deepwater sands. Earth Science Reviews 62, 283-326.
Porębski, S.J., Steel, R.J., 2006. Deltas and sea-level change. Journal of Sedimentary Research 76, 390-403.
Pratson, L.F., Ryan, W.B., Mountain, G.S., Twichell, D.C., 1994. Submarine canyon initiation by downslope-eroding sediment flows: evidence in late Cenozoic strata on the New Jersey continental slope. Geological Society of America Bulletin 106, 395-412.
Prélat, A., Pankhania, S.S., Jackson, C.A.-L., Hodgson, D.M., 2015. Slope gradient and lithology as controls on the initiation of submarine slope gullies; Insights from the North Carnarvon Basin, Offshore NW Australia. Sedimentary Geology 329, 12-17.
Puig, P., Ogston, A., Mullenbach, B., Nittrouer, C., Sternberg, R., 2003. Shelf-to-canyon sediment-transport processes on the Eel continental margin (northern California). Marine Geology 193, 129-149.
Rine, J., Ginsburg, R.N., 1985. Depositional facies of a mud shoreface in Suriname, South America: a mud analogue to sandy, shallow-marine deposits. Journal of Sedimentary Research 55, 633-652.
Roberts, H.H., Huh, O.K., Hsu, S., Rouse, L.J., Rickman, D.A., 1989. Winter storm impacts on the chenier plain coast of southwestern Louisiana. Transactions-Gulf Coast Assocation of Geological Societies 39, 512-522.
Romero-Otero, G., Slatt, R., Pirmez, C., 2010. Detached and shelf-attached mass transport complexes on the Magdalena deepwater fan, Submarine Mass Movements and Their Consequences (Eds D. C. Mosher, L. Moscardelli, R. C. Shipp, J. D. Chaytor, C. D. Baxter, H. J. Lee, and R. Urgeles). Springer Netherlands, pp. 593-606.
Rossi, V.M., Kim, W., López, J.L., Edmonds, D., Geleynse, N., Olariu, C., Steel, R.J., Hiatt, M., Passalacqua, P., 2016. Impact of tidal currents on delta-channel deepening, stratigraphic architecture, and sediment bypass beyond the shoreline. Geology 44, 927-930.
Rossi, V.M., Perillo, M.M., Steel, R.J., Olariu, C., 2017. Quantifying mixed-process variability in shallow-marine depositional systems: What are sedimentary structures really telling us? Journal of Sedimentary Research 87, 1060-1074.

Rossi, V.M., Steel, R.J., 2016. The role of tidal, wave and river currents in the evolution of mixed-energy deltas: Example from the Lajas Formation (Argentina). Sedimentology 63, 824-864.
Sadler, P.M., 1982. Bed-thickness and grain size of turbidites. Sedimentology 29, 37-51.
Schieber, J., Southard, J., Thaisen, K., 2007. Accretion of mudstone beds from migrating floccule ripples. science 318, 1760-1763.
Schwab, W.C., Lee, H.J., Twichell, D.C., Locat, J., Nelson, C.H., McArthur, W.G., Kenyon, N.H., 1996. Sediment mass-flow processes on a depositional lobe, outer Mississippi Fan. Journal of Sedimentary Research 66, 916-927.
Sills, G.C., Elder, D.M., 1986. The transition from sediment suspension to settling bed, Estuarine cohesive sediment dynamics. Springer, pp. 192-205.
Sømme, T.O., Helland-Hansen, W., Granjeon, D., 2009. Impact of eustatic amplitude variations on shelf morphology, sediment dispersal, and sequence stratigraphic interpretation: Icehouse versus greenhouse systems. Geology 37, 587-590.
Sommerfield, C.K., Nittrouer, C.A., 1999. Modern accumulation rates and a sediment budget for the Eel shelf: a flood-dominated depositional environment. Marine Geology 154, 227-241.
Southard, J.B., Lambie, J.M., Federico, D.C., Pile, H.T., Weidman, C.R., 1990. Experiments on bed configurations in fine sands under bidirectional purely oscillatory flow, and the origin of hummocky cross-stratification. Journal of Sedimentary Research 60, 1-17.
Spinelli, G.A., Field, M.E., 2001. Evolution of continental slope gullies on the northern California margin. Journal of Sedimentary Research 71, 237-245.
Steel, R., Crabaugh, J., Schellpeper, M., Mellere, D., Plink-Björklund, P., Deibert, J., Loeseth, T., 2000. Deltas vs. rivers on the shelf edge: their relative contributions to the growth of shelf-margins and basin-floor fans (Barremian and Eocene, Spitsbergen), Deepwater Reservoirs of the World (Eds P. Weimer, R. M. Slatt, J. Coleman, N. C. Rosen, H. Nelson, A. H. Bouma, M. J. Styzen, and D. T. Lawrence). Gulf Coast Section-Society of Economic Paleontologists and Mineralogists Foundation, Houston, pp. 981-1009.
Steel, R., Uroza, C., Huggins, G., Osman, A., Winter, R., 2007. The growth of the Orinoco shelf prism on Trinidad: interaction of sediment supply, tectonics, sea level and basinal processes, Geological Society of Trinidad and Tobago, Annual Meeting, Extended Abstract Volume, pp. 1-12.
Steel, R.J., Carvajal, C., Petter, A.L., Uroza, C., 2008. Shelf and shelf-margin growth in scenarios of rising and falling sea level. Recent Advances in Models of Siliciclastic Shallow-Marine Stratigraphy, SEPM, Special Publication 90, 47-71.
Steel, R.J., Plink-Björklund, P., Aschoff, J., 2012. Tidal deposits of the Campanian Western Interior Seaway, Wyoming, Utah and Colorado, USA, in: Davis, R.A., Dalrymple, R.W. (Eds.), Principles of Tidal Sedimentology. Springer-Verlag, pp. 437-471.

Storms, J.E.A., Hoogendoorn, R.M., Dam, R.A.C., Hoitink, A.J.F., Kroonenberg, S.B., 2005. Late-Holocene evolution of the Mahakam delta, East Kalimantan, Indonesia. Sedimentary Geology 180, 149-166.

Stow, D.A., Mayall, M., 2000. Deep-water sedimentary systems: new models for the 21st century. Marine and Petroleum Geology 17, 125-135.

Strachan, L.J., 2008. Flow transformations in slumps: a case study from the Waitemata Basin, New Zealand. Sedimentology 55, 1311-1332.

Sumner, E.J., Amy, L.A., Talling, P.J., 2008. Deposit structure and processes of sand deposition from decelerating sediment suspensions. Journal of Sedimentary Research 78, 529-547.

Surlyk, F., 1987. Slope and deep shelf gully sandstones, Upper Jurassic, East Greenland. AAPG bulletin 71, 464-475.

Surpless, K.D., Ward, R.B., Graham, S.A., 2009. Evolution and stratigraphic architecture of marine slope gully complexes: Monterey Formation (Miocene), Gaviota Beach, California. Marine and Petroleum Geology 26, 269-288.

Swenson, J.B., Paola, C., Pratson, L., Voller, V.R., Murray, A.B., 2005. Fluvial and marine controls on combined subaerial and subaqueous delta progradation: Morphodynamic modeling of compound-clinoform development. Journal of Geophysical Research 110, F02013.

Sydow, J.C., Finneran, J., Bowman, A.P., 2003. Stacked shelf-edge delta reservoirs of the Columbus Basin, Trinidad, West Indies, in: Roberts, N.C., Rosen, N.C., Fillon, R.F., Anderson, J.B. (Eds.), Shelf-Margin Deltas and Linked Downslope Petroleum Systems: Global Significance and Future Exploration Potential, SEPM, Gulf Coast Section, 23rd Annual Research Conference, Houston, Texas, pp. 441-465.

Sylvester, Z., 2007. Turbidite bed thickness distributions: methods and pitfalls of analysis and modelling. Sedimentology 54, 847-870.

Sylvester, Z., Deptuck, M., Prather, B., Pirmez, C., O'Byrne, C., 2012. Seismic stratigraphy of a shelf-edge delta and linked submarine channels in the northeastern Gulf of Mexico. Application of the Principles of Seismic Geomorphology to Continental-Slope and Base-of-Slope Systems: Case Studies from Seafloor and Near-Seafloor Analogues (Eds B. E. Prather, M. E. Deptuck, D. Mohrig, B. Van Hoorn, and R. B. Wynn): SEPM, Special Publication 99, 31-59.

Ta, T.K.O., Nguyen, V.L., Tateishi, M., Kobayashi, I., Saito, Y., 2005. Holocene delta evolution and depositional models of the Mekong River Delta, southern Vietnam, in: Giosan, L., Bhattacharya, J.P. (Eds.), River Deltas-Concepts, Models, and Examples, SEPM, Special Publication 83, pp. 453-466.

Ta, T.K.O., Nguyen, V.L., Tateishi, M., Kobayashi, I., Tanabe, S., Saito, Y., 2002. Holocene delta evolution and sediment discharge of the Mekong River, southern Vietnam. Quaternary Science Reviews 21, 1807-1819.

Talling, P., Malgesini, G., Sumner, E., Amy, L., Felletti, F., Blackbourn, G., Nutt, C., Wilcox, C., Harding, I., Akbari, S., 2012a. Planform geometry, stacking pattern,

and extrabasinal origin of low strength and intermediate strength cohesive debris flow deposits in the Marnoso-arenacea Formation, Italy. Geosphere 8, 1207-1230.
Talling, P.J., 2001. On the frequency distribution of turbidite thickness. Sedimentology 48, 1297-1329.
Talling, P.J., Amy, L.A., Wynn, R.B., Blackbourn, G., Gibson, O., 2007. Evolution of turbidity currents deduced from extensive thin turbidites: Marnoso Arenacea Formation (Miocene), Italian Apennines. Journal of Sedimentary Research 77, 172-196.
Talling, P.J., Masson, D.G., Sumner, E.J., Malgesini, G., 2012b. Subaqueous sediment density flows: depositional processes and deposit types. Sedimentology 59, 1937-2003.
Talling, P.J., Wynn, R.B., Schmmidt, D.N., Rixon, R., Sumner, E., Amy, L., 2010. How Did Thin Submarine Debris Flows Carry Boulder-Sized Intraclasts for Remarkable Distances Across Low Gradients to the Far Reaches of the Mississippi Fan? Journal of Sedimentary Research 80, 829-851.
Taylor, A., Goldring, R., 1993. Description and analysis of bioturbation and ichnofabric. Journal of the Geological Society 150, 141-148.
Traykovski, P., Geyer, W.R., Irish, J., Lynch, J., 2000. The role of wave-induced density-driven fluid mud flows for cross-shelf transport on the Eel River continental shelf. Continental Shelf Research 20, 2113-2140.
Tripsanas, E.K., Piper, D.J., Jenner, K.A., Bryant, W.R., 2008. Submarine mass-transport facies: New perspectives on flow processes from cores on the eastern North American margin. Sedimentology 55, 97-136.
Trowbridge, J., Kineke, G., 1994. Structure and dynamics of fluid muds on the Amazon continental shelf. Journal of Geophysical Research: Oceans 99, 865-874.
Twichell, D.C., Roberts, D.G., 1982. Morphology, distribution, and development of submarine canyons on the United States Atlantic continental slope between Hudson arid Baltimore Canyons. Geology 10, 408-412.
Tyson, L., Babb, S., Dyer, B., 1991. Middle Miocene tectonics and its effects on late Miocene sedimentation in Trinidad, Transactions of the Second Geological Conference of the Geological Society of Trinidad and Tobago, Trinidad, pp. 26-40.
Uncles, R., Stephens, J., Law, D., 2006. Turbidity maximum in the macrotidal, highly turbid Humber Estuary, UK: flocs, fluid mud, stationary suspensions and tidal bores. Estuarine, Coastal and Shelf Science 67, 30-52.
Uroza, C.A., Steel, R.J., 2008. A highstand shelf-margin delta system from the Eocene of West Spitsbergen, Norway. Sedimentary Geology 203, 229-245.
Vakarelov, B.K., Ainsworth, R.B., MacEachern, J.A., 2012. Recognition of wave-dominated, tide-influenced shoreline systems in the rock record: Variations from a microtidal shoreline model. Sedimentary Geology 279, 23-41.
Vincent, H., 2003. Transition from tidal to fluvial dominated deltaic deposits. A transect through the Morne L'Enfer to basal Erin Formation, Puerto Grande Bay, South Coast, Trinidad, Field Guide, Port of Spain, p. 18.

Vincent, H., 2012. Late Miocene turbidite channel complex of the Cruse Formation, Palo Seco Bay, Trinidad. The Geological Society of Trinidad and Tobago, 5th Geological Conference, 18.
Walsh, J., Nittrouer, C., 2009. Understanding fine-grained river-sediment dispersal on continental margins. Marine Geology 263, 34-45.
Walsh, J., Nittrouer, C., Palinkas, C., Ogston, A., Sternberg, R., Brunskill, G., 2004. Clinoform mechanics in the Gulf of Papua, New Guinea. Continental Shelf Research 24, 2487-2510.
Warne, A.G., Meade, R.H., White, W.A., Guevara, E.H., Gibeaut, J., Smyth, R.C., Aslan, A., Tremblay, T., 2002. Regional controls on geomorphology, hydrology, and ecosystem integrity in the Orinoco Delta, Venezuela. Geomorphology 44, 273-307.
Wei, X., Steel, R.J., Ravnås, R., Jiang, Z., Olariu, C., Li, Z., 2016. Variability of tidal signals in the Brent Delta Front: New observations on the Rannoch Formation, northern North Sea. Sedimentary Geology 335, 166-179.
Wells, J.T., Coleman, J.M., 1978. Longshore transport of mud by waves: northeastern coast of South America. Geologie en Mijbouw 57, 353-359.
Wells, J.T., Coleman, J.M., 1981. Periodic mudflat progradation, northeastern coast of South America: a hypothesis. Journal of Sedimentary Petrology 51, 1069-1075.
Wells, J.T., Roberts, H.H., 1980. Fluid mud dynamics and shoreline stabilization: Louisiana chenier plain. American Society of Civil Engineers, 17th International Coastal Engineering Conference, Proceedings 1, 1382-1401.
Wheatcroft, R., Borgeld, J., 2000. Oceanic flood deposits on the northern California shelf: large-scale distribution and small-scale physical properties. Continental Shelf Research 20, 2163-2190.
Williams, G.E., 1991. Upper Proterozoic tidal rhythmites, South Australia: sedimentary features, deposition, and implications for the earth's paleorotation, in: Smith, D.G., Reinson, G.E., Zaitlin, B.A., Rahmani, R.A. (Eds.), Clastic Tidal Sedimentology: Canadian Society of Petroleum Geologists, Memoir 16, pp. 161-177.
Willis, B.J., 2005. Deposits of tide-influenced river deltas, in: Gioson, L., Bhattacharya, J.P. (Eds.), River Deltas-Concepts, Models, and Examples, SEPM, Special Publication 83, pp. 87-129.
Winter, R., 2006. Reservoir characterization of the Cruse Formation, southern Trinidad, Geological Sciences. University of Texas at Austin, Unpublished MS thesis, p. 85.
Winterwerp, J., De Graaff, R., Groeneweg, J., Luijendijk, A., 2007. Modelling of wave damping at Guyana mud coast. Coastal Engineering 54, 249-261.
Wood, L.J., 2000. Chronostratigraphy and tectonostratigraphy of the Columbus Basin, eastern offshore Trinidad. AAPG bulletin 84, 1905-1928.
Woodside, P.R., 1981. Petroleum geology of Trinidad and Tobago. Oil and Gas Journal 79, 364-389.

Yang, B., Dalrymple, R., Chun, S., 2005. Sedimentation on a wave-dominated, open-coast tidal flat, south-western Korea: summer tidal flat–winter shoreface. Sedimentology 52, 235-252.
Yoshida, S., Steel, R.J., Dalrymple, R.W., 2007. Changes in depositional processes—an ingredient in a new generation of sequence-stratigraphic models. Journal of Sedimentary Research 77, 447-460.
Zhang, J., Steel, R., Ambrose, W., 2016. Greenhouse shoreline migration: Wilcox deltas. AAPG bulletin 100, 1803-1831.
Zhang, J., Steel, R., Ambrose, W., 2017a. Paleocene Wilcox cross-shelf channel-belt history and shelf-margin growth: Key to Gulf of Mexico sediment delivery. Sedimentary Geology 362, 53-65.
Zhang, J., Steel, R., Olariu, C., 2017b. What conditions are required for deltas to reach the shelf edge during rising sea level? Geology 45, 1107-1110.